A PhD thesis

"DESIGN, DEVELOPMENT AND CHARACTERIZATION OF COLON CANCER TARGETING FOLIC ACID CONJUGATED CAPECITABINE NANOPARTICLES"

Submitted to

SUMANDEEP VIDYAPEETH

in partial fulfilment of the requirements
for the award of the degree of

Doctor of Philosophy
in
Pharmaceutical Sciences

By

ANKURKUMAR RAMESHBHAI JAVIA

(Registration No: PhD 006 2011)

Under the guidance of

Dr. A. K. SETH

M. Pharm., Ph. D.

Dean, Faculty of Allied Health Sciences &
Research Director, Sumandeep Vidyapeeth

DEPARTMENT OF PHARMACY,
SUMANDEEP VIDYAPEETH,
PO- PIPARIA, TA- WAGHODIA, VADODARA-391760, GUJARAT

AUGUST 2015

SUMANDEEP VIDYAPEETH

PIPARIA, VADODARA

CERTIFICATE

This is to certify that, this thesis entitled **"DESIGN, DEVELOPMENT AND CHARACTERIZATION OF COLON CANCER TARGETING FOLIC ACID CONJUGATED CAPECITABINE NANOPARTICLES"** submitted by **Mr. ANKURKUMAR RAMESHBHAI JAVIA (Registration No. PhD 006 2011)** in partial fulfilment for the award of degree of **DOCTOR OF PHILOSOPHY IN PHARMACEUTICAL SCIENCES** to Sumandeep Vidyapeeth, Piparia. This work has been carried out under my supervision and guidance. The matter compiled in this thesis has not been submitted earlier for the award of any other degree or fellowship and free from any kind of plagiarism.

Date:

Place:

Dr. A. K. SETH
M. Pharm., Ph. D.
Dean, Faculty of Allied Health Sciences &
Research Director, Sumandeep Vidyapeeth

SUMANDEEP VIDYAPEETH, VADODARA, GUJARAT

SUMANDEEP VIDYAPEETH

PIPARIA, VADODARA

CERTIFICATE

This is to certify that, this thesis entitled **"DESIGN, DEVELOPMENT AND CHARACTERIZATION OF COLON CANCER TARGETING FOLIC ACID CONJUGATED CAPECITABINE NANOPARTICLES"** submitted by **Mr. ANKURKUMAR RAMESHBHAI JAVIA (Registration No. PhD 006 2011)** in partial fulfillment for the award of degree of **DOCTOR OF PHILOSOPHY IN PHARMACEUTICAL SCIENCES** to Sumandeep Vidyapeeth, Piparia. This work has been carried out under the guidance of Dr. A. K. Seth. The matter compiled in this thesis has not been submitted earlier for the award of any other degree or fellowship and free from any kind of plagiarism.

Date:

Place:

ANKURKUMAR RAMESHBHAI JAVIA

Department of Pharmacy,

Sumandeep Vidyapeeth, Piparia

SUMANDEEP VIDYAPEETH, VADODARA, GUJARAT

SUMANDEEP VIDYAPEETH

PIPARIA, VADODARA

DECLARATION

I hereby declare that the topic entitled **"DESIGN, DEVELOPMENT AND CHARACTERIZATION OF COLON CANCER TARGETING FOLIC ACID CONJUGATED CAPECITABINE NANOPARTICLES"** which is submitted herewith to Sumandeep Vidyapeeth, Piparia for the partial fulfillment for the award of degree of Doctor of Philosophy in Pharmaceutical Sciences is the result of work done by me in Department of Pharmacy, Sumandeep Vidyapeeth, under the guidance of Dr. A. K. Seth.

I further declare that the results of this work have not been previously been submitted for any degree or fellowship and free from any kind of plagiarism.

Date:

Place:

ANKURKUMAR RAMESHBHAI JAVIA

Department of Pharmacy,

Sumandeep Vidyapeeth, Piparia

ACKNOWLEDGEMENT

Every event, small or big in nature, itself is a creation. As one flower makes no garland, this research work would not have reaped as fruit without whole hearted encouragement and live involvement of my teachers, friends, family and well wishers. Here I would like to thank the people who had spent their precious time for me and who had directly or indirectly supported me during various stages of my research work.

God is our refuge and strength, a very present help, when we need it most, I thank him for guiding me through rough and torn paths, for always being less than a whisper away……I thank the almighty God, for it is under His grace that we live, learn and flourish !!

In process of research, number of hurdles comes in way. But help of guide and others, could overcome all hurdles and got success. It gives me profound pleasure to express my deep sense of gratitude to my guide, Dr. A. K. Seth, under whose esteemed guidance and supervision, the work presented in this thesis was carried out. I am indebted to him for his self-implemented advices, altruistic attitude, untiring guidance, innovative ideas, constructive criticism and overwhelming cooperativeness. I would also like to thank him for providing necessary infrastructure and facilities for successful completion of my research work.

Besides my advisor, I would like to thank Dr. R. Balaraman, for their insightful comments and encouragement, but also for the hard question which incented me to widen my research from various perspectives.

A journey is easier when you travel together. Interdependence is certainly more valuable than independence. There are some persons who were always there, when I really needed someone my side. They are my colleagues and friends whose presence and encouragement helped me to complete my research work within time.

I also wish to thank non teaching staff of Department of Pharmacy, Sumandeep Vidyapeeth for their help during my research work.

Last but not the least; I pay reverence to my parents and wife for its constant encouragement and moral support.

Finally, I would like to thank all who contributed directly or indirectly in successful completion of this work, as well as expressing my apology that I could not mention personally one by one.

Ankurkumar Rameshbhai Javia

Table of Contents

LIST OF FIGURES

5'-DFCR	5'-deoxy-5-fluorocytidine
5'-DFUR	5'-deoxy-5-fluorouridine
5-FU	5-fluorouracil
%	Percentage
% T	Percentage Transmittance
°C	Degree Centigrade
µg	Microgram
µm	Micrometer
Ab	Absorbance
API	Active Pharmaceutical Ingredient
CDR	Cumulative Drug Release
cm	Centimeter
CS	Chitosan
CS-NPs	Chitosan nanoparticles
D.L	Drug loading
DMEM	Dulbecco's modified eagle medium
DMSO	Dimethyl sulphoxide
DPBS	Dulbecoo's phosphate buffer saline
DPD	Dihydropyrimidine dehydrogenase
EDTA	Ethylene diamine tetraacetate
EE	Entrapment efficiency
ELISA	Enzyme linked immunosorbent assay
FA	Folic acid
FBS	Fetal bovine serum
FA-CS-NPs	Folic acid conjugated Chitosan nanoparticles
FTIR	Fourier transform infrared
FTGM	Fluid thioglycolate medium
Gm	Gram
HBSS	Hank's Balanced Salt solution
hrs	Hours
HT-29	Human colon-cancer cell line
IC_{50}	50% inhibitory concentration
ICH	International conference on harmonization

MCF-7	Human breast-cancer cell line
mg	Milligram
min	Minute
ml	Milliliter
MTT	3-(4,5-dimethylthiazol-2-yl)-2,5 diphenyltetrazolium bromide
NaOH	Sodium Hydroxide
NCCS	National Centre for Cell Science
nm	Nanometer
NPs	Nanoparticles
PBS	Phosphate buffer saline solution
pH	Hydrogen ion concentration
PDT	Population doubling time
RH	Relative humidity
RPM	Revolution per minute
RPMI	Roswell Park Memorial Institute medium
SD	Standard deviation
SEM	Scanning Electron microscope
$t_{1/2}$	Half life
TPP	Tripolyphosphate
TSB	Tryptone soya broth
USP	United state Pharmacopoeia
UV	Ultraviolet
λ_{max}	maximum wavelength

1. INTRODUCTION

1.1 Cancer

1.1.1 Introduction

Cancer is an ailment described by uncontrolled increase and spread of anomalous types of the body's own cells. Malignancy is a class of malady in which a group of cells presents uncontrolled development (division beyond as far as possible), incursion (intrusion on and decimation of nearby tissues) and infrequently metastasis (spread to different areas in the body by means of lymph or blood). Oncology is the branch of health science dealing with the prevention, study, diagnosis and management of cancer. Malignancy may influence individuals at all ages, even babies, yet the danger of most mixed bags increment with age.[1, 2]

1.1.2 Origin

All cancers start in cells, the body's fundamental unit of life. To comprehend tumor, it is important to recognize what happens when typical cells get to be malignancy cells. The body is comprised of numerous sorts of cells. These cells develop and divide in a controlled manner to deliver more cells as they are expected to keep the body sound. At the point when cell get to be old or harmed, they pass on and are supplanted with new cells. In some cases this efficient procedure turns out badly. The hereditary material (DNA) of a cell can get to be harmed or changed, delivering transformations that influence typical cell development and division. At the point when this happens, cells don't undergo the apoptosis when they ought to be and new cells produced when the body does not require them. The additional cells may shape a mass of tissue known as a tumor.[3, 4]

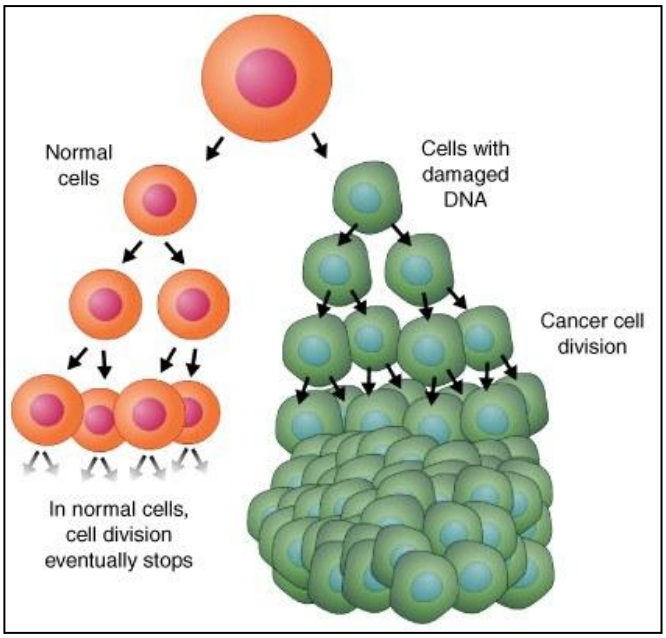

Figure 1.1: Origin of cancer

1.1.3 Types

There are several types of the cancers, based on the body parts affected and the nature of the tissue affected

1. **Neoplasm:** A medical term for cancer or tumor i.e. relatively autonomous growth of tissue, this leads to abnormal growth or mass of tissue which may be a benign or malignant in nature.
2. **Carcinoma:** A cancer that arises from ectoderm or endoderm at tissue (Ectoderm involves skin and nerve tissue. Endoderm involves intestinal tissue and organ).
3. **Sarcoma:** A cancer arises from mesoderm tissue. (mesoderm involves bone, muscles, cartilage etc.)
4. **Teraloma:** A cancer arises from cells of ectoderm, endoderm or mesoderm.
5. **Cancer of blood:** There are two types of blood cancer, leukemia i.e. WBC count more than 10^5 to 10^6 per mm^3 (normal 7500 mm^3) and polycythemia i.e. increase in RBC count.

   The rapid uncontrolled growth of cancerous cells is known as malignant tumor. These cells can then invade & destroy healthy tissues including organs[5]. The comparison between benign and malignant type of the cancer is given in Table 1.1

Table 1.1: Comparison of benign and malignant cancer

Benign	Malignant
Generally encapsulated (Not invasive) Slow growing Do not metastasize Do not interfere with health E.g. **Fibromma** - of fibrous tissue **Lymphoma** - of fat **Osteoma** - of bone	Not encapsulated (invasive) Rapidly growing Metastasize Detrimental to health and life E.g. **Sarcoma** and **Carcinoma**

1.1.4 Pathophysiology

Malignancies are brought on by a progression of mutations. Every mutation modifies the performance of the cell.

Hereditary changes can happen at numerous levels, from addition or loss of whole chromosomes to a transformation influencing a solitary DNA nucleotide. There are two general types of genes, which are influenced by these progressions.

Oncogenes may be ordinary genes, which are expressed at improperly abnormal states. Articulation of these genes advances the threatening phenotype of tumor cells.

Tumor suppressor genes are genes, which repress cell division, survival or different properties of tumor cells. Tumor silencer genes are frequently crippled by malignancy causing DNA changes normally. Changes in numerous genes altogether are responsible to change an ordinary cell into malignant cell.[3, 4] This mechanism involving oncogenes as well as tumor suppressor gene is shown in Figure 1.2

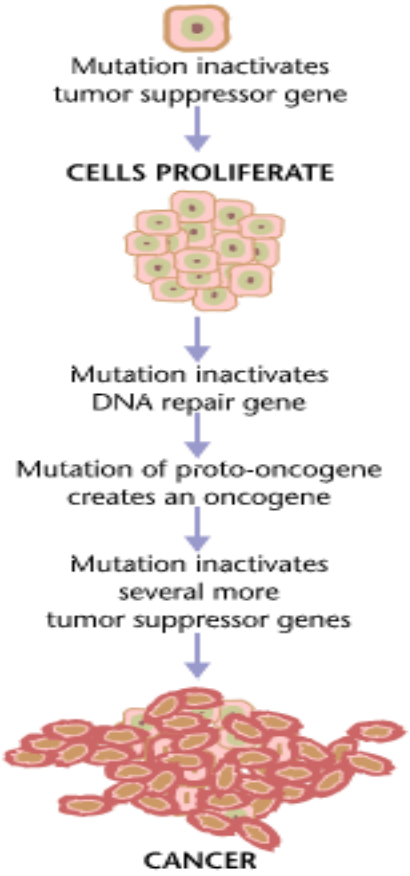

Figure 1.2: Mechanism of cancer

1.1.5 Symptoms

Symptoms of tumor spreading rely on upon the area at which the tumor is located. Cancer symptoms can be partitioned into three categories:[6]

1. Confined symptoms
   Abnormal knots or swelling, Hemorrhage and Jaundice
2. Symptoms of metastasis (spreading)
   Engorged lymph nodes, coughing of blood, abnormally enlarged liver, bone agony, crack of influenced bones and neurological symptoms.
3. Systemic symptoms
   Weight reduction, loss of hunger, weakness, extreme sweating specially at night and iron deficiency.

1.1.6 Risk factors

Following are the factors, which enhance the risk of cancer [7-9]

1. Mutation by chemical carcinogens: chemicals causing mutation, including alcohol and tobacco uncontrolled proliferation
2. Exposure to radiation for prolonged period
3. Viral or bacterial infection
4. Some of the virus species are in charge of 15% of human malignancies around the world, such viruses are, human T-lymphotropic virus, hepatitis B and hepatitis C virus and human papilloma virus.
5. Hormonal irregular characteristics, for instance: Estrogen disparity in females
6. Immune system dysfunction
7. HIV is responsible for various types of cancer, counting kapopsi's sarcoma, non Hodgkin's lymphoma.
8. Hepatitis B and Hepatitis C can cause liver cancer.
9. Epstein Barr virus can cause Hodgkin's lymphoma, which is a cancer of lymphatic system.
10. Risk factors include smoking, obesity, poor diet, lack of exercise and prolong exposure to sunlight.

1.1.7 Prevention

Preventing the cancer can be characterized as dynamic measures to diminish the occurrence of tumor. This can be refined by maintaining a strategic distance from can-

cer-causing agents or modifying their digestion, seeking after a way of life or eating regimen that adjusts cancer bringing variables and/or medicinal intercession, for example, drug prophylaxis, treatment of premalignant sores.[10, 11]

1.1.8 Diagnosis

Numbers of techniques are used for cancer diagnosis, which include[12],

1. Blood test: Some cancer cells release protein in blood. Such blood sample can be tested for cancer detection.
2. X-rays: By taking X-ray of particular organ, cancer can be diagnosed.
3. MRI: Magnetic Resonance (Scan) Imaging is a newer technique to take photography of various organs by different angles.
4. CT Scan: Computerized Tomography also can be used for cancer diagnosis.
5. Endoscopy: By endoscopy we can diagnose the cancer of bowel.
6. Biopsy: It means surgical removal of a small piece of affected tissue is done and tested it for presence of cancerous cell.

1.1.9 Treatment

Cancer can be treated by surgery, chemotherapy, radiation therapy, immunotherapy, monoclonal antibody therapy or other methods. The choice of therapy depends upon the location of and grade of the tumor and the stage of the disease, as well as the general state of the patient.

The treatment of cancer include[13, 14],

1. Surgery – Surgical removal of cancerous tumors
2. Chemotherapy – Using various anticancer agents
3. Radiotherapy – By using X-rays, radium
4. Hormonal therapy – Hormones deactivate cancerous cell functioning.
5. Monoclonal antibody therapy – A dose of readymade monoclonal antibody is given at targeted organ to increase immunity, so also called as targeted therapy.
6. Immunotherapy – Immunity of patient can be increased by administering various immunomodulators.
7. Angiogenesis inhibitor therapy
8. Alternative and complementary therapies

1.1.10 Chemotherapy

Almost all chemotherapeutic agents currently available work to kill cancer by affecting DNA synthesis or function, a process that occur through the cell cycle.
The major categories of chemotherapeutic agents are given in Table 1.2[14]

Table 1.2: classification of drugs used for cancer treatment

A) Drug acting specifically on cells (Cytotoxic medications)	
1. Alkylating specialists	
a) Nitrogen mustards	Ifosfamide , Mechlorethamine, Capecitabine
b) Ethylenimine	Thio-TEPA
c) Alkyl sulfonate	Busulfan, Treosulfan.
d) Nitrosourea	Carmustine, Lomustine, Estramustine
e) Triazine	Dacarbazine
2) Antimetabolites	
a) Folate antagonist	Methotrexate
b) Purine antagonist	6-Mercaptopurine,6-Thioguanine, Azathioprine
c) Pyrimidine antagonist	Capecitabine, 5-Flurouracil (5-FU), Cytarabine
3) Vinca alkaloids	Vincristine, Vinblastine
4) Taxanes	Paclitaxel, Docitaxel
5) Epipodophylotoxin	Etoposide
6) Camptothecin analogues	Topotecan, Irinotecan
7) Antibiotics	Actinomycin-D, Daunorubicin, Mithramycin, Doxorubicin, Bleomycin, Mitomycin
8) Miscellaneous	Hydroxyurea, Procarbazine, Cisplatin
B) Drug altering hormonal meilieu	
1) Glucocorticoids	Prednisolone
2) Estrogen	Fosfestrol, Ethinylestradiol
3) Antiestrogen	Tamoxifen
4) Aantiandrogen	Flutamide
5) 5-α reductase inhibitor	Finasteride
6) GnRH analogues	Naferelin, Gosrelin

1.1.11 Drawbacks of chemotherapy

1.1.11.1 Short term negative side effects

Loss of hair and eyebrows, loss of appetite, having food taste peculiar, mouth sores, nausea, vomiting, loose stools or constipation (due to less food intake), fatigue, mental fogginess and inability to resist infections. Another short term disadvantage is that treatment is time-consuming.[14]

1.1.11.2 Long term side effects

Infertility, heart problems, damage to the central nervous system or damage to vital organs such as the lungs or liver. Another disadvantage is the cost, which many health insurance companies will not entirely pay for.[14]

To overcome of these side effects there are nanoparticles is one of the beneficial method. when nanoparticles are conjugated with folic acid these can be used as targeted drug delivery system and it will not affect the normal cell of the body so there is reduction of side effects and beneficial for target drug delivery system.[14]

1.2 Colorectal cancer

1.2.1 Introduction

Colorectal cancer also regarded as rectal cancer, bowel cancer or colon cancer, is the advancement of the cancer growth at a location of colon and/or rectum i.e. regions of the large intestine. It is because of the strange development of cells that can attack or spread to different parts of the body.[15] Development of the colon cancer from the polyps to advanced stage cancer is shown in Figure 1.3

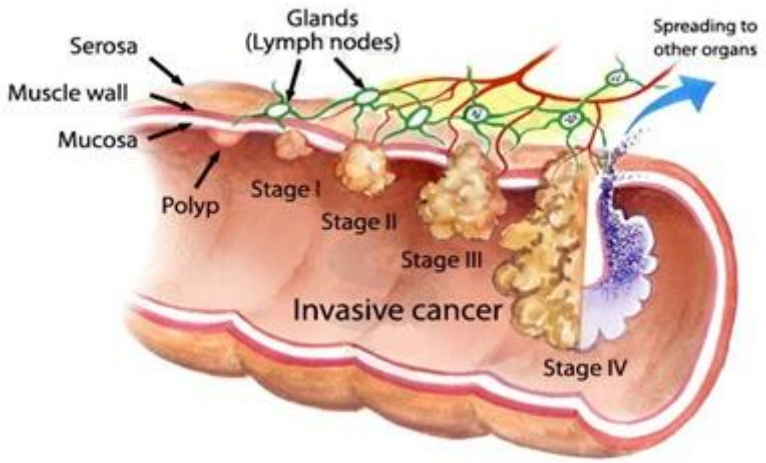

Figure 1.3: Colon cancer and its stage progression

1.2.2 Signs and symptoms

The manifestations of bowel malignancy rely upon two things, first is the area of the cancer in the bowel, and second is the metastatic nature of the cancer that means if cancer is spreaded to the other organs or not. The exemplary cautioning signs include exacerbating stool, blood in stool, reduced stool thickness, and nausea or vomiting in someone more than 50 years of age, while bleeding in bowel or anemia are high hazard highlights in those beyond 50 years old. Other generally portrayed side effects including weight reduction and change in bowel functioning are generally the concern if related with bleeding.[16-18]

1.2.3 Cause

More than 70-90% of colorectal malignancy happens in individuals with next to zero hereditary danger. Other danger elements incorporates more established age, male sex, high admission of fat, liquor or red meat, overweight, smoking and an absence of

physical activity. Roughly, around 10% cases are connected to deficient physical activity. The danger for liquor seems to increment at more prominent than one beverage for each day. A relationship has been found between the measures of liquid taken in, premalignant adenomatous polyps and bowel cancer with no less than 4-5 cups of water, just about 1250mL, associated to lower rates.[15, 19-21]

1.2.4 Pathogenesis

Colon malignancy is arising from the inner cell layers of the colon and/or rectum, in most of the cases, because of the mutation of the WNT signaling pathway, which is found to rise the signaling action artificially. Intestinal crypt stem cell is the usual place where the mutation is most probably occurs.[22] The most frequent mutation in all colorectal malignancy is the APC gene, which delivers the APC protein. This APC protein inhibits the amassing of β-catenin protein; without APC, β-catenin aggregates to abnormal states and moves into the nucleus, ties to DNA, and initiates the expression of genes that are critical for stem cell replenishment and transformation yet when improperly transcribed at abnormal states can bring about malignancy. While APC gene undergoes the mutation in majority of cases of the bowel tumor, a few malignancy have expanded β-catenin on account of changes in β-catenin (CTNNB1) which inhibits its disintegration, or they have mutation(s) in different genes which produces some related protein to APC, for example, AXIN2, AXIN1, NDK1 or TCF72.[23-25]

Past the imperfections in the signaling pathway of WNT-APC-β-catenin, it is also required for some other gene as well for the cell to end up transforming in the cancer state. The p53 protein, expressed by the TP53 gene, regularly screens cell division and executes cells in the events that they have WNT pathway imperfections. In the end, a cell line gains a change in the TP53 gene and change the tissue from a initial epithelial cancer into an intrusive epithelial cell malignancy. However, there is also some instance when p53 gene does not undergo the mutation, but rather another gene express the defensive protein named BAX. [26, 27]

TGF-β and DCC are some of the other routinely deleted-deactivated proteins causing the colon cancer. In more than 50% of the bowel cancer TGF-β is found to be involved by undergoing deactivation mutation, while on the other hand DCC protein may not be mutated to become deactivated when other downstream protein known as

SMAD is mutated. In colon tumor from the DCC concern, its mainly a deletion of DCC gene in its chromosome fragment.[28, 29]

Over expression of the oncogenes cause the colorectal cancer. Case in point, KRAS, RAF, and PI3K proteins expressing genes. Expressed proteins of such oncogenes ordinarily signal the cell to separate and divide in response to the growth factors. Now, when these genes are overexpressed as a result of the mutation, resulting vastly produced protein product can cause the intense cell expansion which ultimately lead to the colon cancer. The sequential mutation can also be a significant, with an essential KRAS mutation that usually cause a self-restricting hyperplastic or marginal progression, yet in the event that happening past an APC mutation it frequently advances to cancer.[30, 31] PTEN, a tumor silencer, ordinarily restrains PI3K, however it may undergoes mutation sometimes and hence get deactivated.[26, 32]

Broad, genome-level investigation has uncovered that colorectal cancers are evidently distinct into two types of malignancy i.e. hypermutated and non-hypermutated.[33] Besides the mutation in oncogene and some deactivation, depicted for the above mentioned genes, non-hypermutated specimens additionally possess mutated gene FAM123B, SOX9, ARID1A, CTNNB1 and ATM. Hypermutated cancers, while advancing through a different types of genetic actions, show mutated forms of BRAF, ACVR2A, MSH3, TGFBR2, SLC9A9, MSH6 and TCF7L2[34, 35]. Basic activity along with these genes, between both cancer sets, is their association in TGF-β and WNT signaling pathways, which thus brings about expanded action of MYC, a focal player in bowel tumor.[33]

1.2.5 Diagnosis

Colon tumor is diagnosed by means of examining a doubtful colon location for possible tumor advancement normally carried out while colonoscopy or sigmoidoscopy, based on the area of a progression. A CT scan of the torso, belly and pelvis then usually determines the degree of malignancy. Additional important imaging test, for example, PET and MRI may also be utilized as a part of specific cases. Then after colorectal tumor staging is done on the basis of TNM system. This TNM system is established by determining degree of spreading of early cancer, and, involvement of lymph nodes if any with its location, and the degree of metastasis.[26, 36]

Investigation outcome of tissue taken from a biopsy or surgery are reported and used for the establishing the microscopic level cell characteristics. A pathology report usually contains information of type and grade of cell. The most widely recognized colon malignancy is adenocarcinoma which represents 98% of cases.[37] Remaining unusual forms of the colorectal cancer incorporate lymphoma and squamous cell carcinoma.

1.2.6 Prevention

Colon malignancy can be made more preventable, through frequent checkup and healthy improvement in lifestyle.[37]

1.2.6.1 Lifestyle

Current dietary suggestions as a prophylactic measure of colorectal malignancy incorporate expanding the utilization of whole grains, fruits and vegetables, and decreasing the consumption of meat.[38, 39] Though the proof of advantage of fiber and vegetables is inadequate,[39] exercise can reasonably diminish the danger of colon cancer.[40]

1.2.6.2 Medication

Celecoxib and aspirin seems to diminish the danger of colon cancer who are more prone to it,[10] though, it is not suggested in those at normal risk.[41] There is conditional confirmation for calcium supplementation yet it is not adequate to make a proposal.[42, 43] It is observed that the blood concentration and consumption of vitamin D is concerned with a quite a retarded danger of colon malignancy.[42, 43]

1.2.7 Management

The management of colon tumor can be targeted for either complete treatment or palliative care. The selection between these two relies upon different variables, including the individual's wellbeing and preferences, and the phase of developed cancer.[44] removing the tumor tissue by surgery is the prime choice if colorectal tumor is diagnosed in initial stage. Nevertheless, if the cancer is in metastasis phase and hence already spreaded in different organs, then the surgery will no longer be the choice. Such advanced colon tumor can reoccur if removed by surgery, therefore management is then targeted for palliative care only, to ease symptoms brought about by the tumor, to make the individual suffer from pain as less as possible.[15, 45]

1.2.7.1 Surgery

An individual with restricted tumor, removing the tumor with surgery is the usual treatment, for the purpose of a complete cure. Open laparotomy or in some cases laparoscopy is the way to do this. This option of surgically removing the tumor can also be chosen even if the metastasis is established but limited to liver or lung only. Usually before performing a surgery, chemotherapy is utilized to reduce a tumor mass, in advanced to uproot it. Lungs and liver are the two places where there is maximum possibility of the reoccurrence of the colon cancer.[15, 46]

1.2.7.2 Chemotherapy

In colorectal cancer, surgery may or may not be accompanied with a chemotherapy. This choice to include chemotherapy before the surgical removal of the colorectal tumor relies on upon the phase of the malignancy.

Chemotherapy is not given with a surgery in stage I colorectal carcinoma. The part of chemotherapy in Stage II colorectal cancer is far from being obviously true, and is typically not offered unless danger elements, for example, T4 tumor or insufficient lymph node detected. Additionally it is also realized that the patients who is having mutated mismatch repair gene do not profit by chemotherapy. However, for stage III and Stage IV colorectal malignancy, chemotherapy is an indispensable piece of treatment.[15, 47]

In the event that malignancy has spread to the lymph nodes or far off organs, which is the situation with stage III and stage IV colorectal cancer individually, including chemotherapy of oxaliplatin, capecitabine or fluorouracil enhance the probabability of better recovery and well being. If the lymph nodes are not contaminated with colorectal metastasis, the advantages of chemotherapy are disputable. On the off chance that the colorectal cancer is broadly metastatic and hence incurable, palliative care will then be the only choice. In this scenario, various distinctive chemotherapeutic drugs may be employed.[48] Chemotherapy drugs for this condition may incorporate irinotecan, capecitabine, oxaliplatin, fluorouracil and tegafur-uracil.[49] The medications capecitabine and fluorouracil are exchangeable, with capecitabine used through oral route while fluorouracil being used through intravenous route. Bevacizumab, an anti angiogenic agent is frequently included as first line treatment. Cetuximab and

panitumumab are the two another class of medications utilized as a part of the second line therapy which inhibits the receptors of epidermal growth factors.[50, 51]

The essential contrast in the way to deal with low stage rectal tumor is the fuse of radiation treatment. Regularly, it is utilized as a part of conjunction with chemotherapy in a neoadjuvant style to empower surgical resection, so that at last as colostomy is not required. On the other hand, it may not be conceivable in low lying tumors, where, a eternal colostomy often needed.[15, 52]

1.2.7.3 Radiation therapy

Though radiation together with chemotherapy may be helpful for rectal malignancy, its utilization in colon tumor is not normally practiced because of the susceptibility of the colon as well as rectum to radiation.[53] Radiotherapy can also be utilized, as chemotherapy can be, in neoadjuvant and adjuvant setting for a few phases of colorectal tumor.[54]

1.3 Targeted Drug Delivery System

1.3.1 Introduction

Paul Ehrlich has coined this drug delivery system as the *Magic Bullet*. This kind of delivery will not only ensure the site specificity but also mitigate the toxicity of drug to non-target sites.

Targeted drug delivery is considered as a method in which drug-carrier complex, delivers drug to the pre-selected cell in a specific manner.

The drug should reach the target cell(s) with the maximum concentration or with maximum effect. This can be achieved by protecting the drug from the bio-environment en-route to the specific cell.[55]

1.3.2 Different concept of targeting the drug to the target site

Different concepts of targeting the drug molecules to a predefined specific location in body incorporates Active targeting, Passive targeting, Inverse targeting, Physical targeting, Ligand mediated targeting, Dual targeting, Combination targeting and Double targeting, as elaborated following.[55]

1.3.2.1 Passive Targeting

Systemic flow is usually portrayed as passive approach of drug transport. Vectoring of drug at predefined site happens due to the body's common reaction to the physico-chemical qualities of a drug or drug-vector complex. It utilizes the characteristic course of bio-dissemination of the vector, and hence it amasses in the target site. [55]

1.3.2.2 Inverse Targeting

It is utilized to bypass the passive uptake of the colloidal transporters by reticuloendothelial system, which causes the aversion of biodistribution tendency of a carrier; therefore, this concept is regarded as the inverse targeting. This kind of targeting is obtained by injecting large amount of blank colloidal carriers or macromolecules. This leads to the blockade of the RES and due to this impairment of the host defense system takes place. Some other appropriate approach is to modify the vectors, like modifying its surface charge, hydrophilicity, surface rigidity, composition and size of vectors for preferred biofate. [55]

1.3.2.3 Active Targeting

For this kind of targeting modification of the carriers is done to get the required bio-fate.

Active targeting can be further categorized as per following[55]

Organ compartmentalization known as first order targeting

Cellular targeting known as second order targeting

Intracellular targeting known as third order targeting

Organ compartmentalization

Sometimes, dissemination of the drug-carrier complex is very confined to the capillary network of a preferred site, tissue or organ. This sort of vectoring can be feasible in lymphatics, plural hole, peritoneal hole, lungs, cerebral ventricles, joints, eyes, and so forth. High scale liposomes of 10 µm are quickly eliminated by means of automatic filtration of lungs, and scale underneath 150 nm is evacuated by tissue macrophages.[55]

Cellular targeting

Vectoring the drug to a particular cell sort, for example, cancer cells while preventing its delivery to the healthy cells is known as the cellular or second order targeting. [55]

Intracellular targeting

It involves the vectoring the drug to the predefined intracellular regions of the aimed cells. Gene delivery of drug to the nucleolus, Ligand-mediated entry of a drug complex into a cell by endocytosis and lysosomal degradation of carrier followed by the release of drug intracellularly are some of the examples of intracellular targeting. [55]

1.3.2.4 Ligand Mediated Targeting

Ligands possess particular affinity to the drug carrier. Specific uptake mechanism can be helpful in attaining the ligand mediated targeting, for example, receptor mediated uptake of natural low density lipoproteins particles and synthetic lipid microemulsions of apoproteins coated moderately reconstituted LDL particles, where conjugated apoprotein play the role of ligand for LDL receptors expressed in the body. [55]

1.3.2.5 Physical Targeting

Specific drug delivery designed and checked at the outer level with the assistance of physical means is regarded as a physical targeting. Qualities of the bio-environment are utilized either to guide the transporter to a specific area or to bring about particular arrival of its substance. Illustration is that of a temperature touchy liposomes, which were produced and targeted to carcinoma cells, the arrival of the drug from the liposomes in the region of the tumor is brought by the serum segments generally the lipoproteins, causing the liberation of the encapsulated drug when phase transits. [55]

1.3.2.6 Dual Targeting

In dual targeting concept, that type of the drug vectoring agent is selected which is having anticancer activity itself as well besides the drug. In this manner there is a collaborations of an anticancer impact of the entrapped anticancer drug as well as the entrapping carrier.[55]

1.3.2.7 Double Targeting

In double targeting approach, appropriate blend is optimized between control of site and the time of drug release. In the first place, the medication is discharged locally at the predefined destinations and the selectivity is expanded by amplification of the spatial selectivity. Therefore this merging of two concepts together and thus making it twofold, is regarded as double targeting. [55] This concept is illustrated in Figure 1.4

1.3.2.8 Combination Targeting

Combination targeting is designed with transporters, polymers and targeting substance with specific structure that could pave the way of drug to pre-aimed sites. For an example, proteins and peptides can be merged with some polymers, for example, polysaccharides as a way of modifying them, so that its physical attributes can be adjusted and hence can be made suitable for focusing to the particular compartments, organs or their tissues.[55]

1.3.2.9 Folate Targeting

The folic acid vitamin enters the cells through a carrier protein, termed as the reduced folate carrier, or via receptor mediated endocytosis facilitated by the folate receptor (FR). [55]

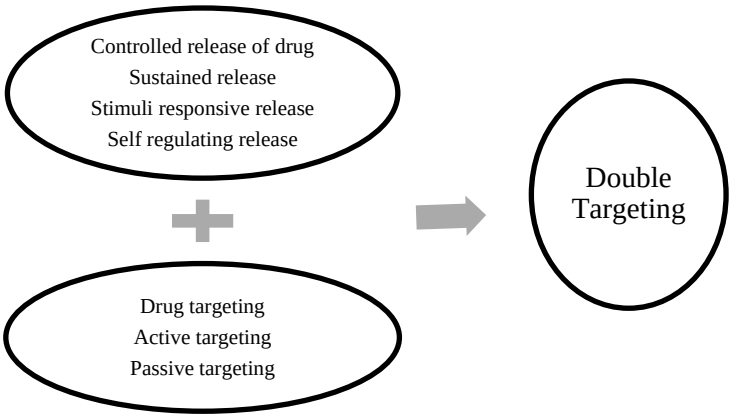

Figure 1.4: Double targeting

1.3.3 Advantages and disadvantages of targeted drug delivery system

Following are the various possible advantages and disadvantages of the targeted drug delivery systems [55]

1.3.3.1 Advantages

Advantages of the targeted drug delivery systems includes Improved therapeutic index, Reduction in dose, Decreased side effect, Decreased toxicity, and Selective treatment of disease

1.3.3.2 Disadvantages

There are also some disadvantages of the targeted drug delivery systems like, Equipment are usually costly, technology itself is still in the development stage, and long-term effect of the targeted drug delivery system is not clear.

1.4 Nanoparticles

Solid particles can be regarded as nanoparticles when their size ranges from 10 to 1000 nm. Nanoparticles comprise of micromolecular resources within which drug is entangled, dispersed, encapsulated, attached or adsorbed.[56, 57]

1.4.1 Nanospheres and Nanocapsules

Nanoparticles can be of two types i.e. Nanospheres and Nanocapsules.

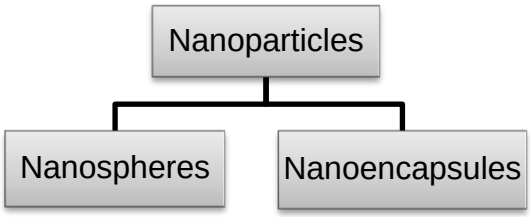

Figure 1.5: Types of nanoparticles

1.4.1.1 Nanospheres

Nanospheres are having a uniform lattice structure within which drug is entangled and scattered.[58]

1.4.1.2 Nanocapsules

In nanocapsules type, drug is encapsulated at the central void of vesicular structure consisting of an internal center encompassed by a polymeric film. For this situation drug is normally in dissolved form in the inward center, yet might likewise be adsorbed to the inner shell surface.[58]

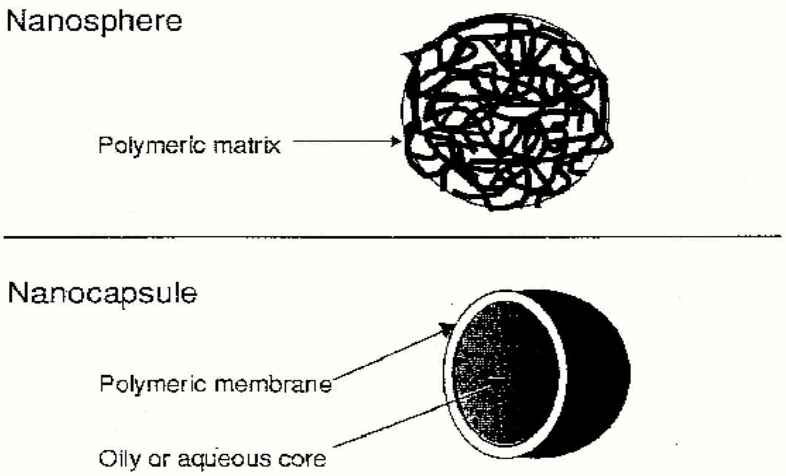

Figure 1.6: Morphology of nanosphere and nanocapsule

1.4.2 The polymers for nanoparticles fabrication

Natural as well as some synthetic polymers are utilized in nanoparticles formulation

1.4.2.1 Natural Hydrophilic Polymers

Some of the frequently used natural hydrophilic polymers are given in Table 1.3[59]

Table 1.3: Natural Hydrophilic Polymers

Proteins	Polysaccharides
Gelatin	Alginate
Albumin	Dextran
Lectins	Chitosan
Legumin	Agarsoe
Viciline	Pullulan

1.4.2.2 Synthetic Hydrophobic Polymer

Synthetic polymer used in drug targeting are either pre-polymerized or polymerized in process. Some of the frequently used synthetic hydrophobic polymers are given in Table 1.4[59]

Table 1.4: Synthetic Hydrophilic Polymers

Pre-polymerized	Polymerized in process
Poly (ε - caprolactone)	Poly(isobutylcynoacrylates)
Poly (lactic acid)	Poly (butylcynoacrylates)
Poly(lactide-co-glycolide)	Polyhexylcyanoacrylates
Polystyrene	Poly (methacrylate)

1.4.3 Methods for Preparation of Nanoparticles

1.4.3.1 Cross-linkage of Amphiphilic Macromolecules

Amphiphilic macromolecules, poly-saccharides and proteins can be utilized in nano-particles formulation. Formulation is usually conducted in two steps initially; the ac-cumulation of amphiphiles took after by stabilization, by either chemical cross-linking or heat denaturation. This process may occur in biphasic o/w or w/o type dispersed

system. The high temperature used in the original method restricts the application of method to heat sensitive drugs. As an alternative to heat stabilization method a chemical cross linking agent, usually gultaraldehyde, is incorporated in to the system. Though the heat borne drawbacks are obviated, yet a need to remove residual cross-linking agent makes the method cumbersome.[60]

1.4.3.2 Solvent Evaporation

By precise RPM, solvent evaporation technique can produce a particles ranging from few nanometers to micrometers with good percentage entrapment of the hydrophobic drug. Initially the polymer and the drug is dissolved in an organic solvent and then after in aqueous solution, the resultant drug-polymer solution is emulsified using suitable stabilizer. Size of the globules can be reduced by elevated sheer stress, aqueous suspension of nanoparticles is obtained by evaporating the organic layer under vaccum, followed by the separation of nanoparticles, and then lyophilizer dries particles.[59]

1.4.3.3 Double Emulsion

Solvent evaporation method can be used when the drug is hyphilic, so formulation of nanoparticles involving a hydrophilic drug, an alternative method of solvent evaporation was established known as double emulsion method in order to get better percentage entrapment. In this method, prepared nanoparticles are separated from the suspension form by vigorous centrifugation and freeze-drying. As this method involves the dissolving the drug in aqueous phase, this method is considered as suitable one for porteinous molecules as they are soluble more in aqueous solvent. For an example bovine serum albumin was successfully entrapped into a nanoparticle prepared using Poly (lactide-co-glycolide). Initially bovine serum albumin (a protein in nature) is dissolved in aqueous solvent and PLGA was dissolved in organic solvent using a Sonicator and then both solution were mixed together to get a w/o emulsion. Then after this emulsion was transferred to the aqueous polyvinyl alcohol solution to obtain a double emulsion. Then, organic phase was evaporated by stirring at lower pressure to get nanoparticles.[59]

1.4.3.4 Emulsion-Diffusion-Evaporation

This technique uses both diffusion as well as evaporation together in nanoparticles formulation. First, while continuous stirring organic solution of a polymer is trans-

ferred into aqueous solvent to produce an emulsion. Suitable emulsifying agent is used which are adsorbed at the interface of the emulsion. Droplet size of the internal phase is narrowed by using Sonicator. Then after water is added to this emulsion which makes the emulsion unstable and shift the organic phase to aqueous phase. This transition creates the super saturation at interface leading to the precipitation of the particles of nano range. During the precipitation, organic layer is evaporated by heating at 40^{o}C.[59, 60]

1.4.3.5 Dispersion Polymerization

Ionic gelation

In this method, chitosan is dissolved in an aqueous acidic solution to obtain the cation of chitosan. This solution is then added drop wise under constant stirring to a poly anionic tripolyphosphate (TPP) solution. Due to complexation between oppositely charged species, chitosan undergoes ionic gelation and precipitates to form spherical particles. Solution, then aggregation and then followed by opalescent suspension happens in sequence after which chitosan-TPP nanoparticles are produced which are separated later on by using centrifugation at 12000 rpm and then particles are dried by lyophilization.[59]

Emulsion cross-linkage technique

In this strategy, first the chitosan solution prepared in aqueous solvent is emulsified in organic solvent to produce the w/o emulsion using appropriate emulsifying agent. Globules are made rigid by adding cross linkers and then produced particles are separated by filtration followed by washing for few times. Here, size of the particles produced by this method depends upon two parameters, first, size of the hardened globules and the RPM. The downside of this technique includes time consuming procedure and additionally utilization of cross-linkers, which may perhaps actuate interaction with drug; on the other hand, complete evacuation of un-responded cross-linkers may be troublesome in this procedure.[60]

Interfacial polymerization

The preformed polymer phase is transformed to an embryonic sheath. A polymer that eventually become core of nanoparticles and drug molecule to be loaded are dissolved in a volatile solvent. The solution is poured in to a non solvent for both polymer and core phase. The polymer phase is separated as a coacervate phase at o/w interface.[59]

Interfacial complexation

The method is based on the process of microencapsulation introduced by Lin and Sun, 1969. In case of nanoparticles preparation, aqueous polyelectrolyte solution is carefully dissolved in reverse micelles in an apolar bulk phase with the help of an appropriate surfactant. Subsequently competing polyelectrolyte is added to the bulk, which allows a layer of insoluble polyelectrolyte complex to coacervate at the interface.[61]

1.4.3.6 Polymer Precipitation Methods

Spray-drying

In spray-drying method, initially chitosan solution is prepared using acetic acid; and then drug is dissolved in chitosan solution. Then after, cross-linker is added to the final solution; which is then passed through the very fine nozzle as an atomized hot air torrent. This ultrafine spraying cause the formation of micro sized globules. During the same atomization, solvent fade away and leads to development of fine and dried particles. Various factors like force at atomization, stream rate of spraying, nozzle size, cross-linking intensity and temperature of inlet air governs the particle size.[59, 60]

Salting-out method

In salting out method, polymer is dissolved in acetone as it is an organic solvent and miscible with water plus also due to its pharmaceutical acknowledgment with respect to lethality. The technique uses salt saturated water as a solvent to prepare a solution of polyvinyl alcohol and then this aqueous phase is mix with the acetone. In spite of the fact that acetone is miscible with water in all proportions, the high salt concentration avoids the miscibility of both phase. Then after both phase is emulsified using suitable emulsifying agent. After emulsification, pure water is added to the emulsion in specific amount, thus bringing about the nanoparticles building up because of the shifting of acetone in water phase.[60, 61]

Solvent Displacement/ Nanoprecipitation

In this strategy polymer solution, solution of lipophilic surfactant and drug solution are mixed together in a water miscible solvent and afterward under stirring; it is transferred to the solvent that contains the dissolved stabilizer. This results in the nanoparticles development because of a quick diffusion of solvent. Hydrophilic drugs are having a little interaction with the polymer in this method as compared to the lipophilic

drug, hence lipophilic drug can give more entrapment, while in case of hydrophilic, drug shift from polymer solution to continuous phase. Many authors have reported the usefulness of this method in different aspect, for example, PLGA nanoparticles of proteins and peptides were produced and it was reported to have a quite better bioavailability of proteins and peptides by this method.[55, 60, 61]

1.4.4 Characterization of Nanoparticles

There are many parameters which must be evaluated in order to characterize the prepared nanoparticles, as mentioned in Table 1.5 [62]

Table 1.5: Characterization of Nanoparticles

Characteristics	Evaluation techniques
Molecular Weight	Gel permeation chromatography
Particle size	Coulter counter Photon correlation spectroscopy Scanning electron microscopy Transmission electron microscopy
Crystal nature	Differential Scanning Calorimetry X-ray diffraction DTA
Density	Helium compression pyncnometry
Lipophilicity	Contact angle measurement Hydrophobic interaction chromatography
Electrical charge	Electrophoresis Amplitude-weighted phase structure determination Laser Doppler anemometry
Surface element analysis	X-ray photoelectron spectroscopy
Surface properties	Static secondary-ion mass spectrometry

1.4.5 Advantages of nanoparticles

Advantages provided by nanoparticles over other conventional formulations includes targeted delivery of the drug, Protection of drug from degradation, Decrease of undesired side effects, Improvement in the bioavailability of the drug, more stability, improved patient compliance.[62]

1.4.6 Pharmaceutical aspects of Nanoparticles

Despite such advantages, some factors about nanoparticle should also be in consideration, like, it should be free from potential toxic impurities**,** it should be easy to store and administer nanoparticles, and it should also be sterile if parenteral use is advocated.[63]

1.5 Cell line

1.5.1 Introduction

A cell line is a populace of cells from an evolved organism that would regularly not multiply uncertainly but rather, because of genetic transformation, have avoided ordinary cell proliferation and rather can continue experiencing vigorous division. The cells in this manner can be developed for extended time *in-vitro*. The genetic transformations needed for making the cells undying can happen normally or be purposefully actuated for exploratory purposes. Undying cell lines are an essential part for exploration into the natural chemistry and cell science of evolved organisms. Cell lines have likewise discovered uses in biotechnology.[64]

Stem cells ought not to be mistaken for cell lines, as stem cells can likewise partition uncertainly, yet frame an ordinary part of the advancement of a multicellular living being.

1.5.2 Relation to natural biology and pathology

Many different undying cell lines are available, some of them are ordinary cell lines means cell lines those are developed from stem cells. Other cell lines are derived from the cancerous cells, known as cancer cell line. Somatic cell that typically cannot split, but because of some mutation, loose the control of the ordinary cell cycle, prompting unrestrained multiplication – this is how cancer develops. Cell lines have experienced comparative genetic transformations (mutations) permitting a cell sort that would regularly not have the capacity to be multiplied *in-vitro*. The birthplaces of some unfading cell lines, for instance MCF-7 human cells, are from actually happening tumors.[65]

1.5.3 Role and uses

Cell lines are generally utilized as a straightforward model for more complicated biological systems, for instance, an investigation of biochemistry and cell science of mammalian cells. The vital benefit of utilizing an unfading cell line for exploration is its everlasting existence; the cells can be developed for indefinite times in artificial nutritional media. This improves investigation of the science of cells that might some way or another have a restricted lifetime.[66]

Cell lines can likewise be cloned as well, offering ascent to a clonal masses that can, therefore, be grown unlimited number of times. This permits an investigation to be rehashed ordinarily on genetically indistinguishable cells that is required for replicable exploratory research. On the other hand, conducting an investigation on normal cells from multiple tissue donors does not have this favorable position.[66]

Cell lines poses numerous scopes in biotechnology where they are a financially savvy method for developing cells like those found in a evolved living being *in-vitro*. The cells are utilized for a wide mixed bag of objectives, from testing harmfulness of new drugs to rDNA based synthesis of protein products of eukaryotic origin.[66]

1.5.4 Limitations

As cell lines frequently start from a natural cells or tissue which have experienced genetical changes to end up becoming an immortal, this phenomena can modify the cell-biology and therefore must be thought seriously about, in any investigation.[66]

1.5.5 Methods for generating cell lines

There are many different approach for creating cell lines:[67]

1. Isolation of cancer cells from a naturally happening malignancy. This is the first strategy for establishing a cell line. Major illustrations incorporate human MCF-7 cells, derived from a breast cancer.
2. Spontaneous or provoked arbitrary mutations to make some of the cells immortal, and then separating the cells that have the capacity to undergo division in uncontrolled manner
3. Injecting a viral gene e.g. the adenovirus E1 that deregulates the cell cycle, same viral gene was utilized to mutate and produce the HEK 293 cell line.
4. Artificially forcing the expression of some vital proteins needed, for instance telomerase that inhibits degradation of chromosome closures in the course of DNA replication in eukaryotes
5. Hybridoma technique, very popular and frequently used for the production of monoclonal antibodies synthesizing B-lymphocyte cell lines, which is produced by blending them with a myeloma cells.

1.5.6 Examples of cell lines

There are a numerous cell lines available for diverse research purpose, each with diverse characteristics. The cell sort they were derived from or are most similar in nature usually categorizes cell line. [69]

1. HT-29 cells – Cell line derived from colon cancer of human origin
2. MCF-7 cells – Cell line derived from breast cancer of human origin
3. HeLa cells – a greatly widely explored human cell line derived from a cervical cancer, most likely from epithelial cells
4. Vero cells – a non-cancerous normal cell line derived from the African green monkey's kidney cells
5. HEK 293 cells – developed from prematurely ended human fetal cells and mutation causing virus
6. A549 cells – developed from the tumor of a malignant patient
7. 3T3 – Cell line derived from a mouse fibroblast developed by a natural mutation in cultured mouse embryo tissue
8. Jurkat – a human cell line isolated from a leukemia patient of T lymphocyte lineage
9. F11 Cells - a rat neuronal cell line derived from the dorsal root ganglia

1.5.7 HT-29 cell line

HT-29 is a adenocarcinoma cell line derived from colorectal cancer of human origin. HT-29 cell extensively express the folate receptors, which can be target by the folate conjugated nanoparticulate drug delivery system.[68]

5-fluorouracil, capecitabine and oxaliplatin, are the standard drugs of choice for the treatment of colorectal cancer. HT-29 cell line was derived from middle aged Caucasian lady with colorectal adenocarcinoma in 1964.[69]

Besides the use of a HT-29 cell line as a xenograft tumor model intended for colorectal adenocarcinoma, it is likewise utilized to study absorption, transport, and discharge by colorectal cells as an *in-vitro* model. Under standard culture conditions, these cells grow as a nonpolarized, undifferentiated multilayer. Altering culture conditions or treating the cells with various inducers, however, results in a differentiated and polarized morphology, characterized by the redistribution of membrane antigens and development of an apical brush-border membrane.[70]

1.5.8 MCF-7 cell line

MCF-7 is a breast cancer cell line isolated in 1970 from a 69-year-old Caucasian woman. MCF-7 cells do not express folate receptors extensively. MCF-7 stands for Michigan Cancer Foundation-7, an institute in Detroit at where the cell line was developed by Herbert Soule and co-workers in 1973.[71] Institute is now renamed as the Barbara Ann Karmanos Cancer Institute.

Before the discovery of MCF-7 cell line, it was impractical for cancer scientists to get a mammary cells that was equipped to stay alive for couple of months.[72] Frances Mallon passed away in 1970, a breast cancer patient, whose cells were wellspring of quite a bit of current information about breast cancer.[73, 74] She was working as a nun in the convent of Immaculate Heart of Mary in Monroe, Michigan as Sister Catherine Frances when a breast cancer cells were isolated from her cancer.

MCF-7 , T-47D and MDA-MB-231 are the three breast cancer cell line that occupies more than 65% of all research literatures specifying the breast cancer cell lines.[75, 76]

1.5.9 Vero cell line

Vero cell line is non-cancerous normal cell line derived from the, Chlorocebus species, African green monkey's kidney cells. Yasumura and Kawakita established the lineage at the Chiba University in Chiba, Japan on 27 March 1962. The first cell line was named "Vero" after a condensing of "verda reno", which signifies "green kidney" in Esperanto, additionally Vero itself signifies "truth" in Esperanto.[77]

Vero cells are utilized for different reasons, as given below:[78]

1. Detecting *E. coli* toxin, which was initially regarded as "Vero toxin" after vero cell line, and later called "Shiga-like toxin" because of its likeness to Shiga toxin detached from Shigella dysenteriae
2. Vero cells also used as a host environment for the cultivation of virus; for instance, to determine whether the replication is occurring or not in the presence of a investigational drug
3. Vero cells are also used as a host cell for eukaryotic parasites, extraordinarily of the trypanosomatids

2. RATIONALE AND OBJECTIVE

2.1 Rationale of research work

Currently there are many drugs with different dosage forms are available in the market for the chemotherapy of cancer, but the prime concern about the anticancer drug is their potent side effects. This problem with anticancer drugs is because of the unfortunate fact that they do not only affect the cancerous cells but also affects the normal cells, which in turn responsible for their side effects. This happens due to non-specific targeting to cancerous cells and hence other normal cells get affected.

To overcome of this problem, Targeting of drugs specifically to the cancerous tissue is an important approach. There are many different newer formulation are being exploited now a days to address this problem, amongst which, nanoparticles conjugated with some targeting moiety have been getting much attention for effective cancer targeting.

Folate receptors (FRs) are over expressed on epithelial cancers of the ovary, mammary gland, colon, lung, prostate, nose, throat, and brain. FRs are also over expressed on malignant tumors, combining with glycosyl phosphatidylinositol (GPI) as a membrane glycoprotein situated at the surface of cancer cells. FRs exhibit limited expression on healthy cells but are often present in large numbers on cancer cells.

Thus, FRs represents an important target for tumor-specific delivery of anticancer drugs. Therefore, controlling the attachment of the ligand, folic acid (FA), chitosan nanoparticles constitutes an important step for FR-mediated targeted delivery of chitosan nanoparticles for anticancer drugs.

Therefore folic acid conjugated chitosan nanoparticles were envisioned to target the capecitabine drug to the colon cancer. The CS-NPs also help to provide sustained release, decrease the dose and frequency of dosing, reduce side effects of cancer treatments.

2.2 Objective

The main objective of this research work was:

To prepare and optimize capecitabine loaded folic acid conjugated chitosan nanoparticles to target the drug delivery to colon- cancer cells to reduce the side effects of the capecitabine

3. REVIEW OF LITERATURE

Agnihotri SA et al. have prepared the capecitabine-loaded semi-interpenetrating network hydrogel microspheres of chitosan-poly(ethylene oxide-*g*-acrylamide) by emulsion crosslinking using glutaraldehyde. Poly(ethylene oxide) was grafted with polyacrylamide by free radical polymerization using ceric ammonium nitrate as a redox initiator. Capecitabine, an anticancer drug, was successfully loaded into microspheres by changing experimental variables such as grafting ratio of the graft copolymer, ratio of the graft copolymer to chitosan, amount of crosslinking agent and percentage of drug loading in order to optimize process variables on drug encapsulation efficiency, release rates, size and morphology of the microspheres. [79]

Cassidy J et al. have analyzed two different capecitabine tablet formulation and compared the bioequivalence for investigating the impact of various parameters on bioavailability of capecitabine and its metabolites. Studied parameters were surface area of body, sex, age and elimination of creatinine. They have found that these factors was not having any noteworthy impact on the pharmacokinetics of capecitabine or its metabolites.[80]

Cassidy J et al. have assessed the security profile of capecitabine utilizing information from an expansive, all around portrayed populace of patients with metastatic colorectal malignancy treated in two stage III studies. They have observed that the Capecitabine showed a less toxicity as compared to 5-fluorouracil and leucovorin, with notably fewer cases of the inflamed mouth mucus, loose motion, nausea, hair loss and reduced neutrophil counts which ultimately cause the less incidents of neutropenic fever/sepsis and hospital admissions.[81]

Weitman SD et al. have studied some epithelial cells *in-vitro*, that a membrane-bound folate receptor initiates the process for cell accumulation of 5-methyltetrahydrofolic acid. This receptor was found to be GP38, an overexpressed, glycosyl-phosphatidylinositol anchored glycoprotein, recognized by two monoclonal antibodies, designated MOv18 and MOv19. Choroid plexus consistently had the largest amount of folate receptor. Other tissues containing substantial amounts of receptor included lung, thyroid, and kidney. The liver, intestines, muscle, cerebellum, cerebrum, and spinal cord were immunologically nonreactive. It was also also demon-

strate that 4 of 6 brain tumors overexpress the folate receptor. These reveal the limited normal tissue distribution of the folate receptor, a cell surface protein that may be a useful immunological or pharmacological target for the development of selective cancer therapy.[82]

Zhenqing H et al. have designed the chitosan nanoparticles and then conjugated them with two ligand i.e. folic acid and methoxy polyethylene glycol, in order to deliver the anticancer drug in extended manner specifically to the malignant cells only. First they have developed the chitosan nanoparticles through the merged principles of two method chemical cross-linking and ionic gelation, and then they have conjugated the nanoparticles first with folic acid and then with methoxy polyethylene glycol. It was observed that expanded measures of nanoparticles conjugated with only folic acid or both ligand were amassed within malignant cells as compared to the non conjugated nanoparticles or those nanoparticles which was conjugated with only methoxy polyethylene glycol. These outcomes recommend that either of the ligand is important for conjugation for significantly delayed drug release as well as drug targeting to malignant cells only.[83]

Yang SJ et al have prepared a folic acid conjugated chitosan nanoparticle as a suitable vehicle for carrying 5-aminolaevulinic acid (5-ALA) to enhance the detection of colorectal cancer cells *in-vivo* after a short-term uptake period. Chitosan can be successfully conjugated with folic acid to produce folic acid−chitosan conjugate, which is then loaded with 5-ALA to create nanoparticles (fCNA). They have demonstrated that fCNA can be taken up more easily by HT29 and Caco-2 cell lines after short-term uptake period, most likely via receptor-mediated endocytosis, and the PpIX accumulates in cancer cells as a function of the folate receptor expression and the folic acid modification. Therefore, the folic acid−chitosan conjugate appears to be an ideal vector for colorectal-specific delivery of 5-ALA for fluorescent endoscopic detection.[84]

Yang SJ et al. have encapsulated indigo carmine into chitosan nanoparticles (CNIC) by the ionic gelation to increase the retention time on intestine surface, and conjugated folic acid with chitosan nanoparticles (fCNIC) to target specifically adenomatous polyps. They have shown that the folic acid conjugation could serve as an ideal vector for a colon-specific targeting system. According to this concept, they have designed a

novel detection system to enhance the accuracy of endoscopic diagnosis for colorectal cancer.[84]

Sahu SK et al. have prepared a doxorubicin nanoparticles by using carboxymethyl chitosan. They have chemically linked the prepared nanoparticle with the bifunctional 2,2′-(ethylenedioxy)-*bis*-(ethylamine) by first conjugating nanoparticles with folic acid. They have shown that the nanoparticle can efficiently deliver the drug specifically to the cancer tissue. Based on the outcome they have concluded that the folic acid-driven cancer targeting drastically enhances the selective internalization of the NPs by cancer cells and hence force the malignant cells to the die.[85]

Li P et al. have prepared the chitosan nanoparticles conjugated with folic acid, thereby creating more promising nanoparticles because the basic functions of chitosan nanoparticles are preserved and additionally folic acid have provided the cancer targeting feature. They have studied the selective internalization of the folic acid conjugated nanoparticles using fluorescent microscopy by employing HT-29 cells, a colon cancer cell line. Based on the outcome they have concluded that the folic acid-driven cancer targeting drastically enhances the selective internalization of the NPs by cancer cells and hence force the malignant cells to the die.[86]

Dube D et al. have prepared folate conjugates (PNIPAM-NH−FA) of a copolymer of *N*-isopropylacrylamide (NIPAM) and amino-*N*‘-ethylenedioxy-bis(ethylacrylamide) by an efficient synthesis leading to random grafting, via a short dioxyethylene spacer, of ∼7 folic acid residues per macromolecule. The cellular uptake of the copolymer was found to be temperature dependent and was competitively decreased by free folic acid, indicating that the polymer uptake is mediated specifically by the folate receptor.[87]

Wu K et al. have assessed the effect of folic acid supplementation on recurrent colorectal adenoma. Their results do not support an overall protective effect of folic acid supplementation on adenoma recurrence. Folic acid supplementation may be beneficial among those with lower folate concentrations at baseline.[88]

Li Q et al. have prepared the nanoparticles of 10-hydroxycamptothecin to vector the drug to malignant tissue. Initially they have done the micronization of the drug, and then human serum albumin was conjugated with folic acid. Finally, they have pre-

pared the 10-hydroxycamptothecinloaded folic acid conjugated human serum albumin nanoparticles using merged principles of NP-coated method and desolvation technique. They have observed that the prepared folic acid linked nanoparticles exhibits much more efficiency in internalizing the drug in SGC7901 cells than non-linked nanoparticles. From this outcome, they concluded that both the method used in combination is efficient for nanoparticle fabrication specifically for poorly water soluble drug. finally they have concluded their work with the outcome that the prepared nanoparticles serves as a efficient drug transporters for vectoring the drug within the malignant tissue.[89]

Yong-Zhong D et al. have developed, by employing a 1-ethyl-3-(3-dimethylaminopropyl) carbodiimide-coupling reaction, stearic acid embedded chitosan micelles conjugated with folic acid, aimed for a gene delivery within a predetermined cells through receptors attribution. Micelle/pDNA composite structure produce when micelles interact with the plasmid DNA, as chitosan carries the positive charge and DNA possess the negative charges. They have observed the enhanced delivery of micelle/pDNA composite within the folate receptors bearing celss, so they conclude that this plasmid DNA delivery efficiency was happening through the endocytosis process accompanied by folate receptor of the concerned cells.[90]

Wang F et al. have prepared a new biocompatiable PTX loaded folic acid conjugated deoxycholic acid-o-carboxymethylated chitosan micelles. It was observed that expanded measures of chitosan micelles conjugated with folic acid were highly amassed within malignant cells as compared to the non conjugated micelles. These outcomes recommend that folic acid mediated drug delivery can significantly target malignant cells.[91]

Zu Y et al. have developed the chitosan nanoparticles loaded with Oligomycin-A and conjugated with folic acid to vector the anticancer drug to the leukemia to solve the issues of drug delivery to healthy cells and the drug's lipophilicity. The prepared nanoparticles have shown the satisfactory extension in the release profile of the drug. They have concluded that FA-Oli-CSNPs can serve as essential drug transporter to vector the drug leukemia cells.[92]

Reddy JA et al. have reviewed that trans-membrane folate receptor (FR) is overpopulated on an extensive variety of human carcinomas, for example, those starting in ovary, bosom, endometrium, lung, cerebrum and kidney. Folic acid is a high fondness ligand of the folate receptors that holds its receptor tying properties when linked to other substances. Hence, folic acid mediated innovation has effectively been employed for the conveyance of radio-imaging and therapeutic drugs, protein toxins, MRI contrast agents, gene transfer vectors, liposomes, antisense oligonucleotides, and immunotherapeutic drugs and ribozymes to folate receptors expressing tumors. These folate-conjugated formulations have delivered significant improvements in vectoring the drug within malignant cell over their non-folate version. Henceforth, it is confident that this cancer specific vectoring will prompt upgrades in the wellbeing and adequacy of concerned anti neoplastic drugs. In this manner, the center of this review was to highlight the present status of folate-mediated innovation with specific accentuation on the late advances in this area and also conceivable way of upcoming advancement.[93]

Pirollo KF et al. have reviewed that incorporation of a tumor-focusing drugs in nanoparticulate drug delivery can builds its *in-vivo* performance. On the other hand, the pharmacokinetics and biodistribution of such nanoparticles is not clearly understood. A few latest articles suggest that tumor-focusing ligands work essentially to increment intracellular uptake of the nanoparticles and don't impact amassing at tumor tissue. Then again, different reports show that they do assume a part in the amassing in the cancer cells. One distinction may be the vicinity or lack of poly-[ethylene glycol] (PEG) in the nanoparticles and its effect on the upgraded penetration and maintenance impact. Further studies are obviously expected completely clarify the impact of carriers on tumor-focusing, systemic conveyance of nanoparticles.[94]

Sonvico F et al. have reviewed that, in the most recent years folate mediated drug delivery has risen as a standout amongst the most encouraging methodology in particular tumor targeting the drugs. Regardless of this developing scenario, a portion of the cell models routinely utilized to explore folate-mediated drug formulation need exact portrayal. Besides, in view of the variability of the folate receptor expression *in-vivo*, it ought to be imperative to assess the bearers in a circumstance of expanding expression levels. The point of this concern is to display an *in vitro* model, comprising of

three diverse cell lines HeLa, MCF7 and KB 3-1 cells, in which the conditions prompting a strong and steady over-population of the folate receptor have been resolved and the amount of receptor present at the surface of the cells evaluated. The chsosen cell lines express different measures of the protein, from a non-noticeable level in MCF7 cell to an abnormal state of over-expression rate in KB cells, bringing about an intriguing scope of conditions helpful for the examination of folate-mediated carriers.[95]

Yonghua Z et al. have examined that cell film related folate receptors are discretely overpopulated in certain human tumors. The high liking of folic acid for folate receptors gives a special chance to utilize folic acid as a carrier to convey anticancer agents to malignant cells. They have prepared folate-grafted liposomes bearing pteroyl-γ-glutamate-cysteine-polyethylene glycol (PEG)- distearoyl phosphatidyl ethanolamine (DSPE) for vectoring the drugs and also genes to tumor cells that shows the over expression of folate receptors. Calcein or doxorubicin loaded folate-grafted liposomes were developed by altered method to increase yield, using pteroyl-γ-glutamate-cysteine-PEG-DSPE as vectoring unit together with non-targeted liposomes with PEG-DSPE. Outcome of a calcein uptake and doxorubicin cytotoxicity in human colon cancer Caco-2 cells and human cervical cancer HeLa-IU_1 cells shown that folate-grafted liposomes were more effective in tumor specific drug delivery which is showing a more folate receptor expression.[96]

Hilgenbrink AR et al. have surveyed that, Folate mediated drug targeting has developed as an new approach for the therapy and imaging of numerous carcinomas and inflammatory disorders. Because of its little sub-atomic size and high tying partiality for cell surface folate receptors (FR), folate conjugates can convey a mixed bag of small molecules to pathologic cells without bringing about damage to ordinary tissues. Compounds that have been effectively conveyed to folate receptors displaying cells, to date, include nanoparticles, immune stimulants, protein toxins, chemotherapeutic agents, imaging agents and liposomes. They have compiled the utilizations of folic acid as a cancer-targeting vector and highlight the different strategies being created for conveyance of anticancer drugs and imaging agents to folate receptors displaying cells.[97]

Turek JJ et al. have demonstrated that proteins conjugated to folic acid may get internalized in cells by means of endocytosis once they tie to trans-membrane folate receptors. They have prepared bovine serum albumin-colloidal gold conjugated with folic acid and studied its uptake using KB cells to determine its intracellular accumulation. From the result they have conclude that the folic acid have specific role in delivering and then internalizing drug in folate receptors positive cancer tissue.[98]

Yingjuan L et al. have explored that, the folate receptor represents a valuable focus for tumor-particular drug targeting, essentially on the grounds of three things. First, folate receptors are overexpressed in different human malignancy, for examples cancer of the ovary, kidney, brain, bosom, lung and myeloid cells; second, folate receptor in healthy tissues are expressed at extremely lower rate and third, folate receptor expression seems to increment as the stage of carcinoma advances. Subsequently, tumors that are most hard to treat by traditional routines may be most effectively focused with folate-connected therapeutics. Folate-intervened macromolecular vectoring *in-vivo* has, be that as it may, yielded just blended results, to a great extent in light of issues with macromolecule entrance of carcinomas. Nevertheless, noticeable illustrations do exist where folate mediated approach has altogether enhanced the result of a macromolecule-based treatment, prompting complete cure of rigid tumors in numerous cases.[99]

Lee RJ et al. have developed targeted delivery of drugs to folate receptor-positive tumor cells by coupling to high affinity ligands, folic acid. Then they found that the small size, convenient availability, simple conjugation chemistry, and presumed lack of immunogenicity of folic acid make it an ideal ligands for targeted delivery to tumors.[100]

Zhang L et al. have formulated the bovine serum albumin nanoparticles (BSANPs) by a coacervation method and chemical cross-linking with glutaraldehyde. Furthermore, the BSANPs were reacted with the activated folic acid to conjugate folate via amino groups of the BSANPs, to improve their intracellular uptake to target cells. The levels of folate-conjugated BSANPs were higher than those of BSANPs and saturable. The association of folate-conjugated BSANPs to SKOV3 cells was inhibited by an excess amount of folic acid, suggesting that the binding and/or uptake were mediated by the folate receptor. Then he implied that the folate-conjugated BSANPs might be

useful as a drug carrier system to deliver drugs into the cells expressing folate receptor.[101]

Mumper RJ et al. have formulated folic acid conjugated nanoparticles by using Emulsifying wax and polyoxyl-2-stearyl ether (Brij 72) which containing high concentrations of gadolinium hexanedione (GdH) (0- 3 mg) have been engineered from oil-in-water micro emulsion templates. Then they found that GdH entrapment and cell uptake were optimized and suggested that engineered folate -coated nanoparticles may serve as effective carrier systems for Gd-NCT of tumors.[102]

Low PS et al have reviewed that folic acid displays multiple desirable characteristics for use in the targeting of cytotoxic drugs and imaging agents to cancer tissue. The use of folate and hope fully many additional targeting ligands yet to be discovered, the prospect of therapy without toxicity.[103]

Chen QI et al has developed bifunctional NPs (BF-NPs), which were based on PLGA–PEG and modified with folic acid and cell penetrating peptide R7 simultaneously. BF-NPs loaded with vincristine sulfate (VCR) were prepared via the water–oil–water emulsion solvent evaporation method. The studies also revealed that BF-NPs were more potent than those of the NPs merely modified by folic acid. The results demonstrated that BF-NPs could be a potential vehicle for delivering chemotherapeutic agents such as VCR and breast cancer therapy.[104]

Li P et al. have summarized drug delivery using nanoparticles (NPs) as carriers for small and large molecules. Targeting delivery of drugs to the diseased lesions is one of the most important aspects of drug delivery system. They have been used *in-vivo* to protect the drug entity in the systemic circulation, restrict access of the drug to the chosen sites and to deliver the drug at a controlled and sustained rate to the site of action. Various polymers have been used in the formulation of nanoparticles for drug delivery research to increase therapeutic benefit, while minimizing side effects. They have summarised the most outstanding contributions in the field of protein nanoparticles used as drug delivery systems. Methods of preparation of protein nanoparticles, characterization, drug loading, release and their applications in delivery of drug molecules and therapeutic genes are considered.[105]

Nesalin AJ et al. had formulated flutamide nanoparticles, a substituted anilide, is a potent anti-androgenic used in the treatment of prostate carcinoma having short biological half-life of 5-6 hrs which is good for the formulation of sustained release dosage form. The nanoparticles of Flutamide were formulated using chitosan polymer by ionic gelation technique. From the drug release studies it was observed that nanoparticles prepared with chitosan in the core: coat ratio 1:4 gives better sustained release for about 12 hrs as compared to other formulations.[106]

Bennett A et al have summarized targeted drug therapy or ‘‘smart’’ drug delivery, potentially combined with simultaneous imaging modalities to monitor the delivery of drugs to specific tissues. The potential to deliver active chemotherapeutic drugs in the vicinity or directly within specific tumors via receptor-mediated pathways, and to image tumors with nanoparticles has been conceptually and experimentally shown for several classes of nanoparticles. Nanoparticles functionalized with the vitamin folic acid are of particular interest, as varieties of malignant tumors are known to overexpress the folate receptor. They have summarized several nanoparticle architectures with improved retention time, administration route; biocompatibility, absorption, and clearance are being proposed and are in late stage clinical development. Their review highlights some of the most important concepts related to nanoparticles and folate-mediated drug delivery and imaging in cancer research.[107]

Li J et al have prepared a magnetic iron oxide nanoparticles conjugated with folic acid to detect the cancer *in-vivo* using magnetic resonance imaging. They have turned out with the outcomes that the folic acid conjugated magnetic iron oxide nanoparticles can be utilized as an effective nano-scale probe for magnetic resonance imaging of malignant cells *in-vitro* and a xenografted tumor model *in-vivo* by means of a dynamic folic acid mediated pathway.[108]

Mumper RJ et al have studied the cell uptake, biodistribution and tumor retention of folate-coated and PEG-coated gadolinium (Gd) nanoparticles. Gd is a potential agent for neutron capture therapy (NCT) of tumors. They have found that both folate-coated and PEG-coated nanoparticles had comparable tumor accumulation. However, the cell uptake and tumor retention of folate-coated nanoparticles was significantly enhanced over PEG-coated nanoparticles. Thus, the benefits of folate ligand coating were to facilitate tumor cell internalization and retention of Gd-nanoparticles in the tumor tis-

sue. They have concluded that engineered nanoparticles may have potential in tumor-targeted delivery of Gd thereby enhancing the therapeutic success of NCT.[109]

Ma Y et al have studied the biodistribution profile of the PLGA nanoparticles with dual surface modifications of PEG and folic acid (FA) in mice xenografted with MDA-MB-231 human breast cancer cells with high expression of folate receptor (FR); and to illustrate that the modified nanoparticles can target the loaded indocyanine green (ICG) to the tumor with high FR expression. They have found that ICG concentration in plasma from the DM-NP group was significantly higher than the NM-NP group. Therefore they have Concluded that the accumulation of DM-NP into the tumor was significantly higher than NM-NP due to the long circulation and FR-mediated uptake.[110]

Du Z et al have synthesized and characterised folate-poly(ethylene glycol) and poly(-benzyl l-glutamate) diblock copolymer (FEG) and than used it for the preparation of Paclitaxel (PTX)-loaded FEG micelles. They have found that the FITC-labeled FEG micelles were selectively transported to the folate receptor positive [FR(+)] HepG-2 cells, but not the FR(−) A549 cells. This results suggested that FEG micelles could be transported into FR(+) HepG-2 cells by a FR-mediated endocytosis. There for they have concluded FEG micelles as a promising carrier for targeted delivery of hydrophobic anticancer drug, such as PTX.[111]

Paolino D et al have utilized folic acid molecules as crucial cancer targeting vector for tumor specific delivery of prepared supramolecular vesicular aggregates (SVAs), fabricated by self-assembling liposomes and polyasparthydrazide co-polymers. They have grafted the MCF-7 cells to NOD-SCID mice to generate breast cancer animal model and then they have used this model to evaluate the cancer specificity of SVAs. From the outcome they have concluded that supramolecular systems can be used as novel drug delivery system prepared through self-assembling liposomes and biocompatible polymers to be conceivably utilized for cancer therapy.[112]

Lin J et al have prepared pluronic F127 self-assembled; polyacrylic acid-bound iron oxides (PAAIO) micelles conjugated with folic acid and investigated its drug delivery and the MRI properties. They have utilized lipophilic color Nile red typified into the hydrophobic poly(propylene oxide) slot of PF127 as a model medication and as a flu-

orescent agent with the end goal of magnetic resonance imaging and as bearers for drug delivery. Utilizing a flow cytometry, laser confocal scanning microscopy, and atomic absorption spectroscopy they have studied FA–PF127–PAAIO, together with a targeting ligand, shows a increased subcellular internalization into KB cells.[113]

Li J et al prepared a magnetic iron oxide nanoparticles conjugated with folic acid to detect the cancer *in-vivo* using magnetic resonance imaging. They have turned out with the outcomes that the folic acid conjugated magnetic iron oxide nanoparticles can be utilized as an effective nano-scale probe for magnetic resonance imaging of malignant cells *in-vitro* and a xenografted tumor model *in-vivo* by means of a dynamic folic acid mediated pathway.[108]

Khoee S et al have synthesized a novel nanocarrier based on methacrylated poly(lactic-co-glycolic acid) (mPLGA) as a lipophilic domain, acrylated methoxy poly(ethylene glycol) (aMPEG) as hydrophilic part and N-2-[(tert-butoxycarbonyl)amino] ethyl methacrylamide (Boc-AEMA) as pH-responsive segment. They have produced amphiphilic brushlike copolymer by radical polymerization of the above-mentioned three modified monomers, from which targeted copolymer was produced through the reaction with activated folic acid. Using this targeteg polymer they have produced a quercetin-loaded nanoparticles using nanoprecipitation method. Dynamic light scattering (DLS) analysis showed that the produced nanoparticles had nanometric size (<100 nm) and low polydispersity in size at different pHs. Higuchi and KorsmeyerePeppas models were applied to evaluate release mechanisms and kinetics.[114]

Majd MH et al have synthesized tamoxifen (TMX) loaded folic acid (FA) armed Fe_3O_4 NPs to target the folate receptor (FR) positive cancer cells. The engineered MNPs were further characterized and examined in the human breast cancer MCF-7 cells that express FR. Fluorescence microcopy and flow cytometry analyses revealed substantial interaction of Fe_3O_4-APSPEG- FA-TMX NPs with the FR-positive MCF-7 cells. Cytotoxicity analysis resulted in significant growth inhibition in MCF-7 cells treated with Fe_3O_4-APS-PEG-FA-TMX NPs. Based on these findings, they have concluded TMX loaded FA-armed PEGylated MNPs as a novel multifunctional nanomedicine/theranostic for concurrent targeting, imaging and therapy of the FR-positive cancer cells.[115]

Song H et al have been prepared doxorubicin loaded folic acid-chitosan conjugated nanoparticles (FA-CS NPs) and evaluated their targeting specificity on tumor cells by ionic cross linking method, and folic acid (FA) was conjugated with CS NPs by electrostatic interaction. They have observed that, FA-CS NPs Compared with the non-conjugated CS NPs showed much higher cell uptaking ability due to the known folate-receptor mediated endocytosis. Therefore they have concluded FA-CS NPs as a potential way to enhance efficiency of antitumor drug by folate receptor mediated targeting delivery.[116]

Hejazi R et al. have reviewed the feasibility of chitosan as a polymer for novel drug delivery system. Chitosan, a natural polymer obtained by alkaline deacetylation of chitin, is non-toxic, biocompatible, and biodegradable. These properties make chitosan a good candidate for the development of conventional and novel gastrointestinal (GI) drug and gene delivery systems. They have summarized the recent applications of chitosan in oral and/or buccal delivery, stomach-specific drug delivery, intestinal delivery, and colon-specific drug delivery. Based on numerous research papers thay have concluded a chitosan to be a promising material for GI drug and gene delivery applications as many derivatives and formulations are being examined.[117]

Tian XX et al. have prepared the chitosan nanoparticles of PS4A, a proteoglycans, with considerable immunological and antineoplastic activity, isolated from the *Mycobacterium vaccae*. They have found that chitosan nanoparticles, readily prepared without the use of organic solvents, are a suitable vehicle for the delivery of these immunostimulants from *M. vaccae;* the formulations might find application as antitumour agents.[118]

Janes KA et al. have fabricated and assessed chitosan nanoparticles as vectors for the anthracycline drug, doxorubicin (DOX). By confocal studies, they have found that DOX was not discharged in the cell medium but rather entered the cells while remaining attached to the nanoparticles. Along these lines they have finished up the chitosan nano-particles as a practical approach to capture the fundamental medication DOX and to convey it into the cells in its dynamic structure.[119]

Katas H et al. have explored chitosan nanoparticles as a siRNA vector due to its advantages such as low toxicity, biodegradability and biocompatibility, by two methods

of ionic cross-linking, simple complexation and ionic gelation using sodium tripolyphosphate (TPP). They have found chitosan–TPP nanoparticles with entrapped siRNA to be better vectors as siRNA delivery vehicles compared to chitosan–siRNA complexes possibly due to their high binding capacity and loading efficiency. Therefore they have concluded that chitosan–TPP nanoparticles are potential vector candidates for safer and cost-effective siRNA delivery.[120]

Qi L et al. have prepared chitosan nanoparticles by ionic gelation of chitosan with tripolyphosphate anions, to evaluate the *in-vitro* antibacterial activity of chitosan nanoparticles and copper-loaded nanoparticles against various microorganisms. The antibacterial activity of chitosan nanoparticles and copper-loaded nanoparticles against *E. coli*, *S. choleraesuis*, *S. typhimurium*, and *S. aureus* was evaluated by calculation of minimum inhibitory concentration (MIC) and minimum bactericidal concentration (MBC). Results show that chitosan nanoparticles and copper-loaded nanoparticles could inhibit the growth of various bacteria tested. Their MIC values were less than 0.25 μg/mL, and the MBC values of nanoparticles reached 1 μg/mL.[121]

Luo Y et al. have prepared the selenite-loaded chitosan (CS) nanoparticles using tripolyphosphate (TPP) as a cross-linking agent with or without zein (a water insoluble corn protein) coating, to obtain selenite supplement formulations with low toxicity and improved antioxidant property. They have found that chitosan nanoparticles have successfully sustained the release of the selenite, while zein coating on chitosan nanoparticles were found to enhance the encapsulation efficiency and release time of selenite drastically. Moreover, due to high antioxidant activity of CS, the *in-vitro* antioxidant properties of selenite-loaded CS/TPP nanoparticles were significantly enhanced, compared with pure selenite.[122]

Dung TH et al. have prepared and investigated antisense oligonucleotide loaded chitosan nanoparticles for the release of oligonucleotide. From the results they have suggested that the sustained release of oligonucleotide from chitosan nanoparticles may be suitable for the local therapeutic application in periodontal diseases.[123]

Gan Q et al. have fabricated chitosan nanoparticles, via different preparation protocols to explore the polyionic coacervation fabrication process, and associated processing conditions so that the drug encapsulation and subsequent release can be sys-

tematically and predictably manipulated. In that study they have found that the polyionic coacervation process for fabricating protein loaded chitosan nanoparticles offers simple preparation conditions and a clear processing window for manipulation of physiochemical properties of the nanoparticles (e.g., size and surface charge), which can be conditioned to exert control over protein encapsulation efficiency and subsequent release profile.[124]

Wang SL et al. have used chitosan nanoparticle-mediated delivery of a shRNA-expressing vector to inhibit *TGFB1* expression in the human rhabdomyosarcoma cell line RD. Knockdown of *TGFB1* by shRNA resulted in a decrease in RD cell growth *in-vitro* and tumorigenicity in nude mice. The efficiency of *TGFB1* gene silencing varied with the selection of targeting sites. These data suggest that chitosan nanoparticle-mediated delivery of an shRNA produces efficient *TGFB1* knockdown in rhabdomyosarcoma cells and may be a method of choice for shRNA delivery for gene therapy.[125]

Lopez-Leon T et al. have prepared the nanogel particles of chitosan by ionic cross-linking with tripolyphosphate (TPP). They have found that the nanoparticle show good swelling property, depending on the pH, which can be controlled to release the drug at desired rate.[126]

Nasti A et al. have studied the influence of a number of orthogonal factors (pH, concentrations, ratios of components, different methods of mixing) in the preparation of chitosan/triphosphate (TPP) nanoparticles and in their coating with hyaluronic acid (HA). They have aimed this study for the minimisation of size polydispersity, the maximisation of zeta potential and long-term stability, and at the control over average nanoparticle size. They have found that HA-coating was beneficial in the reduction of toxicity and suggested that the uncoated chitosan/TPP nanoparticles had toxic effects following internalisation rather than membrane disruption.[127]

Wu Y et al. have prepared the ammonium glycyrrhizinate-loaded chitosan nanoparticles by ionic gelation of chitosan with tripolyphosphate anions (TPP). They have observed that nanoparticles have good ammonium glycyrrhizinate loading efficiency. The encapsulation efficiency was decreasing with the increase of ammonium glycyrrhizinate concentration and chitosan concentration. The introduction of PEG

was also observed to decrease significantly the positive charge of particle surface. Finally they have come up with the conclusion that chitosan can complex TPP to form stable cationic nanoparticles for subsequent ammonium glycyrrhizinate loading.[128]

Berthold A et al. have prepared the chitosan microspheres by a novel precipitation process using sodium sulfate as precipitant. After preparation, they have investigated the loading property with various anti-inflammatory drugs. Drug liberation was tested *in-vitro* using side-by-side diffusion cells with a dialysis membrane made of cellulose acetate. They have found that the highest loading was achieved with prednisolone sodium phosphate (PSP) and the adsorbed drug was present in an amorphous form. They have also observed that the drug release from the microspheres was dependent on the drug-polymer ratio.[129]

4. PLAN OF WORK

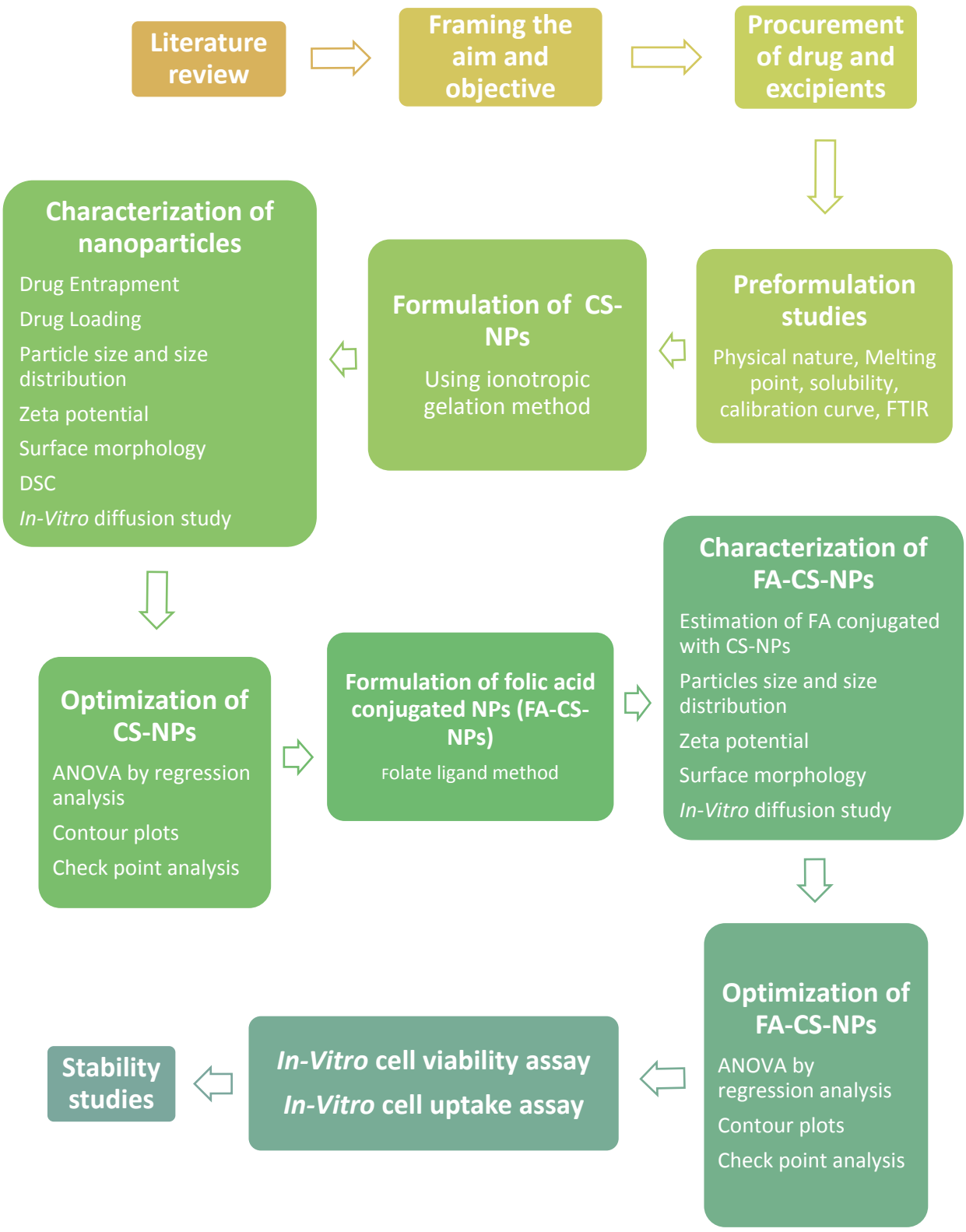

5. MATERIAL AND METHODS

5.1 Materials and Instruments

The following drug, excipients, chemicals, media, cell-lines, glasswares and instruments were used for the formulation and evaluation of FA-CS-NPs.

5.1.1 Materials

Drug, various excipients and reagents used in the study are given in Table 5.1

Table 5.1: List of drug, excipients and reagents

Sr. No.	Materials	Suppliers / Manufacturer
	Drug	
1.	Capecitabine	Gift sample from sun pharma.Vadodara
	Excipients	
2.	Chitosan	Balaji drugs, Surat
3.	Sodium tripolyphosphate	Krishna chemicals, Vadodara
4.	Acetic acid	Aatur Instu chem., Vadodara
5.	Sodium hydroxide	Suvidhan Laboratories, Baroda
6.	Folic acid	Suvidhan Laboratories, Baroda
	Reagents	
7.	Trypan blue	Hyclone, Lot no: JRH27098, 100 ml
8.	Triton X	MP Biomedicals, Lot No: 8009H
9.	DMSO cell culture grade	MP Biomedicals, Lot No: R20759
10.	10000 U/ml Penicillin G, 10000 µg/ml Streptomycin, 25 µg/ml Amphotericin B	Hyclone, Lot no: JRM28184, 100 ml
11.	EDTA	MP Biomedicals, Lot No: 6941H
12.	Rhodamine B	HiMedia
13.	0.25% Trypsin 1X	Invitrogen, Lot No: 1376596
14.	DPBS/modified 1X (Dulbecoo's phosphate buffer saline)	Hyclone, Lot No: ASA28462, 100 ml
15.	HBSS –1X (Hank's Balanced Salt solution)	Hyclone, Lot no:ARL27892, 500 ml

5.1.2 Nutritional Media

Various cell culture media used in the study are given in Table 5.2

Table 5.2: List of Nutritional Media

Sr. No.	Media	Source
1.	DMEM (Dulbecoos Modified Eagels medium, low glucose with glutamine)	US Biological, Lot No: L7020976
2.	RPMI1640 (with L-glutamine)	Hyclone, Lot no: ARB25753A
3.	FBS (Fetal Bovine Serum, South Ameri-can origin, 500 ml)	Bioclot, Lot No:07310
4.	Fluid thioglycolate media (FTGM)	HiMedia, Lot No: M059374
5.	Tryptone Soya broth (TSB)	HiMedia, Lot No: M043461

5.1.3 Cell line

Various cell lines for in vitro study used in the research work are given in Table 5.3

Table 5.3: List of cell line

Sr. No.	Cell line	Type	Origin	Species	Source
1.	VERO	Normal (non-cancerous)	Kidney	African green monkey	NCCS, Pune
2.	HT-29	cancerous	Colon	Human	NCCS, Pune
3.	MCF-7	cancerous	Breast	Human	NCCS, Pune

5.1.4 Cell- proliferation kit

1. Cell proliferation kit (MTT), 2500 tests, (Roche, Lot No: 13363700)

5.1.5 Glasswares and plastic wares

Important glasswares and plastic wares, apart from the common and routinely used, are given in Table 5.4

Table 5.4: List of glasswares and plastic wares

Sr. No.	Glasswares/plastic wares
1.	96-well microtiter plate (Flat Bottom, U Bottom, V Bottom)
2.	Tissue culture flasks (25 cm^2 T Flask vented and non-vented, 75 cm^2 T Flask vented, 150 cm^2 T Flask vented)
3.	Falcon tubes (15ml, 50ml)
4.	Cryotubes (2ml)
5.	Cell scrapper
6.	Micro tips (Blue 1000µl, Yellow 200µl, White 10 µl) (Volex)
7.	Reagent bottles (100ml, 250 ml, 500 ml, 1000 ml)
8.	Haemocytometer

5.1.6 Instruments

Various important instruments and equipments used in the study are given in Table 5.5

Table 5.5: List of Instruments

Sr.No.	Equipments	Source
1.	Electronic Balance	Ohaus corporation, pine brook, NJ,USA
2.	Magnetic stirrer	Remi Service Pvt Ltd,Mumbai,India
3.	Mechanical stirrer	MAC, mumbai
4.	Sonicator	MAC, mumbai
5.	Cooling centrifuge	Remi Service Pvt Ltd,Mumbai,India
6.	FT-IR Spectrophotometer	Shimadzu Corporation, Japan
7.	UV – Visible Spectrometer	UV-1800,Shimadzu Corporation, japan
8.	Lyophilizer	Macro scientific works
9.	Scanning electron microscope	Model-JSM-5610LV, JEOL
10.	Zeta-sizer	Malvern instrument LTD,UK
11.	Stability chamber	Macro scientific work PVT LTD,Delhi
12.	Fluorescence inverted micrscope	Leica DM IL, Germany
13.	Biosafety cabinet class-II	Esco, Singapore
14.	Cytotoxic safety cabinet	Esco, Singapore
15.	CO_2 incubator	RS Biotech, mini galaxy A, Scotland

16.	Deep freezer	Dairei, Denmark
17.	ELISA plate reader	Thermo, USA
18.	Micropipettes	Eppendorff, Germany
19.	RO water system	Millipore, USA
20.	Electronic water bath	Genie, India

5.2 Drug profile

5.2.1 Capecitabine

Capecitabine (Xeloda, Roche) is an orally-administered chemotherapeutic agent used in the treatment of numerous cancers. Capecitabine is a prodrug, that is enzymatically converted to 5-fluorouracil (5-FU) in the body.[130, 131]

5.2.1.1 Medical uses

It is used in the treatment of the following cancers[132, 133]

a. Colorectal cancer (either as neoadjuvant therapy with radiation, adjuvant therapy or for metastatic cases)
b. Breast cancer (metastatic or as monotherapy/ combo therapy; this is licensed as a second-line treatment in the UK)
c. Gastric cancer (off-label in the US; this is a licensed indication in the UK)
d. Oesophageal cancer (off-label in the US)

5.2.1.2 Adverse effects

Following are some common adverse effect of capecitabine[134]

- Appetite loss
- Diarrhea
- Vomiting
- Nausea
- Stomatitis
- Fatigue
- Weakness
- Hand-foot syndrome
- Oedema
- Fever
- Pain
- Headache
- Hair loss
- Dermatitis
- Indigestion
- Shortness of breath
- Eye irritation

5.2.1.3 Contraindications

Capecitabine is contraindicated in the following conditions[135]

a. History of hypersensitivity to fluorouracil, capecitabine or any of its excipients
b. Patients with Dihydropyrimidine dehydrogenase (DPD) deficiency
c. Pregnancy and lactation
d. Patients with pre-existing blood dyscrasias
e. Patients with severe hepatic impairment or severe renal impairment
f. Treatment with sorivudine or its chemically related analogues, such as brivudine

5.2.1.4 Drug interactions

Drugs which are known to interact with capecitabine include[130-132]

a. Sorivudine or its analogues, such as, brivudine
b. Allopurinol as it decreases the efficacy of 5-FU.
c. CYP2C9 substrates, including, warfarin and other coumarin-derivatives anti-coagulants
d. Phenytoin, as it increases the plasma concentrations of phenytoin.
e. Calcium folinate may enhance the therapeutic effects of capecitabine by means of synergising with its metabolite, 5-FU. It may also induce more severe diarrhoea by means of this synergy.

5.2.1.5 Systematic (IUPAC) name

Pentyl [1- (3, 4 - dihydroxy - 5 – methyltetrahydrofuran – 2 – yl) – 5 – fluoro -2 – oxo - 1*H* - pyrimidin – 4 – yl] carbamate[130]

5.2.1.6 Chemical structure

Chemical structure of capecitabine is given in Figure 5.1[131]

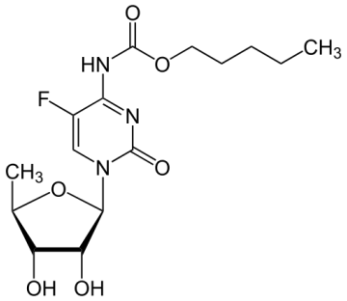

Figure 5.1: Chemical structure of capecitabine

5.2.1.7 Pharmacokinetic parameters, Chemical data and Clinical data

Pharmacokinetic parameters, Chemical data and clinical data is given in Table 5.6, Table 5.7 and Table 5.8 respectively [130-132, 136]

Table 5.6: Pharmacokinetic parameters of capecitabine

Pharmacokinetic Parameter	**Value**
Absorption	Readily absorbed through the GI tract (~70%)
Metabolism	Hepatic, to 5'-deoxy-5-fluorocytidine (5'-DFCR), 5'-deoxy-5-fluorouridine (5'-DFUR) (inactive); neo-

	plastic tissue, 5'-DFUR to active fluorouracil
BCS class	Class-I
Protein binding	< 60% (mainly albumin)
Solubility	Soluble in water (26mg/ml), ethanol (207mg/ml), methanol (40mg/ml), DMF (14mg/ml), DMSO (72mg/ml) at 25^{o}C
Bioavailability	Extensive
Half-life	38–45 minutes
Excretion	Renal (95.5%), faecal (2.6%)
pK value	pKa:5.41, pKb:1.75
Affected organisms	Humans and other mammals

Table 5.7: Chemical data of capecitabine

Chemical data	**Value**
Formula	$C_{15}H_{22}FN_3O_6$
Mol. mass	359.35 g/mol
Melting point	115-120^{o}C

Table 5.8: Clinical data of capecitabine

Clinical data	**Value**
Brand name	Xeloda (Roche)
Routes	oral

5.2.1.8 Mechanism of action

Capecitabine is metabolized to 5-FU which in turn is a thymidylate synthase inhibitor, hence inhibiting the synthesis of thymidine monophosphate (ThMP), the active form of thymidine which is required for the *de novo* synthesis of DNA and RNA during gene expression.[130-132, 135]

5.2.1.9 Pharmacodynemics

Capecitabine is a fluoropyrimidine carbamate with antineoplastic activity indicated for the treatment of metastatic breast cancer and colon cancer. It is an orally administered systemic prodrug that has little pharmacologic activity until it is converted to fluorouracil by enzymes that are expressed in higher concentrations in many tumors.

Fluorouracil it then metabolized both normal and tumor cells to 5-fluoro-2′-deoxyuridine 5′-monophosphate (FdUMP) and 5-fluorouridine triphosphate (FUTP).[130-132, 135]

5.3 Excipients profile

5.3.1 Chitosan

Chitosan is a sugar that is obtained from the hard outer skeleton of shelfish, including crab, lobster and shrimp. Some people apply chitosan directly to their gums to treat inflammation that can lead to tooth loss (periodontitis), or chew gum that contains chitosan to prevent "cavities" (dental caries). In an effort to help "donor tissue" re-build itself, plastic surgeons sometimes apply chitosan directly to places from which they have taken tissue to be used elsewhere. In pharmaceutical manufacturing, chitosan is used as a filler in tablets; as a carrier in controlled release drug; to improve the way certain drug dissolve; and to make bitter tastes in solutions taken by mouth.[137]

5.3.1.1 Chemical formula

$C_6H_{11}NO_4X_2$ [137, 138]

5.3.1.2 Molecular weight

3800g/mol to 20,000 g/mol [137]

5.3.1.3 Chemical structure

Chemical structure of chitosan is given in Figure 5.2[124]

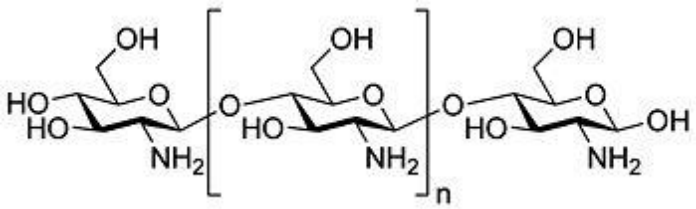

Figure 5.2: Chemical structure of chitosan

5.3.1.4 Chemical IUPAC name

Poly [(1,4)-N-acetyl-D-glucose-2-amine)]

5.3.1.5 Physical nature

Bright white, odorless powder

5.3.1.6 Solubility

Water-soluble and a bioadhesive which readily binds to negatively charged surfaces such as mucosal membranes.[137, 139]

5.3.1.7 Hydrophobicity

-1.8

5.3.1.8 Dissociation constant

6.5

5.3.1.9 Melting point

270-274^{o}C

5.3.1.10 Uses

Patients with kidney failure who are on long term hemodialysis. When taken by these patients, chitosan may reduse high cholesterol; help to correct anemia; and improve physical strength, appetite and sleep. Treating periodontistis, a dental condition. Applying chitosan ascorbate directly to the gums seems to help in the treatment of periodontitis. Helping to remake tissue after plastic surgery. Applying N-carboxybutyl chitosan directly seems to help donor site tissue rebuild in plastic surgery.[137]

5.3.1.11 Adverse effect

When taken by mouth, it might cause mild stomach upset, constipation or gas. Not enough is known about the use of chitosan during pregnancy and breast-feeding. Stay on the safe side and avoid use.[137-139]

5.3.2 Sodium tripolyphosphate

Sodium triphosphate **(**STP, sometimes STPP or sodium tripolyphosphate or TPP**)** is an inorganic compound with formula $Na_5P_3O_{10.}$ It is the sodium salt of the polyphosphatepenta-anion, which is the conjugate base of triphosphoric acid. it is produced on a large scale as a component of many domestic and industrial products,

especially detergents. Environmental problems associated with eutrophication are attributed to its widespread use.[138, 139]

5.3.2.1 Chemical formula

$Na_5P_3O_{10}$

5.3.2.2 Physical nature

White powder

5.3.2.3 Chemical structure

Chemical structure of the TPP is shown in Figure 5.3

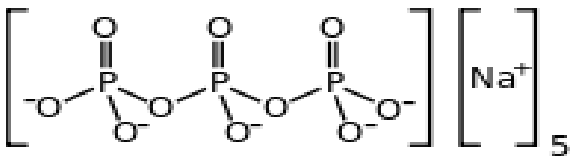

Figure 5.3: Chemical structure of TPP

5.3.2.4 Solubility

It is soluble in water 14.5 g/100ml (25^{o}C)

5.3.2.5 Melting point

622-625^{o}C

5.3.2.6 Uses

STTP is a preservative for seafood, meats, poultry and animal feeds.

5.3.2.7 Adverse effect

The toxicity of polyphosphates is low, as the lowest LD50 after oral administration is >1,000 mg/kg body weight. No mutagenic or carcinogenic effects nor reproductive effects have been noted. Salts of polyphosphate anions are moderately irritating to skin and mucous memberane because they are mildly alkaline.[138, 139]

5.3.4 Folic acid

Folate and folic acid derive their names from the Latin word folium, which means "leaf". Folate occurs naturally in many foods and, among plants, are especially plentiful in dark green leafy vegetables. Folic acid is itself not biologically active, but its

biological importance is due to tetrahydrofolate and other derivatives after its conversion to dihydrofolic acid in the liver.[140]

5.3.4.1 Chemical formula

$C_{19}H_{19}N_7O_6$ [103]

5.3.4.2 Physical nature

Yellowish to orange crystalline powder[140]

5.3.4.3 Chemical structure

Chemical structure of the folic acid is given in Figure 5.4[84]

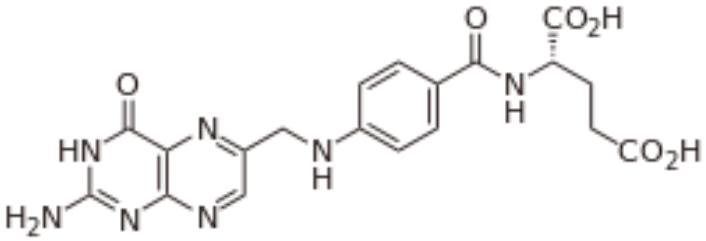

Figure 5.4: Chemical structure of folic acid

5.3.4.4 Solubility

soluble in dilute acids and alkaline solutions[140, 141]

5.3.4.5 Use

Folic acid is used for preventing and treating low blood levels of folic acid (folic acid deficiency), as well as its complications, including anemia and the inability of the bowel to absorb nutrients properly. Also used for other conditions commonly associated with folic acid deficiency, including liver disease, alcoholism, and kidney dialysis. Some people use folic acid to prevent colon cancer or cervical cancer. It is also used to prevent heart disease and stroke. Folic acid is used for memory loss, age-related hearing loss, reducing signs of aging, weak bones (osteoporosis), sleep problems, depression, muscle pain, AIDS. Some people apply folic acid directly to the gum for treating gum infection.[140]

5.4 Methodology

5.4.1 Preformulation study

It is the first step in rational development of dosage forms of drug substance. Preformulation testing is defined as an investigation of physical and chemical properties of a drug substance alone and when combined with excipients. The overall objective of preformulation testing is to generate information useful to the formulator in developing stable and bioavailable dosage forms that can be mass-produced.

Following preformulation studies were carried out

5.4.1.1 Color, odor, taste and appearance

The drug was evaluated for its color, odor and taste.

5.4.1.2 Melting point determination

Melting point of the drug sample was determined by capillary method using melting point apparatus.

5.4.1.3 Determination of λ_{max} of capecitabine

Stock solution (1000µg/ml) of capecitabine in Phosphate buffer pH 7.4 was prepared. This solution was appropriately diluted with the same solvent to obtain stock solution of (100µg/ml). The resultant solution was scanned in the range of 200 nm – 400 nm in UV-Visible spectrophotometer. It showed λ_{max} 240 nm in phosphate buffer pH 7.4 for capecitabine. In the same way λ_{max} was also determined in water and 1%v/v acetic acid as a requirement to assess the solubility of capecitabine in later stage.

5.4.1.4 Determination of λ_{max} of folic acid

Stock solution (1000µg/ml) of folic acid in Phosphate buffer pH 7.4 was prepared. This solution was appropriately diluted with the same solvent to obtain stock solution of (100µg/ml). The resultant solution was scanned in the range of 200 nm – 400 nm in UV-Visible spectrophotometer. It showed λ_{max} 283 nm in phosphate buffer pH 7.4 for folic acid.

5.4.1.5 Determination of calibration curve

Spectrophotometric analysis of capecitabine and folic acid was carried out on double beam UV-spectrophotometer (UV-1800, shimazdu, japan).

Standard calibration curve of capecitabine in water

Capecitabine (25 mg) was dissolved in 25 ml distilled water in volumetric flask to obtain a stock solution of 1000 μg/ml concentration. From the stock solution 10ml of solution diluted with 100 ml water to obtain 100μg/ml. This solution (100 μg/ml) was further diluted with water to obtain solution of 5 to 40 μg/ml. Absorbance of each aliquots was measured at 240nm using UV-Visible spectrophotometer and water was taken as blank. The standard curve was generated for the entire range from 5 to 40 μg/ml.

Standard calibration curve of capecitabine in Phosphate buffer pH 7.4

Capecitabine (25 mg) was dissolved in 25 ml phosphate buffer pH 7.4, in volumetric flask, to obtain a stock solution of 1000 μg/ml concentration. From the stock solution 10ml of solution diluted with 100ml to obtain 100μg/ml. This solution (100 μg/ml) was further diluted with phosphate buffer pH 7.4 to obtain solution of 5 to 40 μg/ml. Absorbance of each solution was measured at 240 nm using UV-Visible spectrophotometer and phosphate buffer pH 7.4 was taken as blank. The standard curve was generated for the entire range from 5 to 40 μg/ml.

5.4.1.6 Solubility study

Solubility of the drug was determined by saturation equilibrium method. Excess quantity of capecitabine was added in to the 10ml volumetric flask and then volume was made up to 10ml mark with water, and then mixture was place in incubator shaker overnight, to get saturated solution of drug in water. Next day, undissolved drug was separated from the solution by filtering the mixture from whatman filter paper. Supernatant was diluted appropriately with water and the absorbance was determined using UV-visible spectrophotometer at 240 nm, where water was used as a reference solvent. Concentration of the drug was calculated from the standard calibration curve of drug taken in water. Using same method, solubility of capecitabine was also determined in phosphate buffer saline solution pH 7.4 and 1% v/v acetic acid.

5.4.1.7 Standard calibration curve of folic acid in Phosphate buffer pH 7.4

Folic acid (10 mg) was dissolved in 10 ml 20%w/v NaOH solution, in volumetric flask, to obtain a stock solution of 1000 μg/ml concentration. This stock solution was diluted with phosphate buffer pH 7.4 and volume was made up to 100 ml, to obtain

100μg/ml concentration. This solution (100 μg/ml) was further diluted with phosphate buffer pH 7.4 to obtain solution of 4 to 20 μg/ml. Absorbance of each solution was measured at 283 nm using UV-Visible spectrophotometer and phosphate buffer pH 7.4 was taken as blank. The standard curve was generated for the entire range from 05 to 40 μg/ml.

5.4.1.8 Drug – Excipients compatibility study

Infrared spectra of pure drug, polymer, as well as for combination of drug-polymer were taken by KBr pellet technique and were recorded in the range of 4000 – 400cm^{-1} by using FT-IR Spectrophotometer Shimadzu.

5.5 Formulation of CS-NPs

5.5.1 Method of preparation

Chitosan nanoparticles were prepared by ionic cross linking of chitosan solution with TPP anions. Chitosan was dissolved in 50ml aqueous solution of acetic acid (1% v/v) to prepare various concentrations (0.5mg/ml, 1mg/ml, 1.5mg/ml). Under magnetic stirring at room temperature, 0.5 mg/ml, 0.75 mg/ml, and 1.0 mg/ml concentration of 20 ml TPP aqueous solution was added dropwise using syringe needle into chitosan solution containing 25 mg of capecitabine. pH was adjusted to 6.0 by adding 0.1 N NaOH. The stirring was continued for about 30 minutes. The resultant nanoparticles suspensions were centrifuged at 12000 rpm for 30 minutes. Particles get settled down and separated from clear supernatant. The Particles obtained after centrifugation were finally freeze dried and stored in air tight close container. The formation of the nano-particles was because of the interaction between the negative groups of the TPP and the positively charged amino groups of chitosan (ionic gelation).[83, 92, 116]

5.5.2 Factorial Designs

Formulation were prepared by applying 3^2 full factorial design. Chitosan and TPP concentration were considered as dependent variable whereas amount of drug, strength of acetic acid solution and stirring speed was kept constant throughout for-mulation process. Factorial design for the preparation of CS-NPs is given in Table 5.9

Table 5.9: Factorial design

Factor	Level		
	Low	**Medium**	**High**
X_1	0.5mg/ml	01mg/ml	1.5mg/ml
X_2	0.5mg/ml	0.75mg/ml	01mg/ml
Factorial levels	-1	0	+1

X_1- concentration of chitosan in 1%v/v Acetic Acid; X_2 -concentration of TPP in water. Amount of drug (capecitabine) was kept constant (25mg).

5.5.3 Formulation codes for CS-NPs

Levels of both the variables for each batch of the CS-NPs are shown in Table 5.10

Table 5.10: Formulation codes for CS-NPs

Batch Code	X_1	X_2
CS-NPs -1	−1	−1
CS-NPs -2	−1	0
CS-NPs -3	−1	+1
CS-NPs -4	0	−1
CS-NPs -5	0	0
CS-NPs -6	0	+1
CS-NPs -7	+1	−1
CS-NPs -8	+1	0
CS-NPs -9	+1	+1

5.6 Characterization of CS-NPs

5.6.1 Percentage Yield

The yield of production of nanoparticles of various batches were calculated using the weight of the final product after drying with respect to the initial total weight of the drug and polymer used for preparation of nanoparticles and percent production yield were calculated as per the formula mentioned below.

$$\% \text{ yield} = \frac{\text{Practical mass}}{\text{Theoritical mass}} \times 100$$

5.6.2 Drug entrapment efficiency

First of all the prepared chitosan nanoparticles were separated from supernatant by centrifugation at 12000 RPM for 30 minutes, by using a REMI cooling centrifuge. Then, the nanoparticles pellets and supernatant was separated. Amount of the free drug present in supernatant was analyzed by appropriately diluting supernatant in wa-

ter and absorbance was taken against water as a blank on UV-Visible Spectrophotometer at 240nm. To find out percentage entrapment following equation was used.

$$\% \text{ Drug Entrapment} = \frac{\text{Total Drug taken} - \text{drug in supernatant}}{\text{Total drug taken}} \times 100$$

5.6.3 Percentage Drug content

% Drug content was calculated using following equation

$$\% \text{ Drug content } = \frac{\text{Amount of drug entraped in NPs}}{\text{Total Weight of NPs}} \times 100$$

5.6.4 *In-vitro* drug release

In-vitro drug release from all 09 batches of CS-NPs was carried out by dialysis bag diffusion method. A 4–5 cm long portion of the dialysis bag was made into a dialysis sac by folding and tying up one end of the bag with thread. It was then filled up with phosphate-buffer pH 7.4 and examined for the leaks. The sac was then emptied and NPs dispersion (equivalent to 10 mg drug) was accurately transferred into sac which served as the donor compartments. The sac was once again examined for leak and then suspended in the glass beakers containing 50 ml phosphate-buffer pH 7.4, which become the receptor compartment. Aliquots were taken at 1,2,3,4,5,6,7,8 12, 24 and 48 hours and analyzed spectrophotometrically at 240 nm. Fresh buffer was used to replenish the receptor compartment at each time to maintain sink condition.

5.7 Optimization of CS-NPs

Optimization of the prepared 09 batches of CS-NPs was done by considering the effect of variables and interaction between them, on the percentage entrapment efficiency as a response, as follows.

5.7.1 Interaction between the factors

The statistical evaluation of all the obtained results data was carried out by analysis of variance (ANOVA) using Microsoft Excel Version-2007. The significant factors in the equations were selected for conducting the regression analysis. The terms of full model having non-significant p value (> 0.05) have negligible contribution in obtaining dependent variables and thus neglected. The equations represent the quantitative effect of the formulation variables on responses.

5.7.2 Construction of contour plots

Two-dimensional and three-dimensional contour plots were constructed using reduced polynomial equation. Contour plots were used to find out the appropriate combination of the both variables giving the maximum percentage entrapment of the drug. Contour plots were constructed by using sigma plot version 11.0 (Systat software Inc.).

5.7.3 Evaluation of model / Check point analysis

In order to assess the reliability of the model, a checkpoint analysis was done to confirm the effect of the independent variables on the dependent variables. Any two values of the independent variables were selected from the contour graph and the responses were estimated by using the equations and experimental procedure, and then both these values, predicted and experimental, were compared and difference was recorded as a percentage error.

5.8 Evaluation of optimized CS-NPs

Optimized CS-NPs-8 was further evaluated for particle size, size distribution, zeta potential, FTIR study, DSC study, SEM and drug release kinetics

5.8.1 Particle size and zeta potential

The particle size distribution of the nanoparticle reflects its penetration efficiency during tissue transportation, because less the size better is the penetration. A narrow particle size distribution also contributes to the better stability as particles of similar size intends less to aggregate. Zeta potential of nanoparticles reflects the electric potential of particles and is used to characterize the surface charge properties and to determine whether the charged particle is encapsulated within the center or adsorbed on to the surface of nanoparticles. The particle size and zeta potential of NPs was recorded using Malvern particle size analyzer. CS-NPs batch optimized using the response % entrapment and *In-Vitro* drug release were subjected to particles size distribution and zeta potential analysis. This study was carried out at Parul University, Vadodara.

5.8.2 Scanning Electron Microscopy (SEM)

Scanning Electron Microscopy is a technique that produce largely magnified image by using electrons instead of light to form an image. Electron gun produces a beam of electrons which follows the vertical path through the microscope between electro-

magnetic field and lenses towards the sample due to which electron and X-rays are ejected from sample. The surface morphology of Capecitabine loaded optimized CS-NPs-8 were determined using scanning electron microscope (SEM). This study was carried out at M S University, Vadodara.

5.8.3 FT-IR study

Infrared spectra of optimized batch of CS-NPs was taken by KBr pellet technique and were recorded in the range of 4000 – 400cm^{-1} by using FT-IR Spectrophotometer (Shimadzu) and then it was compared with the spectra of capecitabine alone to check whether the drug is interacting with the excipients or not.

5.8.4 Differential Scanning Calorimetry

Thermogram of pure drug capecitabine and optimized batch of CS-NPs were obtained by using Differential scanning calorimeter. Then after, both the thermograms obtained, were compared with each other to confirm about the interaction between the capecitabine and excipients, weather it is happening or not, in optimized CS-NPs. It was carried out at S.K. Patel College of Pharmacy, Kherva, Mehsana.

5.8.5 Drug release kinetics

In order to investigate the mechanism of drug release from an optimized CS-NPs formulation, the release data obtained from in-vitro release studies were fitted to various kinetics equations. The kinetics models used were a zero order equation (Qt = Q0 – K0t), first order equation (lnQt = lnQ0 – Kt), and Higuchi‘s equation (Qt = Kht1/2). Where Qt is the percent of drug released at time t, Q0 is the initial amount of drug present in optimized CS-NPs and K0, K and Kh were constant of the equation of zero order, first order and Higuchi model respectively.

5.9 Conjugation of folic acid to optimized CS-NPs

CS-NPs-8 was found to be optimized one and it was used in the conjugation of folic acid on chitosan nanoparticles

5.9.1 Method of preparation

Folic acid conjugated CS-NPs (FA-CS-NPs) were prepared by applying 3^3 full factorial design. Varying amount of folic acid was dissolved in 10mL 20%w/v aqueous solution of sodium hydroxide and dropped into 10mL phosphate buffer suspension

(pH 7.4) containing 20mg of optimized Chitosan nanoparticles, CS-NPs-8, under varying stirring speed, using mechanical stirrer, for different duration of time. The collected products were centrifuged at 10000 rpm for 20 min, nanoparticles were separated and freeze-dried.[116]

Mechanism of folic acid conjugation with nanoparticles is given in Figure 5.5

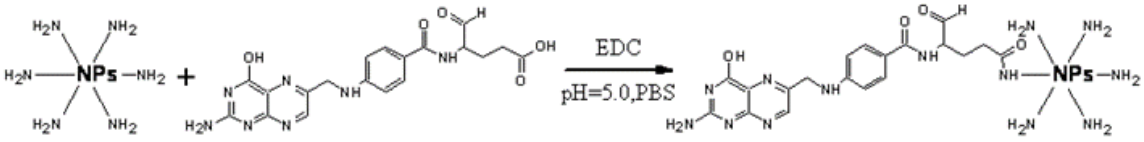

Figure 5.5: Mechanism of folic acid conjugation with nanoparticles

5.9.2 Factorial design

Formulation were prepared by applying 3^3 full factorial design. Folic acid amount, RPM and reaction time considered as dependent variable. Factorial design for the preparation of FA-CS-NPs is given in Table 5.11

Table 5.11: Factorial designs

Factor	Level		
	Low	**Medium**	**High**
X_1 (Amount of folic acid)	2.5mg	5.0mg	7.5mg
X_2 (RPM)	500	700	900
X_3 (Reaction time)	10	20	30
Factorial levels	-1	0	+1

Amount of CS-NPs was kept constant (20mg).

5.9.3 Formulation codes for FA-CS-NPs

Levels of each three the variables for all batches of the FA-CS-NPs are shown in Table 5.12

Table 5.12: Formulation codes for FA-CS-NPs

Batch Code	X_1	X_2	X_3
FA-CS-NPs -1	−1	−1	−1
FA-CS-NPs -2	−1	−1	0
FA-CS-NPs -3	−1	−1	+1
FA-CS-NPs -4	−1	0	−1
FA-CS-NPs -5	−1	0	0
FA-CS-NPs -6	−1	0	+1
FA-CS-NPs -7	−1	+1	−1
FA-CS-NPs -8	−1	+1	0
FA-CS-NPs -9	−1	+1	+1
FA-CS-NPs -10	0	−1	−1
FA-CS-NPs -11	0	−1	0
FA-CS-NPs -12	0	−1	+1
FA-CS-NPs -13	0	0	−1
FA-CS-NPs -14	0	0	0
FA-CS-NPs -15	0	0	+1
FA-CS-NPs -16	0	+1	−1
FA-CS-NPs -17	0	+1	0
FA-CS-NPs -18	0	+1	+1
FA-CS-NPs -19	+1	−1	−1
FA-CS-NPs -20	+1	−1	0
FA-CS-NPs -21	+1	−1	+1
FA-CS-NPs -22	+1	0	−1
FA-CS-NPs -23	+1	0	0
FA-CS-NPs -24	+1	0	+1
FA-CS-NPs -25	+1	+1	−1
FA-CS-NPs -26	+1	+1	0
FA-CS-NPs -27	+1	+1	+1

5.10 Characterization of FA-CS-NPs

5.10.1 Percentage Yield

The yield of production of FA-CS-NPs of all 27 batches were calculated using the weight of the final product, after drying, with respect to the initial total weight of the drug and excipients used for conjugation of the folic acid to the optimized CS-NPs and percent yield was calculated as per the formula mentioned below.

$$\% \text{ yield} = \frac{\text{Practical mass}}{\text{Theoritical mass}} \times 100$$

5.10.2 Percentage folic acid conjugation efficiency

First of all the prepared folic acid conjugated CS-NPs were separated by centrifugation at 10000 RPM for 20 minutes, by using a REMI cooling centrifuge. Then, the FA-CS-NPs pellets and supernatant was separated.

Supernatant was appropriately diluting phosphate buffer pH 7.4 and absorbance was taken against phosphate buffer pH 7.4 as a blank on UV-Visible Spectrophotometer at 283nm to determine concentration of free folic acid. Percentage entrapment was calculated using following equation was used.

$$\% \text{ Folic acid conjugation} = \frac{\text{Total FA taken} - \text{FA in supernatant}}{\text{Total FA taken}} \times 100$$

5.10.3 Percentage folic acid loading

% FA loading was calculated using following equation

$$\% \text{ Folic acid Loading } = \frac{\text{FA cojugated on CS} - \text{NPs}}{\text{Total Weight of FA} - \text{CS} - \text{NPs}} \times 100$$

5.10.4 *In*-Vitro drug release

In-Vitro drug release from all the prepared 27 batches of FA-CS-NPs was carried out by dialysis bag diffusion method. A 4–5 cm long portion of the dialysis bag was made into a dialysis sac by folding and tying up one end of the bag with thread. It was then filled up with phosphate-buffer pH 7.4 and examined for the leaks. The sac was then emptied and FA-CS-NPs dispersion (equivalent to 10 mg drug) was accurately transferred into sac which served as the donor compartments. The sac was once again examined for leak and then suspended in the glass beaker containing 50 ml phosphate-buffer pH 7.4, which become the receptor compartment. Aliquots were taken at 1, 2, 3, 4, 5, 6, 7, 8, 12, 24, 48 and 72 hours and analyzed spectrophotometrically at 240 nm. Fresh buffer was used to replenish the receptor compartment at each time to maintain sink condition.

5.11 Optimization of FA-CS-NPs

Optimization of the prepared FA-CS-NPs was done by considering the effect of variables and interaction between them, on the percentage folic acid conjugation as a response, as follows.

5.11.1 Interaction between the factors

The statistical evaluation of all the obtained results data was carried out by analysis of variance (ANOVA) using Microsoft Excel Version-2007. The significant factors in the equations were selected for conducting the regression analysis. The terms of full model having non-significant p value (> 0.05) have negligible contribution in obtaining dependent variables and thus neglected. The equations represent the quantitative effect of the formulation variables on responses.

5.11.2 Construction of contour plots

Two-dimensional and three-dimensional contour plots were constructed using reduced polynomial equation. Initially variable-1 was kept constant at level -1 and first contour plot was constructed by varying the levels of variable-2 and variable-3. Then after another two contour plots were made by keeping the variable constant at level 0 and level +1 respectively. In the same way another three contour plots were constructed by keeping the level of variable-2 constant at -1, 0 and +1 respectively. Finally, another three contour plot were constructed by keeping the level of variable-3 constant at -1, 0 and +1 respectively. These 09 Contour plots were used to find out the appropriate combination of the all three variables giving the maximum percentage folic acid conjugation. Contour plots were constructed by using sigma plot version 11.0 (Systat software Inc.).

5.11.3 Evaluation of model / Check point analysis

In order to assess the reliability of the model, a checkpoint analysis was done to confirm the effect of the independent variables on response. Any three values of the independent variables were selected from the contour graph and the responses were estimated by using the equations and experimental procedure, and then both these values, predicted and experimental, were compared and difference was recorded as a percentage error.

5.12 Evaluation of optimized FA-CS-NPs

Optimized CS-NPs-8 was further evaluated for particle size, size distribution, zeta potential, FTIR study, DSC study, SEM and drug release kinetics

5.12.1 Particle size distribution and zeta potential

The particle size distribution of the nanoparticle reflects its penetration efficiency during tissue transportation, because less the size better is the penetration. A narrow particle size distribution also contributes to the better stability as particles of similar size intends less to aggregate. Zeta potential of nanoparticles reflects the electric potential of particles and is used to characterize the surface charge properties and to determine whether the charged particle is encapsulated within the center or adsorbed on to the surface of nanoparticles. The particle size and zeta potential of Optimized FA-CS-NPs was assessed using Malvern particle size analyzer. This study was carried out at Parul University, Vadodara.

5.12.2 Scanning Electron Microscopy (SEM)

Scanning Electron Microscopy is a technique that produce largely magnified image by using electrons instead of light to form an image. Electron gun produces a beam of electrons which follows the vertical path through the microscope between electromagnetic field and lenses towards the sample due to which electron and X-rays are ejected from sample. The surface morphology of capecitabine loaded optimized FA-CS-NPs were determined using scanning electron microscope (SEM). This study was carried out at M S University, Vadodara.

5.12.3 FT-IR study

Infrared spectra of optimized batch of FA-CS-NPs was taken by KBr pellet technique and were recorded in the range of 4000 – 400cm^{-1} by using FT-IR Spectrophotometer (Shimadzu) and then it was compared with the spectra of capecitabine alone to check whether the drug is interacting with the excipients or not.

5.12.4 Differential Scanning Clorimetry

Thermogram of pure drug capecitabine and optimized batch of FA-CS-NPs were obtained by using Differential scanning calorimeter. Then after, both the thermograms obtained, were compared with each other to confirm about the interaction between the capecitabine and excipients, weather it is happening or not, in optimized FA-CS-NPs. It was carried out at S.K. Patel College of Pharmacy, Kherva, Mehsana.

5.12.5 Drug release kinetics

In order to investigate the mechanism of drug release from an optimized FA-CS-NPs formulation, the release data obtained from *in-vitro* release studies were fitted to various kinetics equations. The kinetics models used were a zero order equation ($Q_t = Q_0 – K_0t$), first order equation ($lnQ_t = lnQ_0 – K_t$), and Higuchi's equation ($Q_t = K_h\mathbf{t}_{1/2}$). Where Q_t is the percent of drug released at time t, Q_0 is the initial amount of drug present in optimized FA-CS-NPs and K_0, K and K_h were constant of the equation of zero order, first order and Higuchi model respectively.

5.13 *In-Vitro* cell viability assay

5.13.1 Characterization of cell lines and culture media

Characterization is essential, not only when deriving new lines, but also when a cell line is obtained from a cell bank or other laboratory. Cultures were examined under an inverted phase microscope before start of experiments and frequent assessments are made of the viability of the cell population throughout the experimental periods.[64-66, 78]

5.13.1.1 Testing for Microbial Contamination

The two methods were used to check for bacterial and fungal contamination. Detection carried out using special media like Fluid thiogycolate media (TGM) and Tryptone Soya broth (TSB) and direct observation using Grams stain.

Contamination by bacteria, yeast or fungi was detected by an increase in turbidity of the medium and/or a decrease in pH (yellow in media containing phenol red as a pH indicator). Cells were inspected daily for presence or absence of microbial growth.

Protocol

1. Cell lines were cultured in the absence of antibiotics prior to testing using 25cm^2 non-vented T flask.
2. In case of adherent cell line, attached cells were bringing in to into suspension using a cell scraper. Suspension cell lines were tested directly.
3. 1.5ml test sample (Cells) were Inoculated in to two separate test tubes of each containing Thioglycollate Medium (TGM) and Tryptone Soya broth (TSB).
4. 0.1ml *E.Coli*, 0.1ml *B. subtilis and* 0.1ml *C. sporogenes* inoculated in to separate test tubes (duplicate) containing (TGM) and (TSB) t as positive

controls where as two separate test tubes of each containing (TGM) and (TSB) un-inoculated as negative controls.[78]

Broths were incubated as follows:

a. For TSB, one broth of each pair were incubated at 32ºC the other at 22ºC for 4 days
b. For TGM, one broth of each pair were incubated at 32ºC the other at 22ºC for 4 days
c. For the TGM inoculated with *C.sporogenes* incubate at 32ºC for 4 days
d. Test and Control broths were examined for turbidity after 4 days.

5.13.1.2 Criteria for a Validity of results

If control broths show evidence of bacteria and fungi within 4 days of incubation in all positive control broths and the negative control broths show no evidence of bacteria and fungi.

Criteria for a Positive Result

Test broths containing bacteria or fungi show turbidity.

Criteria for a Negative Result

Test broths should be clear and show no evidence of turbidity.

5.13.2 Preparation of media

5.13.2.1 Preparation of DMEM

10.7gm of DMEM powder was added in 1litre of distilled water and then it was stir continuously until clear solution formed. To this, $NaHCo_3$ was added to maintain pH 7.0-7.2 and then solution was filtered using membrane filtration assembly. It was Stored in reservoir bottle under room temperature.

5.13.2.2 Preparation of the Trypsin dilution

5ml of Trypsin solution was pipette out in to 50ml falcon tube containing 45ml of PBS using 10ml pipette.

5.13.3 Determination of cell viability, density and PDT

The quantification of cellular growth, including proliferation and viability, has become an essential tool for working on cell-based studies.

5.13.3.1 Cell viability by Trypan Blue Dye Exclusion Method

The viability of cells was determined by the Trypan Blue dye exclusion method. It takes advantage of the ability of healthy cells with uncompromised cytoplasmic membrane integrity to exclude dyes such as trypan blue.[78]

Haemocytometer Cell Counts

1. Hemocytometer and cover slip were cleaned and wiped with 70% alcohol. Than cover slip were placed on haemocytometer.
2. In separate 2ml centrifuge tube, cell suspension (cells in culture media) was added. Than two fold dilution of reaction mixture was prepared by mixing aliquot of 0.1 ml cell suspensions with 0.1 ml trypan blue.
3. Afterwards 0.1ml of Cell suspension was then placed in to chamber of haemocytometer.
4. By using a Lieca inverted microscope, numbers of cells were counted in $1mm^2$ area with use of 10X objective.
5. Viable and non-viable cells were counted in both halves of the chamber[78]

Calculations

(1) Total number of viable cells = A x Bx C x 10^4

(2) Total dead cell count = A x B x D x 10^4 Where,

A = Vol. of cell solution (ml)

B = Dilution factor in trypan blue

C = Mean number of unstained cells

D = Mean number of dead/stained cells

10^4 = Conversion of 0.1 mm^3 to ml

(3) Total cell count = Viable cell count + dead cell count

% viability = (Viable cell count/Total cell count) X 100

5.13.3.2 Cell density

It was particularly important in case of adherent cell line like MCF-7, HT-29 and VERO. It was calculated by following equation:

[No. of cells /well or flask] / [surface area of well or flask]

5.13.3.3 Population doubling time (PDT)

It is the time expressed in hours, taken for cell number to double and is reciprocal of the multiplication rate. (1/r)

N^H= no. of cells harvested at the end of growth period that is t_2

N^I = no. of cells inoculated at time t_1= 0

Number of generation (n) = 3.32 ($\log N^H$ — $\log N^I$)

PDT = total time elapsed/no. of generations = 1/r

5.13.3.4 Multiplication rate (r)

No. of generation that occurs per unit time and is usually expressed as population doubling in 24 hours.

$r = 3.32 (\log N^H — \log N^I)/t_2\text{-}t_1$.

5.13.4 Subculturing /Passaging of cell lines

MCF-7, HT-29 and VERO are adherent cell line, which were subcultured as per following protocol.

1. All the reagents and cell lines were bring at room temperature before start of sub culture which include FBS, DMEM, EDTA –Trypsin solution (Trypsin-EDTA made by diluting the stock 1/10 by adding PBS only) and antibiotics. Cell line was handled under cytotoxicity cabinet to prevent cross contamination of cell lines.
2. Cells were subcultured when they were about 80-90% confluence.
3. Cells were washed with 0.1 ml DPBS- EDTA solution (1mM EDTA) per cm^2 of flask. The monolayer adhere to flask was gently rinsed by rocking the flask back and forth.
4. After 5 minutes, aspirate offs the excess PBS-EDTA from the flask.
5. To the above flask, 0.1-0.2 ml trypsin /cm^2 was added until the entire monolayer was covered, than flask was incubate for 3-5 min at room temperature to detach the cells from monolayer.
6. Cells were dispersed into a single cell suspension by pippeting the cell solution up and down. These Cells were added in to media flask (DMEM + BSS) containing FBS in it (FBS inactivates the trypsin, which was why it had to be rinsed off with DPBS-EDTA initially)

7. Cells were counted by haemocytometer and diluted to the appropriate concentration for seeding. Finally, the appropriate volume of cell suspension were added in to a new flask containing medium along with 1% antibiotic solution and Place flask in 5 % CO_2 incubator at 37°C.[78]

This splitting/passage was repeated every 3-4 days, so that they were not diluted too much or overgrown.

5.13.5 Design of 96-well plate

Design of the 96-well plate framed for the *in-vitro* viability assay is shown in Figure 5.6

	1	2	3	4	5	6	7	8	9	10	11	12	
A					10 µg/ml	20 µg/ml	40 µg/ml	60 µg/ml	80 µg/ml	100 µg/ml	NC	PC	Capecitabine
B					10 µg/ml	20 µg/ml	40 µg/ml	60 µg/ml	80 µg/ml	100 µg/ml	NC	PC	
C					10 µg/ml	20 µg/ml	40 µg/ml	60 µg/ml	80 µg/ml	100 µg/ml	NC	PC	CS-NPs
D					10 µg/ml	20 µg/ml	40 µg/ml	60 µg/ml	80 µg/ml	100 µg/ml	NC	PC	
E					10 µg/ml	20 µg/ml	40 µg/ml	60 µg/ml	80 µg/ml	100 µg/ml	NC	PC	Blank FA-CS-NPs
F					10 µg/ml	20 µg/ml	40 µg/ml	60 µg/ml	80 µg/ml	100 µg/ml	NC	PC	
G					10 µg/ml	20 µg/ml	40 µg/ml	60 µg/ml	80 µg/ml	100 µg/ml	NC	PC	Capecitabine loaded FA-CS-NPs
H					10 µg/ml	20 µg/ml	40 µg/ml	60 µg/ml	80 µg/ml	100 µg/ml	NC	PC	

Where, PC= positive control (cells + media; no drug),
NC=Negative control (only complete media; no cells; no drug)

Figure 5.6: Plate design

5.13.6 Experimental setup

5.13.6.1 Cell Lines and Culture Medium

MCF-7, HT-29 and VERO cell cultures, used in these experiments, were purchased from National Centre for Cell Science (NCCS), Pune. Stock cells of these cell lines were cultured in DMEM, supplemented with 10% FBS (fetal bovine serum). Along with media, cells were also supplemented with 5% HBSS, penicillin, streptomycin and Amphotericin-B (MP Biomedicals, Lot No: R23253, Hyclone, Lot no: JRM28184), in a humidified atmosphere of 5% CO_2 at 37°C until confluence attain. The cells were dissociated with 0.2% trypsin, 0.02% EDTA in phosphate buffer saline solution. The stock cultures were grown initially in 25 cm^2 tissue culture flasks, than

in 75 cm^2 and finally in 150 cm^2 tissue culture flask and all cytotoxicity experiments were carried out in 96 well microtitre plates. 5 X 10^4 cells/well were added in to each well of 96 well plate. It was calculated as follow.

5.13.6.2 Calculation for number of cells in 96-well plates

For this, number of cells required for 100 wells ≈96 well, was calculated

No. of cells/well x 100

= 5 x 10^4 x 100

= 5 x 10^6 cells/plate

Total volume of media for 100 wells

= volume of media/well x 100

= 100 µl x 100

= 10 ml

Therefore, 5 X 10^6 cells in 10ml of medium is required for one plate, and then required volume of cell suspension was added in to each wells.

5.13.6.3 Design of experiment

Cell lines in exponential growth phase were washed, trypsinized and re-suspended in complete culture media. Cells were seeded at 5x10^4 cells/well in 96 well microtitre plate and incubated for 72 hr during which a partial monolayer forms. The cells were then exposed to various concentrations of the test compounds, as indicated in plate design. Control wells were filled only with maintenance medium. The plates were incubated at 37 °C in a humidified incubator with 5% CO2 for a period of 72 h. Morphological changes of drug treated cells were examined using an inverted microscope at different time intervals and compared with the cells serving as control. At the end of 72h, cellular viability was determined using MTT assay.

5.13.7 Screening of test compounds by MTT assay

1. Cells were preincubated at a concentration of 1× 10^6 cells/ml in culture medium, taken in T flask, for 3 h at 37°C and 6.5% CO_2.
2. Cells were seeded at a concentration of 5× 10^4 cells/well in 100 µl culture medium and various amounts of nanoparticles (final drug concentration varying 10-100 µg/ml) were added into microplates (tissue culture grade, 96 wells, flat bottom).
3. Cell cultures were incubated for 24 h at 37°C and 6.5% CO2.

4. 10 µl MTT labeling mixture was added and incubate for 4 h at 37°C and 6.5% CO_2.
5. The formazan crystals that formed were solubilized by adding 150 µl solubilization solution (isopropanol containing 0.01N HCl) each well and incubated for overnight
6. Number of viable cells in each well was determined from the absorbance at 570 nm in a 96-well plate reader.[78, 83, 89, 101, 116]

5.13.7.1 Data interpretation

Absorbance values that are lower than the control cells indicate a reduction in the rate of cell proliferation. Conversely, a higher absorbance indicates an increase in cell proliferation.

After 72hr, the cytotoxicity data was evaluated by determining absorbance and calculating the correspondent chemical concentrations. Linear regression analysis with 95% confidence limit and R^2 were used to define dose-response curves and to compute the concentration of test compounds required, to reduce absorbance of the formazan by 50% (IC_{50}).

Percentage cell growth inhibition or percentage cytotoxicity was calculated by following formula

% viability = $(A_T-A_B) / (A_C-A_B)$ X 100

Where,
$A_{T=}$Absorbance of treated cells (drug)
$A_{B=}$Absorbance of blank (only media)
$A_{C=}$Absorbance of control (untreated)

There by,
% cytotoxicity = 100 - % cell survival

5.14 *In-vitro* cell uptaking assay

In-vitro cell uptake assay was done by fluorescent microscopy by labeling the nano-particles with fluorescent dye, rhodamine B, as given below.

5.14.1 Labeling of rhodamine B to FA-CS-NPs

Five milligrams of rhodamine B isothiocyanate was dissolved in 1 ml of DMSO. Rhodamine B solution, 200µl, was added to 1 ml of 10 mg/ ml CS-NPs and FA-CS-NPs separately, and then 1 ml of 2M pH 9.0 Na2CO3/NaHCO3 buffer was added to the mixtures, which was kept for 12 h at 4°C under dark condition, and the mixture was dialyzed against distilled water to remove the free rhodamine B.[83]

Mechanism of rhodamine B labeling to NPs is given in Figure 5.7.

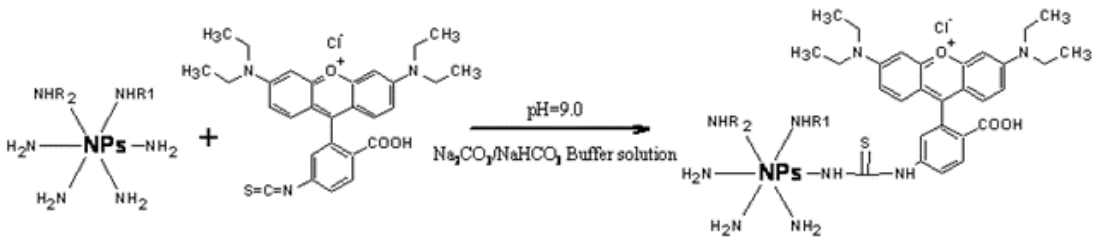

Figure 5.7: Mechanism of rhodamine B labeling to CS-NPs

5.14.2 Assay protocol

Cell uptaking of the nanoparticles by various cell-lines was done to analyze the cancer targeting of the drug by folic acid conjugated chitosan nanoparticles. Same procedure was used to evaluate the colon-cancer targeting ability of optimized CS-NPs and FA-CS-NPs, as given below[78, 83, 89-91, 101, 116]

1. HT-29, VERO and MCF-7 cells were incubated separately in 6-well plate at 37°C and 5% CO_2.
2. After 24 h, rhodamine B labeled optimized CS-NPs-8 and FA-CS-NPs-12 were added into the medium and incubated with cells, separately.
3. The cells were then harvested by trypsinization and centrifuged at 1,000 rpm for 05 min at 4°C.
4. Finally, the cells were resuspended in 500µl of PBS and stored on ice until analysis
5. The fluorescence intensity was measured using confocal laser scanning microscopy.

5.15 Stability study

5.15.1 Stability study of optimized CS-NPs

The stability study was carried out for Capecitabine loaded optimized CS-NPs as per ICH guidelines. Nanoparticles of the optimized batch were placed in screw capped glass container and stored at various ICH storage condition which are 25^0 C ± 2^0C (60%± 5%RH) and 40^0 C ± 2^0C (75%± 5%RH) for a period of 90 days. The samples were analyzed for physical appearance, percentage drug content and drug release study at regular interval of 15 days.

5.15.2 Stability study of optimized FA-CS-NPs

The stability study was carried out for Capecitabine loaded optimized FA-CS-NPs as per ICH guidelines. FA-CS-NPs of the optimized batch were placed in screw capped glass container and stored at various ICH storage condition which are 25^0 C ± 2^0C (60%± 5%RH) and 40^0 C ± 2^0C (75%± 5%RH) for a period of 90 days. The samples were analyzed for physical appearance, percentage drug content and drug release study at regular interval of 15 days.

6. RESULTS

6.1 Preformulation study

Various preformulation parameters were evaluated before formulation of the nanoparticles and the results were as per following

6.1.1 Physical nature of drug

Color, odor and appearance are the primary criteria to check the authenticity of any drug or excipients. A result of such parameters for capecitabine is given in Table 6.1.

Table 6.1: Color, Odor and Appearance of capecitabine

Sr No.	Parameter	observations
1	Color	White
2	Odor	Odorless
3	Appearance	Crystalline powder

6.1.2 Solubility of capecitabine in water

Solubility of capecitabine was evaluated in water, phosphate buffer solution pH 7.4 and 1% v/v acetic acid and the result is given in Table 6.2.

Table 6.2: solubility of capecitabine in various solvents

Sr No.	Solvent	Solubility	Terms
1	Water	25±0.19 mg/ml	sparingly soluble
2	1% v/v acetic acid	28.24±0.08 mg/ml	sparingly soluble
3	Phosphate buffer solution pH-7.4	31.21±0.11 mg/ml	sparingly soluble

6.1.3 Melting point of capecitabine

Melting point of capecitabine was determined for its authenticity and purity, and the result is given in Table 6.3.

Table 6.3: Melting point of capecitabine

Reported Melting Point	Observed Melting Point
115-120^{0}C	117 - 121^{0}C

6.1.4 λ_{max} of capecitabine and folic acid

Wavelength for the maximum absorbance (λ_{max}) was determined for capecitabine as well as folic acid using spectrophotometer and the result of the same is given in Table 6.4

Table 6.4: λ_{max} of capecitabine and folic acid

Chemical	λmax (nm)
Capecitabine (in PBS pH 7.4)	240
Capecitabine (in 1% v/v acetic acid)	243
Capecitabine (in Water)	240
Folic acid	283

6.1.5 Calibration curve of capecitabine

Calibration curve of the capecitabine in water was evaluated in triplicate using spectrophotometer at λmax 240nm. Data of the same is given in Table 6.5 and graph of the calibration curve is given in Figure 6.1

Table 6.5: Calibration curve of capecitabine in water at λmax 240 nm

Sr. No.	Conc. (µg/ml)	Absorbance			Mean ± SD
		I	II	III	
1	5	0.098	0.099	0.098	0.098±0.000577
2	10	0.193	0.195	0.194	0.194±0.001
3	20	0.411	0.411	0.413	0.412±0.001155
4	30	0.709	0.703	0.71	0.707±0.003786
5	40	0.968	0.97	0.96	0.966±0.005292

n=3

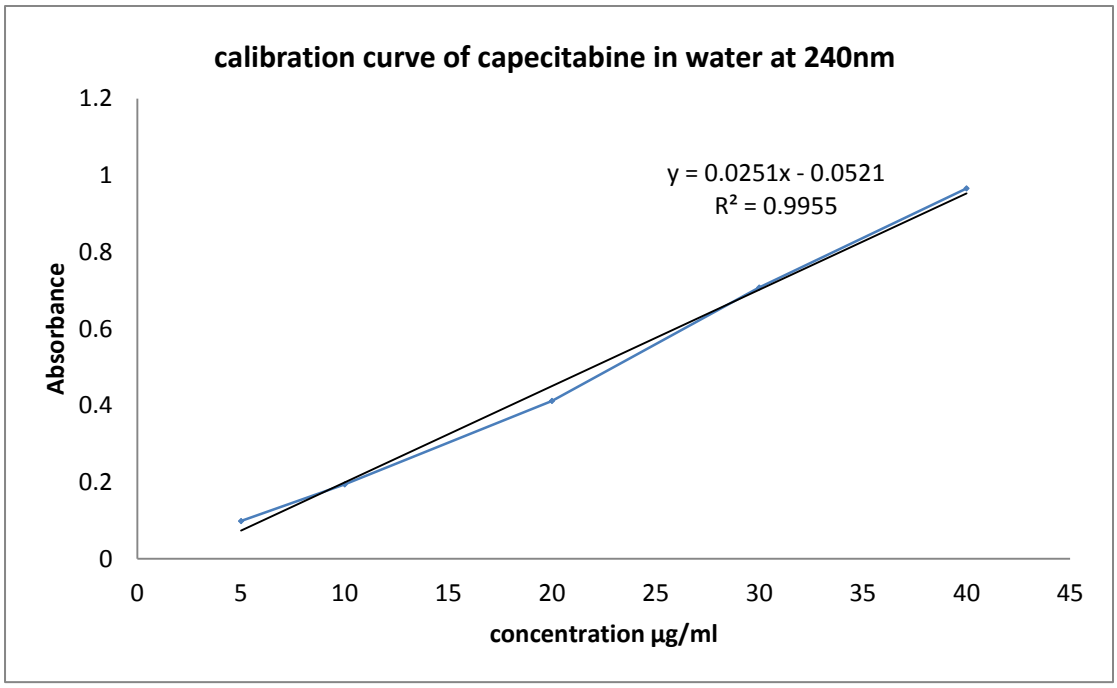

n=3

Figure 6.1: Calibration curve of capecitabine in water at λmax 240 nm

Calibration curve of the capecitabine in phosphate buffer solution-pH 7.4 was evaluated in triplicate using spectrophotometer at λmax 240nm. Data of the same is given in Table 6.6 and graph of the calibration curve is given in Figure 6.2

Table 6.6: Calibration curve of capecitabine in PBS pH 7.4 at λmax 240 nm

Sr. No.	Conc. (µg/ml)	Absorbance			Mean ± SD
		I	II	III	
1	5	0.105	0.099	0.101	0.101±0.003055
2	10	0.199	0.201	0.196	0.198±0.002517
3	20	0.438	0.441	0.435	0.438±0.003
4	30	0.724	0.72	0.728	0.724±0.004
5	40	0.987	0.99	0.985	0.987±0.002517

n=3

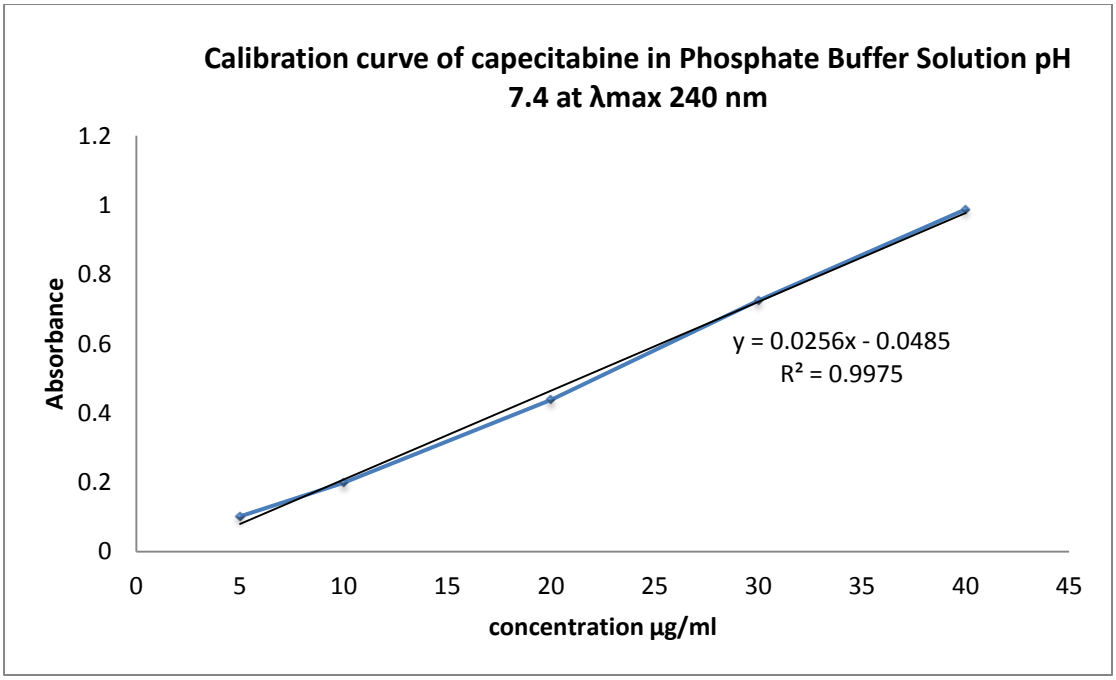

n=3

Figure 6.2: Calibration curve of capecitabine in Phosphate Buffer Solution pH 7.4 at λmax 240 nm

6.1.6 Calibration curve of folic acid in pH buffer 7.4

Calibration curve of folic acid in phosphate buffer solution-pH 7.4 was evaluated in triplicate using spectrophotometer at λmax 283nm. Data of the same is given in Table 6.7 and graph of the calibration curve is given in Figure 6.3

Table 6.7: Calibration curve of folic acid in PBS pH 7.4 at λmax 283nm

Sr. No.	Conc. (µg/ml)	Absorbance			Mean(±SD)*
		I	II	III	
1	4	0.251	0.250	0.252	0.251±0.001
2	8	0.507	0.506	0.505	0.506±0.0011
3	12	0.666	0.667	0.667	0.667±0.002
4	16	0.897	0.898	0.897	0.897±0.0011
5	20	1.139	1.139	1.138	1.139±0.015

n=3

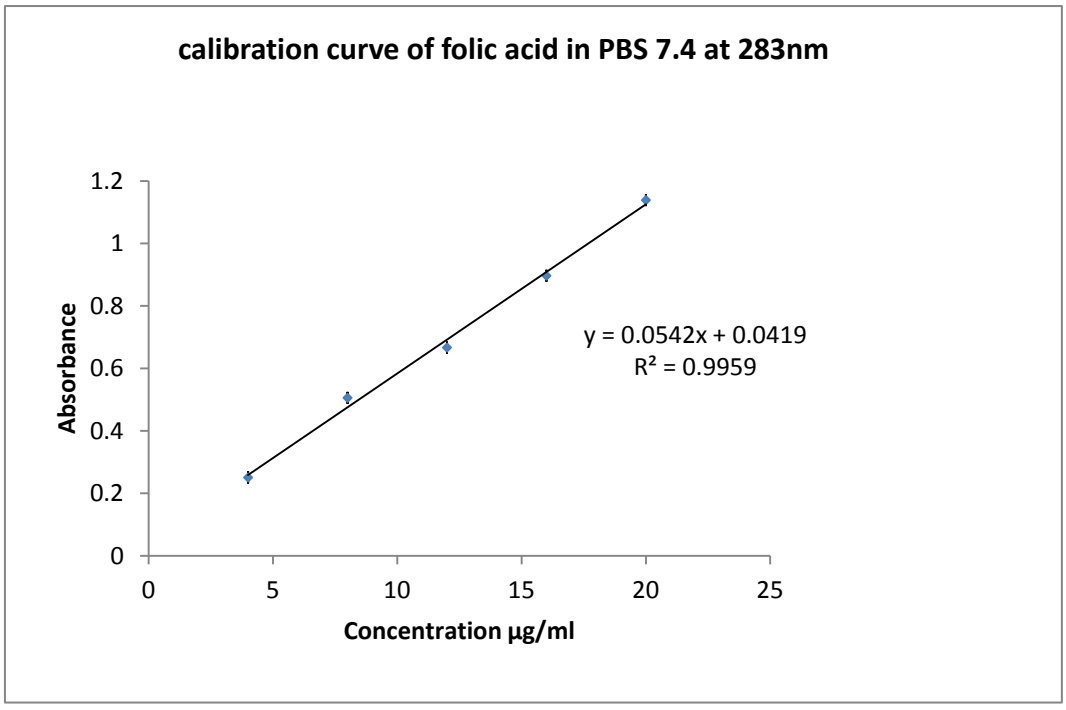

n=3

Figure 6.3: Calibration curve of folic acid in phosphate buffer saline solution pH 7.4 at λmax 283 nm

6.1.7 FT-IR studies

FT-IR study was carried out to evaluate the compatibility of capecitabine with excipients. For this purpose the IR spectra of alone capecitabine, alone chitosan, alone TPP, alone folic acid and then mixture of all these were taken, which are given in Figure 6.4, Figure 6.5, Figure 6.6, Figure 6.7 and Figure 6.8 respectively.

6.1.7.1 Capecitabine

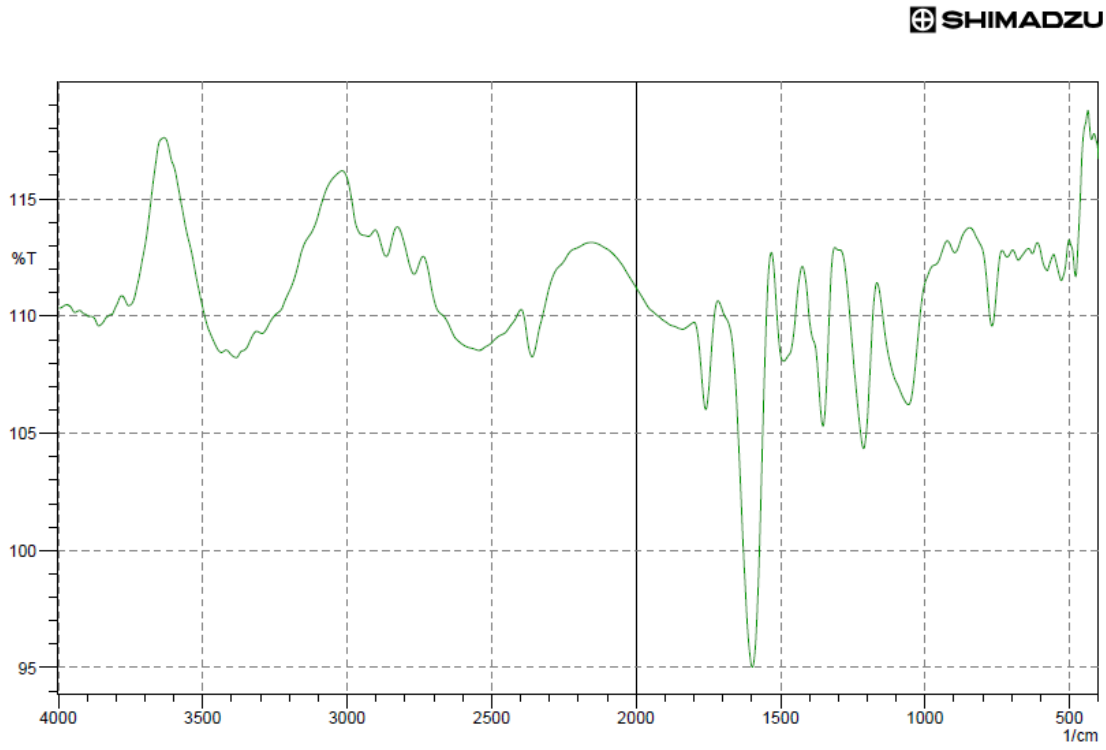

Figure 6.4: FT-IR Spectrum of capecitabine in range 4000 to 400 cm^{-1}

6.1.7.2 Chitosan

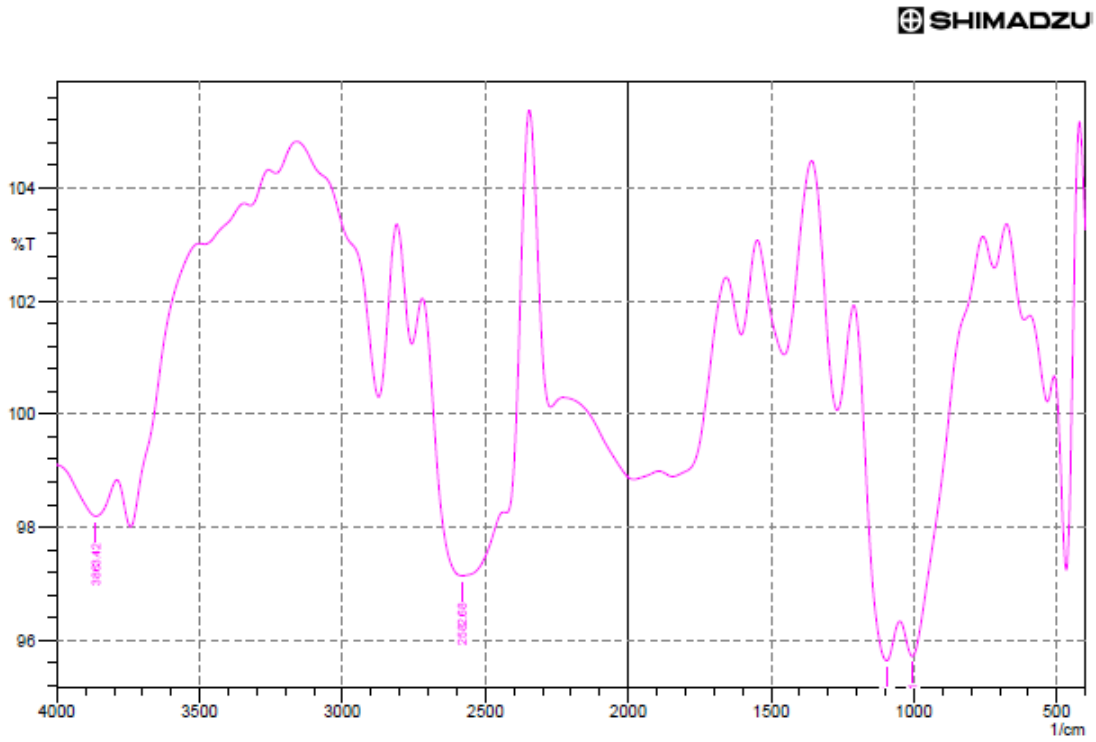

Figure 6.5: FT-IR Spectrum of Chitosan in range 4000 to 400 cm^{-1}

6.1.7.3 TPP

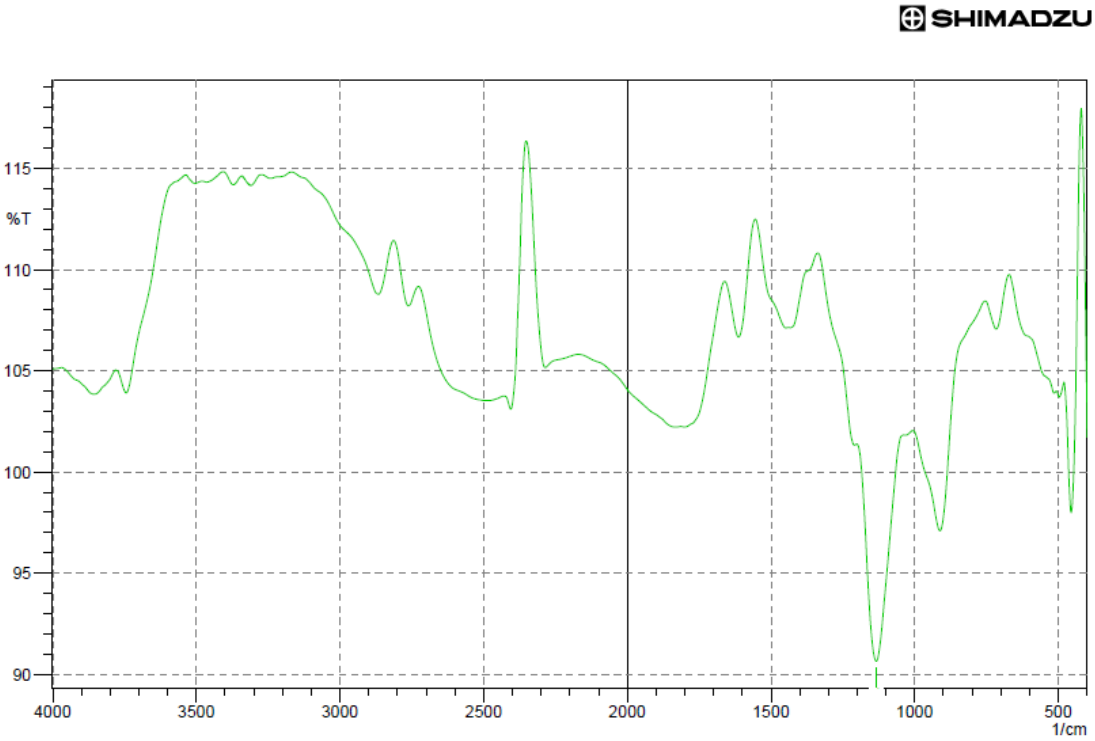

Figure 6.6: FT-IR Spectrum of TPP in range 4000 to 400 cm^{-1}

6.1.7.4 Folic acid

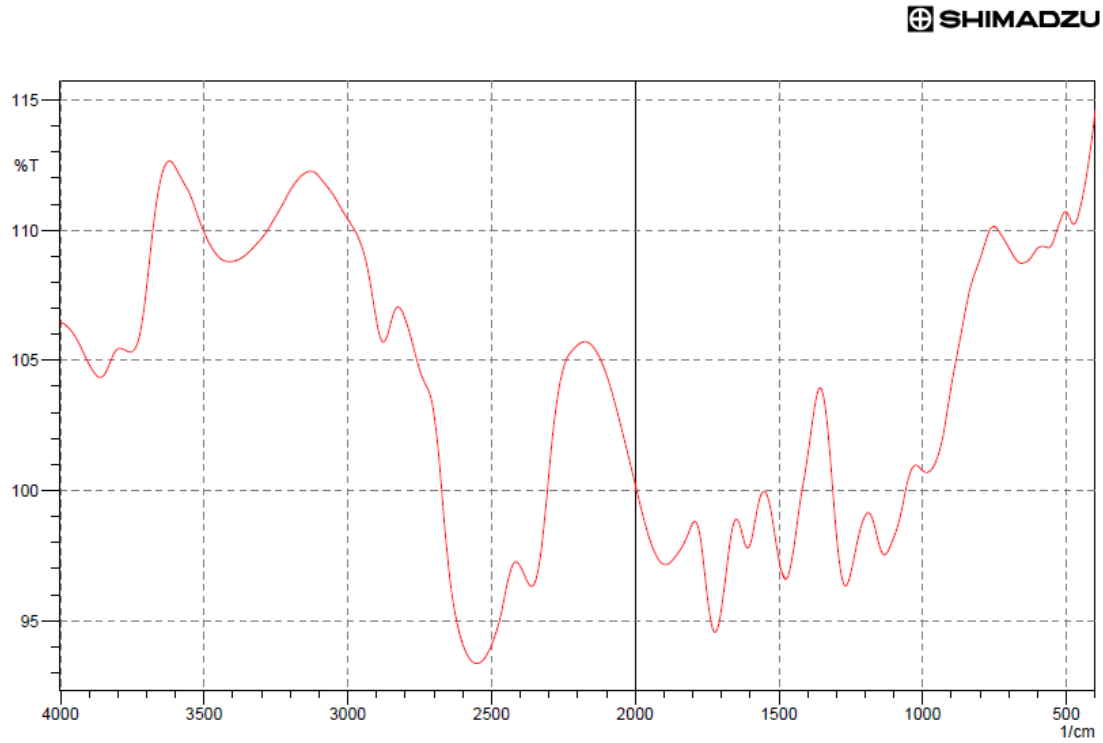

Figure 6.7: FT-IR Spectrum of folic acid in range 4000 to 400 cm^{-1}

6.1.7.5 Mixture of capecitabine + chitosan + TPP + folic acid

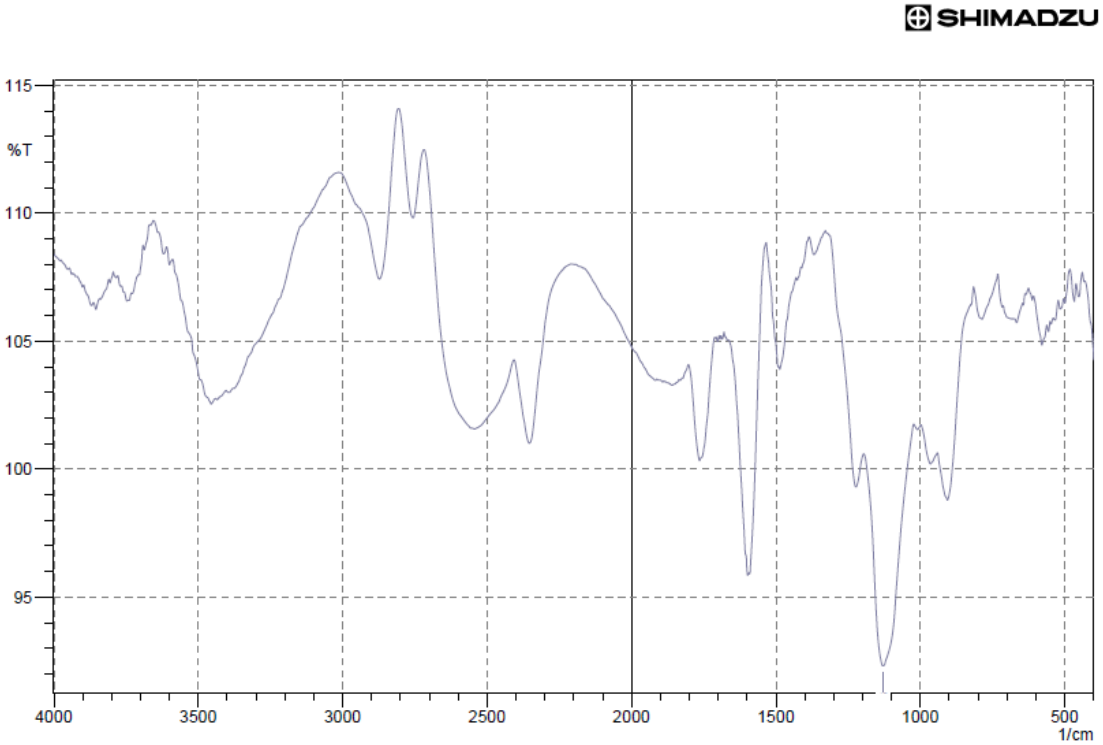

Figure 6.8: FT-IR Spectrum of mixture of capecitabine + chitosan + TPP + folic acid in range 4000 to 400 cm^{-1}

6.2 Characterization of CS-NPs

6.2.1 % yield, % entrapment efficiency (EE) and % drug content

Data for the % yield, % entrapment efficiency (EE) and % drug content are given in Table 6.8 and graphically represented in Figure 6.9, Figure 6.10 and Figure 6.11 respectively

Table 6.8: Data of % yield, % entrapment efficiency (EE) and % drug content of capecitabine CS-NPs

Batch No.	%Yield	%EE	%Drug content
CS-NPs -1	69.6±1.4	45.7±1.5	25.18±0.62
CS-NPs -2	66.38±1.21	57.94±1.25	27.2±0.76
CS-NPs -3	62.07±0.95	52.9±1.023	24.85±.54
CS-NPs -4	65.2±2.06	63.01±2.53	27.56±0.91
CS-NPs -5	70.1±1.3	80.15±1.32	28.67±1.04
CS-NPs -6	73.9±0.96	76.57±2.5	25.87±0.82
CS-NPs -7	54.17±2.5	60.39±2.21	24.66±0.85
CS-NPs -8	69.64±1.11	85.74±2.36	29.9±0.91
CS-NPs -9	70.06±0.93	81.19±3.21	23.03±0.43

*n=3

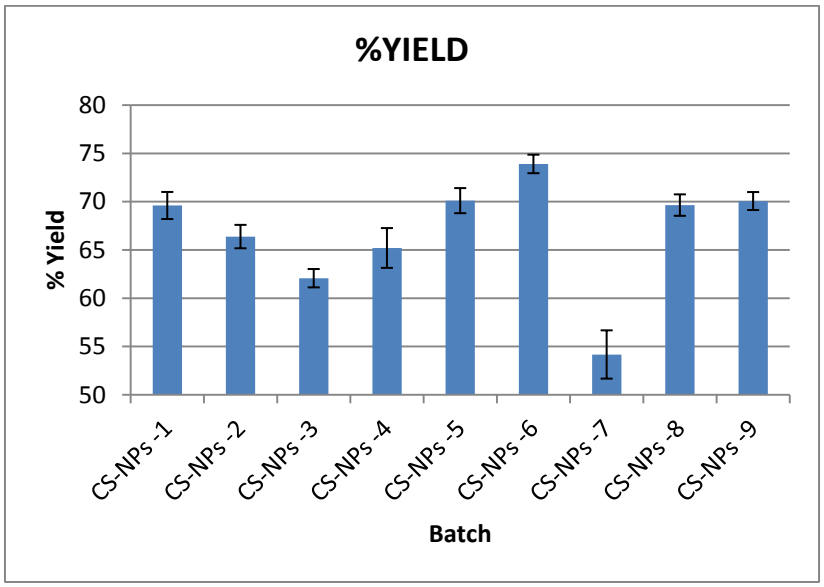

Figure 6.9: Column diagram for % yield of CS-NPs

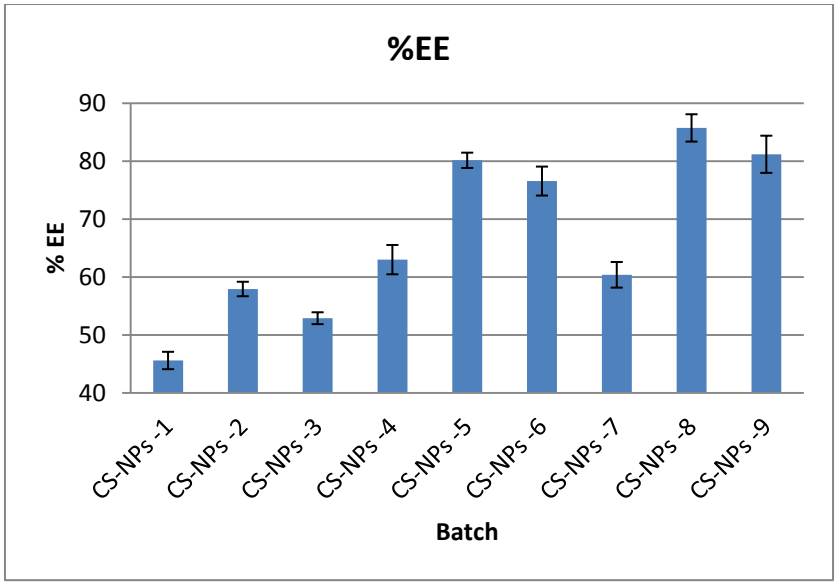

Figure 6.10: Column diagram for % Entrapment efficiency of capecitabine in CS-NPs

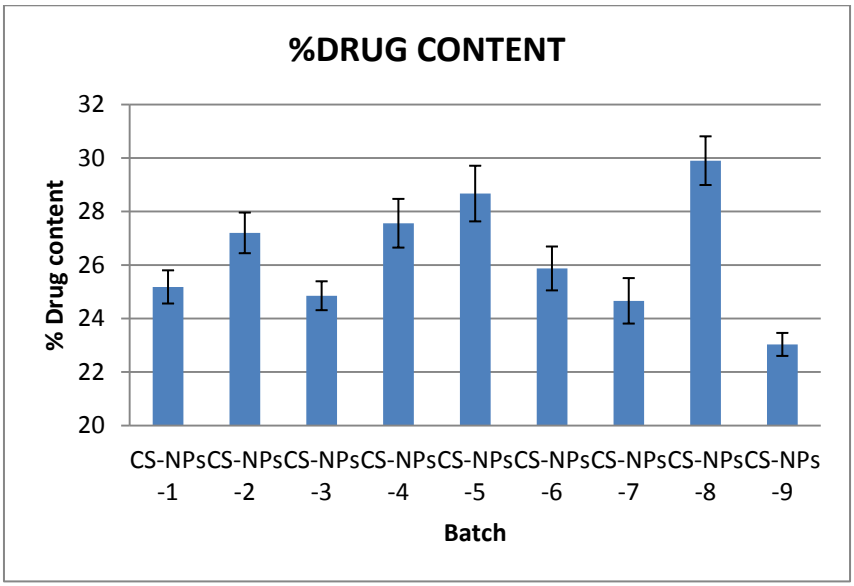

Figure 6.11: Column diagram for % drug content in CS-NPs

6.2.2 *In-Vitro* Diffusion Study of CS-NPs

Drug release from the chitosan nanoparticles was evaluated by in-vitro diffusion study and its drug release data of all 09 batches are given in Table 6.9 and Table 6.10. Percentage cumulative drug release profile against time is graphically represented in Figure 6.12 for batches CS-NPs-1 to 3, Figure 6.13 for batches CS-NPs-4 to 6 and Figure 6.14 for batches CS-NPs-7 to 9

Table 6.9: Release profile of CS-NPs-1 to CS-NPs-5 batches.

Time (hrs)	%CDR				
	CS-NPs-1	CS-NPs-2	CS-NPs-3	CS-NPs-4	CS-NPs-5
0	0	0	0	0	0
1	5.5±0.57	11.2±0.41	5.8±0.45	3.5±0.61	6.8±0.32
2	7.1±0.92	18.9±0.56	7.1±0.71	4.5±0.82	11.6±0.64
3	9.3±0.97	25.1±0.65	9.9±0.91	6.21±0.91	13.9±1.15
4	13.01±1.01	31.7±1.06	13.9±0.95	8.1±0.96	31.2±0.86
5	14.08±1.53	36.1±1.11	16.7±1.02	11.4±1.04	38.6±1.1
6	18.2±1.87	41.9±2.1	19.6±1.15	25.9±1.7	45.22±1.5
7	23.4±2.08	45.4±2.05	25.4±2.1	39.06±1.31	52.6±1.61
8	36.8±1.26	52.1±1.57	32.7±2.11	47.4±2.28	59.7±2.4
12	53.01±1.58	62.02±2.01	56.7±1.71	67.27±2.2	70.12±1.38
24	73.29±2.01	74.04±2.13	77.72±1.97	81.09±1.72	85.17±1.65
48	73.5±2.15	74.8±2.20	78.9±2.15	82.11±2.11	85.7±2.15

*n=3

Table 6.10: Release profile of CS-NPs-6 to CS-NPs-9 batches

Time (hrs)	%CDR			
	CS-NPs-6	CS-NPs-7	CS-NPs-8	CS-NPs-9
0	0	0	0	0
1	2.7±0.21	1.4±1.1	1.1±1.2	2.1±0.83
2	6.52±0.64	3.43±0.51	5.7±1.15	3.76±1.15
3	9.07±0.82	4.53±0.65	8.9±1.1	5.97±0.95
4	12.57±0.95	13.14±0.84	16.47±0.94	11.98±1.1
5	27.32±1.6	17.13±1.31	19.2±0.86	22.37±0.92
6	40.67±1.38	21.12±1.15	28.9±1.4	35.47±1.11
7	51.87±2.2	29.68±1.6	39.4±2.2	49.77±2.3
8	61.67±1.2	45.7±2.15	51.27±2.1	56.9±2.05
12	70.77±2.04	71.23±2.3	69.1±1.2	72.6±2.2
24	87.34±1.82	90.31±2.21	93.48±2.06	87.36±1.85
48	88.12±1.4	90.93±2.6	94.4±2.15	87.2±1.3

n=3

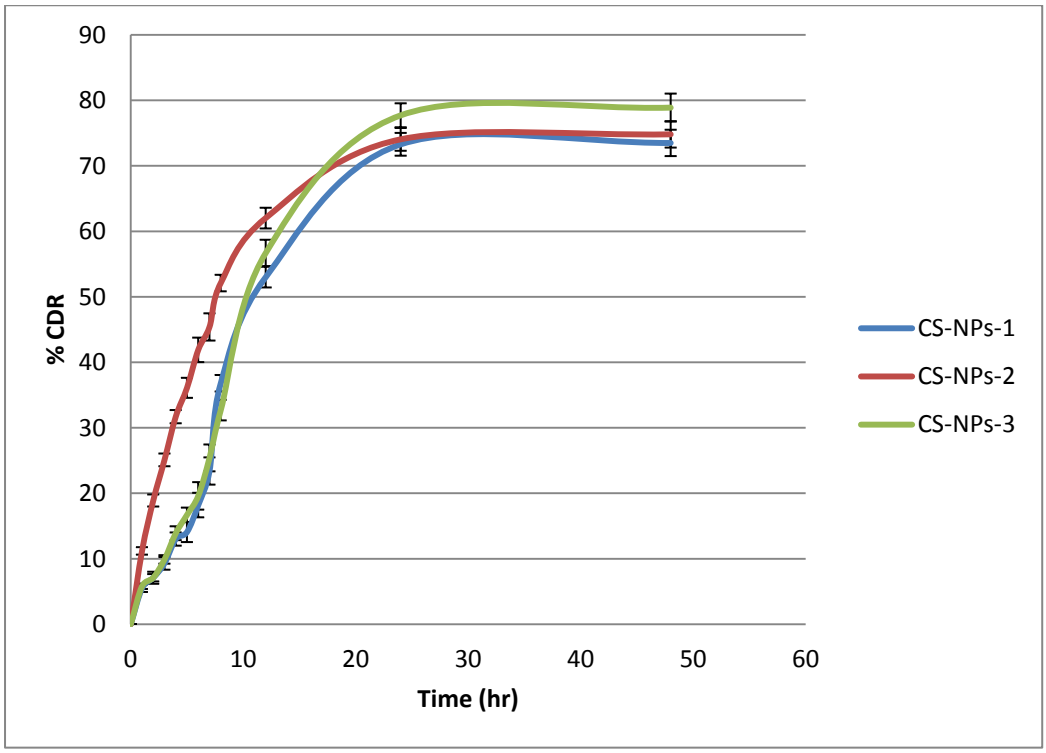

Figure 6.12: *In-Vitro* drug release profile of batch CS-NPs-1 to CS-NPs-3

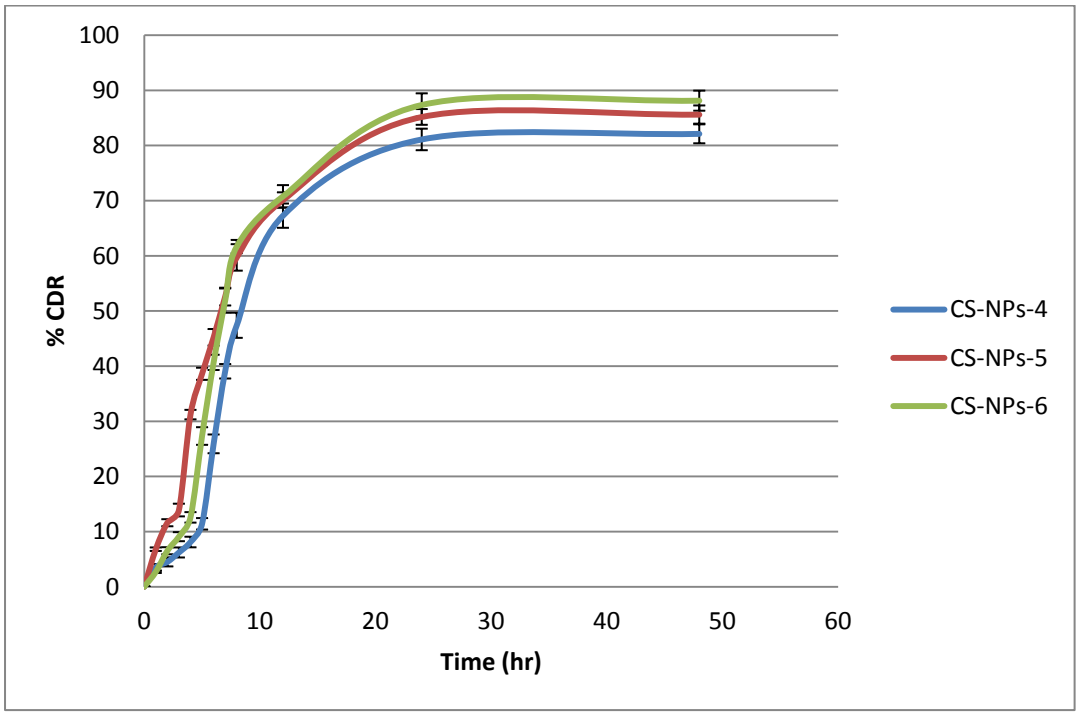

Figure 6.13: *In-Vitro* drug release profile of batch CS-NPs-4 to CS-NPs-6

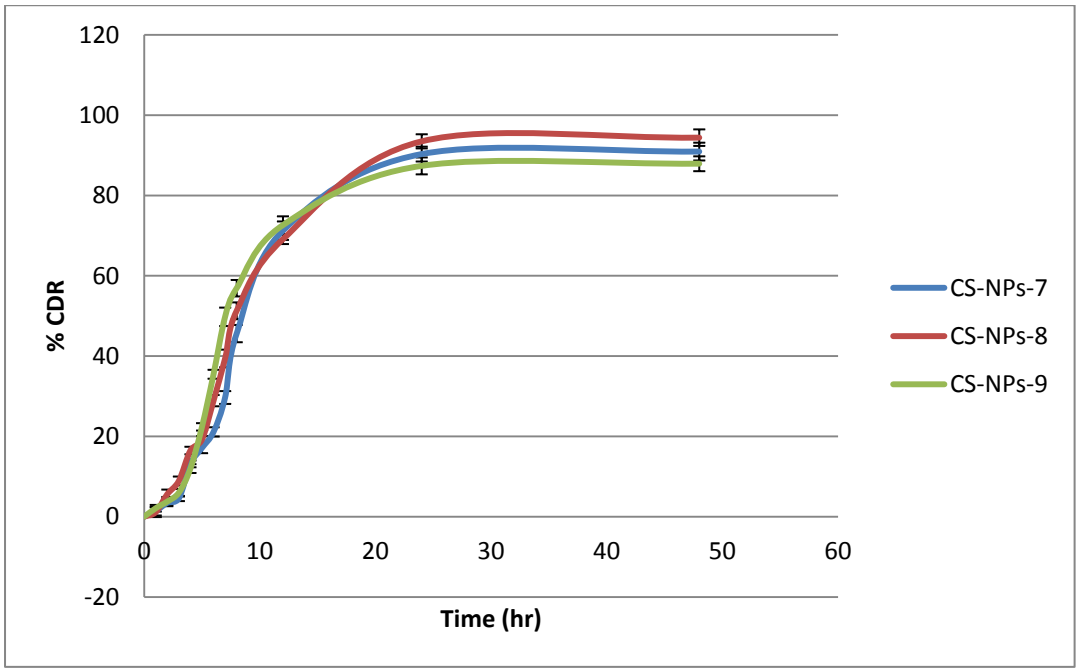

Figure 6.14: *In-Vitro* drug release profile of batch CS-NPs-7 to CS-NPs-9

6.3 Optimization of CS-NPs

6.3.1 Interaction between the factors

Various batches of CS-NPs with experimental entrapment efficiency along with interaction factors are presented in Table 6.11 and P-values of all these interaction factors obtained by the ANOVA of response surface quadratic model is given in Table 6.12

Table 6.11: Various batches of CS-NPs with experimental percentage entrapment efficiency along with interaction factors

Batch No.	X_1	X_2	$(X_1)^2$	$(X_2)^2$	X_1X_2	%EE
CS-NPs -1	-1	-1	1	1	1	45.6
CS-NPs -2	-1	0	1	0	0	57.94
CS-NPs -3	-1	1	1	1	-1	52.9
CS-NPs -4	0	-1	0	1	0	63.01
CS-NPs -5	0	0	0	0	0	80.15
CS-NPs -6	0	1	0	1	1	76.57
CS-NPs -7	1	-1	1	1	-1	60.39
CS-NPs -8	1	0	1	0	0	85.74
CS-NPs -9	1	1	1	1	1	81.19

Table 6.12: Analysis of variance for response surface quadratic model

	Coefficients	Standard Error	P-value
Intercept	80.12	1.83	0.000026
X_1	11.81	0.99	0.0013
X_2	6.43	1.01	0.0078
$(X_1)^2$	-8.26	1.76	0.0182
$(X_2)^2$	-11.85	1.73	0.0063
X_1X_2	3.07	1.15	0.0756

From the above Table 6.12 full polynomial equation was derived as per follows

$$\% \text{ EE} = 80.12 + 11.81X_1 + 6.43X_2 - 8.26(X_1)^2 - 11.85(X_2)^2 + 3.07X_1X_2$$

Then after, interaction factor showing P-value more than 0.05 was omitted and reduced surface quadratic model was obtained by regression analysis as shown in Table 6.13

Table 6.13: Analysis of variance for response surface reduced quadratic model

	Coefficients	Standard Error	P-value
Intercept	80.80	2.88	9.58E-06
X_1	11.81	1.58	0.0017
X_2	6.94	1.58	0.0117
$(X_1)^2$	-9.28	2.73	0.0273
$(X_2)^2$	-11.33	2.73	0.0143

From above Table 6.13 reduced polynomial equation was derived as per follows

$$\% \text{ EE} = 80.80 + 11.81X_1 + 6.94X_2 - 9.28(X_1)^2 - 11.33(X_2)^2$$

Predicted values of % EE of CS-NPs by response surface reduced quadratic model was compared with the real experimental value of all 09 batches of CS-NPs to calculate the difference in terms of % error, as shown in Table 6.14

Table 6.14: Experimental versus predicted values of % entrapment efficiency of CS-NPs by response surface reduced quadratic model

Batch	Experimental %EE	Predicted %EE	Residuals	% Error
CS-NPs -1	45.6	44.84	0.76	1.69
CS-NPs -2	57.94	60.04	-2.10	-3.50
CS-NPs -3	52.9	51.56	1.34	2.61
CS-NPs -4	63.01	61.84	1.17	1.89
CS-NPs -5	80.15	80.12	0.03	0.04
CS-NPs -6	76.57	77.78	-1.20	-1.55
CS-NPs -7	60.39	62.32	-1.93	-3.10
CS-NPs -8	85.74	83.67	2.07	2.47
CS-NPs -9	81.19	81.33	-0.14	-0.17

Finally, results of ANOVA of full and reduced quadratic model was compared, as summarized in Table 6.15, to calculate the F value as per calculation given below. Then this calculated F value was compared with the table value of F value to know whether the effect of interaction factor on response is significant or not, and also to justify the omission of non-significant interaction factor while obtaining the reduced surface quadratic model.

Table 6.15: Results of ANOVA of full model and reduced model

		df	SS	MS	F	R^2
Regression	FM	5	1597.83	319.57	54.28	0.989
	RM	4	1555.84	388.96	26.08	0.963
Residual	FM	3	17.66	5.89		
	RM	4	59.65	14.91		

df – degree of freedom, SS – sum of squares, MS – mean sum of squares, FM – full model, RM – reduced model

SSE2-SSE1=59.65-17.66=41.99

No. of terms omitted is during the reduced model = 01

MS of Error of FM=5.89

$$\text{F Calculated} = \frac{\dfrac{\text{SSE 2} - \text{SSE 1}}{\text{No of non significant terms omitted}}}{\text{MS of error of FM}}$$

$$= \frac{\dfrac{59.65 - 17.66}{1}}{5.89} = 7.13$$

Therefore, F value (Calculated) = 7.13, and from the table of F value, it was found to be, F value (Tabulated) = 11.35.

Hence, F calculated < F tabulated

6.3.2 Construction of contour plots

2D contour plot and 3D response surface plot of CS-NPs is given in Figure 6.15 and Figure 6.16 respectively

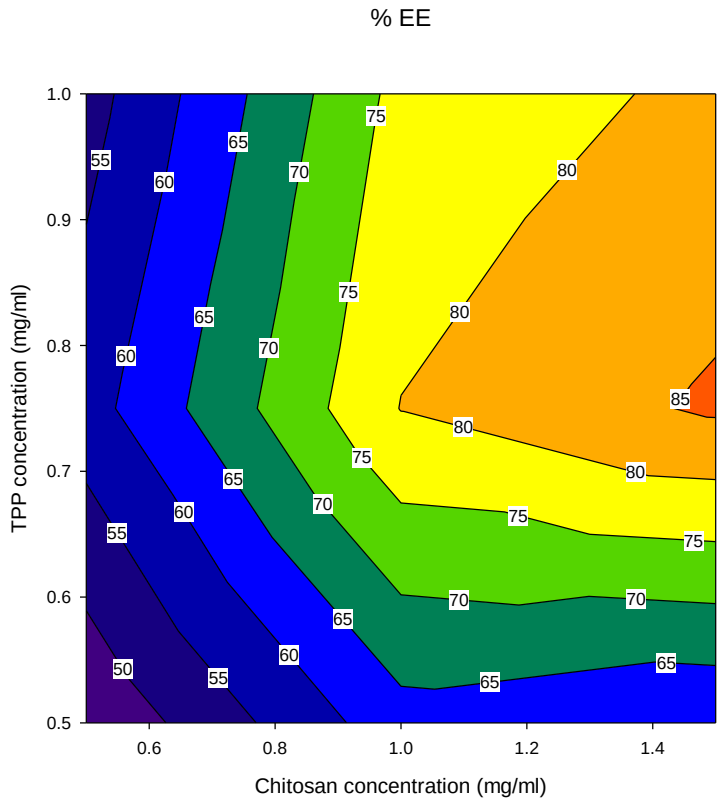

Figure 6.15: 2D Contour plot of CS-NPs for the effect of variables on the % EE response

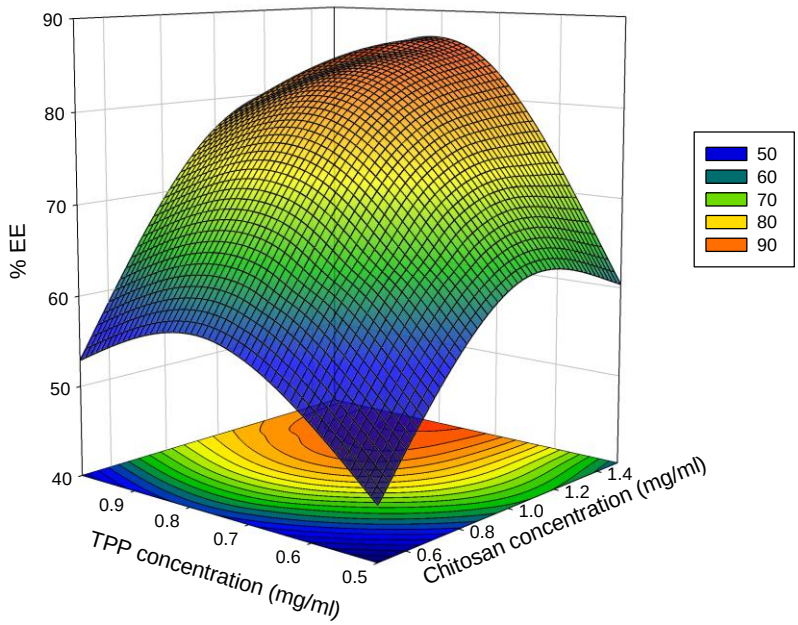

Figure 6.16: 3D plot of CS-NPs for the effect of variables on the % EE response

6.3.3 Evaluation of model / Check point analysis

Result of the check point analysis of the CS-NPs is summarized in Table 6.16

Table 6.16: Check point analysis of CS-NPs from the contour plot

Test batches	Response	Factors		Predicted value	Experimental value	% Error
		X_1	X_2			
Batch 1	% EE	1.5	0.75	85.74	84.29	1.69
Batch 2	% EE	1.5	0.76	85.95	83.82	2.48
Batch 3	% EE	1.5	0.77	86.29	84.75	1.78

6.4 Evaluation of Optimized CS-NPs

6.4.1 Particle size distribution and zeta potential

Optimized chitosan nanoparticle CS-NPs-8 was analyzed for its size, size distribution and electrical charge that they carry, using a Malvern particle size analyzer. Result is given in Figure 6.17 and Figure 6.18 respectively.

Size Distribution Report by Intensity
v2.1

Malvern

Sample Details

Sample Name:	CS-NPs		
SOP Name:			
General Notes:			
File Name:	SUMANDEEP.dts	**Dispersant Name:**	1% acetic acid
Record Number:	23	**Dispersant RI:**	1.330
Material RI:	1.59	**Viscosity (mPa.s):**	0.8872
Material Absorbtion:	0.010	**Measurement Date and Time:**	Thursday, February 13, 2014 ...

System

Temperature (°C):	25.0	**Duration Used (s):**	70
Count Rate (kcps):	228.9	**Measurement Position (mm):**	4.65
Cell Description:	Disposable sizing cuvette	**Attenuator:**	11

Results

			Size (d.nm):	% Intensity	Width (d.n...
Z-Average (d.nm):	87.23	**Peak 1:**	98.1	82.7	94.74
PdI:	0.113	**Peak 2:**	11.13	17.3	1.732
Intercept:	1.01	**Peak 3:**	0.000	0.0	0.000
Result quality :	Refer to quality report				

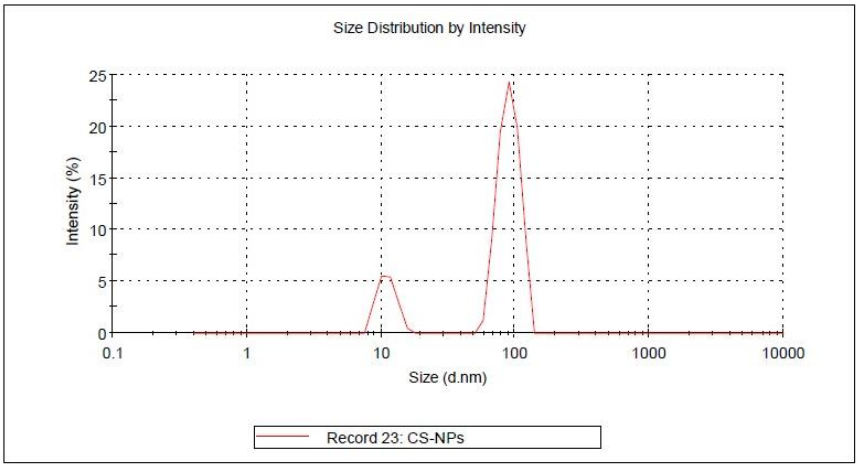

Figure 6.17: Particle size distribution of CS-NPs-8

Zeta Potential Report

v2.1

Malvern

Sample Details

Sample Name:	CS-NPs
SOP Name:	
General Notes:	

File Name:	SUMANDEEP.dts	**Dispersant Name:**	1% acetic acid
Record number:	13	**Dispersant RI:**	1.330
Date and Time:	Thursday, February 13, 2014	**Viscosity (cP):**	0.8872
		Dispesant Dielectric Constant:	78.5

System

Temperature (°C):	25.0	**Zeta Runs:**	70
Count Rate (kcps):	252.5	**Measurement Position (mm):**	2.00
Cell Description:	Clear disposable zeta cell	**Attenuator:**	7

Results

			Mean (mV):	**Area (%)**	**Width (mV)**
Zeta Potential (mv):	-35.9	**Peak 1:**	-35.9	100	3.85
Zeta Deviation (mv):	3.85	**Peak 2:**	0.000	0.0	0.000
Conductivity (mS/cm):	0.745	**Peak 3:**	0.000	0.0	0.000

Result quality : Refer to quality report

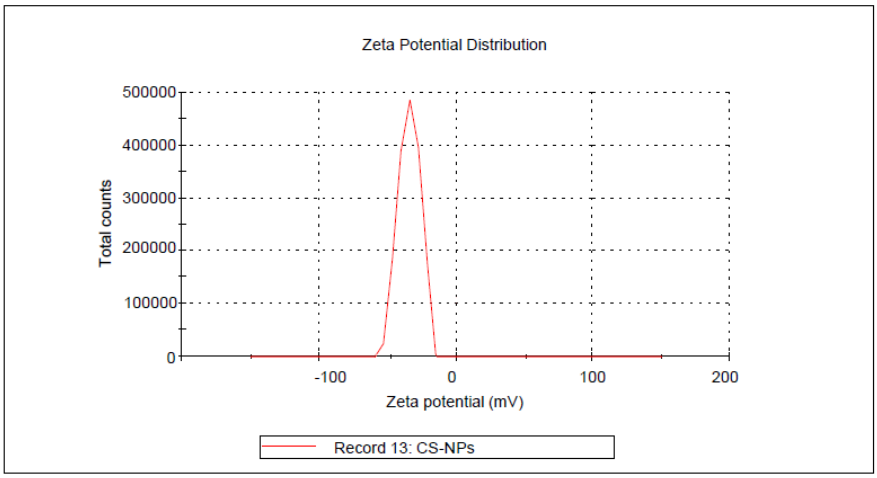

Figure 6.18: Zeta potential of CS-NPs-8

6.4.2 Scanning Electron microscopy

Surface morphology of optmized chitosan nanoparticles, CS-NPs-8, was evaluated by scanning electron microscopy, and the result of the same is given in Figure 6.19.

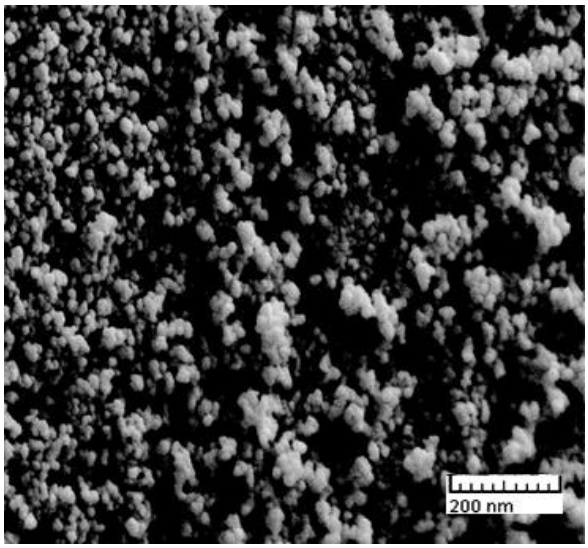

Figure 6.19: Scanning electron microscopic photograph of CS-NPs-8

6.4.3 FT-IR study

In the optimized chitosan nanoparticle, CS-NPs-8, compatibility of capecitabine with excipients was evaluated by taking the FT-IR spectra of CS-NPs-8, and compared it with the FT-IR spectrum of capecitabine. This comparison is given in Figure 6.20

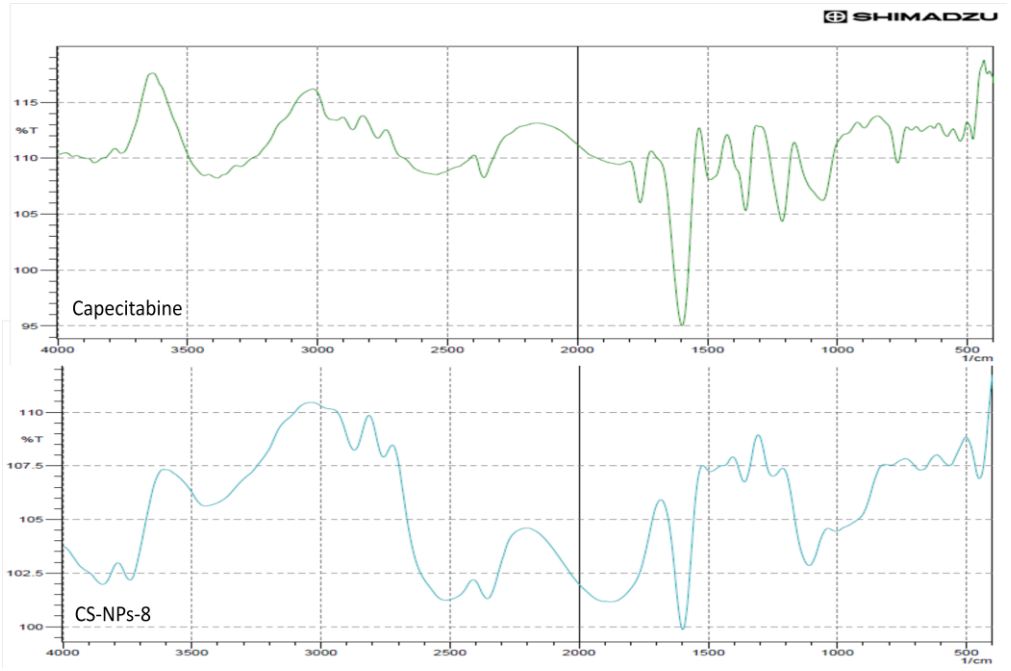

Figure 6.20: Comparison of FT-IR Spectrum of capecitabine and CS-NPs-8 in range 4000 to 400 cm^{-1}

6.4.4 Differential scanning calorimetry

Optimized chitosan nanoparticle, CS-NPs-8, were subjected to the differential scanning calorimetry to make the final confirmation about the compatibility of capecitabine with excipients by taking the DSC thermogram of CS-NPs-8, and compared it with the DSC thermogram of capecitabine. This comparison is given in Figure 6.21

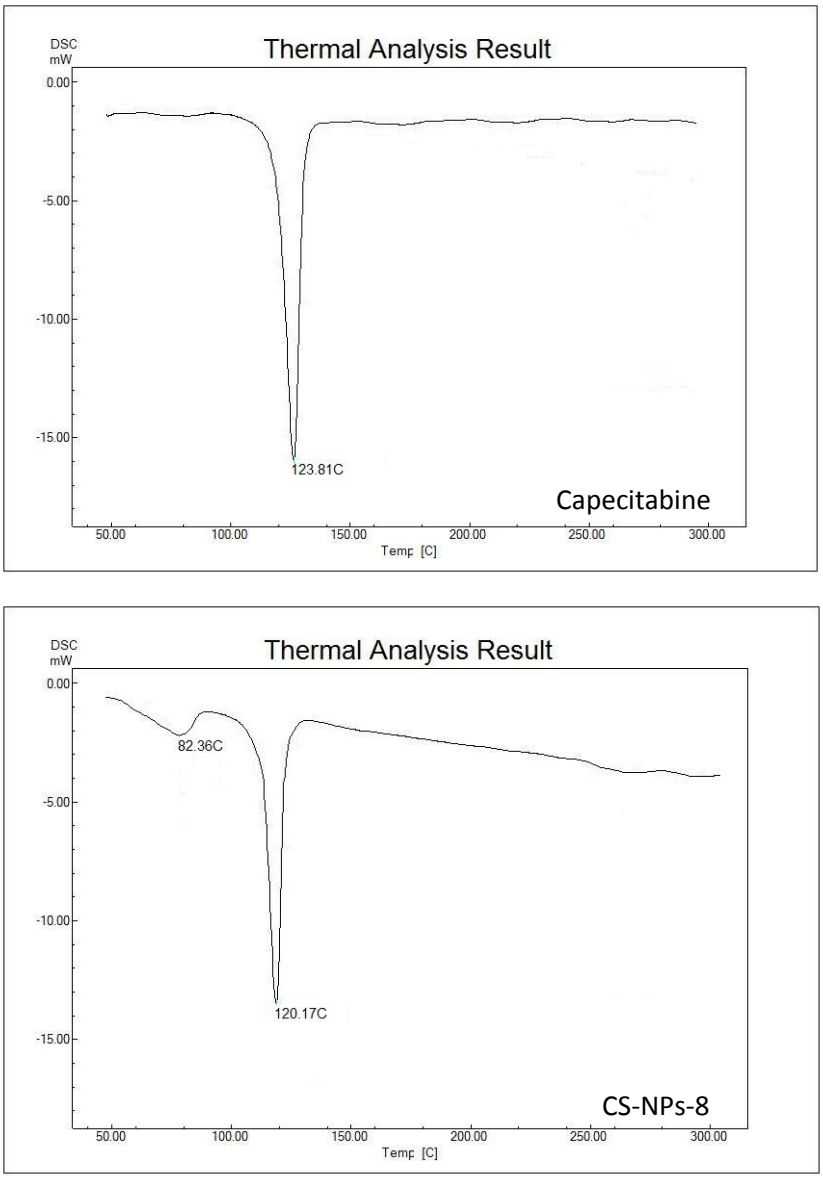

Figure 6.21: DSC thermogram of capecitabine and optimized CS-NPs-8

6.4.5 Drug release kinetics

Correlation coefficient of zero order, first order and higuchi model of drug release kinetics from optimized CS-NPs-8 is summarized in Table 6.17

Table 6.17: Drug release kinetics for an optimized formulation CS-NPs-8

Optimized formulation (CS-NPs-8)	Release kinetic model		
	Zero order	First order	Higuchi model
	R^2	R^2	R^2
	0.733	0.869	0.874

Drug release from optimized CS-NPs-8 as per the zero order, first order and higuchi model of the release kinetics are graphically represented in Figure 6.22, Figure 6.23 and Figure 6.24 respectively.

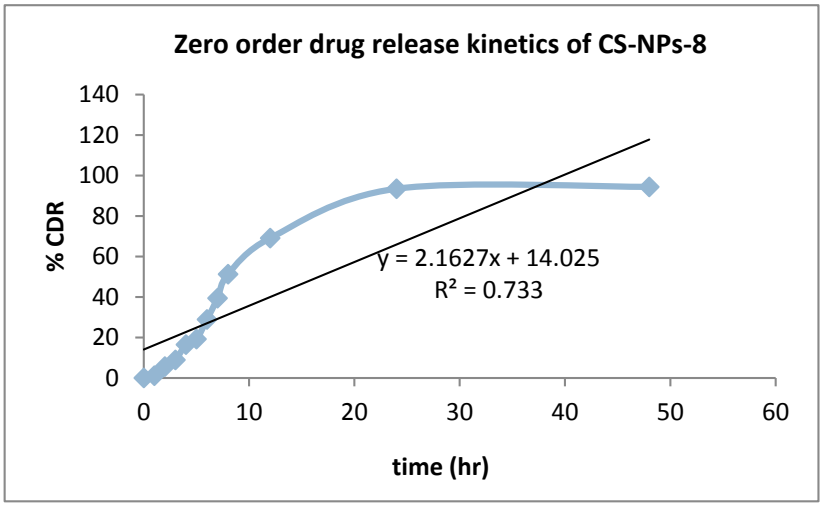

Figure 6.22: Zero order drug release kinetics of CS-NPs-8

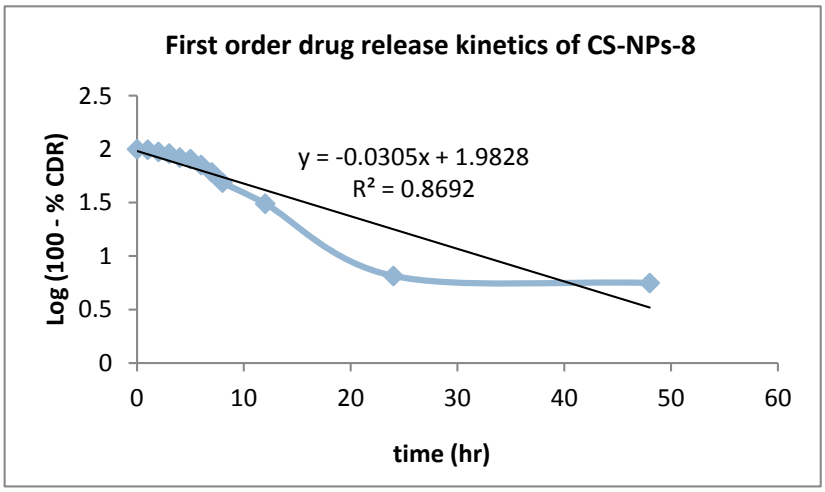

Figure 6.23: First order drug release kinetics of CS-NPs-8

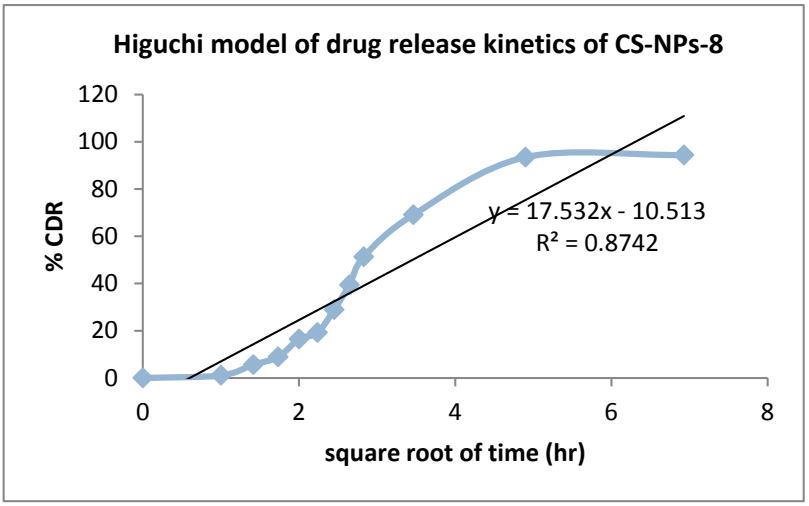

Figure 6.24: Higuchi model of drug release kinetics of CS-NPs-8

6.5 Characterization of FA-CS-NPs

6.5.1 % yield, % conjugation efficiency and % folic acid loading

Data for the % yield, % folic acid conjugation efficiency (CE) and % folic acid loading are given in Table 6.18 and graphically represented in Figure 6.25, Figure 6.26 and Figure 6.27 respectively

Table 6.18: % Yield, % Conjugation efficiency, and % FA loading of FA-CS-NPs

Batch No.	% Yield	% CE	% FA Loading
FA-CS-NPs-1	78.03±1.56	61.53±1.23	6.97±0.32
FA-CS-NPs-2	90.18±1.63	73.86±1.48	8.48±0.55
FA-CS-NPs-3	80.35±.81	87.78±0.96	7.91±0.15
FA-CS-NPs-4	88.19±2.28	68.39±2.17	6.15±0.28
FA-CS-NPs-5	79.17±0.97	70.64±1.41	7.39±0.34
FA-CS-NPs-6	93.13±1.73	62.19±1.64	9.31±0.54
FA-CS-NPs-7	87.65±2.51	51.59±2.03	8.49±0.25
FA-CS-NPs-8	88.74±1.55	68.17±1.36	6.82±0.31
FA-CS-NPs-9	81.28±1.65	59.27±1.59	8.97±0.41
FA-CS-NPs-10	88.06±2.22	63.94±2.33	13.91±0.63
FA-CS-NPs-11	82.12±1.68	78.38±1.57	16.25±0.74
FA-CS-NPs-12	95.23±0.81	91.23±0.82	18.57±1.03
FA-CS-NPs-13	86.73±2.47	69.81±1.20	14.75±0.58
FA-CS-NPs-14	80.09±1.60	64.45±1.47	13.92±0.72
FA-CS-NPs-15	93.27±2.03	85.17±1.70	17.7±0.80
FA-CS-NPs-16	85.71±1.42	55.33±2.11	12.19±0.40
FA-CS-NPs-17	89.37±1.57	69.76±1.40	11.28±0.69
FA-CS-NPs-18	75.82±1.67	70.11±1.60	16.66±0.76
FA-CS-NPs-19	79.63±2.19	52.57±0.85	14.02±0.64
FA-CS-NPs-20	73.27±2.33	45.23±2.02	15.93±0.72
FA-CS-NPs-21	76.89±1.48	64.48±3.29	16.13±0.87
FA-CS-NPs-22	77.47±1.10	48.79±0.82	13.32±0.61
FA-CS-NPs-23	81.95±2.28	41.47±0.97	10.22±0.65
FA-CS-NPs-24	75.37±1.41	62.41±1.85	15.9±0.36
FA-CS-NPs-25	75.74±2.03	38.19±0.76	12.11±0.45
FA-CS-NPs-26	79.28±1.17	44.79±2.90	13.09±0.60
FA-CS-NPs-27	70.99±2.32	59.53±1.19	16.36±0.83

n=3

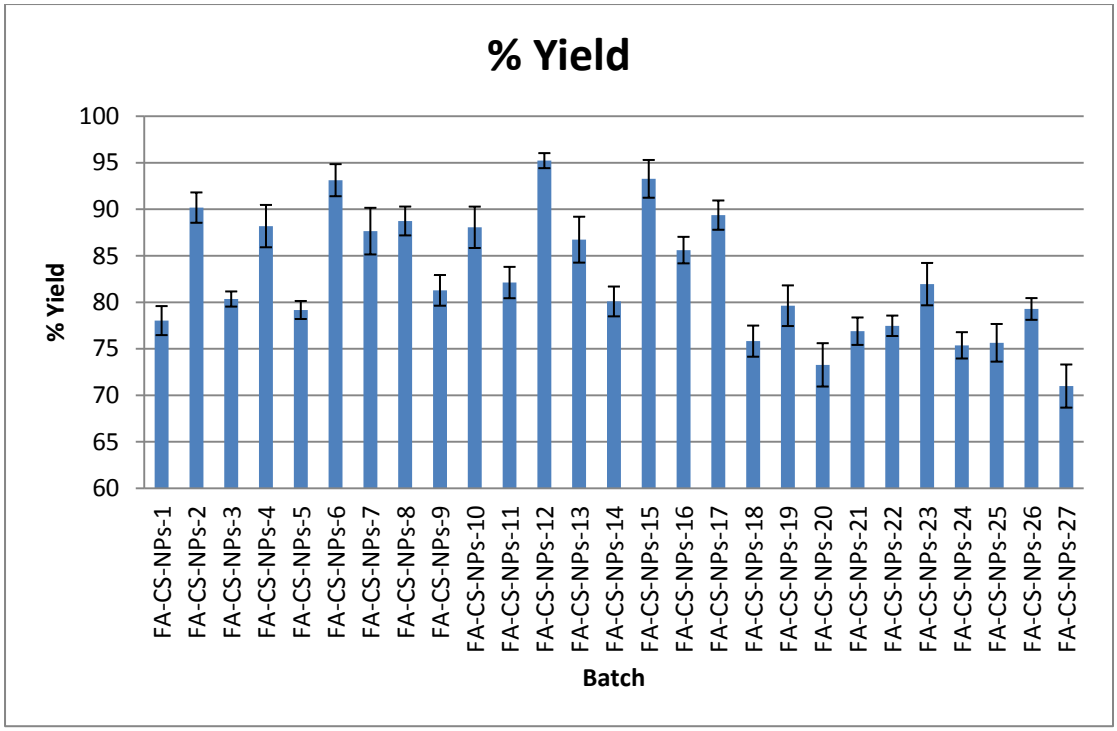

Figure 6.25: Column diagram for % yield of FA- CS-NPs

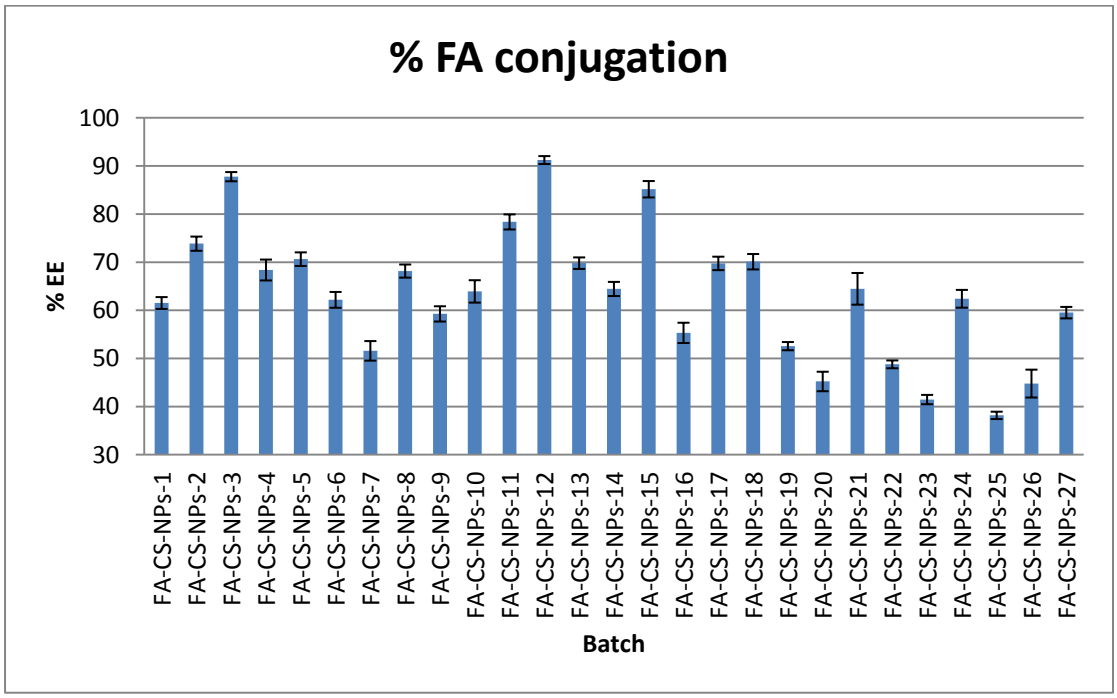

Figure 6.26: Column diagram for % Conjugation efficiency of folic acid in FA-CS-NPs

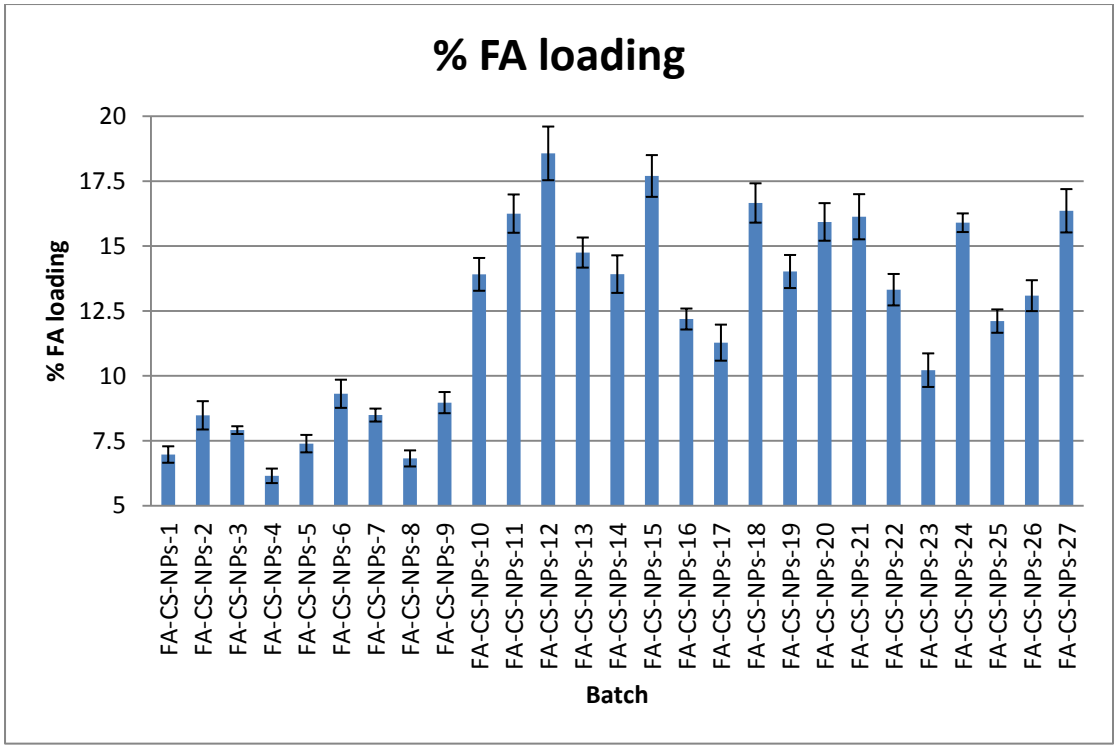

Figure 6.27: Column diagram for % FA loading in FA-CS-NPs

6.5.2 In-Vitro Diffusion of capecitabine from FA-CS-NPs

Drug release from the folic acid conjugated chitosan nanoparticles was evaluated by in-vitro diffusion study and its drug release data of all 27 batches is given in Table 6.19, Table 6.20, Table 6.21, Table 6.22, Table 6.23 and Table 6.24. Percentage cumulative drug release profile against time is graphically represented in Figure 6.28 for batches FA-CS-NPs-1 to 3, Figure 6.29 for batches FA-CS-NPs-4 to 6, Figure 6.30 for batches FA-CS-NPs-7 to 9, Figure 6.31 for batches FA-CS-NPs-10 to 12, Figure 6.32 for batches FA-CS-NPs-13 to 15, Figure 6.33 for batches FA-CS-NPs-16 to 18 , Figure 6.34 for batches FA-CS-NPs-19 to 21, Figure 6.35 for batches FA-CS-NPs-22 to 24, and Figure 6.36 for batches FA-CS-NPs-25 to 27.

Table 6.19: Release profile of FA-CS-NPs-1 to 5

Time (hrs)	%CDR				
	FA-CS-NPs-1	FA-CS-NPs-2	FA-CS-NPs-3	FA-CS-NPs-4	FA-CS-NPs-5
0	0	0	0	0	0
1	0	0	0	0	0
2	2.89±0.92	2.08±0.56	2.29±0.71	3.24±0.82	2.41±0.64
3	6.02±0.97	5.31±0.65	5.79±0.91	6.63±0.91	5.82±1.15
4	13.31±1.01	12.47±1.06	12.93±0.95	14.78±0.96	13.12±0.86
5	25.12±1.53	24.18±1.11	24.67±1.02	25.56±1.04	24.85±1.1
6	32.23±1.87	31.24±2.1	31.85±1.15	33.47±1.7	32.09±1.5
7	41.31±2.08	40.51±2.05	41.02±2.1	42.85±1.31	41.16±1.61
8	49.08±1.26	48.14±1.57	48.76±2.11	50.38±2.28	48.89±2.4
12	72.77±1.58	71.63±2.01	72.11±1.71	74.26±2.2	72.36±1.38
24	85.91±1.74	84.72±1.83	85.06±1.68	86.52±1.95	85.27±1.43
48	91.85±2.013	90.75±2.13	91.18±1.97	92.63±1.72	91.47±1.65
72	92.67±2.15	91.83±2.2	92.28±2.15	93.21±2.11	92.55±2.15

n=3

Table 6.20: Release profile of FA-CS-NPs-6 to 10

Time (hrs)	%CDR				
	FA-CS-NPs-6	FA-CS-NPs-7	FA-CS-NPs-8	FA-CS-NPs-9	FA-CS-NPs-10
0	0	0	0	0	0
1	0	0	0	0	0
2	1.05±0.64	1.99±0.51	2.94±1.15	1.46±1.15	0
3	4.28±0.82	5.22±0.65	6.13±1.1	4.69±0.95	1.59±1.1
4	11.44±0.95	12.38±0.84	13.64±0.94	11.85±1.1	8.75±1.14
5	23.15±1.6	24.09±1.31	25.23±0.86	23.56±0.92	20.46±1.66
6	30.21±1.38	31.15±1.15	32.68±1.4	30.62±1.11	27.52±2
7	39.48±2.2	40.42±1.6	41.79±2.2	39.89±2.3	36.79±2.21
8	47.11±1.2	48.05±2.15	49.67±2.1	47.52±2.05	44.42±1.39
12	70.6±2.04	71.54±2.3	73.35±1.2	71.01±2.2	67.91±1.71
24	83.69±2.11	84.63±1.85	86.11±1.76	84.1±2.1	81±1.87
48	89.72±1.82	90.66±2.21	92.25±2.06	90.13±1.85	87.03±2.143
72	90.8±1.4	91.74±2.6	93.17±2.15	91.21±1.3	88.11±2.28

n=3

Table 6.21: Release profile of FA-CS-NPs-11 to 15

Time (hrs)	%CDR				
	FA-CS-NPs-11	FA-CS-NPs-12	FA-CS-NPs-13	FA-CS-NPs-14	FA-CS-NPs-15
0	0	0	0	0	0
1	0	0	0	0	0
2	0	0	0	0	0
3	2.34±0.78	1.21±1.04	1.25±1.04	1.55±1.28	1.54±0.95
4	6.71±1.19	3.58±1.08	8.41±1.09	8.71±0.99	3.74±1.08
5	11.39±1.24	8.84±1.15	20.12±1.17	20.42±1.23	9.34±1.73
6	19.68±2.23	16.75±1.28	27.18±1.83	27.48±1.63	17.63±1.51
7	29.56±2.18	25.49±2.23	36.45±1.44	36.75±1.74	25.89±2.33
8	40.71±1.7	37.31±2.24	44.08±2.41	44.38±2.53	37.92±1.33
12	58.16±2.14	52.56±1.84	67.57±2.33	67.87±1.51	53.31±2.17
24	78.32±1.96	71.32±1.81	80.66±2.08	80.96±1.56	71.79±2.24
48	91.25±2.26	90.36±2.1	86.69±1.85	86.99±1.78	90.72±1.95
72	93.33±2.33	92.47±2.28	87.77±2.24	88.07±2.28	92.46±1.53

n=3

Table 6.22: Release profile of FA-CS-NPs-16 to 20

Time (hrs)	%CDR				
	FA-CS-NPs-16	FA-CS-NPs-17	FA-CS-NPs-18	FA-CS-NPs-19	FA-CS-NPs-20
0	0	0	0	0	0
1	0	0	0	0	0
2	0	0.12±0.1	0	0	0
3	2.89±0.78	3.35±1.23	2.12±1.08	1.42±0.84	2.45±0.52
4	10.05±0.97	10.51±1.07	6.25±1.23	8.58±0.88	7.25±0.93
5	21.76±1.44	22.22±0.99	10.28±1.05	20.29±1.4	11.58±0.98
6	28.82±1.28	29.28±1.53	18.54±1.24	27.35±1.74	21.34±1.97
7	38.09±1.73	38.55±2.33	29.37±2.43	36.62±1.95	30.68±1.92
8	45.72±2.28	46.18±2.23	40.49±2.18	44.25±1.13	40.95±1.44
12	69.21±2.43	69.67±1.33	58.28±2.33	67.74±1.45	58.39±1.88
24	82.3±1.98	82.76±1.89	78.65±2.23	80.83±1.61	80.26±1.7
48	88.33±2.34	88.79±2.19	88.79±1.98	86.86±1.883	90.13±2
72	89.41±2.73	89.87±2.28	91.21±1.43	87.94±2.02	93.41±2.07

n=3

Table 6.23: Release profile of from FA-CS-NPs-21 to 25

Time (hrs)	%CDR				
	FA-CS-NPs-21	FA-CS-NPs-22	FA-CS-NPs-23	FA-CS-NPs-24	FA-CS-NPs-25
0	0	0	0	0	0
1	0	0	0	0	0
2	0	0	0.65±0.51	0	0
3	2.27±0.78	1.96±0.78	3.88±1.02	2.53±0.69	3.01±0.52
4	6.81±0.82	9.12±0.83	11.04±0.73	7.37±0.82	10.17±0.71
5	11.12±0.89	20.83±0.91	22.75±0.97	11.74±1.47	21.88±1.18
6	19.26±1.02	27.89±1.57	29.81±1.37	21.69±1.25	28.94±1.02
7	28.43±1.97	37.16±1.18	39.08±1.48	30.91±2.07	38.21±1.47
8	41.58±1.98	44.79±2.15	46.71±2.27	41.24±1.07	45.84±2.02
12	57.79±1.58	68.28±2.07	70.2±1.25	58.72±1.91	69.33±2.17
24	78.34±1.55	81.37±1.82	83.29±1.3	80.83±1.98	82.42±1.72
48	89.11±1.84	87.4±1.59	89.32±1.52	90.57±1.69	88.45±2.08
72	92.46±2.02	88.48±1.98	90.4±2.02	93.45±1.27	89.53±2.47

n=3

Table 6.24: Release profile of FA-CS-NPs-26 and 27

Time (hrs)	%CDR	
	FA-CS-NPs-26	FA-CS-NPs-27
0	0	0
1	0	0
2	0	0
3	2.15±0.97	2.36±0.82
4	9.31±0.81	7.31±0.97
5	21.02±0.73	11.42±0.79
6	28.08±1.27	20.89±0.98
7	37.35±2.07	29.57±2.17
8	44.98±1.97	40.75±1.92
12	68.47±1.07	57.62±2.07
24	81.56±1.63	79.24±1.97
48	87.59±1.93	91.54±1.72
72	88.67±2.02	92.78±1.17

n=3

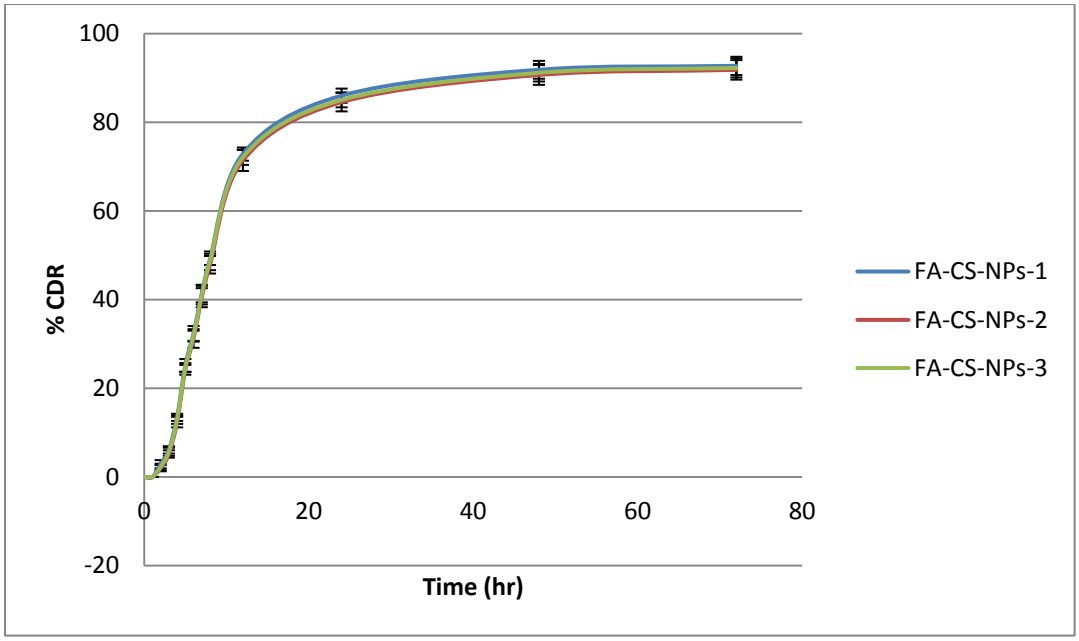

Figure 6.28: *In-Vitro* drug release profile of batch FA-CS-NPs-1 to 3

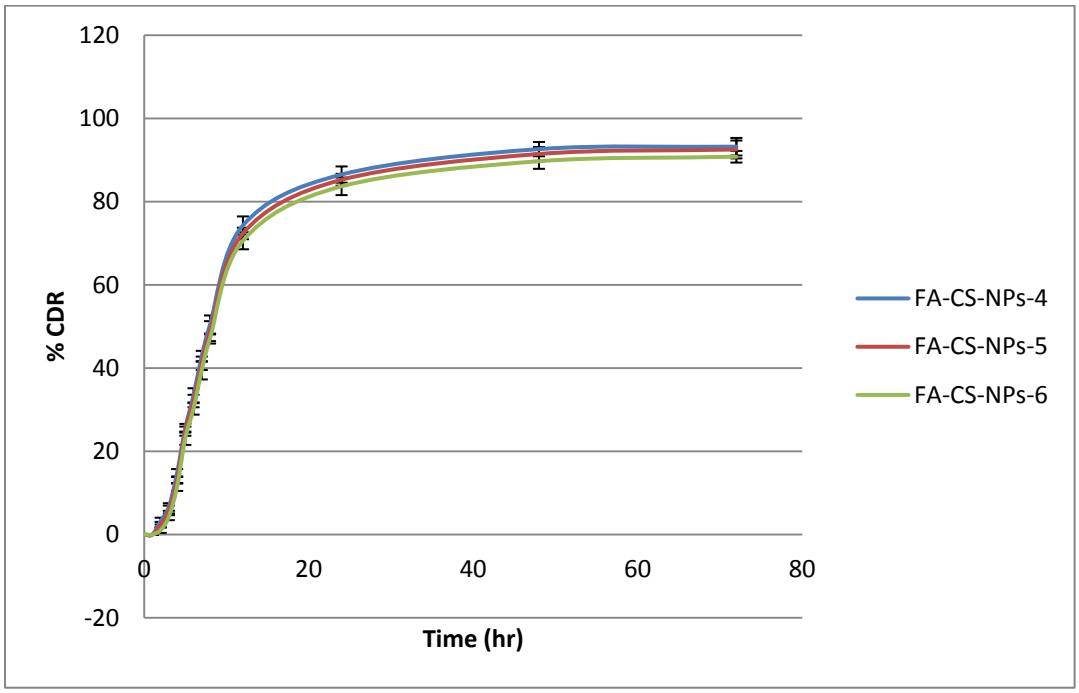

Figure 6.29: *In-Vitro* drug release profile of batch FA-CS-NPs-4 to 6

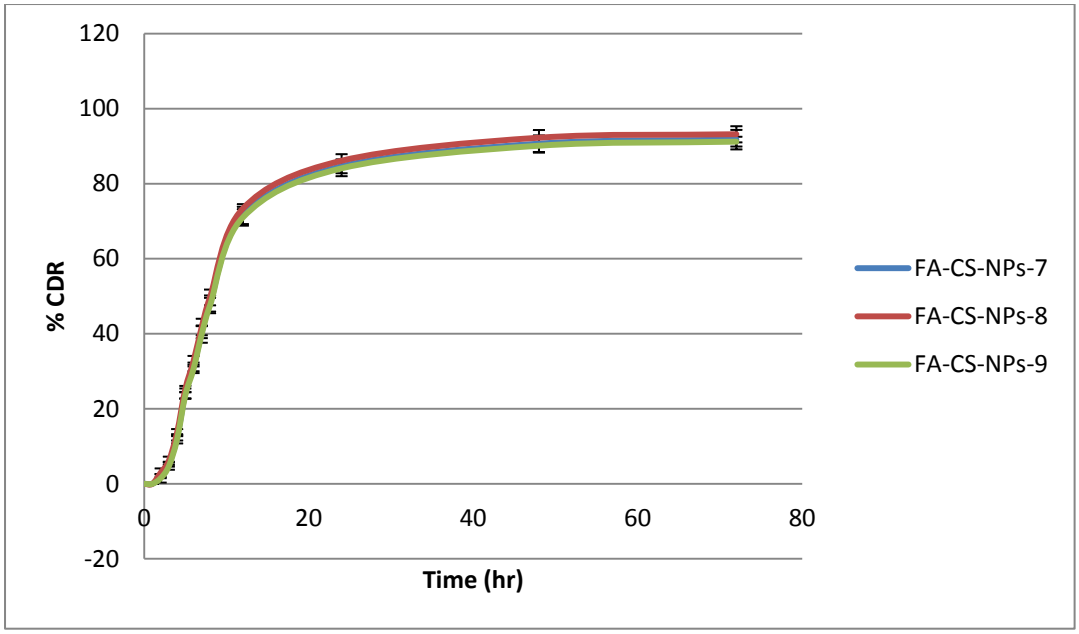

Figure 6.30: *In-Vitro* drug release profile of batch FA-CS-NPs-7 to 9

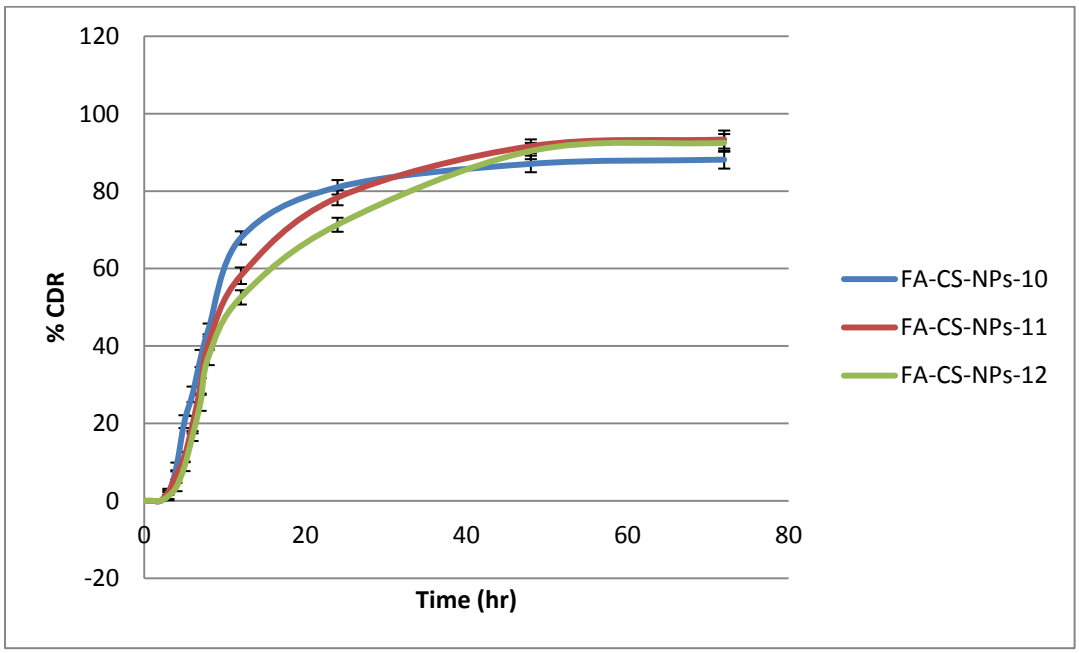

Figure 6.31: *In-Vitro* drug release profile of batch FA-CS-NPs-10 to 12

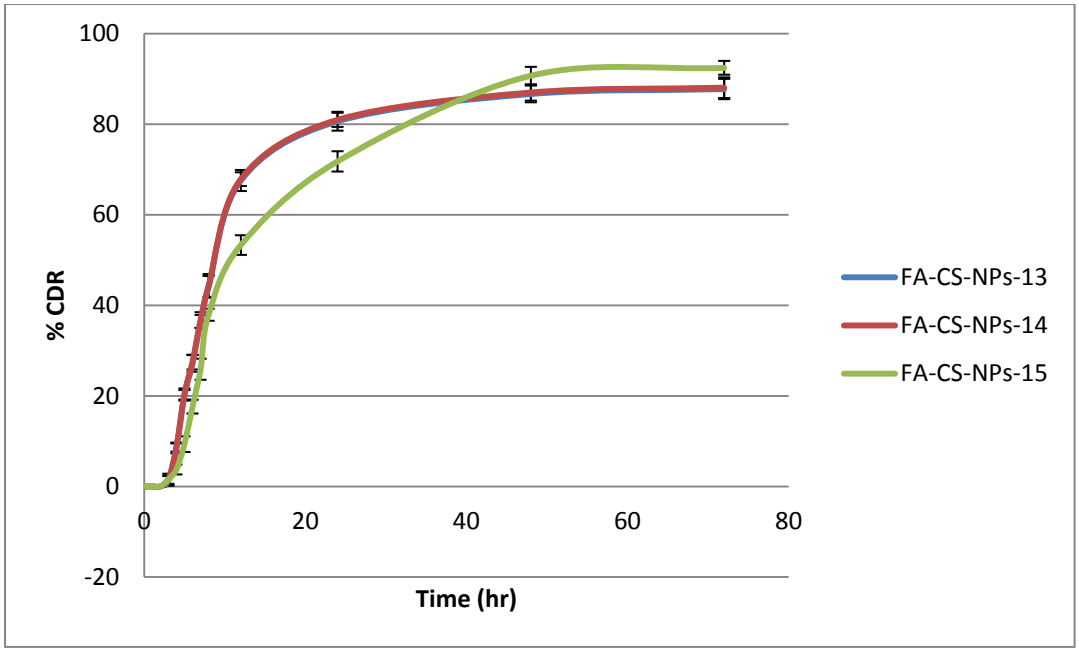

Figure 6.32: *In-Vitro* drug release profile of batch FA-CS-NPs-13 to 15

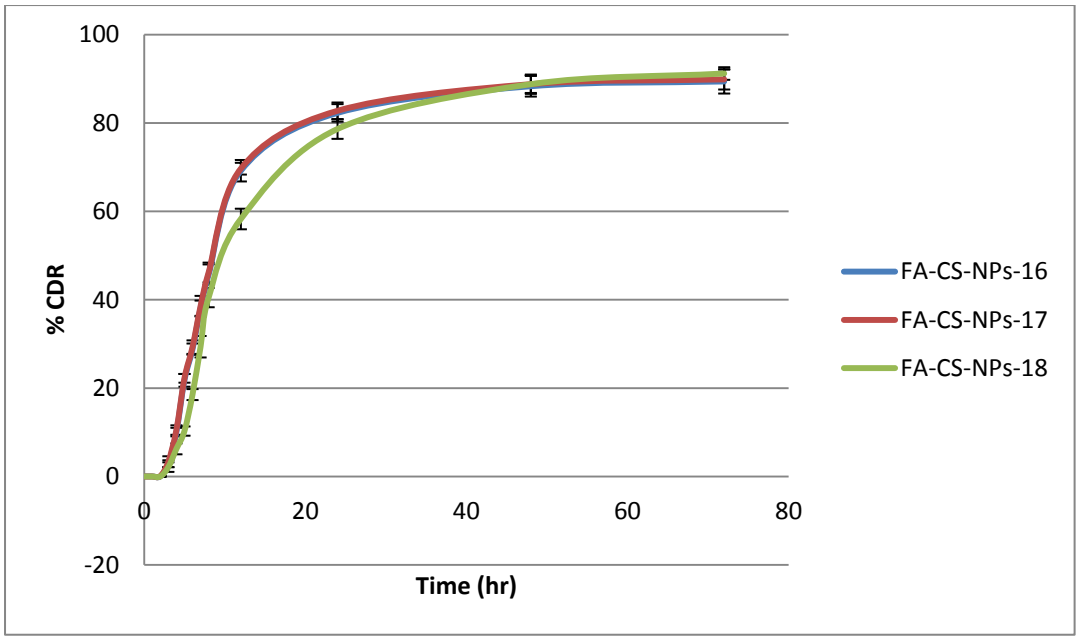

Figure 6.33: *In-Vitro* drug release profile of batch FA-CS-NPs-16 to 18

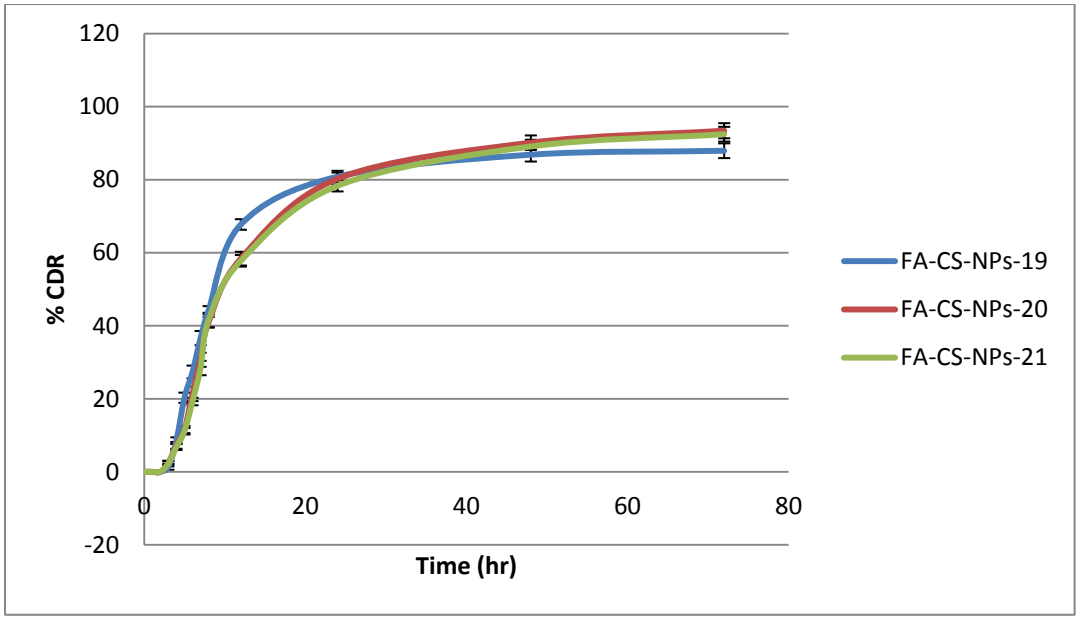

Figure 6.34: *In-Vitro* drug release profile of batch FA-CS-NPs-19 to 21

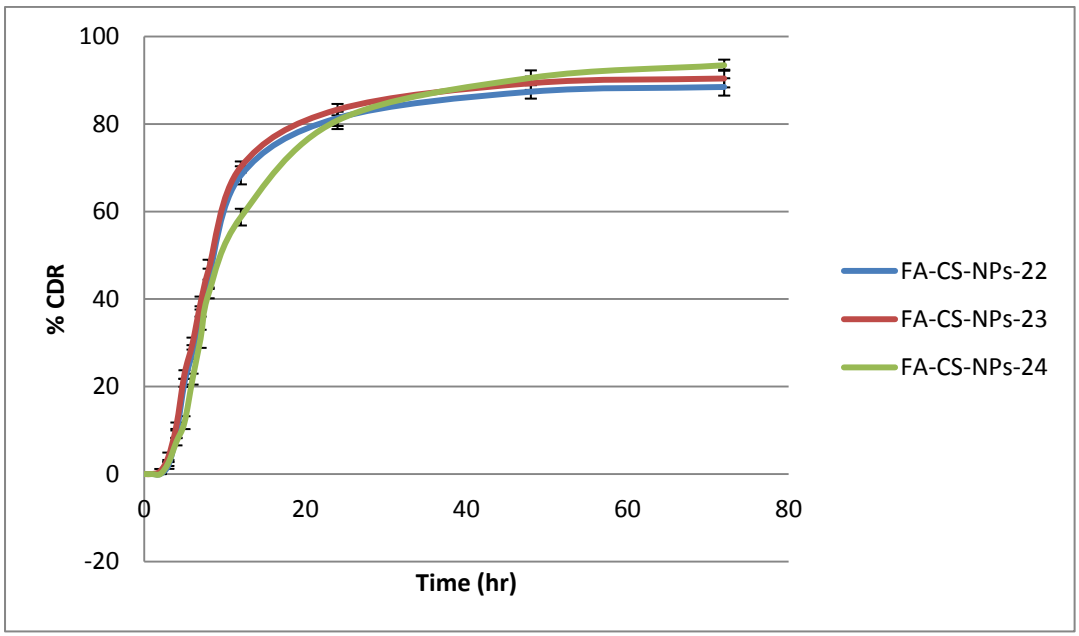

Figure 6.35: *In-Vitro* drug release profile of batch FA-CS-NPs-22 to 24

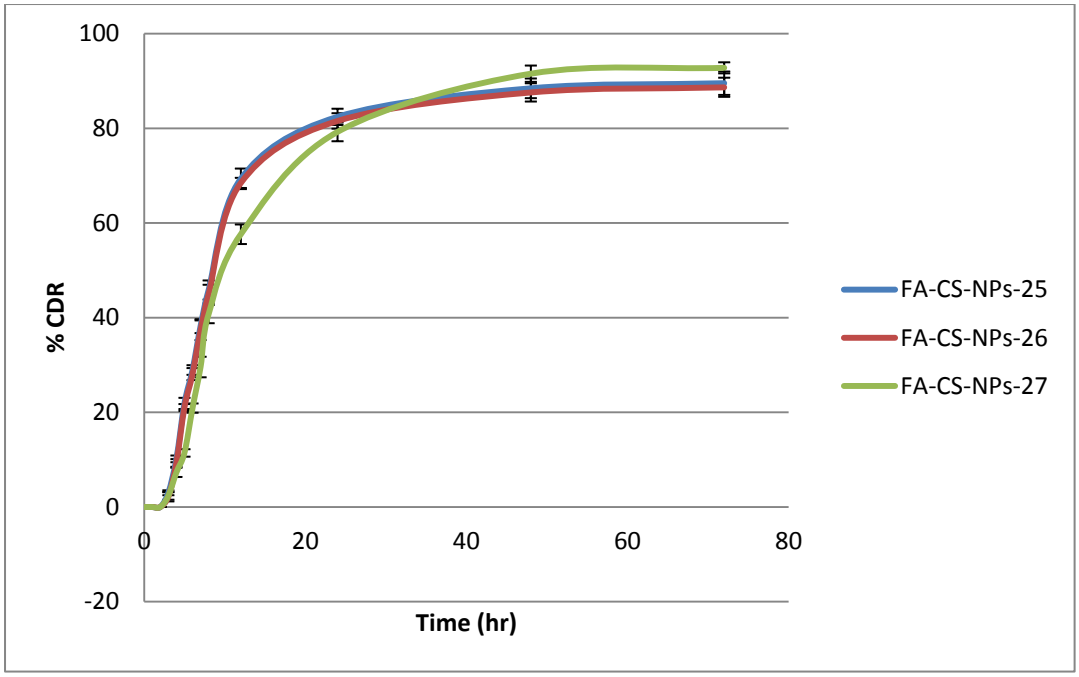

Figure 6.36: *In-Vitro* drug release profile of batch FA-CS-NPs-25 to 27

6.6 Optimization of FA-CS-NPs

6.6.1 Interaction between the factors

Various batches of FA-CS-NPs with experimental conjugation efficiency along with interaction factors are presented in Table 6.25 and P-values of all these interaction factors obtained by the ANOVA of response surface quadratic model is given in Table 6.26

Table 6.25: Various batches of FA-CS-NPs with experimental % folic acid conjugation efficiency (%CE) along with all interaction factors

Batch No.	X_1	X_2	X_3	$(X_1)^2$	$(X_2)^2$	$(X_3)^2$	X_1X_2	X_2X_3	X_1X_3	$X_1X_2X_3$	%CE
FA-CS-NPs-1	-1	-1	-1	1	1	1	1	1	1	-1	61.53
FA-CS-NPs-2	-1	-1	0	1	1	0	1	0	0	0	73.86
FA-CS-NPs-3	-1	-1	1	1	1	1	1	-1	-1	1	87.78
FA-CS-NPs-4	-1	0	-1	1	0	1	0	1	0	0	68.39
FA-CS-NPs-5	-1	0	0	1	0	0	0	0	0	0	70.64
FA-CS-NPs-6	-1	0	1	1	0	1	0	-1	0	0	62.19
FA-CS-NPs-7	-1	1	-1	1	1	1	-1	1	-1	1	51.59
FA-CS-NPs-8	-1	1	0	1	1	0	-1	0	0	0	68.17
FA-CS-NPs-9	-1	1	1	1	1	1	-1	-1	1	-1	59.27
FA-CS-NPs-10	0	-1	-1	0	1	1	0	0	1	0	63.94
FA-CS-NPs-11	0	-1	0	0	1	0	0	0	0	0	78.38
FA-CS-NPs-12	0	-1	1	0	1	1	0	0	-1	0	91.23
FA-CS-NPs-13	0	0	-1	0	0	1	0	0	0	0	69.81
FA-CS-NPs-14	0	0	0	0	0	0	0	0	0	0	64.45
FA-CS-NPs-15	0	0	1	0	0	1	0	0	0	0	85.17
FA-CS-NPs-16	0	1	-1	0	1	1	0	0	-1	0	55.33
FA-CS-NPs-17	0	1	0	0	1	0	0	0	0	0	69.76
FA-CS-NPs-18	0	1	1	0	1	1	0	0	1	0	70.11
FA-CS-NPs-19	1	-1	-1	1	1	1	-1	-1	1	1	52.57
FA-CS-NPs-20	1	-1	0	1	1	0	-1	0	0	0	45.23
FA-CS-NPs-21	1	-1	1	1	1	1	-1	1	-1	-1	64.48
FA-CS-NPs-22	1	0	-1	1	0	1	0	-1	0	0	48.79
FA-CS-NPs-23	1	0	0	1	0	0	0	0	0	0	41.47
FA-CS-NPs-24	1	0	1	1	0	1	0	1	0	0	62.41
FA-CS-NPs-25	1	1	-1	1	1	1	1	-1	-1	-1	38.19
FA-CS-NPs-26	1	1	0	1	1	0	1	0	0	0	44.79
FA-CS-NPs-27	1	1	1	1	1	1	1	1	1	1	59.53

Table 6.26: Analysis of variance for response surface quadratic model

	Coefficients	Standard Error	P-value
Intercept	70.99	3.52	8.43E-13
X_1	-8.11	1.63	0.0001
X_2	-5.68	1.63	0.0031
X_3	7.34	1.63	0.0004
$(X_1)^2$	-13.08	2.82	0.0003
$(X_2)^2$	-0.61	2.82	0.8328
$(X_3)^2$	2.16	2.82	0.4561
X_1X_2	2.03	2.00	0.3240
X_2X_3	1.60	2.00	0.4359
X_1X_3	-1.80	2.00	0.3794
$X_1X_2X_3$	3.50	2.44	0.1714

From the above Table 6.26, full polynomial equation was derived as per follows

$$\% \text{ EE} = 70.99 - 8.11X_1 - 5.68X_2 + 7.34X_3 - 13.08(X_1)^2 - 0.61(X_2)^2 + 2.16(X_3)^2 + 2.03X_1X_2 + 1.6X_2X_3 - 1.8X_1X_3 + 3.5X_1X_2X_3$$

Then after, interaction factor showing P-value more than 0.05 was omitted (shown in shadowed cells) and reduced surface quadratic model was obtained by regression analysis as shown in Table 6.27

Table 6.27: Analysis of variance for response surface reduced quadratic model

	Coefficients	Standard Error	P-value
Intercept	72.02	2.26	6.67E-20
X_1	-8.10	1.59	4.42E-05
X_2	-5.68	1.59	0.0018
X_3	7.33	1.59	0.00014
$(X_1)^2$	-13.08	2.76	0.0001

From above Table 6.27 reduced polynomial equation was derived as per follows

$$\% \text{ EE} = 72.02 - 8.1X_1 - 5.68X_2 + 7.33X_3 - 13.08(X_1)^2$$

Predicted values of % EE of FA-CS-NPs by response surface reduced quadratic model was compared with the real experimental value of all 27 batches of FA-CS-NPs to calculate the difference in terms of % error, as shown in Table 6.28.

Table 6.28: Experimental versus predicted values of % folic acid conjugation efficiency (%CE) of CS-NPs by response surface reduced quadratic model

Batch	Experimental %CE	Predicted %CE	Residuals	% Error
FA-CS-NPs-1	61.53	60.95	-0.61	-0.95
FA-CS-NPs-2	73.86	74.04	0.18	0.25
FA-CS-NPs-3	87.78	89.14	1.23	1.55
FA-CS-NPs-4	68.39	69.98	1.39	2.33
FA-CS-NPs-5	70.64	71.25	0.57	0.86
FA-CS-NPs-6	62.19	60.56	-1.95	-2.63
FA-CS-NPs-7	51.59	51.22	-0.39	-0.72
FA-CS-NPs-8	68.17	69.38	1.09	1.78
FA-CS-NPs-9	59.27	57.97	-1.51	-2.20
FA-CS-NPs-10	63.94	63.00	-1.03	-1.46
FA-CS-NPs-11	78.38	78.49	0.11	0.14
FA-CS-NPs-12	91.23	92.30	0.99	1.17
FA-CS-NPs-13	69.81	70.70	0.82	1.27
FA-CS-NPs-14	64.45	63.36	-1.21	-1.68
FA-CS-NPs-15	85.17	86.17	0.93	1.17
FA-CS-NPs-16	55.33	54.78	-0.5	-1.00
FA-CS-NPs-17	69.76	70.34	0.54	0.83
FA-CS-NPs-18	70.11	69.57	-0.57	-0.78
FA-CS-NPs-19	52.57	53.15	0.54	1.11
FA-CS-NPs-20	45.23	43.78	-1.81	-3.20
FA-CS-NPs-21	64.48	64.58	0.11	0.16
FA-CS-NPs-22	48.79	49.74	0.84	1.95
FA-CS-NPs-23	41.47	40.25	-1.51	-2.95
FA-CS-NPs-24	62.41	63.14	0.68	1.17
FA-CS-NPs-25	38.19	38.25	0.06	0.16
FA-CS-NPs-26	44.79	44.73	-0.05	-0.13
FA-CS-NPs-27	59.53	60.81	1.12	2.15

Finally, results of ANOVA of full and reduced quadratic model was compared, as summarized in Table 6.29, to calculate the F value as per calculation given below. Then after, this calculated F value was compared with the table value of F value to know whether the effect of interaction factor on response is significant or not, and also to justify the omission of non-significant interaction factor while obtaining the reduced surface quadratic model.

Table 6.29: Results of ANOVA of full model and reduced model

		df	SS	MS	F	R^2
Regression	FM	10	4007.01	400.71	8.38	0.84
	RM	4	3759.83	939.96	20.43	0.79
Residual	FM	16	764.81	47.81		
	RM	22	1011.98	45.99		

df – degree of freedom, SS – sum of squares, MS – mean sum of squares, FM – full model, RM – reduced model

SSE2-SSE1=1011.98-764.81=247.17

No. of terms omitted while obtaining a reduced model were 06

MS of Error of FM=47.81

$$\text{F Calculated} = \frac{\dfrac{\text{SSE 2} - \text{SSE 1}}{\text{No of non significant terms omitted}}}{\text{MS of error of FM}}$$

$$= \frac{\dfrac{1011.98 - 764.81}{6}}{47.81} = 0.86$$

Therefore, F value (Calculated) = 0.86, and from the table of F value, it was found to be, F value (Tabulated) = 3.48.

Hence, F calculated < F tabulated

6.6.2 Construction of contour plots

2D contour plot and 3D response surface plot of FA-CS-NPs for the effect of variables, folic acid amount and RPM, on the response, % folic acid conjugation, when third variable reaction time was kept constant at level -1, 0 and +1 is given in Figure 6.37, Figure 6.39 and Figure 6.41 respectively. While 3D response surface plot for the same is given in Figure 6.38, Figure 6.40 and Figure 6.42 respectively.

In the same way three 2D contour plots was constructed by keeping the variable RPM constant at -1, 0, and +1 as shown in Figure 6.43, Figure 6.45 and Figure 6.47 respectively. While 3D response surface plot for the same is given in Figure 6.44, Figure 6.46 and Figure 6.48 respectively.

Finally, three 2D contour plots was constructed by keeping the variable folic acid amount constant at -1, 0, and +1 as shown in Figure 6.49, Figure 6.51 and Figure 6.53 respectively. While 3D response surface plot for the same is given in Figure 6.50, Figure 6.52 and Figure 6.54 respectively.

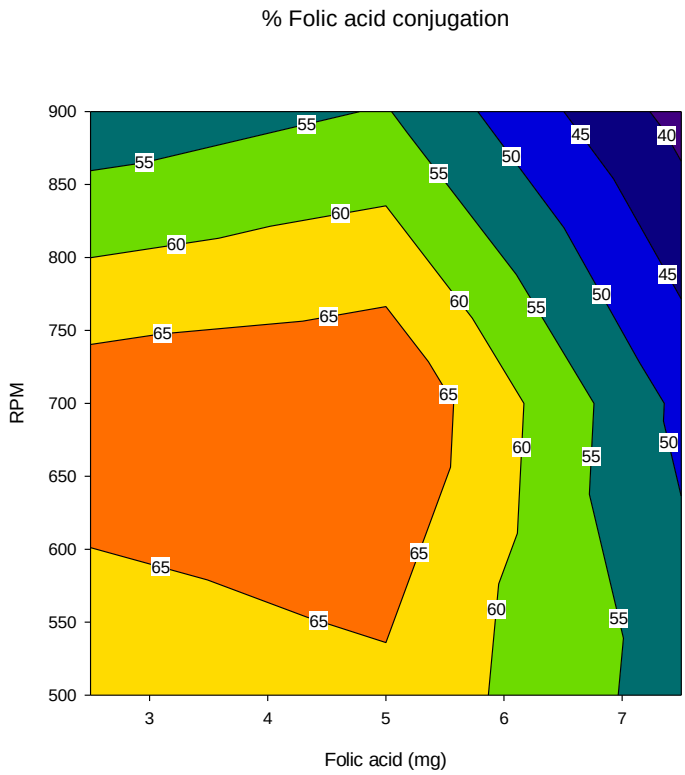

Figure 6.37: 2D Contour plot of FA-CS-NPs for the effect of variables, folic acid amount and RPM, on the response, % folic acid conjugation, when third variable reaction time was kept constant at level (-1)

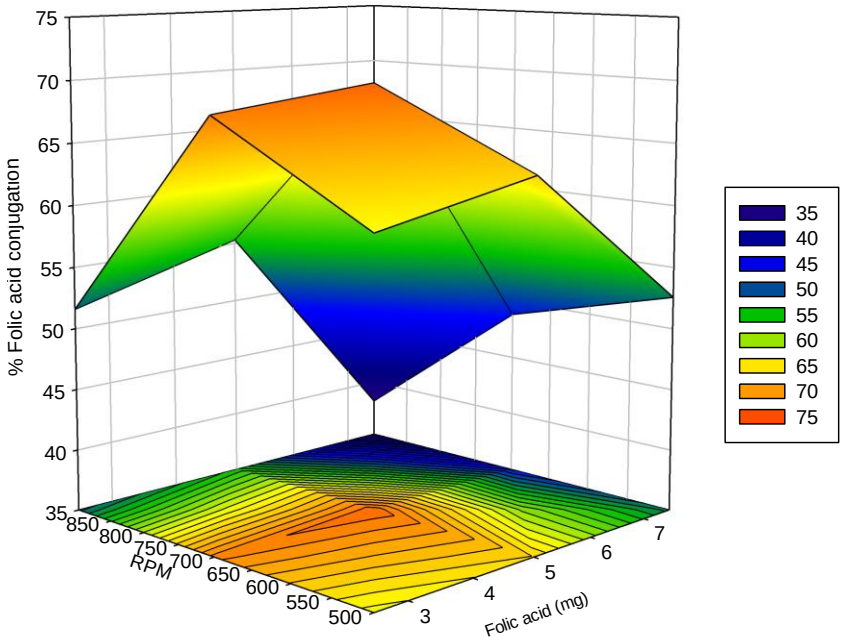

Figure 6.38: 3D surface response plot of FA-CS-NPs for the effect of variables, folic acid amount and RPM, on the response, % folic acid conjugation, when third variable reaction time was kept constant at level (-1)

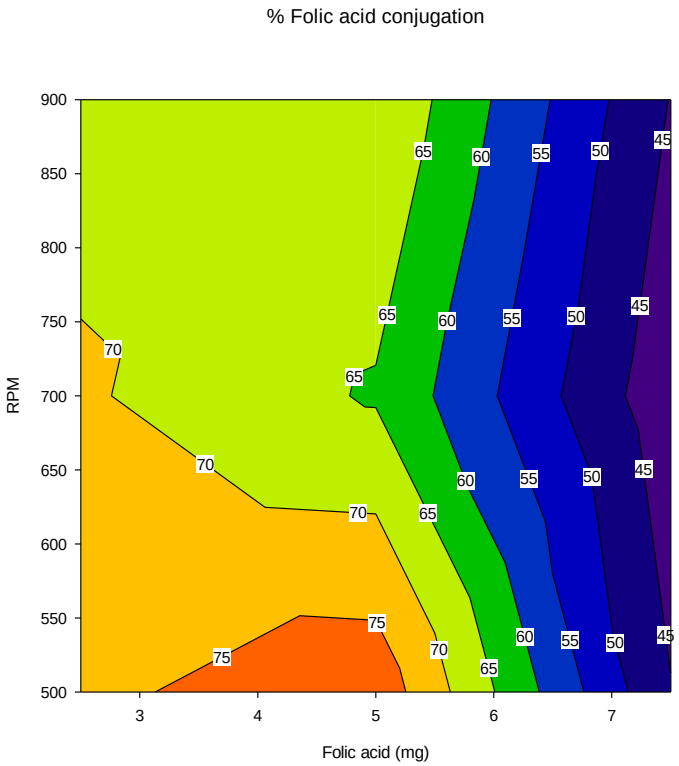

Figure 6.39: 2D Contour plot of FA-CS-NPs for the effect of variables, folic acid amount and RPM, on the response, % folic acid conjugation, when third variable reaction time was kept constant at level (0)

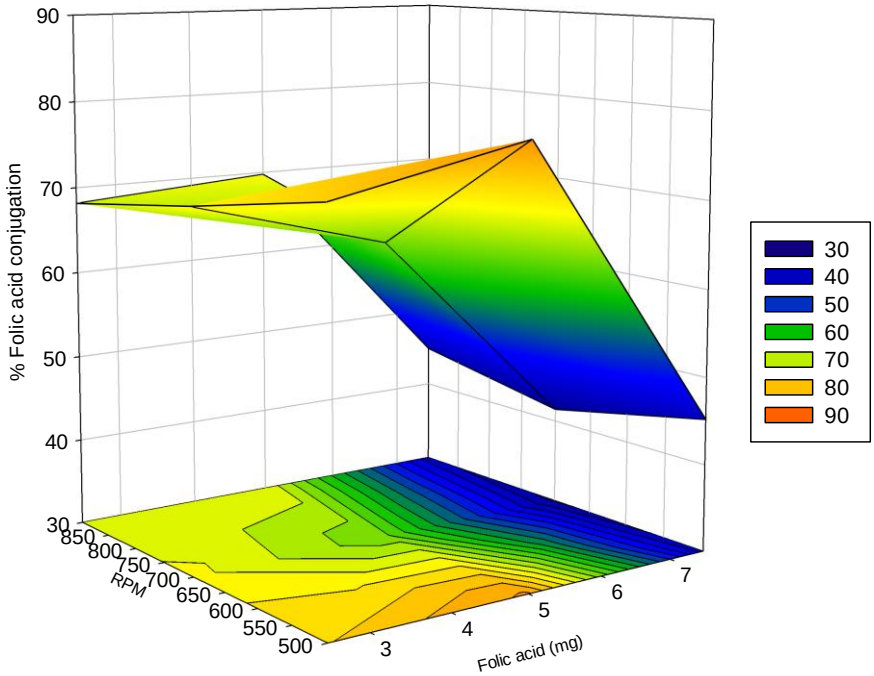

Figure 6.40: 3D surface response plot of FA-CS-NPs for the effect of variables, folic acid amount and RPM, on the response, % folic acid conjugation, when third variable reaction time was kept constant at level (0)

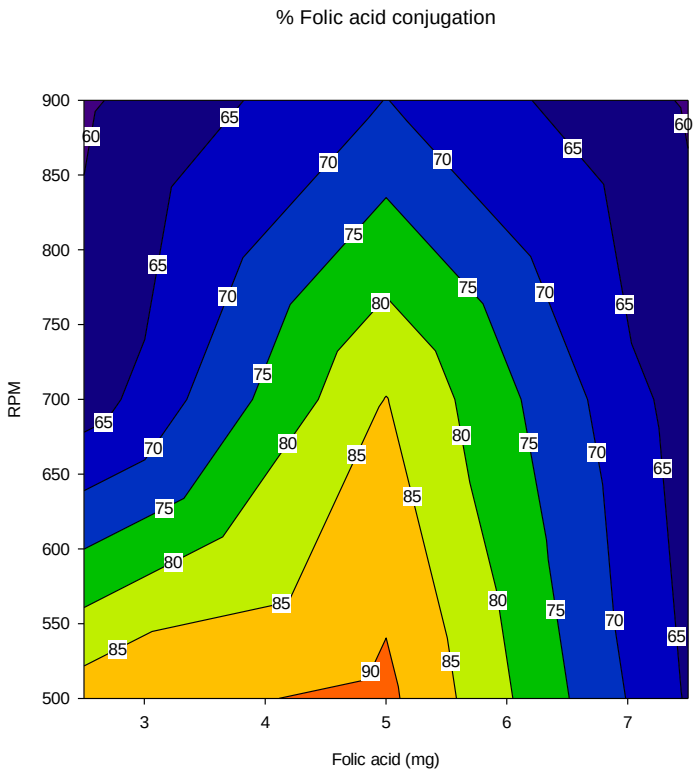

Figure 6.41: 2D Contour plot of FA-CS-NPs for the effect of variables, folic acid amount and RPM, on the response, % folic acid conjugation, when third variable reaction time was kept constant at level (+1)

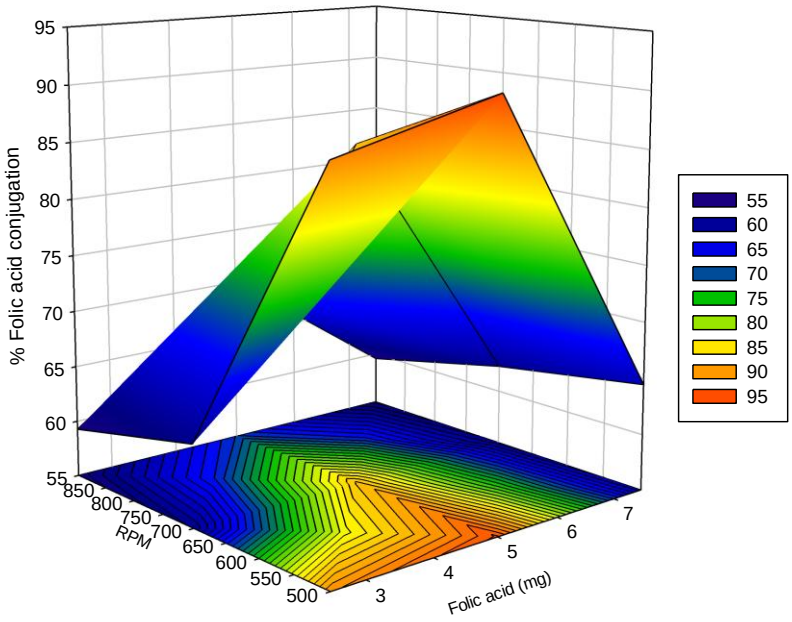

Figure 6.42: 3D surface response plot of FA-CS-NPs for the effect of variables, folic acid amount and RPM, on the response, % folic acid conjugation, when third variable reaction time was kept constant at level (+1)

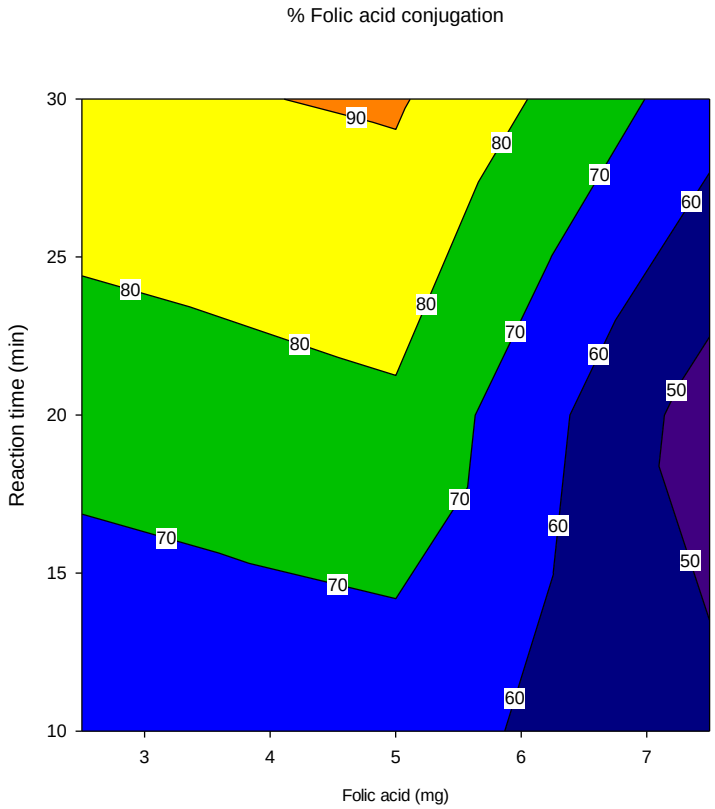

Figure 6.43: 2D Contour plot of FA-CS-NPs for the effect of variables, folic acid amount and reaction time, on the response, % folic acid conjugation, when third variable RPM was kept constant at level (-1)

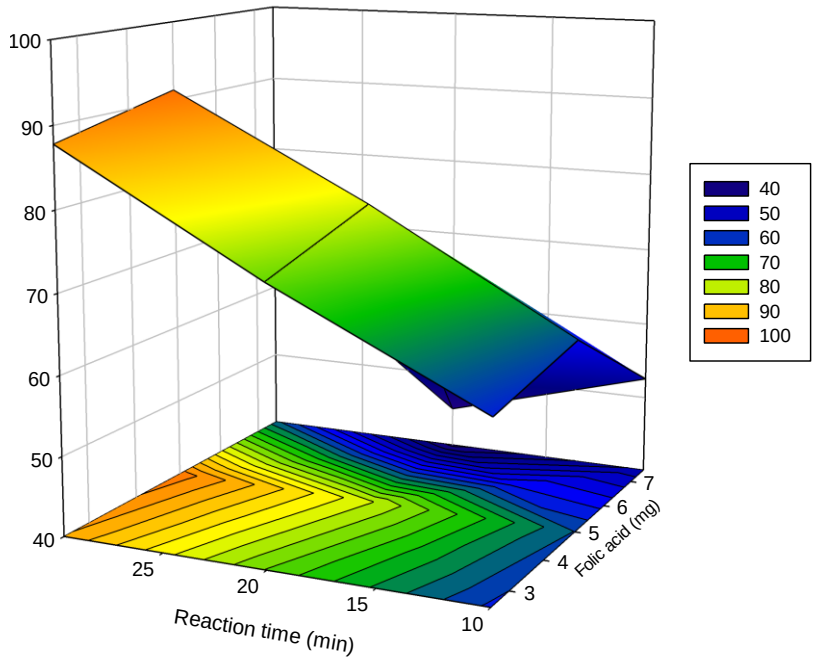

Figure 6.44: 3D surface response plot of FA-CS-NPs for the effect of variables, folic acid amount and reaction time, on the response, % folic acid conjugation, when third variable RPM was kept constant at level (-1)

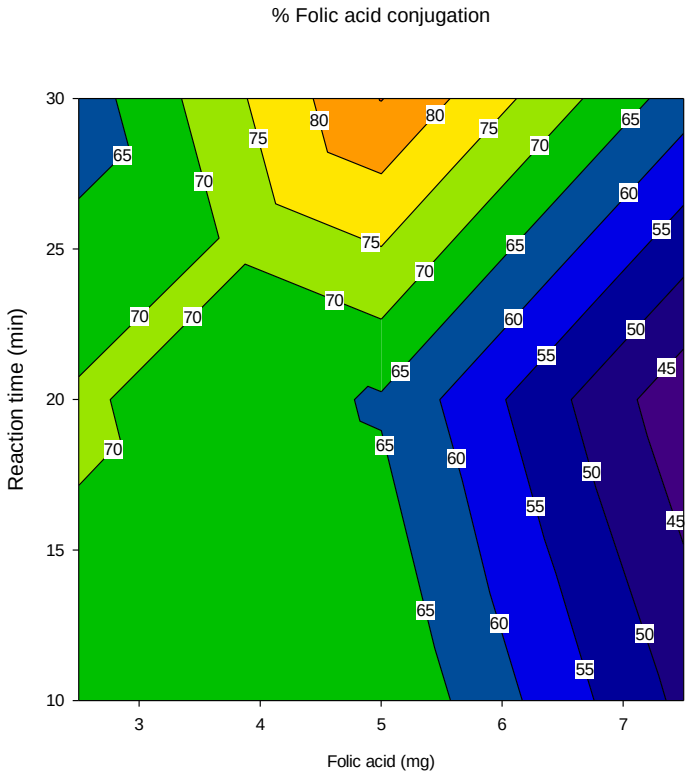

Figure 6.45: 2D Contour plot of FA-CS-NPs for the effect of variables, folic acid amount and reaction time, on the response, % folic acid conjugation, when third variable RPM was kept constant at level (0)

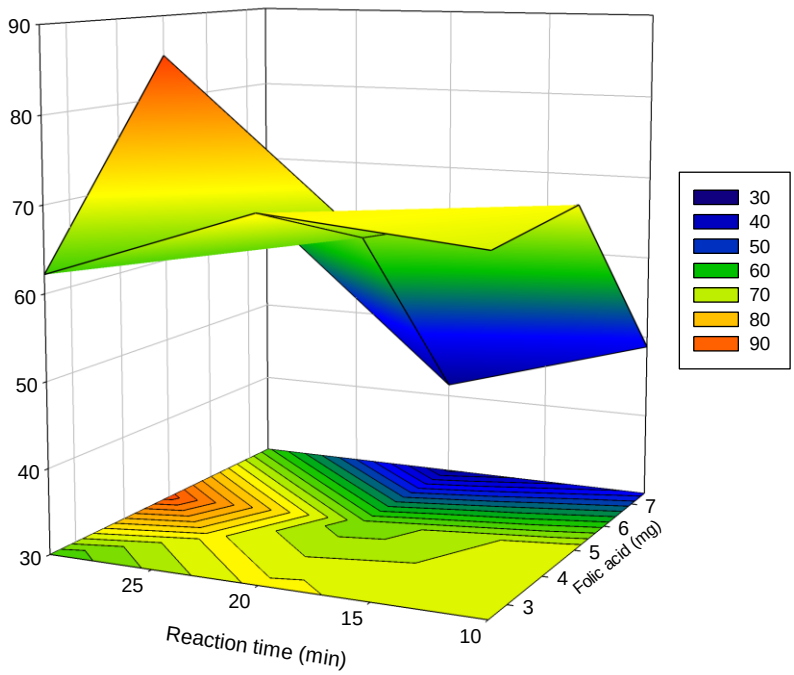

Figure 6.46: 3D surface response plot of FA-CS-NPs for the effect of variables, folic acid amount and reaction time, on the response, % folic acid conjugation, when third variable RPM was kept constant at level (0)

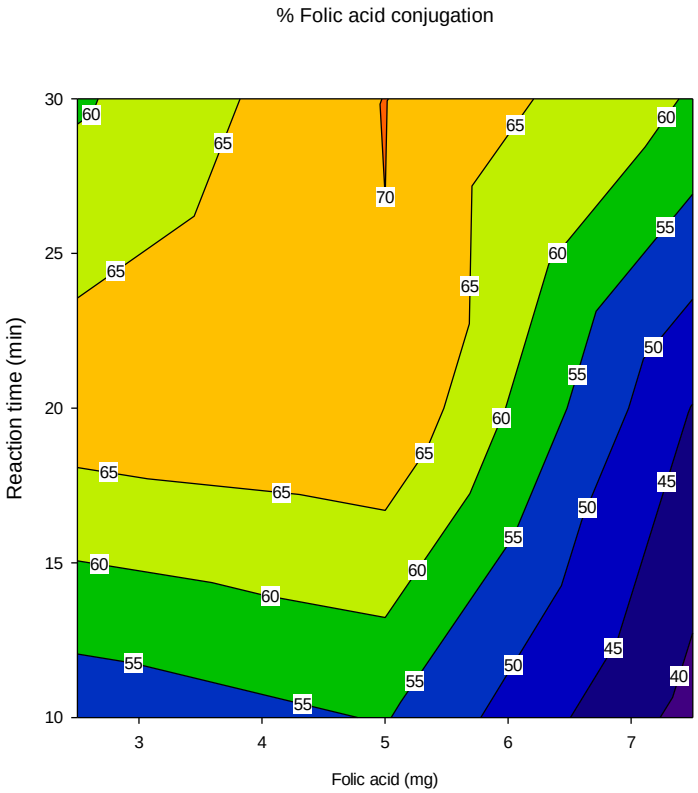

Figure 6.47: 2D Contour plot of FA-CS-NPs for the effect of variables, folic acid amount and reaction time, on the response, % folic acid conjugation, when third variable RPM was kept constant at level (+1)

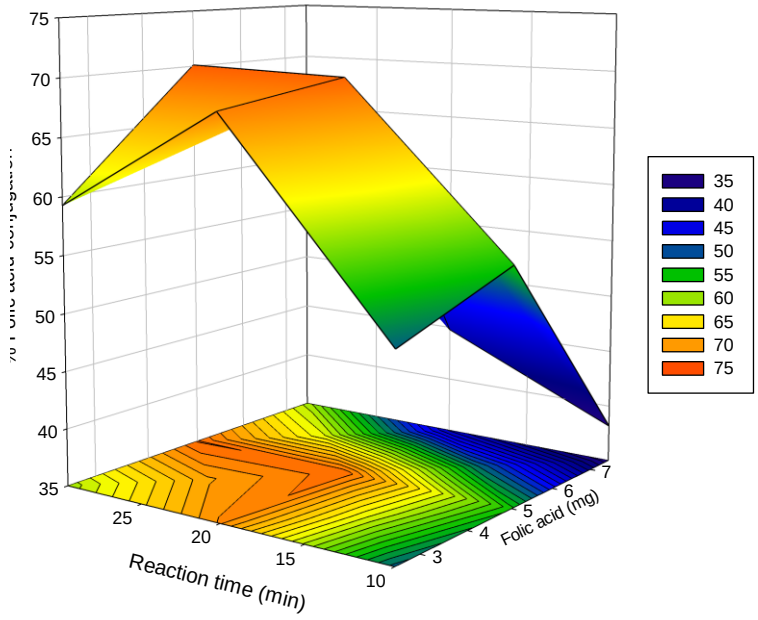

Figure 6.48: 3D surface response plot of FA-CS-NPs for the effect of variables, folic acid amount and reaction time, on the response, % folic acid conjugation, when third variable RPM was kept constant at level (+1)

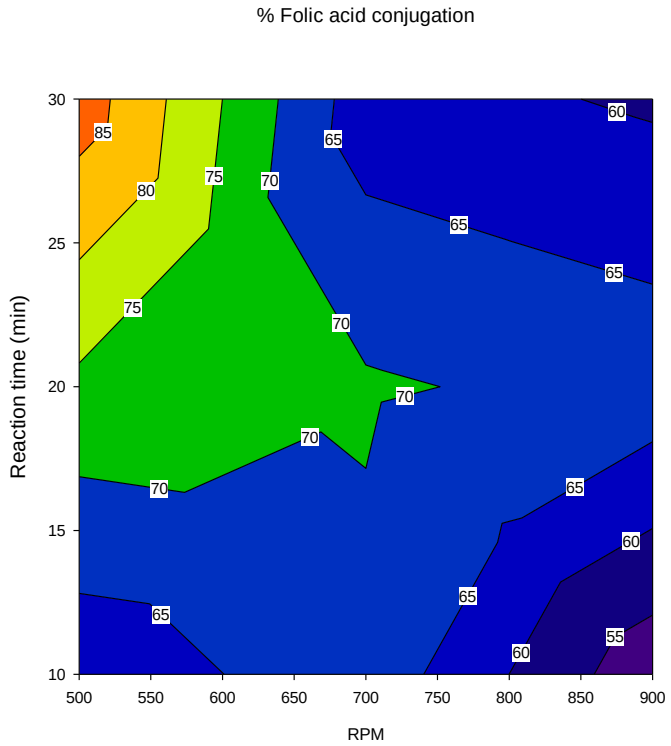

Figure 6.49: 2D Contour plot of FA-CS-NPs for the effect of variables, reaction time and RPM, on the response, % folic acid conjugation, when third variable folic acid amount was kept constant at level (-1)

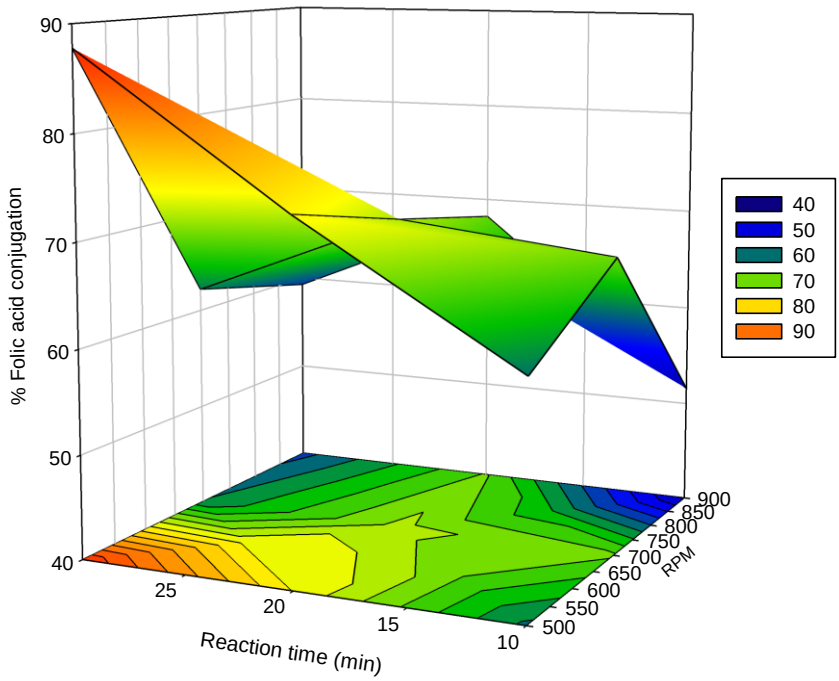

Figure 6.50: 3D surface response plot of FA-CS-NPs for the effect of variables, reaction time and RPM, on the response, % folic acid conjugation, when third variable folic acid amount was kept constant at level (-1)

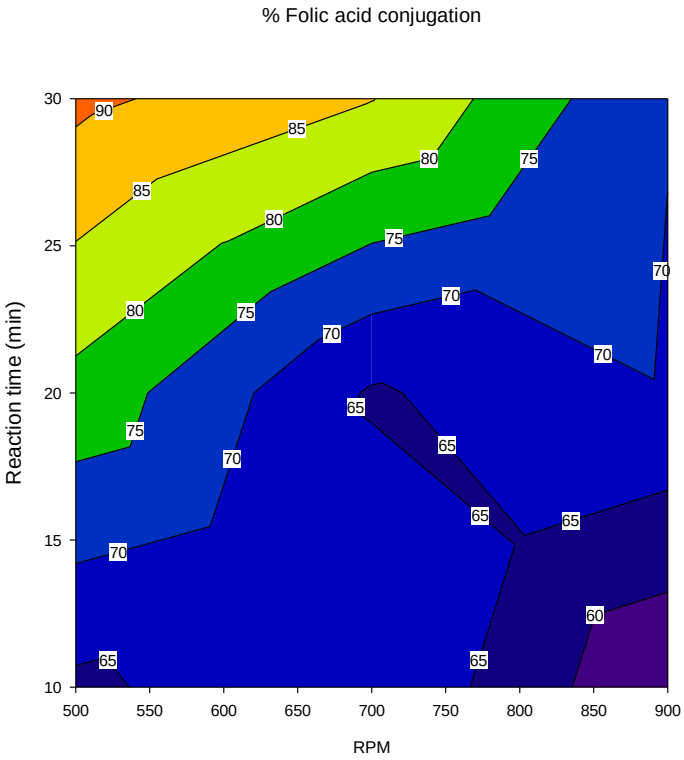

Figure 6.51: 2D Contour plot of FA-CS-NPs for the effect of variables, reaction time and RPM, on the response, % folic acid conjugation, when third variable folic acid amount was kept constant at level (0)

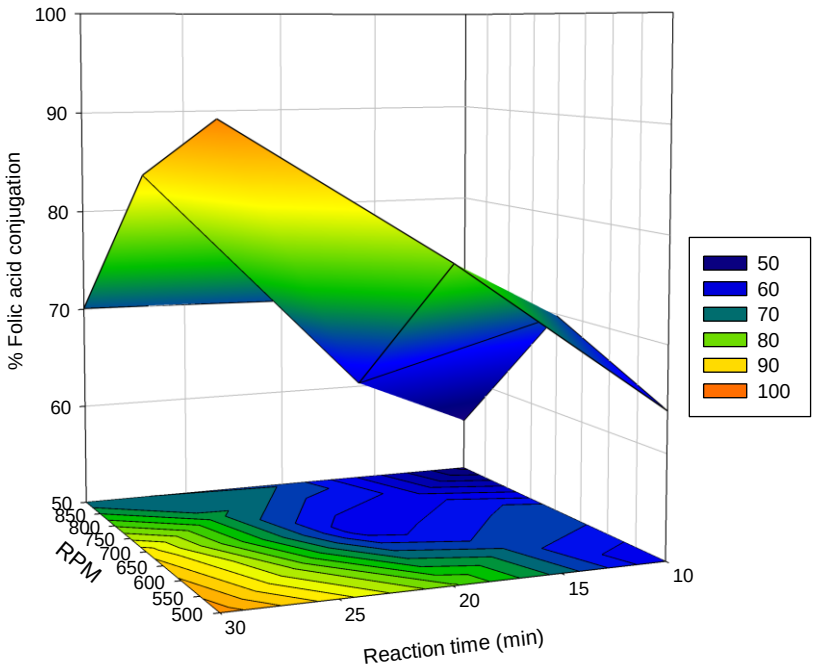

Figure 6.52: 3D surface response plot of FA-CS-NPs for the effect of variables, reaction time and RPM, on the response, % folic acid conjugation, when third variable folic acid amount was kept constant at level (0)

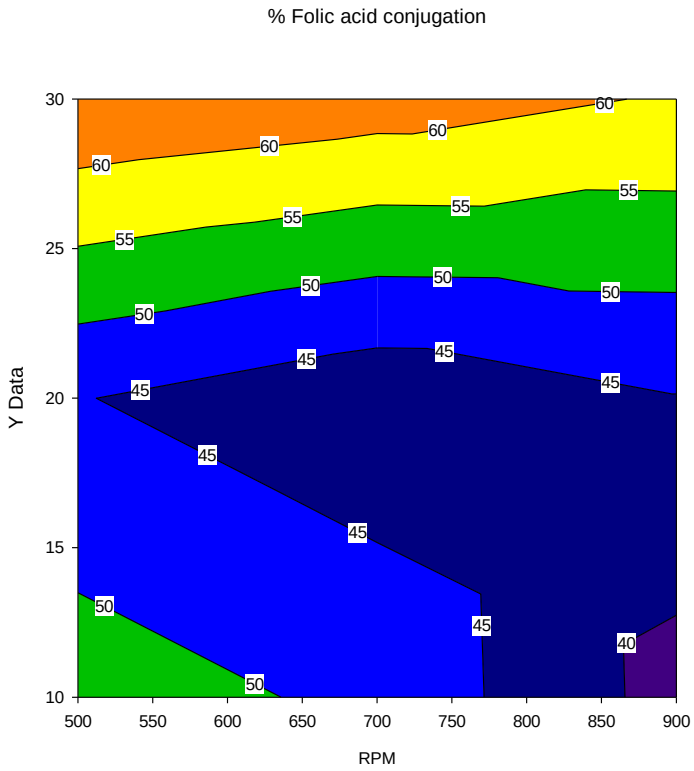

Figure 6.53: 2D Contour plot of FA-CS-NPs for the effect of variables, reaction time and RPM, on the response, % folic acid conjugation, when third variable folic acid amount was kept constant at level (+1)

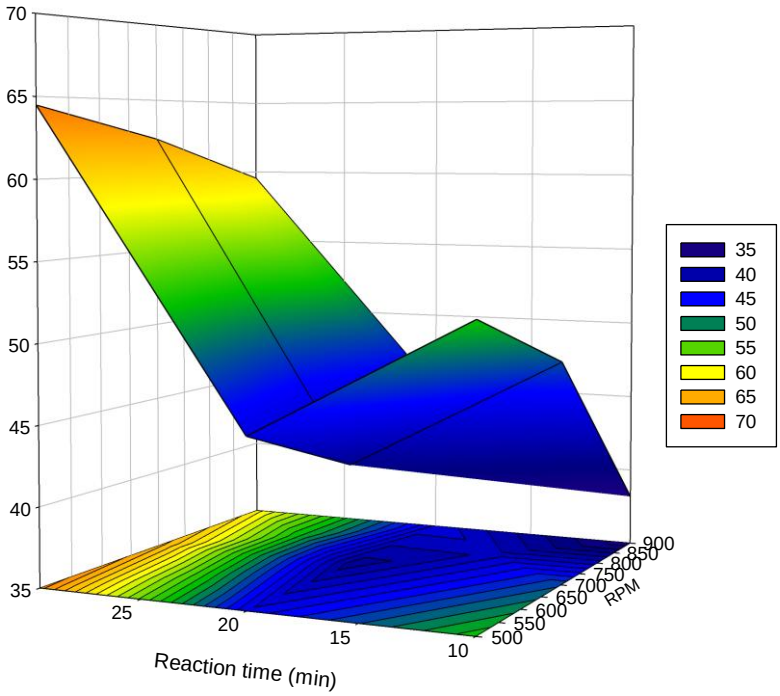

Figure 6.54: 3D surface response plot of FA-CS-NPs for the effect of variables, reaction time and RPM, on the response, % folic acid conjugation, when third variable folic acid amount was kept constant at level (+1)

6.6.3 Evaluation of model / Check point analysis

Result of the check point analysis for the FA-CS-NPs is summarized in Table 6.30

Table 6.30: Check point analysis of FA-CS-NPs from the contour plot

Test batches	Response	Factors			Predicted value	Experimental value	% Error
		X_1	X_2	X_3			
Batch 1	% CE	5mg	500	30	92.26	90.79	1.96
Batch 2	% CE	5mg	500	29	91.48	89.32	2.36
Batch 3	% CE	5mg	500	28	90.23	88.57	1.84

6.7 Evaluation of optimized FA-CS-NPs-12

6.7.1 Particle size distribution and zeta potential of FA-CS-NPs

Folic acid conjugated chitosan nanoparticle was analyzed for its size, size distribution and electrical charge that they carry, using a Malvern particle size analyzer. Result of the same for batch FA-CS-NPs-12 is given in Figure 6.55 and Figure 6.56 respectively.

Size Distribution Report by Intensity
v2.1

Malvern

Sample Details

Sample Name:	FA-CS-NPs
SOP Name:	mansettings.nano
General Notes:	

File Name:	SUMANDEEP.dts	**Dispersant Name:**	Water
Record Number:	23	**Dispersant RI:**	1.330
Material RI:	1.59	**Viscosity (mPa.s):**	0.8872
Material Absorbtion:	0.010	**Measurement Date and Time:**	Thursday, February 13, 2014 ...

System

Temperature (°C):	25.0	**Duration Used (s):**	70
Count Rate (kcps):	228.9	**Measurement Position (mm):**	4.65
Cell Description:	Disposable sizing cuvette	**Attenuator:**	11

Results

			Size (d.nm):	% Intensity	Width (d.n...
Z-Average (d.nm):	121.9	**Peak 1:**	130.7	82.7	94.74
PdI:	0.124	**Peak 2:**	19.13	17.3	1.732
Intercept:	1.01	**Peak 3:**	0.000	0.0	0.000

Result quality : Refer to quality report

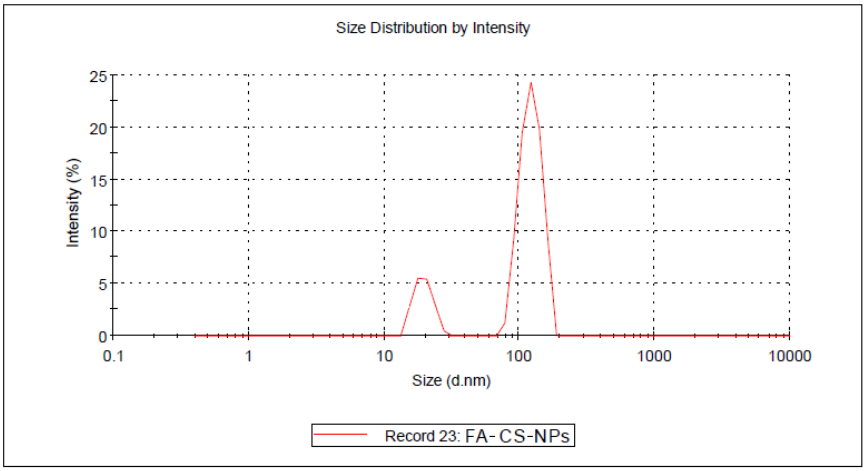

Figure 6.55: Particle size distribution of FA-CS-NPs-12

Zeta Potential Report

v2.1

Malvern

Sample Details

Sample Name:	FA-CS-NPs
SOP Name:	
General Notes:	

File Name:	SUMANDEEP.dts	**Dispersant Name:**	1% acetic acid
Record number:	14	**Dispersant RI:**	1.370
Date and Time:	Thursday, February 13, 2014	**Viscosity (cP):**	0.8541
		Dispesant Dielectric Constant:	77.1

System

Temperature (°C):	25.0	**Zeta Runs:**	70
Count Rate (kcps):	252.5	**Measurement Position (mm):**	2.00
Cell Description:	Clear disposable zeta cell	**Attenuator:**	7

Results

			Mean (mV):	**Area (%)**	**Width (mV)**
Zeta Potential (mv):	-30.9	**Peak 1:**	-30.9	100	3.88
Zeta Deviation (mv):	3.74	**Peak 2:**	0.000	0.0	0.000
Conductivity (mS/cm):	0.737	**Peak 3:**	0.000	0.0	0.000

Result quality : Refer to quality report

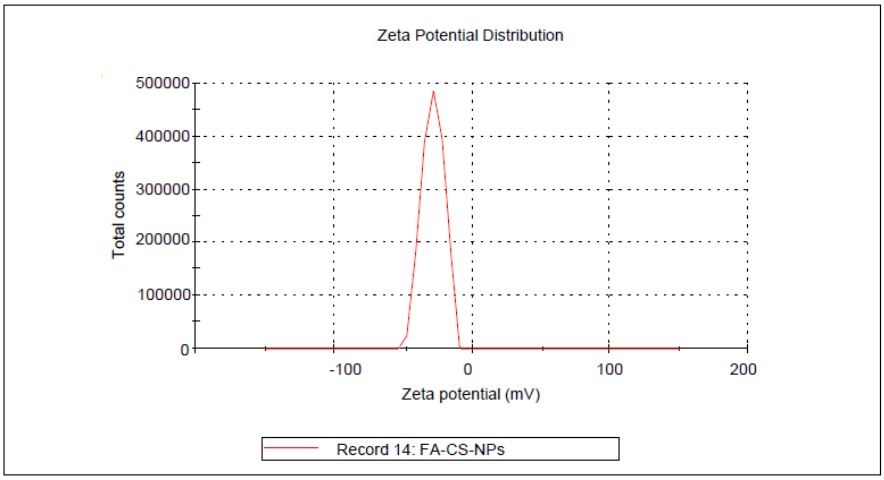

Figure 6.56: Zeta potential distribution of FA-CS-NPs-12

6.7.2 Scanning Electron Microscopy

surface morphology of optimized folic acid conjugated chitosan nanoparticle, FA-CS-NPs-12, was evaluated by scanning electron microscopy, and the result of the same is given in Figure 6.57.

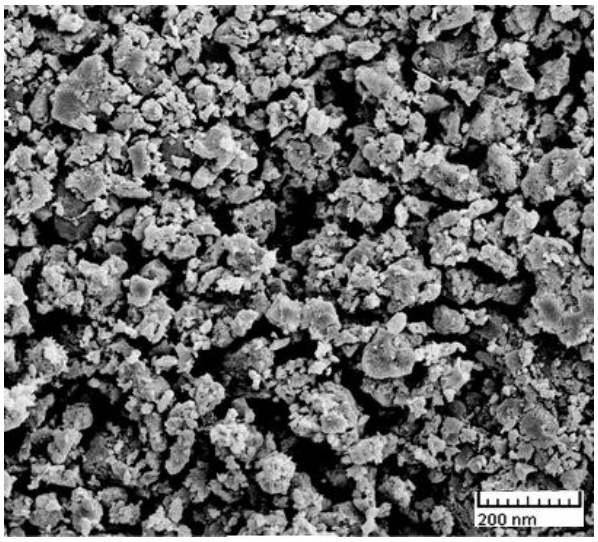

Figure 6.57: SEM photograph of folic acid conjugated nanoparticles, FA-CS-NPs-12

6.7.3 FT-IR study

In optimized folic acid conjugated chitosan nanoparticle, FA-CS-NPs-12, compatibility of capecitabine with excipients was evaluated by taking the FT-IR spectra of FA-CS-NPs-12, and then it was compared with the FT-IR spectra of capecitabine alone, as given in Figure 6.58.

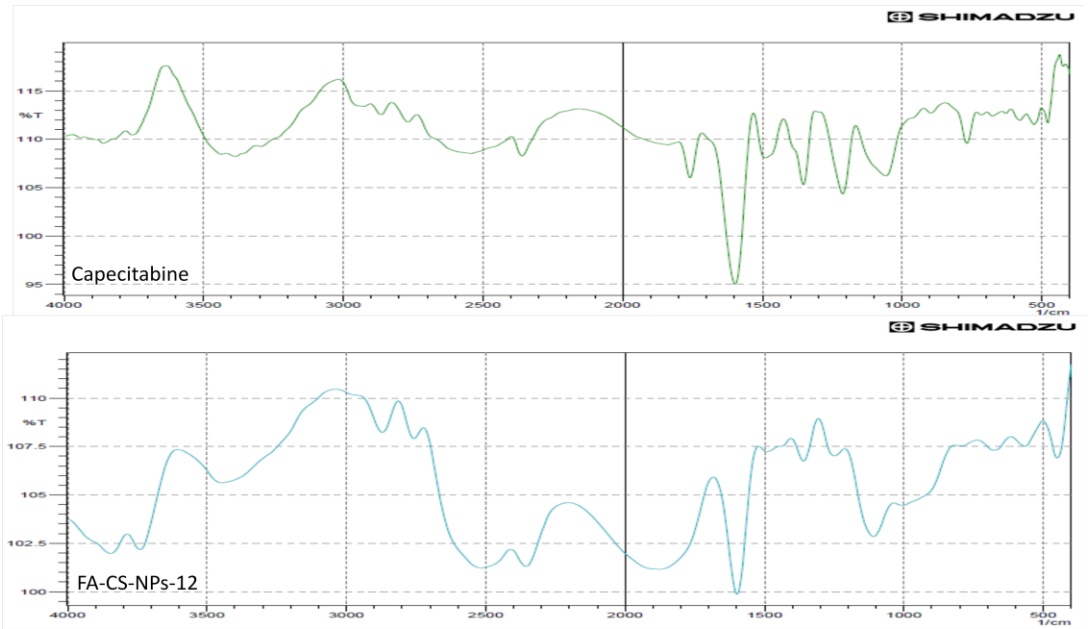

Figure 6.58: FT-IR Spectrum of capecitabine and optimized FA-CS-NPs-12 in range 4000 to 400 cm^{-1}

6.7.4 Differential scanning calorimetry

Optimized chitosan nanoparticle, FA-CS-NPs-12, were subjected to the differential scanning calorimetry to make the final confirmation about the compatibility of capecitabine with excipients by taking the DSC thermogram of FA-CS-NPs-12, and compared it with the DSC thermogram of capecitabine. This comparison is given in Figure 6.59

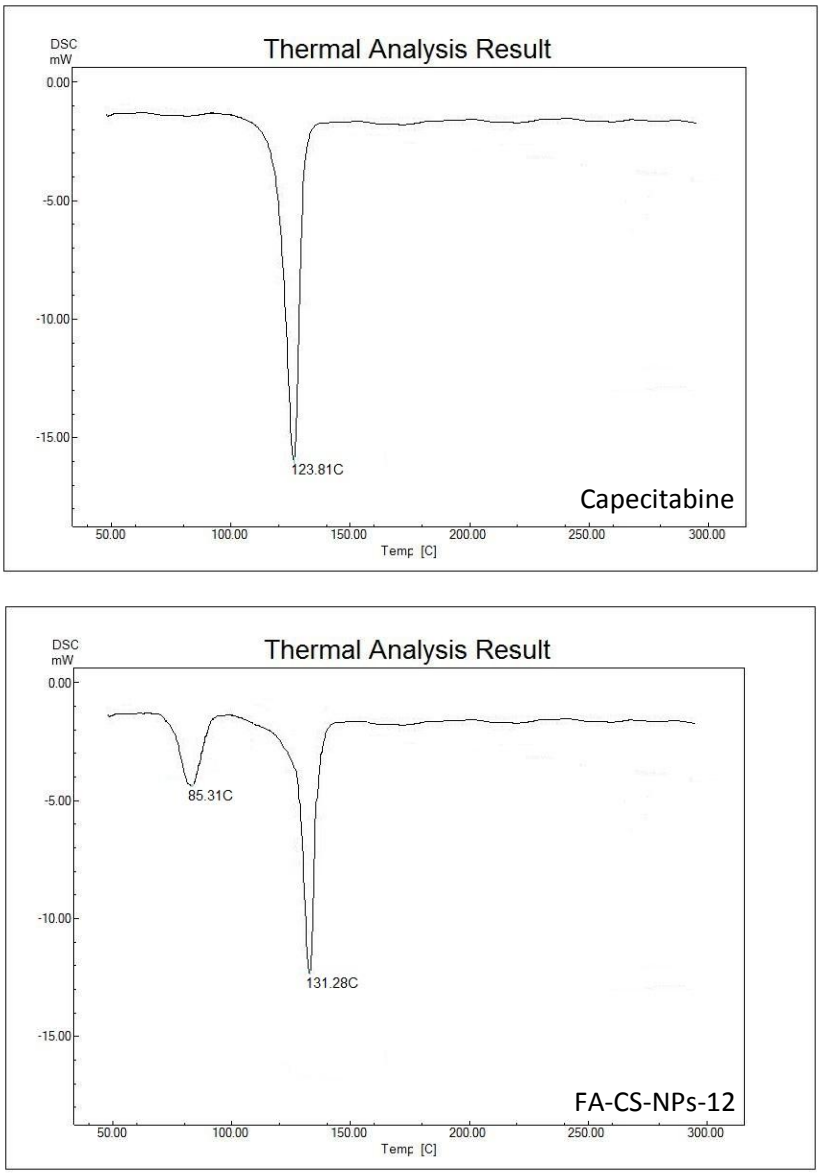

Figure 6.59: DSC thermogram of capecitabine and FA-CS-NPs-12

6.7.5 Drug release kinetics

Correlation coefficient of zero order, first order and higuchi model of drug release kinetics from optimized FA-CS-NPs-12 is summarized in Table 6.31

Table 6.31: Drug release kinetics for an optimized formulation FA-CS-NPs-12

Optimized formulation (FA-CS-NPs-12)	Release kinetic model		
	Zero order	First order	Higuchi model
	R^2	R^2	R^2
	0.795	0.950	0.902

Drug release from optimized FA-CS-NPs-12 as per the zero order, first order and higuchi model of the release kinetics are graphically represented in Figure 6.60, Figure 6.61 and Figure 6.62 respectively.

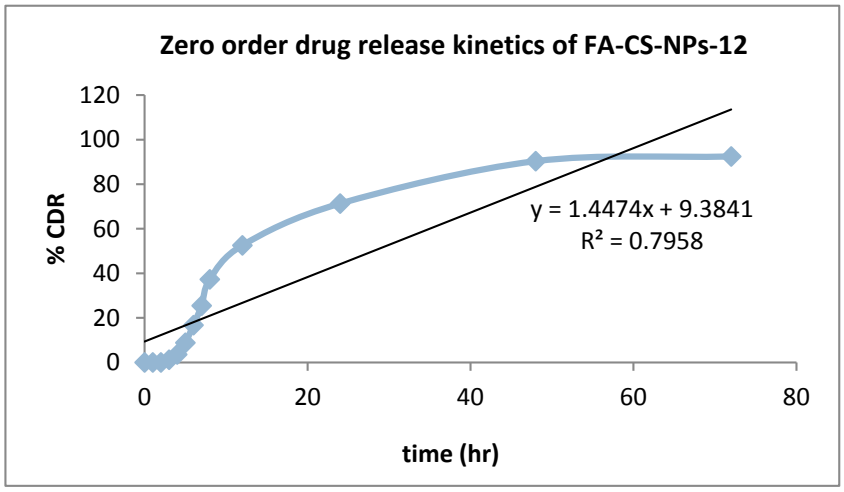

Figure 6.60: Zero order drug release kinetics of FA-CS-NPs-12

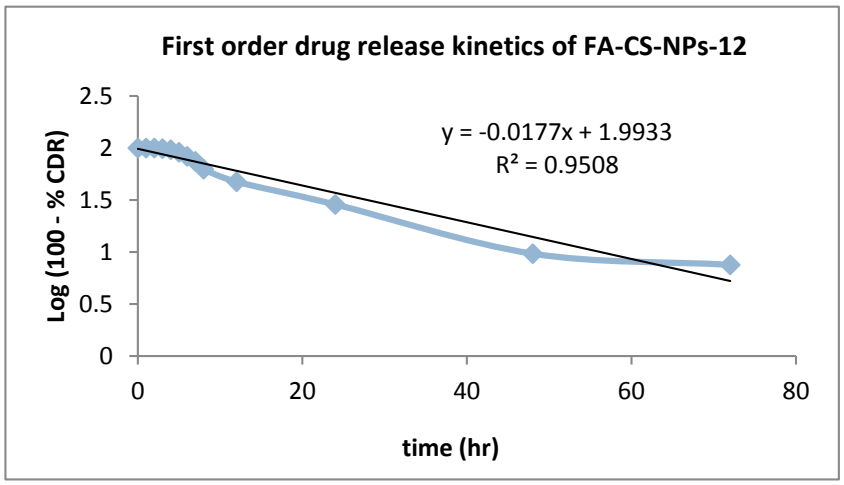

Figure 6.61: First order drug release kinetics of FA-CS-NPs-12

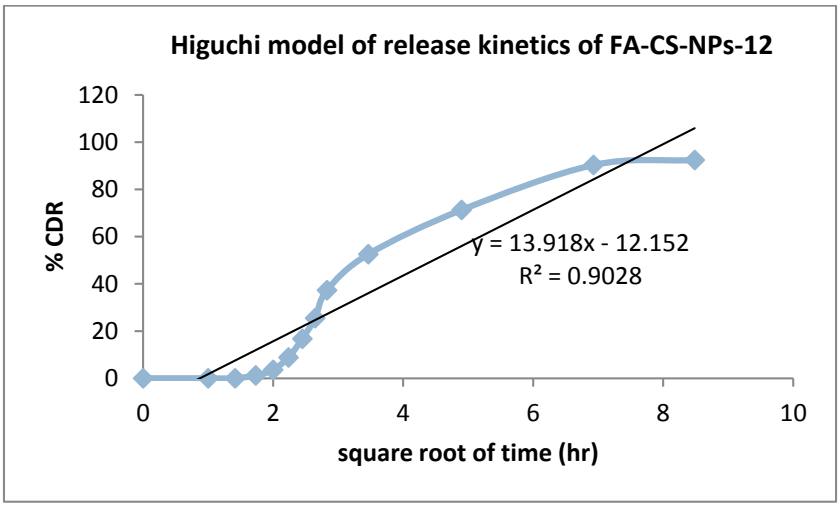

Figure 6.62: Higuchi model of drug release kinetics of FA-CS-NPs-12

6.8 *In-vitro* cell viability assay

Capecitabine loaded as well as blank FA-CS-NPs, capecitabine alone, and capecitabine loaded CS-NPs were evaluated for its efficacy to inhibit the growth of three different cell lines, HT-29, Vero, and MCF-7; and the outcome of this study is given in Table 6.32, Table 6.33 and Table 6.34 respectively. These percentage inhibition data is graphically represented in Figure 6.63.

6.8.1 Percentage inhibition of HT-29 cell line

Table 6.32: Percentage inhibition of HT-29 cell line

Concentration of capecitabine	FA-CS-NPs	Capecitabine	Blank FA-CS-NPs	CS-NPs
100µg/ml	72.01	50.37	-4.83	52.58
80µg/ml	55.77	37.97	-13.88	35.79
60µg/ml	44.17	27.51	-16.22	27.33
40µg/ml	17.71	-5.59	-9.10	9.43
20µg/ml	-1.90	1.32	-0.33	2.55
10µg/ml	8.14	7.23	-1.82	2.15

6.8.2 Percentage inhibition of Vero cell line

Table 6.33: Percentage inhibition of Vero cell line

Concentration of capecitabine	FA-CS-NPs	Capecitabine	Blank FA-CS-NPs	CS-NPs
100µg/ml	2.49	2.36	-1.59	1.28
80µg/ml	-11.80	-13.56	-8.10	-14.29
60µg/ml	-16.17	-9.78	-6.69	-13.95
40µg/ml	-13.22	-13.40	-8.45	-7.61
20µg/ml	-3.28	-6.12	-5.52	-10.18
10µg/ml	-5.45	-7.65	-4.44	-8.33

6.8.3 Percentage inhibition of MCF-7 cell line

Table 6.34: Percentage inhibition of MCF-7 cell line

Concentration of capecitabine	FA-CS-NPs	Capecitabine	Blank FA-CS-NPs	CS-NPs
100µg/ml	9.84	18.67	-3.86	7.97
80µg/ml	-7.97	-13.03	-7.29	-13.21
60µg/ml	-9.82	-13.40	-7.91	-18.51
40µg/ml	-15.15	-15.22	-11.71	-22.97
20µg/ml	-3.46	-11.16	-7.14	-23.11
10µg/ml	-16.20	-16.08	-8.17	-24.68

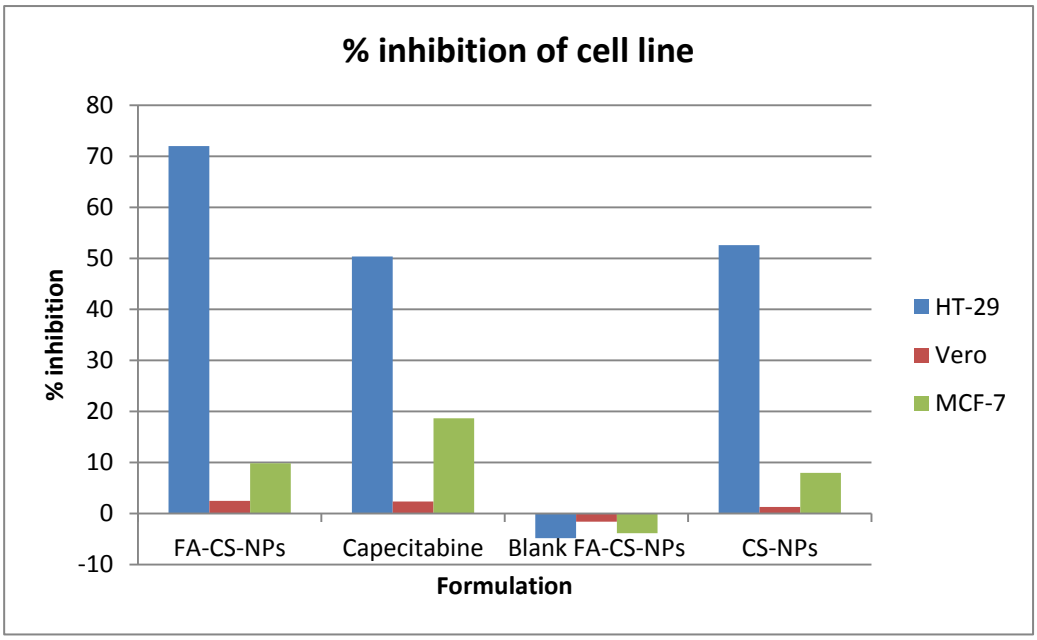

Figure 6.63: % inhibition of HT-29, Vero and MCF-7 cell line by various nanoparticles and capecitabine

6.9 *In-vitro* cell uptake study

In-vitro cell uptake study was performed to evaluate the folate receptor mediated cell-internalization of optimized folic acid conjugated nanoparticles, FA-CS-NPs-12. Result of this study is given in Figure 6.64.

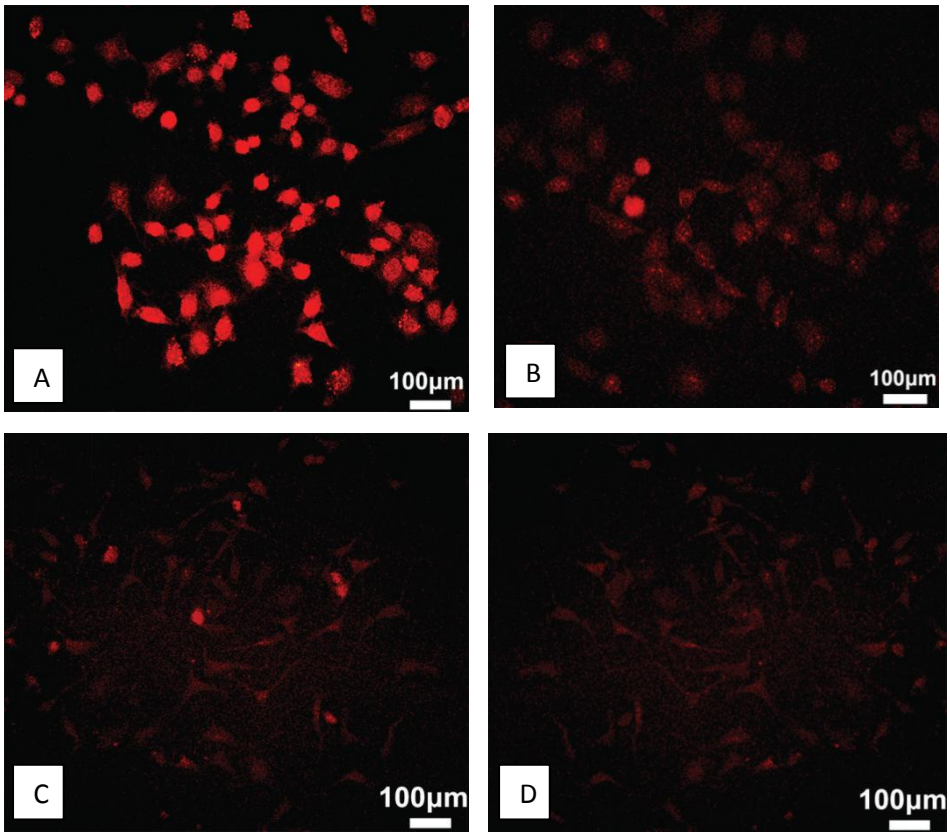

Figure 6.64: Fluorescent microscopy of A) FA-CS-NPs-12 and B) CS-NPs-8 in HT-29 cell; and C) FA-CS-NPs-12 and D) CS-NPs-8 in MCF-7 cells

6.10 Stability Study

6.10.1 Change in Physical appearance and % Drug content of optimized CS-NPs-8

Change in physical appearance and % drug content of optimized chitosan nanoparticle, CS-NPs-8 was analyzed for the periods of 90 day to check its stability. Data of this study for CS-NPs-8 is given in Table 6.35.

Table 6.35: Stability studies of CS-NPs-8

Storage condition	Tested after time (days)	Physical appearance	% Drug content
$25^{o}C \pm 2^{o}C$ (60%± 5%RH)	0	No change	29.74±0.025
	15	No change	29.68±0.011
	30	No change	29.42±0.015
	45	No change	29.28±0.012
	60	No change	29.12±0.031
	75	No change	28.78±0.059
	90	No change	28.29±0.042
$40^{o}C \pm 2^{o}C$ (75%± 5%RH)	0	No change	29.74±0.025
	15	No change	29.32±0.022
	30	No change	29.09±0.061
	45	No change	28.68±0.052
	60	No change	28.32±0.042
	75	No change	28.11±0.034
	90	No change	27.79±0.037

6.10.2 Change in Physical appearance and % Drug content of optimized FA-CS-NPs-12

Change in physical appearance and % drug content of folic acid cojugated chitosan nanoparticle was analyzed for the periods of 90 day to check its stability. Data of this study for FA-CS-NPs-12 is given in Table 6.36.

Table 6.36: Stability studies of FA-CS-NPs-12

Storage condition	Tested after time (days)	Physical appearance	% Drug content
$25^{o}C \pm 2^{o}C$ (60%± 5%RH)	0	No change	27.74±0.014
	15	No change	27.65±0.023
	30	No change	27.39±0.031
	45	No change	27.26±0.026
	60	No change	27.09±0.040
	75	No change	26.69±0.033
	90	No change	26.21±0.017
$40^{o}C \pm 2^{o}C$ (75%± 5%RH)	0	No change	27.74±0.025
	15	No change	27.32±0.064
	30	No change	27.09±0.057
	45	No change	26.68±0.044
	60	No change	26.32±0.028
	75	No change	26.11±0.059
	90	No change	25.79±0.035

n=3

6.10.3 *In-Vitro* drug release profile of CS-NPs-8

Percentage cumulative drug release was also studied for the purpose of stability evaluation of optimized chitosan nanoparticle, CS-NPs-8. % CDR was evaluated at the interval of 15 days, up to the 90 days. Result of this study for CS-NPs-8 stored at $25^{o}C \pm 2^{o}C$ is given in Table 6.37, and for CS-NPs-8 stored at $40^{o}C \pm 2^{o}C$ is given in Table 6.38. These data are represented graphically in Figure 6.65.

Table 6.37: Release profile of CS-NPs-8 during stability studies at $25^{o}C \pm 2^{o}C$ and 60%± 5 % RH

Time (hrs)	% CDR						
	Initial	15 days	30 days	45 days	60 days	75 days	90 days
0	0	0	0	0	0	0	0
1	1.1±0.57	1.04±0.21	0.98±0.31	0.91±0.23	0.85±0.34	0.79±0.44	0.73±0.36
2	5.7±0.92	5.36±0.65	5.12±0.84	4.89±0.71	4.65±0.78	4.41±0.97	4.17±0.84
3	8.9±0.97	8.64±0.86	8.37±0.93	8.11±0.62	7.85±0.99	7.59±1.06	7.32±0.75
4	16.47±1.01	16.18±0.94	15.89±1.02	15.59±0.85	15.30±1.07	15.01±1.15	14.72±0.98
5	19.2±1.53	18.97±1.13	18.75±1.07	18.52±1.32	18.29±1.26	18.07±1.2	17.84±1.45
6	28.9±1.87	28.40±1.4	27.90±1.62	27.41±1.37	26.91±1.53	26.41±1.75	25.91±1.5
7	39.4±2.08	38.90±2.2	38.41±2.31	37.91±1.74	37.41±2.33	36.92±2.44	36.42±1.87
8	51.27±1.26	50.65±2.11	50.02±2.9	49.40±2.21	48.78±2.24	48.16±3.03	47.53±2.34
12	69.1±1.58	68.48±1.87	67.86±2.46	67.24±2.65	66.62±2	66.00±2.59	65.38±2.78
24	93.48±2.013	92.61±2.15	91.74±2.91	90.88±2.76	90.01±2.28	89.14±3.04	88.27±2.89
48	94.4±2.15	93.47±2.27	92.54±2.78	91.62±2.83	90.69±2.4	89.76±2.91	88.83±2.96

n=3

Table 6.38: Release profile of CS-NPs-8 during stability studies at $40^{o}C \pm 2^{o}C$ and 75% ± 5% RH

Time (hrs)	% CDR						
	Initial	15 days	30 days	45 days	60 days	75 days	90 days
0	0	0	0	0	0	0	0
1	1.1±0.57	1.00±0.37	0.91±0.35	0.81±0.28	0.71±0.26	0.62±0.22	0.52±0.18
2	5.7±0.92	5.28±0.75	4.96±0.88	4.64±0.64	4.32±0.79	4.00±0.74	3.67±0.62
3	8.9±0.97	8.52±0.66	8.14±0.97	7.76±0.55	7.38±0.88	7.00±0.95	6.62±0.83
4	16.47±1.01	15.98±0.89	15.49±1.06	15.00±0.78	14.51±0.97	14.02±1.03	13.52±0.91
5	19.2±1.53	18.77±1.36	18.35±1.11	17.92±1.25	17.50±1.02	17.07±1.22	16.64±1.10
6	28.9±1.87	28.14±1.41	27.37±1.66	26.61±1.30	25.84±1.57	25.08±1.49	24.31±1.37
7	39.4±2.08	38.74±1.78	38.08±2.35	37.42±1.67	36.76±2.26	36.10±2.29	35.44±2.17
8	51.27±1.26	50.44±2.25	49.60±2.94	48.77±2.14	47.94±2.85	47.11±2.20	46.27±2.08
12	69.1±1.58	68.18±2.69	67.26±2.5	66.34±2.58	65.42±2.41	64.50±1.96	63.58±1.84
24	93.48±2.013	92.30±2.80	91.12±2.95	89.93±2.69	88.75±2.86	87.57±2.24	86.39±2.12
48	94.4±2.15	93.15±2.87	91.89±2.82	90.64±2.76	89.38±2.73	88.13±2.36	86.87±2.24

n=3

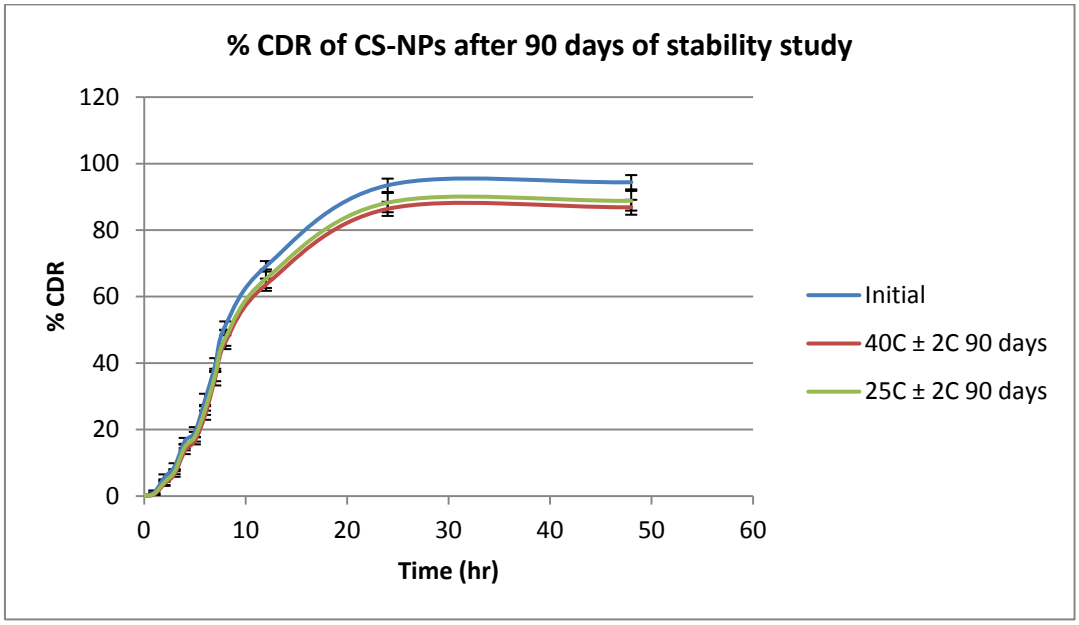

Figure 6.65: Comparison of *in-vitro* drug release profile of CS-NPs-8 before and after storage for 90 days, at 25° C ± 2°C and 40° C ± 2°C

6.10.4 *In-Vitro* drug release profile of FA-CS-NPs-12

Percentage cumulative drug release was also studied for optimized folic acid conjugated chitosan nanoparticle, FA-CS-NPs-12 for the purpose of stability evaluation. Percentage CDR was evaluated at the interval of 15 days, up to the 90 days. Result of this study for FA-CS-NPs-12 stored at $25^{o}C \pm 2^{o}C$ is given in Table 6.39, and for FA-CS-NPs-12 stored at $40^{o}C \pm 2^{o}C$ is given in Table 6.40. These data are represented graphically in Figure 6.66.

Table 6.39: Release profile of FA-CS-NPs-12 during stability studies at $25^{o}C \pm 2^{o}C$ and 60% ± 5% RH

Time (hrs)	% CDR						
	Initial	15 days	30 days	45 days	60 days	75 days	90 days
0	0	0	0	0	0	0	0
1	0	0	0	0	0	0	0
2	0	0	0	0	0	0	0
3	1.21±0.54	1.21±0.39	1.18±0.95	1.16±0.58	1.09±0.43	0.95±0.38	0.91±0.52
4	3.58±1.09	3.4±0.99	3.37±1.08	3.34±0.97	3.26±1.07	3.19±1.23	3.06±0.93
5	8.84±1.17	8.66±1.23	8.63±1.73	8.08±1.44	7.67±0.99	7.18±1.05	6.74±0.98
6	16.75±1.83	16.45±1.63	16.42±1.51	15.94±1.28	15.82±1.53	15.73±1.05	15.59±1.97
7	25.49±1.44	25.34±1.74	25.29±2.33	25.17±1.73	25.09±2.33	24.73±1.24	24.46±1.92
8	37.31±2.41	37.27±2.53	37.14±1.33	37.03±2.28	36.93±2.23	36.31±2.43	35.75±1.44
12	52.56±2.33	52.46±1.51	52.23±2.17	52.18±2.43	51.94±1.33	51.13±2.18	50.68±1.88
24	71.32±2.08	71.21±1.5	71.18±2.24	71.05±1.98	70.94±1.89	70.12±2.33	69.46±1.70
48	90.36±1.85	90.23±1.78	90.11±1.95	89.96±2.34	89.67±2.19	89.09±1.98	88.29±2.00
72	92.47±2.24	92.32±2.28	92.19±2.53	92.03±2.73	91.73±2.28	91.34±2.43	90.72±2.07

n=3

Table 6.40: Release profile of FA-CS-NPs-12 during stability studies at $40^{o}C \pm 2^{o}C$ and 75% ± 5% RH

Time (hrs)	% CDR						
	Initial	15 days	30 days	45 days	60 days	75 days	90 days
0	0	0	0	0	0	0	0
1	0	0	0	0	0	0	0
2	0	0	0	0	0	0	0
3	1.21±0.54	1.12±0.83	0.93±0.83	0.83±0.91	0.82±0.91	0.76±0.65	0.72±0.82
4	3.58±1.09	3.31±0.8	3.24±1.19	3.12±0.96	2.94±0.96	2.57±0.86	2.38±0.95
5	8.84±1.17	8.57±1.43	8.19±1.11	7.83±1.04	7.42±1.04	6.93±1.1	6.49±1.6
6	16.75±1.83	16.36±1.77	15.93±2.10	15.57±1.7	15.25±1.7	14.76±1.5	14.22±1.38
7	25.49±1.44	25.15±1.98	24.82±2.15	24.39±1.31	24.11±1.31	23.91±1.61	22.47±2.2
8	37.31±2.41	37.08±1.26	36.84±1.98	36.57±2.28	36.07±2.28	35.81±2.4	34.74±1.2
12	52.56±2.33	52.17±1.48	51.91±2.37	51.38±2.2	50.03±2.2	49.49±1.38	48.18±2.04
24	71.32±2.08	71.12±1.60	70.82±2.09	70.63±1.95	70.05±1.95	68.74±1.43	67.23±2.11
48	90.36±1.85	89.95±2.01	89.37±2.23	89.09±1.72	88.31±1.72	87.05±1.65	86.07±1.82
72	92.47±2.24	92.03±2.05	91.49±2.20	91.03±2.11	90.28±2.11	89.11±2.15	87.64±2.40

n=3

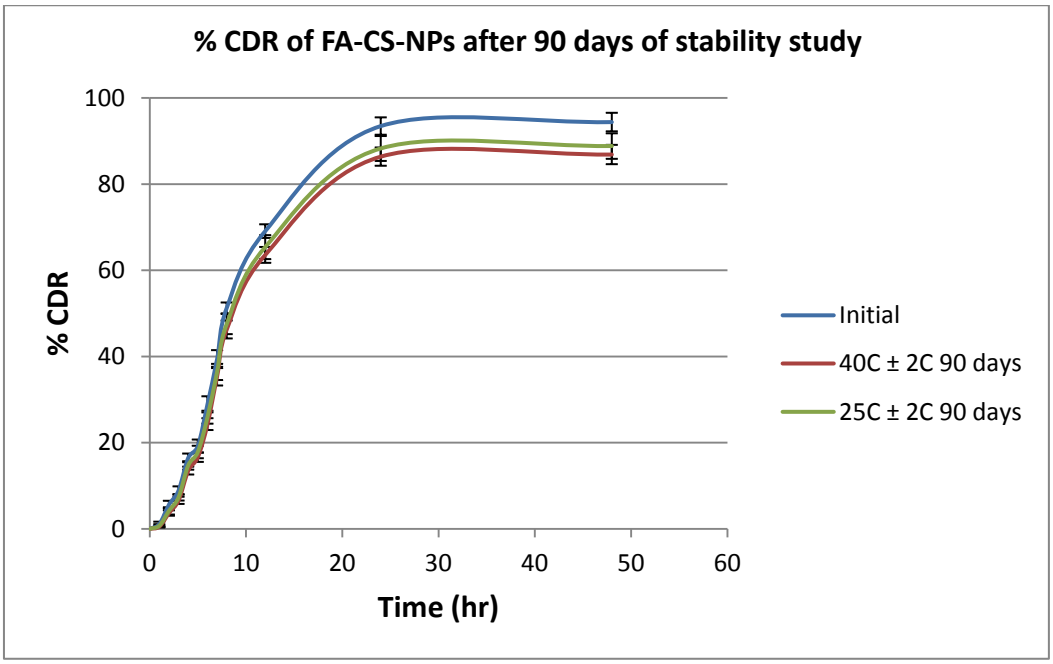

Figure 6.66: Comparison of *in-vitro* drug release profile of FA-CS-NPs-12 before and after storage for 90 days, at 25° C ± 2°C and 40° C ± 2°C

7. DISCUSSION

The research work emphasis on fabrication of folic acid conjugated chitosan nanoparticle for targeting the capecitabine to the colon cancer. Initially capecitabine loaded chitosan-TPP nanoparticles were prepared using ionic gelation method, and then optimized nanoparticles were conjugated with the folic acid. The result obtained in this study indicates that, capecitabine can be effectively loaded in chitosan nanoparticle system, resulting in formulation that considerably sustain the release rate of drug, and precisely targeting the drug only to the folate-receptor expressing colon cancer cells and not to the normal healthy cells, thus contributing to reduced dose and toxicity of the drug.

7.1 Preformulation study

Before development of formulation, it is necessary to perform the preformulation study for drug molecule to develop optimized formulation with required characteristics.

Preformulation can be defined as investigation of physical and chemical properties of drug substance alone and when combined with excipients. Preformulation studies are the first step in the rational development of dosage form of a drug substance. The objectives of preformulation studies are to develop a portfolio of information about the drug substance, so that this information is useful to develop formulation. Preformulation investigations are designed to identify those physicochemical properties and excipients that may influence the formulation design, method of manufacture, and pharmacokinetic-biopharmaceutical properties of the resulting product. Followings studies were performed for the drug and excipients used for the formulation development.

In Preformulation study, all the characteristics of drug were observed like physical appearance, melting point, solubility in different solvents and compatibility study with other excipients used for the formulation development. To estimate the drug amount in the formulation and % CDR, maximum wavelength i.e. λmax and linearity curve were determined in various solvents used in the study by UV spectrophotometric technique and plotted.

7.1.1 Physical nature of capecitabine

Physical nature of capecitabine like color, odor, and appearance was observed physically. The drug was found to be white, odorless and free flowing powder, which serves as a primary identification of drug (Table 6.1).

7.1.2 Melting point determination

Melting point is a good indication of purity of the sample since the presence of relatively small amount of impurity can be detected by a lowering as well as widening in the melting point range. Melting point for the drug was determined by capillary method using melting point testing apparatus. It found in the range of 117 ˚C – 121 ˚C, which was similar as reported melting point for the drug capecitabine in the literature. Henceforth, it may indicate that the drug sample does not contain any impurity (Table 6.3).

7.1.3 Solubility analysis

Solubility of capecitabine was determined by saturation equilibrium method with water. Solubility of capecitabine in various solvents like distilled water, aqueous acetic acid (1 % v/v), and in phosphate buffer pH 7.4 was found to be 25.12±0.19 mg/ml, 28.24±0.08 mg/ml and 31.21 ± 0.11 mg/ml respectively. It indicates that capecitabine is sparingly soluble in each of the solvents used as per the terminology defined in Indian Pharmacopoeia for the solubility. It was noted that this much solubility in distilled water, aqueous acetic acid and in phosphate buffer was sufficient to estimate it in the formulation as well as for drug release study. Solubility of the capecitabine in distilled water was found to be similar as per reported solubility (Table 6.2).

7.1.4 Determination of λmax of capecitabine

First step in development of UV spectroscopic method is screening of each component expected to present in drug sample prepared for estimation of drug content in formulation and in diffusion media over UV range. Excipients should not interfere with drug peak at absorption maxima (λmax) of drug and if any excipients interfere with drug peak then method should be modified accordingly. The λmax of drug acapecitabine having concentration 10 µg/ml was found to be 240 nm in each solvent i.e. in distilled water, phosphate buffer pH 7.4 and in aqueous acetic acid (1% v/v) while screened over entire UV range 200 – 400 nm. So, 240 nm was used as wave-

length for estimation of drug amount present in formulation and drug release from CS-NPs and FA-CS-NPs (Table 6.4).

7.1.5 Calibration curve of the capecitabine

Before determining the calibration curve, stability of the capecitabine in each solvent i.e. in distilled water, phosphate buffer pH 7.4 and aqueous acetic acid was ascertained by observing the changes in the absorbance of the solution at the analytical wavelength over a period of 48 hr at room temperature. It was observed that no change in λmax and absorbance over period of 48 hr proves that drug was stable in each solvent for the period of 48 hr.

The calibration curve for the drug capecitabine were taken in distilled water and phosphate buffer pH 7.4 at 240 nm absorption maxima using UV – Visible spectrophotometer. It was found that drug was giving the linearity in concentration range of 5 – 40 µg/ml in each solvent. The regression value (R^2) for distilled water and phosphate buffer pH 7.4 was found to be 0.995 and 0.997 respectively. It indicates that the calibration curve obtained in each solvent was linear in the range of prepared concentrations of drug (Table 6.5, Table 6.6, Figure 6.1, and Figure 6.2).

7.1.6 Determination of λmax of folic acid

Folic acid is used as a colon cancer targeting carrier, conjugated on chitosan nanoparticles. λmax of folic acid was required to be determined because on a later stage of folic acid conjugation on chitosan nanoparticles, % conjugation was calculated by indirect method through determining the folic acid concentration present in the supernatant. Therefore calibration of folic acid in phosphate buffer solution was a necessary step for which λmax determination was inevitable.

The λmax of folic acid having concentration 10 µg/ml was found to be 283 nm in phosphate buffer pH 7.4 while screened over entire UV range 200 – 400 nm. So, 283 nm was used as wavelength for estimation of folic acid amount present in supernatant to calculate the % conjugation of the folic acid after fabrication of folic acid conjugated chitosan nanoparticles (Table 6.4).

7.1.7 Calibration curve of the folic acid

The calibration curve for the folic acid was taken in phosphate buffer solution pH 7.4 at 283 nm absorption maxima using UV – Visible spectrophotometer. It was found

that folic acid was giving the linearity in concentration range of 4 – 20 µg/ml. The regression value (R^2) was found to be 0.995. It indicates that the calibration curve obtained in phosphate buffer solution pH 7.4 was linear in the range of prepared concentrations of folic acid (Table 6.7 and Figure 6.3).

7.1.8 Compatibility study

Compatibility of capecitabine with excipients used in nanoparticle formulation was analyzed by FTIR spectroscopy. The spectra of drug alone and in combination with other excipients as physical mixture used for the formulation development were taken in the wavelength region of 4000–400 cm^{-1}. All spectras were compared with the spectrum of drug to check any interaction was there or not in between drug molecule and excipients. No major changes were observed in the functional groups peak for capecitabine in any spectra when compared it with spectrum of pure drug. So, it was considered that there was no any interaction takes place in between drug and excipients used for the formulation development and they were compatible with drug (Figure 6.4, Figure 6.5, Figure 6.6, Figure 6.7 and Figure 6.8).

7.2 Formulation of chitosan nanoparticles

There are numbers of methods reported for preparation of nanoparticles. From these, ionotropic gelation method was selected for the present study as it could be feasible and easy to formulate nanoparticles at laboratory scale with small particle size and high entrapment efficiency

Chitosan nanoparticles were prepared by ionic gelation method. 1% v/v acetic acid solvent was used to dissolve drug and polymer. The amount of drug was kept constant while the concentration of chitosan and TPP was varied. During the trial batches it was founded that the concentration of chitosan lower than 0.5mg/ml was not able to entrap the drug while concentration exceeding 1.5mg/ml was not showing any apparent rise in percentage drug entrapment. In the same way for TPP, the effective range of concentration was found to be 0.5mg/ml to 1mg/ml. Therefore using these range of chitosan and TPP concentration range 09 batches was formulated by varying the chitosan and TPP concentration within the above mentioned range using 3^2 full factorial design (Table 5.9 and Table 5.10).

7.3 Characterization of chitosan nanoparticles

% Entrapment Efficiency, % yield, % drug content and % CDR of each batch was evaluated and from the results of the of %EE and % CDR CS-NPs was optimized using the contour plots and response surface quadratic mode, done by regression analysis. CS-NPs-8 was found to be optimized batch and then it was further subjected to particle size analysis, surface morphology by SEM, FT-IR study, DSC study, Drug release kinetics, *In-vitro* cell viability assay, *In-vitro* cell uptake assay and stability study.

7.3.1 Percentage yield

The percentage yield for each formulated batches was found to be in the range of 54.17±2.5 to 73.9±0.96. It was observed that production yield was varied with change in concentration of chitosan or sodium TPP. Batch CS-NPs-6 shows the maximum production yield containing 1 mg/ml chitosan concentration and 1 mg/ml sodium TPP concentration. It was also found that, the formulation containing similar concentration of chitosan and sodium TPP were gave higher yield as compared to other formulation batches (Table 6.8 and Figure 6.9).

7.3.2 Entrapment efficiency

Entrapment efficiency was determined for all 09 batches and it was obtained in the range of 45 to 85%. The maximum entrapment was in batch CS-NPs-8, 85.74±2.36. This may be because of optimum concentration of chitosan as well as of TPP. Initially as concentration of TPP increases, the entrapment was also found to be increasing up to certain limit, but as concentration further increases, the entrapment was decreasing. This suggest that at lower level TPP is not sufficient enough to crosslink all chitosan used, and at higher concentration TPP might be causing the over cross linking which is reducing the entrapment. For chitosan, higher level was observed to cause maximum entrapment, which suggests that the 1:3 capecitabine chitosan ratio is optimum (Table 6.8 and Figure 6.10).

7.3.3Ppercentage drug content

Percentage drug content was determined for all nine batches, and were obtained in the range from 23.03±0.43 to 29.9±0.91. It was required to determine to perform the in-vitro drug release study as an equivalent amount of drug can be calculated from percentage drug content (Table 6.8 and Figure 6.11).

7.3.4 In –vitro drug release studies

The *In-Vitro* drug release of drug capecitabine from all the nanoparticles batches was carried out by using dialysis method in phosphate buffer pH 7.4 for 48 hrs. The cumulative percentage release of capecitabine from the prepared nanoparticles was obtained from 73.5±2.15 to 94.4±2.15. Highest drug release found in CS-NPs-8 might be because of the better through entrapment of the drug in chitosan network within nanoparticle, because the same batch also exhibits the maximum drug entrapment. These outcome suggest that the 1.5mg/ml and 0.75mg/ml concentration of the chitosan and TPP respectively can be concluded as a optimum in order to get the maximum possible capecitabine entrapment and more percentage drug release with extended time (Table 6.9, Table 6.10, Figure 6.12, Figure 6.13 and Figure 6.14).

7.4 Optimization of chitosan nanoparticles

The popular method in the development and optimization of the drug delivery system is response surface methodology (RSM). Depending on the principles of design of experiments, the methodology involves the use of various types of experimental designs, generation of polynomial mathematical equations and plotting the response over the experimental domain to choose the optimum formulation. A full factorial statistical design is one type of RSM. It specifies the required experimental runs and consumes less time and thus provides a far more efficient and cost-effective technique than the conventional techniques of formulation and optimization of dosage forms.

Based on obtained result for characterization of nanoparticle, it was found that change in the concentration of chitosan and sodium TPP has higher influence on entrapment efficiency. Thus, a 3^2 full factorial design was employed in optimizing the formula. The concentration of chitosan (X_1) and concentration of sod TPP (X_2) were taken as the independent variables whereas the entrapment efficiency was taken as the dependent variable.

7.4.1 Fitting the model to the data

Entrapment efficiency was obtained by conducting systematic experiments at various levels and was subjected to regression analysis. All the responses observed for 09 formulations prepared were simultaneously fitted to linear, quadratic and cubic models manually and the responses were evaluated using the data analysis feature of Mi-

crosoft Excel 2007. It was found that the best-fitted model was quadratic model. Thus a polynomial equation of the full model was obtained. The entrapment efficiency for the all prepared 09 batches showed a variation in the range of 45.6±1.5% to 85.74±2.36 %.

Non-significant terms, showing the P-values > 0.05 were rejected and reduced model was obtained and regression of the reduced model was carried out. Significance of each coefficient was established by P value. Lower the magnitude of the P value, more significant is the corresponding coefficient.

Based on the P value, X_1, X_2, $(X_1)^2$, and $(X_2)^2$ factors were found to be significant while the factor X_1X_2 was found to be insignificant. In addition, the F value was obtained from the full and reduced models. As the calculated F value was found to be less than the tabular F value, it can be concluded that the neglected terms do not significantly contribute in the prediction of the entrapment efficiency using reduced polynomial equation. The value of the coefficient of X_1 was found to be greatest. From this, it was concluded that X_1 is the factor that affects the entrapment efficiency maximum.

The determination coefficient R^2 gives an excellent idea about the goodness of the fit of the model. The R^2 values for the full and the reduced model ware found to be 0.989 and 0.963 respectively. From this, we can conclude that above 90% of the variations are explained by the model. Lastly, high values of the correlation coefficient for the full model and the reduced model implies a very good correlation between the selected independent variables (Table 6.11 to Table 6.15).

7.4.2 Contour plots and response surface analysis

Two-dimensional contour plots and three dimensional response surface plots were prepared for the response 'percentage entrapment efficiency'. It was found that as the values of chitosan and TPP were low, the entrapment was also low. But an increase in the concentrations also increased the entrapment efficiency. This was further confirmed by plotting response surface plots that depicted the same results. Thus from the plots a range was established for the independent variables. It was found that when chitosan is taken in the range of 1.4 – 1.5 mg/ml and sodium TPP was taken in the range of 0.7 – 0.8mg/ml, satisfactory entrapment can be achieved. However maxi-

mum entrapment could be achieved at 0.75mg/ml sodium TPP solution and 1.5 mg/ml chitosan concentration that represent the batch CS-NPs-8, and same batch has also given maximum drug release after 48hr, there for batch CS-NPs-8 was concluded as a optimized batch (Figure 6.15 and Figure 6.16).

7.4.3 Check point analysis

From the two-dimensional contour plots, prepared for the response 'percentage entrapment efficiency', any three random points was selected and predicted percentage EE at that selected chitosan concentration and TPP concentration was noted. Percentage EE was also obtained experimentally by preparing the three different batches of CA-NPs using the three randomly selected levels of chitosan and TPP concentration. Then after difference between predicted and experimental percentage EE was calculated to obtain the percentage error. It was found that none of these three batch shows % error more than ±5%, which suggest the reliability of predicted values of the selected response '% EE' from the contour plots (Table 6.16).

7.5 Evaluation of optimized chitosan nanoparticles

7.5.1 Particle size analysis

Particle size determination was done by using Malvern particle analyzer instrument for the optimized batch CS-NPs-8. Average particle size was found to be 87.23 nm with maximum intensity and volume. This much reduced particles sized nanoparticle can serve better internalization in colon cancer cells hence better effect of capecitabine against colon cancer. From this data, it could be said that the nanoparticles has been formed successfully by using ionic cross linking method (Figure 6.17).

7.5.2 Polydispersibility index (PDI)

Particles with the less PDI has more uniform size distribution which can help preventing the aggregation resulting in better stability of nanoparticles, because in broad size distribution, smaller particles can adhere to the larger particle and hence can lead to the aggregation. PDI of the optimized chitosan nanoparticles, CS-NPs-8 was found to be 0.113, which is quite a narrow size distribution and contributes to the stability of nanoparticles (Figure 6.17).

7.5.3 Zeta potential

As Zeta Potential is an important tool for prediction of long term stability and understanding the state of the nanoparticle surface. The value greater than + 25 mV or less than – 25 mV have high degree of stability. Zeta potential of the optimized chitosan nanoparticles, CS-NPs-8 was found to be -35.9 mV which suggests that CS-NPs-8 can remain stable without undergoing an aggregation (Figure 6.18).

7.5.4 Scanning Electron Microscopy (SEM)

The surface morphology of optimized formulation CS-NPs-8 was studied using scanning electron microscopy. SEM is an instrument that produces largely magnified image by using electrons instead of light. Electron gun produces a beam of electrons, which follows the vertical path through the microscope between electromagnetic fields and lenses towards the sample due to which electrons, and X-rays are ejected from sample. The particle shape was found to be fairly spherical structure with smooth surface (Figure 6.19).

7.5.5 FT-IR study

Compatibility of capecitabine with excipients within the optimized chitosan nanoparticles, CS-NPs-8 was analyzed by FTIR spectroscopy. The spectra of drug alone and CS-NPs-8 were taken in the wavelength region of 4000–400 cm^{-1}. All spectras were compared with the spectrum of drug to check any interaction was there or not in between drug molecule and excipients. No major changes were observed in the functional groups peak for capecitabine in any spectra of CS-NPs-8 when compared it with spectrum of pure drug. So, it was considered that there was no interactions in between drug and excipients present in the CS-NPs (Figure 6.20).

7.5.6 Differential scanning calorimetry

Differential scanning calorimetry is widely used in thermal analysis to monitor endothermic processes (melting, solid-solid phase transitions and chemical degradation) as well as exothermic processes (crystallization and oxidative decomposition). It could be extremely useful since it indicates the existence of possible drug-excipients or excipient-excipient interactions in formulation. Thermogram of pure drug capecitabine shows an endothermic peak at 123.81 ºC which indicates the purity of the drug as the reported melting point of the capecitabine was 123.27 ºC. The thermogram of an op-

timized CS-NPs-8 shows two endothermic peaks at 120.17 ºC and 82.36 ºC. In this, endothermic peak at 120.17 ºC indicates the presence of drug and its stability into the CS-NPs-8 (Figure 6.21).

7.5.7 Drug release kinetics

The *in-vitro* release profile of an optimized CS-NPs-8 were fitted in various kinetic dissolution models like zero order, first order and Higuchi respectively. As indicated by higher R^2 values, the drug release from optimized formulation follows first order release and Higuchi model. Since it was confirmed as Higuchi model, the release mechanism was swelling and diffusion controlled (Figure 6.22, Figure 6.23 and Figure 6.24).

7.6 Formulation of FA-CS-NPs

The optimized chitosan nanoparticles CS-NPs-8 were conjugated with folic acid. However, conjugation between CS-NPs and FA was due to the fact that cationic amino group of chitosan had strong electrostatic interaction with anionic carboxyl group of FA. Three variables were selected to apply the 3^3 factorial design for the statistical evaluation of effect of all variables on the various parameters of the FA-CS-NPs. Range of the each of three variables was identified by preparing and analyzing the various trial batches at different random levels of all three variable. As a result of such trial study, range of the variable 'folic acid concentration' was found to be 2.5mg to 7.5mg per 20mg of chitosan nanoparticles. Range for the variable 'RPM' was found to be 10 to 30 rpm while the range for the variable 'reaction time' was found to be 10 to 30 minutes (Table 5.11 and Table 5.12).

7.7 Characterization of FA-CS-NPs

7.7.1 Percentage conjugation

Percentage conjugation was determined for all 27 batches and it was obtained in the range of 38.19±0.76 to 91.23±0.82%. The maximum folic acid conjugation was in batch FA-CS-NPs-12, 91.23±0.82%. This suggest that the optimum value for the variable folic acid concentration was found to be 5mg per 20mg of chitosan nanoparticles, while for RPM variable it was found to be 500rpm and for reaction time variable it was found to be 30 minutes (Table 6.18 and Figure 6.26).

7.7.2 *In –vitro* drug release studies

The *In-Vitro* drug release of drug capecitabine from the various folic acid conjugated nanoparticles formulations was carried out by using dialysis method in phosphate buffer pH 7.4 for 72 hrs. The cumulative percentage release of capecitabine from the prepared nanoparticle batch FA-CS-NPs-12 was found to be 92.47±2.28. The drug moved through inside pores in nanoparticles slowly and fell into the medium by diffusion. FA-CS NPs suggested that they had potential as a long-lasting and effective drug delivery system (Table 6.19 to Table 6.24, Figure 6.28 to Figure 6.36).

7.8 Optimization of FA-CS-NPs

The popular method in the development and optimization of the drug delivery system is response surface methodology (RSM). Depending on the principles of design of experiments, the methodology involves the use of various types of experimental designs, generation of polynomial mathematical equations and plotting the response over the experimental domain to choose the optimum formulation. A full factorial statistical design is one type of RSM. It specifies the required experimental runs and consumes less time and thus provides a far more efficient and cost-effective technique than the conventional techniques of formulation and optimization of dosage forms.

Based on obtained result for characterization of folic acid conjugated chitosan nanoparticle, it was found that change in the folic acid ratio, RPM and reaction time has higher influence on conjugation efficiency. Thus, a 3^3 full factorial design was employed in optimizing the formula. The amount of folic acid (X_1), RPM (X_2) and reaction time (X_3) were taken as the independent variables whereas the cojugation efficiency was taken as the dependent variable.

7.8.1 Fitting the model to the data

conjugation efficiency was obtained by conducting systematic experiments at various levels and was subjected to regression analysis. All the responses observed for all 27 formulations prepared were simultaneously fitted to linear, quadratic and cubic models manually and the responses were evaluated using the data analysis feature of Microsoft Excel 2007. It was found that the best-fitted model was quadratic model. Thus a polynomial equation of the full model was obtained. The conjugation efficiency for

the all prepared 27 batches showed a variation in the range of 38.19±0.76% to 91.23±0.82 %.

Non-significant terms, showing the P-value > 0.05 were rejected, and reduced model was obtained and regression of the reduced model was carried out. Significance of each coefficient was established by P value. Lower the magnitude of the P value, more significant is the corresponding coefficient.

Based on the P value, X_1, X_2, X_3 and $(X_1)^2$ factors were found to be significant while all other factors were found to be insignificant. In addition, the F value was obtained from the full and reduced models. As the calculated F value was found to be less than the tabular F value, it can be concluded that the neglected terms do not significantly contribute in the prediction of the conjugation efficiency using reduced polynomial equation.

The determination coefficient R^2 gives an excellent idea about the goodness of the fit of the model. The R^2 values for the full and the reduced model ware found to be 0.839 and 0.788 respectively. From this, we can conclude that above 80% of the variations are explained by the model. Lastly, high values of the correlation coefficient for the full model and the reduced model implies a very good correlation between the selected independent variables (Table 6.25 to Table 6.29).

7.8.2 Contour plots and response surface analysis

Total 09 two-dimensional contour plots and 09 three-dimensional response surface plots were prepared for the response 'percentage conjugation efficiency'. By comparing all these contour plots with each other, the common area in which there was a maximum percentage conjugation was obtained. A common zone where a maximum conjugation can obtained was representing the 5mg folic acid/20mg of CS-NPs-8, 500 RPM and 30 minutes of reaction time that represent the batch FA-CS-NPs-12, and same batch has also given maximum drug release amongst other batches after 72hr, there for batch FA-CS-NPs-12 was concluded as a optimized batch (Figure 6.37 to Figure 6.54).

7.8.3 Check point analysis

From the various two-dimensional contour plots, prepared for the response 'percentage conjugation efficiency', any three random points was selected and predicted per-

centage conjugation at that selected levels of all three variables were noted. Percentage conjugation was also obtained experimentally by preparing the three different batches of FA-CA-NPs using the three randomly selected points from contour plots. Then after difference between predicted and experimental percentage conjugation was calculated to obtain the percentage error. It was found that none of these three batch shows % error more than ±5%, which suggest the reliability of predicted values of the selected response '% conjugation' from the contour plots (Table 6.30).

7.9 Evaluation of optimized FA-CS-NPs

7.9.1 Particle size analysis

Particle size determination was done by using Malvern particle analyzer instrument for the optimized batch of folic acid conjugated chitosan nanoparticles, FA-CS-NPs-12. Average Particle size was found to be 121.9 nm with maximum intensity and volume, while average particle size of CS-NPs-9 was observed 87.23. Hence, particles size was observed to be slightly increasing when folic acid was conjugated on optimized CS-NPs, that is because of the peripheral conjugation of folic acid surrounding the particle surface. Much reduced sized nanoparticle can serve better internalization in colon cancer cells hence better effect of capecitabine against colon cancer (Figure 6.55).

7.9.2 Polydispersibility index (PDI)

Particles with the less PDI has more uniform size distribution which can help preventing the aggregation resulting in better stability of nanoparticles, because in broad size distribution, smaller particles can adhere to the larger particle and hence can lead to the aggregation. PDI of the optimized folic acid conjugated chitosan nanoparticles, FA-CS-NPs-12 was found to be 0.124, which is quite a narrow size distribution and contributes to the stability of nanoparticles (Figure 6.55).

7.9.3 Zeta potential

As Zeta Potential is an important tool for prediction of long term stability and understanding the state of the nanoparticle surface. The value greater than + 25 mV or less than – 25 mV have high degree of stability. Zeta potential of the optimized folic acid conjugated chitosan nanoparticles, FA-CS-NPs-12 was found to be -30.9 mV which

suggests that FA-CS-NPs-12 can remain stable without undergoing an aggregation (Figure 6.56).

7.9.4 Scanning Electron Eicroscopy (SEM)

The surface morphology of optimized formulation FA-CS-NPs-12 was studied using scanning electron microscopy. SEM is an instrument that produces largely magnified image by using electrons instead of light. Electron gun produces a beam of electrons, which follows the vertical path through the microscope between electromagnetic fields and lenses towards the sample due to which electrons, and X-rays are ejected from sample. The particle shape was not found complete spherical and smooth surface as found in CS-NPs. This can because of the irregular conjugation of the folic acid on the surface of the chitosan nanoparticle during the conjugation process (Figure 6.57).

7.9.5 FT-IR study

Compatibility of capecitabine with excipients within the optimized folic acid conjugated chitosan nanoparticle, FACS-NPs-12 was analyzed by FTIR spectroscopy. The spectra of drug alone and FA-CS-NPs-12 were taken in the wavelength region of 4000–400 cm^{-1}. All spectras were compared with the spectrum of drug to check any interaction was there or not in between drug molecule and excipients. No major changes were observed in the functional groups peak for capecitabine in any spectra of FA-CS-NPs-12 when compared it with spectrum of pure drug. So, it was considered that there was no interactions in between drug and excipients present in the FA-CS-NPs (Figure 6.58).

7.9.6 Differential scanning calorimetry

Differential scanning calorimetry is widely used in thermal analysis to monitor endothermic processes (melting, solid-solid phase transitions and chemical degradation) as well as exothermic processes (crystallization and oxidative decomposition). It could be extremely useful since it indicates the existence of possible drug-excipients or excipient-excipient interactions in formulation. Thermogram of pure drug capecitabine shows an endothermic peak at 123.81 ºC which indicates the purity of the drug as the reported melting point of the capecitabine was 123.27 ºC. The thermogram of an optimized FA-CS-NPs-12 shows two endothermic peaks at 131.28 ºC and 85.31 ºC. In

this, endothermic peak at 131.28 ºC indicates the presence of drug and its stability within the FA-CS-NPs-12 (Figure 6.59).

7.9.7 Drug release kinetics

The *in-vitro* release profile of an optimized FA-CS-NPs-12 was fitted in various kinetic dissolution models like zero order, first order and Higuchi respectively. As indicated by higher R^2 values, the drug release from optimized formulation follows first order release and Higuchi model. Since it was confirmed as Higuchi model, the release mechanism was swelling and diffusion controlled (Figure 6.60, Figure 6.61 and Figure 6.62).

7.10 *In-vitro* cell viability assay

Capecitabine loaded FA-CS-NPs was accessed for its anti-cancer activity *in-vitro* against two cancer cell lines HT-29, a human colon cancer cell line and MCF-7, human breast cancer cell line; while its cytotoxic effect was evaluated by using normal cell line VERO. FA-CS-NPs have shown good anti cancer activity against HT-29 cell line but not shown against MCF-7 and VERO, which reflects its colon specificity because of the fact that the colon cancer cells over express the folate receptor unlike the MCF-7 and VERO cell line (Figure 6.63).

7.11 *In-vitro* cell uptake study

In-Vitro cell uptake study shows that, when rhodamine labeled CS-NPs-8 and FA-CS-NPs-12 were mixed with the two different cancer cell lines HT-29 and MCF-7 separately, CS-NPs-8 were not been internalized within any of the cancer cell line, while FA-CS-NPs were found highly accumulated inside the HT-29 but fails to gain entry in MCF-7 cells. These results shows that the FA-CS-NPs were getting internalized only within the HT-29 cancer cell line because its expressing the folate receptors while MCF-7 cancer cell line is not expressing the folate receptor that much, therefore FA-CS-NPs couldn't gain the entry in MCF-7 as intensely as they have in HT-29 cell line. These outcomes suggest that the folate receptors positive colon cancer can be successfully targeted by folic acid conjugated nanoparticle of anticancer drug (Figure 6.64).

7.12 Stability studies

The optimized formulation CS-NPs-8 and FA-CS-NPs-12 was subjected to stability studies at various ICH storage conditions i.e. 25 ºC ± 2 oC/60 ± 5 % RH and 40 ºC ± 2oC/75 ± 5 % RH for a period of 90 days. The formulation was evaluated for physical appearance, drug content and in-vitro drug release study at regular interval of 15 days. No major changes were observed in physical appearance, drug content and *in-vitro* drug release profile when stored at room temperature. Also, at 40 ºC ± 2oC/75 ± 5 % RH storage condition, no major changes were observed in physical appearance as well as in drug content, while very minor decline were observed in in-vitro release data at the end of 90 days study. It indicates that the formulation were stable at various ICH storage condition for longer period (Table 6.35 to Table 6.40).

8. CONCLUSION

Colorectal cancer is a disease originating from the epithelial cells, lining the colon or rectum of the gastrointestinal tract. Capecitabine is one of the choices for the treatment of colon cancer. Generally, capecitabine is given in the form of tablet dosage form which has many disadvantages like, delivery of the drug to the healthy cells as well which must not happen, poor patient compliance, larger drug dose etc. Therefore, to target the capecitabine with suitable novel drug delivery system at specific site of action in controlled manner is thought to be beneficial approach.

From research literature, it was found that certain cancer express folate receptors on the cell surface and these receptors are over expressed on colon cancer cells. To support this, preparation and optimization of folic acid-targeted capecitabine loaded nanoparticles as a delivery system for the effective treatment of colon cancer, was the goal of this study. For that purpose, chitosan nanoparticles have been prepared by using ionic gelation method which was, later on, conjugated with folic acid as a targeting carrier.

In chitosan nanoparticle formulation, some parameters such as chitosan concentration and sodium TPP concentration have been studied as they affect the percentage entrapment efficiency. 3^2 full factorial design was used to statistically optimize parameters and evaluate the main effects of these individual variables on the percentage entrapment, particle size and drug release. The particle size was found to be ~87 nm, spherical in shape. IR spectra have confirmed that there was no any interaction between drug and excipients. From the result, it was concluded that concentration of chitosan, 1.5mg/ml and sodium TPP, 1.5mg/ml were found to be optimum for the preparation of optimized chitosan nanoparticles.

The developed and optimized chitosan nanoparticles were conjugated with folic acid as a targeting tool. This conjugation was carried out using 3^3 factorial design to statistically optimize three parameters i.e. concentration of folic acid, rpm and reaction time; and evaluate the main effects of these individual variables on the percentage folic acid conjugation. Drug loaded folic acid conjugated chitosan nanoparticles were also evaluated for particle size analysis, compatibility and SEM study. it confirms the conjugation of folic acid as increased particle size ~ 122 nm was observed.

In-vitro cytotoxicity study was carried out using two cancer cell line, folate receptor positive colon cancer cell line HT-29 and folate receptor negative breast cancer cell line MCF-7. From the results of *in-vitro* cytotoxicity study, it was concluded that capecitabine loaded formulations were highly effective on colon cancer cell line HT-29 and not on the MCF-7 cell line which lacks the folate receptors expression. The FA-CS-NPs formulation were readily taken by HT-29 cell while non-cojugated CS-NPs were not getting internalized with much intensity as compared to folic acid conjugated CS-NPs which indicates that the FA-CS-NPs have good potential as a carrier for the targeting and releases the drug capecitabine in controlled manner.

Finally, capecitabine loaded folic acid-conjugated colon-targeted chitosan nanoparticles, was successfully developed and optimized which can specifically target the colon cancer cells with less side effects and improved efficacy.

Bibliography

1. Walker R, Whittlesea C. Clinical pharmacy and therapeutics: Elsevier Health Sciences; 2011.
2. Organization WH. WHO Media centre. Cancer Fact sheet N 297. 2011.
3. Lahtz C, Pfeifer GP. Epigenetic changes of DNA repair genes in cancer. Journal of molecular cell biology. 2011;3(1):51-8.
4. Merlo LM, Pepper JW, Reid BJ, Maley CC. Cancer as an evolutionary and ecological process. Nature Reviews Cancer. 2006;6(12):924-35.
5. Danaei G, Vander Hoorn S, Lopez AD, Murray CJ, Ezzati M. Causes of cancer in the world: comparative risk assessment of nine behavioural and environmental risk factors. The Lancet. 2005;366(9499):1784-93.
6. Tolar J, Neglia JP. Transplacental and other routes of cancer transmission between individuals. Journal of pediatric hematology/oncology. 2003;25(6):430-4.
7. Anand P, Kunnumakara AB, Sundaram C, Harikumar KB, Tharakan ST, Lai OS, et al. Cancer is a preventable disease that requires major lifestyle changes. Pharmaceutical research. 2008;25(9):2097-116.
8. Kuper H, Adami HO, Boffetta P. Tobacco use, cancer causation and public health impact. Journal of internal medicine. 2002;251(6):455-66.
9. Sasco A, Secretan M, Straif K. Tobacco smoking and cancer: a brief review of recent epidemiological evidence. Lung cancer. 2004;45:S3-S9.
10. Cooper K, Squires H, Carroll C, Papaioannou D, Booth A, Logan R, et al. Chemoprevention of colorectal cancer: systematic review and economic evaluation. 2010.
11. Schwartz GG, Blot WJ. Vitamin D status and cancer incidence and mortality: something new under the sun. Journal of the National Cancer Institute. 2006;98(7):428-30.
12. Anguiano L, Mayer DK, Piven ML, Rosenstein D. A literature review of suicide in cancer patients. Cancer nursing. 2012;35(4):E14-E26.

13. Rampling R, James A, Papanastassiou V. The present and future management of malignant brain tumours: surgery, radiotherapy, chemotherapy. Journal of Neurology, Neurosurgery & Psychiatry. 2004;75(suppl 2):ii24-ii30.

14. Lind M. Principles of cytotoxic chemotherapy. Medicine. 2004;32(3):20-5.

15. Watson AJ, Collins PD. Colon cancer: a civilization disorder. Digestive diseases. 2011;29(2):222-8.

16. Astin M, Griffin T, Neal RD, Rose P, Hamilton W. The diagnostic value of symptoms for colorectal cancer in primary care: a systematic review. British Journal of General Practice. 2011;61(586):e231-e43.

17. Adelstein B-A, Macaskill P, Chan SF, Katelaris PH, Irwig L. Most bowel cancer symptoms do not indicate colorectal cancer and polyps: a systematic review. BMC gastroenterology. 2011;11(1):65.

18. Slaughter DP, Southwick HW, Smejkal W. "Field cancerization" in oral stratified squamous epithelium. Clinical implications of multicentric origin. Cancer. 1953;6(5):963-8.

19. Lee I-M, Shiroma EJ, Lobelo F, Puska P, Blair SN, Katzmarzyk PT. Effect of physical inactivity on major non-communicable diseases worldwide: an analysis of burden of disease and life expectancy. The Lancet. 2012;380(9838):219-29.

20. Fedirko V, Tramacere I, Bagnardi V, Rota M, Scotti L, Islami F, et al. Alcohol drinking and colorectal cancer risk: an overall and dose–response meta-analysis of published studies. Annals of oncology. 2011;22(9):1958-72.

21. Valtin H. "Drink at least eight glasses of water a day." Really? Is there scientific evidence for "8× 8"? American Journal of Physiology-Regulatory, Integrative and Comparative Physiology. 2002;283(5):R993-R1004.

22. Ionov Y, Peinado MA, Malkhosyan S, Shibata D, Perucho M. Ubiquitous somatic mutations in simple repeated sequences reveal a new mechanism for colonic carcinogenesis. Nature. 1993;363(6429):558-61.

23. Levin B. Inflammatory bowel disease and colon cancer. Cancer. 1992;70(S3):1313-6.

24. Xie J, Itzkowitz SH. Cancer in inflammatory bowel disease. World journal of gastroenterology: WJG. 2008;14(3):378.

25. Giovannucci E, Ogino S. DNA methylation, field effects, and colorectal cancer. Journal of the National Cancer Institute. 2005;97(18):1317-9.

26. Triantafillidis JK, Nasioulas G, Kosmidis PA. Colorectal cancer and inflammatory bowel disease: epidemiology, risk factors, mechanisms of carcinogenesis and prevention strategies. Anticancer research. 2009;29(7):2727-37.

27. Galiatsatos P, Foulkes WD. Familial adenomatous polyposis. The American journal of gastroenterology. 2006;101(2):385-98.

28. Mehlen P, Fearon ER. Role of the dependence receptor DCC in colorectal cancer pathogenesis. Journal of clinical oncology. 2004;22(16):3420-8.

29. Bernstein C, Bernstein H, Payne CM, Dvorak K, Garewal H. Field defects in progression to gastrointestinal tract cancers. Cancer letters. 2008;260(1):1-10.

30. Vogelstein B, Kinzler KW. Cancer genes and the pathways they control. Nature medicine. 2004;10(8):789-99.

31. Nguyen H, Loustaunau C, Facista A, Ramsey L, Hassounah N, Taylor H, et al. Deficient Pms2, ERCC1, Ku86, CcOI in field defects during progression to colon cancer. Journal of visualized experiments: JoVE. 2010(41).

32. Rubin H. Fields and field cancerization: The preneoplastic origins of cancer. Bioessays. 2011;33(3):224-31.

33. Muzny DB CK, Dinh HH, Drummond JA, Fowler G, Kovar CL, Lewis LR, Morgan MB, Newsham IF, Reid JG, Santibanez J, Shinbrot E, Trevino LR, Wu YQ, Wang M, Gunaratne P, Donehower LA, Creighton CJ, Wheeler DA, Gibbs RA, Lawrence MS, Voet D, Jing R, Cibulskis K, Sivachenko A, Stojanov P, McKenna A, Lander ES, Gabriel S. Comprehensive molecular characterization of human colon and rectal cancer. Nature. 2012;487(7407):330-7.

34. Stein U, Walther W, Arlt F, Schwabe H, Smith J, Fichtner I, et al. MACC1, a newly identified key regulator of HGF-MET signaling, predicts colon cancer metastasis. Nature medicine. 2008;15(1):59-67.

35. Stein U. MACC1-a novel target for solid cancers. Expert opinion on therapeutic targets. 2013;17(9):1039-52.

36. Tsao J-L, Yatabe Y, Salovaara R, Järvinen HJ, Mecklin J-P, Aaltonen LA, et al. Genetic reconstruction of individual colorectal tumor histories. Proceedings of the National Academy of Sciences. 2000;97(3):1236-41.

37. Schottenfeld D, Fraumeni Jr JF. Cancer epidemiology and prevention: Eastbourne, UK; WB Saunders Co; 1982.

38. Campos F, Logullo Waitzberg A, Kiss D, Waitzberg D, Habr-Gama A, Gama-Rodrigues J. Diet and colorectal cancer: current evidence for etiology and prevention. Nutr Hosp. 2005;20(1):18-25.

39. Doyle VC. Nutrition and colorectal cancer risk: a literature review. Gastroenterology Nursing. 2007;30(3):178-82.

40. Harriss D, Atkinson G, Batterham A, George K, Tim Cable N, Reilly T, et al. Lifestyle factors and colorectal cancer risk (2): a systematic review and meta-analysis of associations with leisure-time physical activity. Colorectal disease. 2009;11(7):689-701.

41. Giardiello F, Offerhaus G, DuBois R. The role of nonsteroidal anti-inflammatory drugs in colorectal cancer prevention. European Journal of Cancer. 1995;31(7):1071-6.

42. Ma Y, Zhang P, Wang F, Yang J, Liu Z, Qin H. Association between vitamin D and risk of colorectal cancer: a systematic review of prospective studies. Journal of Clinical Oncology. 2011;29(28):3775-82.

43. Yin L, Grandi N, Raum E, Haug U, Arndt V, Brenner H. Meta-analysis: serum vitamin D and colorectal adenoma risk. Preventive medicine. 2011;53(1):10-6.

44. Stein A, Atanackovic D, Bokemeyer C. Current standards and new trends in the primary treatment of colorectal cancer. European Journal of Cancer. 2011;47:S312-S4.

45. Brenner H, Stock C, Hoffmeister M. Effect of screening sigmoidoscopy and screening colonoscopy on colorectal cancer incidence and mortality: systematic review and meta-analysis of randomised controlled trials and observational studies. BMJ: British Medical Journal. 2014;348.

46. Siegel RL, Ward EM, Jemal A. Trends in colorectal cancer incidence rates in the United States by tumor location and stage, 1992–2008. Cancer Epidemiology Biomarkers & Prevention. 2012;21(3):411-6.

47. Mitrovic B, Schaeffer DF, Riddell RH, Kirsch R. Tumor budding in colorectal carcinoma: time to take notice. Modern Pathology. 2012;25(10):1315-25.

48. Hewitson P, Glasziou P, Watson E, Towler B, Irwig L. Cochrane systematic review of colorectal cancer screening using the fecal occult blood test (hemoccult): an update. The American journal of gastroenterology. 2008;103(6):1541-9.

49. Mayer RJ. Chemotherapy for metastatic colorectal cancer. Cancer. 1992;70(S3):1414-24.

50. Shaib W, Mahajan R, El-Rayes B. Markers of resistance to anti-EGFR therapy in colorectal cancer. Journal of gastrointestinal oncology. 2013;4(3):308.

51. Winawer S, Fletcher R, Rex D, Bond J, Burt R, Ferrucci J, et al. Colorectal cancer screening and surveillance: clinical guidelines and rationale—update based on new evidence. Gastroenterology. 2003;124(2):544-60.

52. Sostres C, Gargallo CJ, Lanas A. Aspirin, cyclooxygenase inhibition and colorectal cancer. World journal of gastrointestinal pharmacology and therapeutics. 2014;5(1):40.

53. DeVita VT, Lawrence TS, Rosenberg SA. DeVita, Hellman, and Rosenberg's cancer: principles & practice of oncology. Vol. 2: Wolters Kluwer/Lippincott Williams & Wilkins; 2008.

54. Qaseem A, Denberg TD, Hopkins RH, Humphrey LL, Levine J, Sweet DE, et al. Screening for colorectal cancer: a guidance statement from the American College of Physicians. Annals of internal medicine. 2012;156(5):378-86.

55. Vyas SP, Khar RK. Targeted & Controlled Drug Delivery: Novel Carrier Systems: CBS publishers & distributors; 2004.

56. Brannon-Peppas L, Blanchette JO. Nanoparticle and targeted systems for cancer therapy. Advanced drug delivery reviews. 2012;64:206-12.

57. Sinha R, Kim GJ, Nie S, Shin DM. Nanotechnology in cancer therapeutics: bioconjugated nanoparticles for drug delivery. Molecular cancer therapeutics. 2006;5(8):1909-17.

58. Kreuter J. Nanoparticles—a historical perspective. International Journal of Pharmaceutics. 2007;331(1):1-10.

59. Mohanraj V, Chen Y. Nanoparticles-a review. Tropical Journal of Pharmaceutical Research. 2007;5(1):561-73.

60. Soppimath KS, Aminabhavi TM, Kulkarni AR, Rudzinski WE. Biodegradable polymeric nanoparticles as drug delivery devices. Journal of controlled release. 2001;70(1):1-20.

61. Pathak Y, Thassu D. Drug delivery nanoparticles formulation and characterization: Informa Healthcare New York; 2009.

62. Gelperina S, Kisich K, Iseman MD, Heifets L. The potential advantages of nanoparticle drug delivery systems in chemotherapy of tuberculosis. American journal of respiratory and critical care medicine. 2005;172(12):1487-90.

63. Marcato PD, Durán N. New aspects of nanopharmaceutical delivery systems. Journal of Nanoscience and Nanotechnology. 2008;8(5):2216-29.

64. Drexler HG, Dirks WG, MacLeod R. False human hematopoietic cell lines: cross-contaminations and misinterpretations. Leukemia. 1999;13(10):1601-7.

65. Cabrera C, Cobo F, Nieto A, Cortés J, Montes R, Catalina P, et al. Identity tests: determination of cell line cross-contamination. Cytotechnology. 2006;51(2):45-50.

66. Dunham JH, Guthmiller P. Doing good science: Authenticating cell line identity. Promega Notes. 2009;101:15-8.

67. Irfan Maqsood M, Matin MM, Bahrami AR, Ghasroldasht MM. Immortality of cell lines: challenges and advantages of establishment. Cell biology international. 2013;37(10):1038-45.

68. Cohen E, Ophir I, Shaul YB. Induced differentiation in HT29, a human colon adenocarcinoma cell line. Journal of cell science. 1999;112(16):2657-66.

69. Fogh J, Fogh JM, Orfeo T. One hundred and twenty-seven cultured human tumor cell lines producing tumors in nude mice. Journal of the National Cancer Institute. 1977;59(1):221-6.

70. Nautiyal J, Kanwar SS, Yu Y, Majumdar A. Combination of dasatinib and curcumin eliminates chemo-resistant colon cancer cells. J Mol Signal. 2011;6(7).

71. Soule H, Vazquez J, Long A, Albert S, Brennan M. A human cell line from a pleural effusion derived from a breast carcinoma. Journal of the National Cancer Institute. 1973;51(5):1409-16.

72. Levenson AS, Jordan VC. MCF-7: the first hormone-responsive breast cancer cell line. Cancer research. 1997;57(15):3071-8.

73. Lacroix M, Leclercq G. Relevance of breast cancer cell lines as models for breast tumours: an update. Breast cancer research and treatment. 2004;83(3):249-89.

74. Ross DT, Perou CM. A comparison of gene expression signatures from breast tumors and breast tissue derived cell lines. Disease markers. 2001;17(2):99-109.

75. Charafe-Jauffret E, Ginestier C, Monville F, Finetti P, Adelaide J, Cervera N, et al. Gene expression profiling of breast cell lines identifies potential new basal markers. Oncogene. 2005;25(15):2273-84.

76. Lacroix M, Toillon R-A, Leclercq G. p53 and breast cancer, an update. Endocrine-related cancer. 2006;13(2):293-325.

77. Desmyter J, Melnick JL, Rawls WE. Defectiveness of interferon production and of rubella virus interference in a line of African green monkey kidney cells (Vero). Journal of virology. 1968;2(10):955-61.

78. Freshney RI. Culture of specific cell types. 6th ed: Wiley Online Library; 2005.

79. Agnihotri SA, Aminabhavi TM. Novel interpenetrating network chitosan-poly (ethylene oxide-< i> g</i>-acrylamide) hydrogel microspheres for the controlled release of capecitabine. International journal of pharmaceutics. 2006;324(2):103-15.

80. Cassidy J, Twelves C, Cameron D, Steward W, O'Byrne K, Jodrell D, et al. Bioequivalence of two tablet formulations of capecitabine and exploration of age, gender, body surface area, and creatinine clearance as factors influencing systemic exposure in cancer patients. Cancer chemotherapy and pharmacology. 1999;44(6):453-60.

81. Cassidy J, Twelves C, Van Cutsem E, Hoff P, Bajetta E, Boyer M, et al. First-line oral capecitabine therapy in metastatic colorectal cancer: a favorable safety profile compared with intravenous 5-fluorouracil/leucovorin. Annals of Oncology. 2002;13(4):566-75.

82. Weitman SD, Lark RH, Coney LR, Fort DW, Frasca V, Zurawski VR, et al. Distribution of the folate receptor GP38 in normal and malignant cell lines and tissues. Cancer research. 1992;52(12):3396-401.

83. Hou Z, Zhan C, Jiang Q, Hu Q, Li L, Chang D, et al. Both FA-and mPEG-conjugated chitosan nanoparticles for targeted cellular uptake and enhanced tumor tissue distribution. Nanoscale research letters. 2011;6(1):1-11.

84. Yang S-J, Lin F-H, Tsai K-C, Wei M-F, Tsai H-M, Wong J-M, et al. Folic acid-conjugated chitosan nanoparticles enhanced protoporphyrin IX accumulation in colorectal cancer cells. Bioconjugate chemistry. 2010;21(4):679-89.

85. Sahu SK, Mallick SK, Santra S, Maiti TK, Ghosh SK, Pramanik P. In vitro evaluation of folic acid modified carboxymethyl chitosan nanoparticles loaded with doxorubicin for targeted delivery. Journal of Materials Science: Materials in Medicine. 2010;21(5):1587-97.

86. Li P, Wang Y, Zeng F, Chen L, Peng Z, Kong LX. Synthesis and characterization of folate conjugated chitosan and cellular uptake of its nanoparticles in HT-29 cells. Carbohydrate research. 2011;346(6):801-6.

87. Dubé D, Francis M, Leroux J-C, Winnik FM. Preparation and tumor cell uptake of poly (N-isopropylacrylamide) folate conjugates. Bioconjugate chemistry. 2002;13(3):685-92.

88. Wu K, Platz EA, Willett WC, Fuchs CS, Selhub J, Rosner BA, et al. A randomized trial on folic acid supplementation and risk of recurrent colorectal adenoma. The American journal of clinical nutrition. 2009;90(6):1623-31.

89. Li Q, Liu C, Zhao X, Zu Y, Wang Y, Zhang B, et al. Preparation, characterization and targeting of micronized 10-hydroxycamptothecin-loaded folate-conjugated human serum albumin nanoparticles to cancer cells. Int J Nanomedicine. 2011;6(3):1-9.

90. Du Y-Z, Cai L-L, Li J, Zhao M-D, Chen F-Y, Yuan H, et al. Receptor-mediated gene delivery by folic acid-modified stearic acid-grafted chitosan micelles. International journal of nanomedicine. 2011;6:1559.

91. Wang F, Chen Y, Zhang D, Zhang Q, Zheng D, Hao L, et al. Folate-mediated targeted and intracellular delivery of paclitaxel using a novel deoxycholic acid-O-carboxymethylated chitosan-folic acid micelles. Int J Nanomedicine. 2012;7(145):325-37.

92. Zu Y, Zhao Q, Zhao X, Zu S, Meng L. Process optimization for the preparation of oligomycin-loaded folate-conjugated chitosan nanoparticles as a tumor-targeted drug delivery system using a two-level factorial design method. International journal of nanomedicine. 2011;6:3429.

93. Reddy J, Allagadda V, Leamon C. Targeting therapeutic and imaging agents to folate receptor positive tumors. Current pharmaceutical biotechnology. 2005;6(2):131-50.

94. Pirollo KF, Chang EH. Does a targeting ligand influence nanoparticle tumor localization or uptake? Trends in biotechnology. 2008;26(10):552-8.

95. Sonvico F, Dubernet C, Marsaud V, Appel M, Chacun H, Stella B, et al. Establishment of an in vitro model expressing the folate receptor for the investigation of targeted delivery systems. Journal of drug delivery science and technology. 2005;15(6):407-10.

96. Zhang Y, Guo L, Roeske RW, Antony AC, Jayaram HN. Pteroyl-γ-glutamate-cysteine synthesis and its application in folate receptor-mediated cancer cell targeting using folate-tethered liposomes. Analytical biochemistry. 2004;332(1):168-77.

97. Hilgenbrink AR, Low PS. Folate receptor-mediated drug targeting: From therapeutics to diagnostics. Journal of pharmaceutical sciences. 2005;94(10):2135-46.

98. Turek JJ, Leamon CP, Low PS. Endocytosis of folate-protein conjugates: ultrastructural localization in KB cells. Journal of Cell Science. 1993;106(1):423-30.

99. Lu Y, Low PS. Folate-mediated delivery of macromolecular anticancer therapeutic agents. Advanced drug delivery reviews. 2012;64:342-52.

100. Lee RJ, Low PS. Folate-mediated tumor cell targeting of liposome-entrapped doxorubicin in vitro. Biochimica et Biophysica Acta (BBA)-Biomembranes. 1995;1233(2):134-44.

101. Zhang L, Hou S, Mao S, Wei D, Song X, Lu Y. Uptake of folate-conjugated albumin nanoparticles to the SKOV3 cells. International journal of pharmaceutics. 2004;287(1):155-62.

102. Oyewumi MO, Mumper RJ. Influence of formulation parameters on gadolinium entrapment and tumor cell uptake using folate-coated nanoparticles. International journal of pharmaceutics. 2003;251(1):85-97.

103. Low PS, Kularatne SA. Folate-targeted therapeutic and imaging agents for cancer. Current opinion in chemical biology. 2009;13(3):256-62.

104. Chen J, Li S, Shen Q. Folic acid and cell-penetrating peptide conjugated PLGA–PEG bifunctional nanoparticles for vincristine sulfate delivery. Eur J Pharm Sci. 2012;47(2):430-43.

105. Li P, Dai Y-N, Zhang J-P, Wang A-Q, Wei Q. Chitosan-Alginate nanoparticles as a novel drug delivery system for nifedipine. International journal of biomedical science: IJBS. 2008;4(3):221.

106. Nesalin JAJ, Smith AA. Preparation and evaluation of chitosan nanoparticles containing zidovudine. Asian J Pharm Sci. 2012;7:80-4.

107. Garcia-Bennett A, Nees M, Fadeel B. In search of the Holy Grail: folate-targeted nanoparticles for cancer therapy. Biochemical pharmacology. 2011;81(8):976-84.

108. Li J, Zheng L, Cai H, Sun W, Shen M, Zhang G, et al. Polyethyleneimine-mediated synthesis of folic acid-targeted iron oxide nanoparticles for< i> in vivo</i> tumor MR imaging. Biomaterials. 2013;34(33):8382-92.

109. Oyewumi MO, Yokel RA, Jay M, Coakley T, Mumper RJ. Comparison of cell uptake, biodistribution and tumor retention of folate-coated and PEG-coated gadolinium nanoparticles in tumor-bearing mice. Journal of Controlled Release. 2004;95(3):613-26.

110. Ma Y, Sadoqi M, Shao J. Biodistribution of indocyanine green-loaded nanoparticles with surface modifications of PEG and folic acid. International journal of pharmaceutics. 2012;436(1):25-31.

111. Du Z, Pan S, Yu Q, Li Y, Wen Y, Zhang W, et al. Paclitaxel-loaded micelles composed of folate-poly (ethylene glycol) and poly (γ-benzyl l-glutamate) diblock copolymer. Colloids and Surfaces A: Physicochemical and Engineering Aspects. 2010;353(2):140-8.

112. Paolino D, Licciardi M, Celia C, Giammona G, Fresta M, Cavallaro G. Folate-targeted supramolecular vesicular aggregates as a new frontier for effective anticancer treatment in< i> in vivo</i> model. European Journal of Pharmaceutics and Biopharmaceutics. 2012;82(1):94-102.

113. Lin J-J, Chen J-S, Huang S-J, Ko J-H, Wang Y-M, Chen T-L, et al. Folic acid–Pluronic F127 magnetic nanoparticle clusters for combined targeting, diagnosis, and therapy applications. Biomaterials. 2009;30(28):5114-24.

114. Khoee S, Rahmatolahzadeh R. Synthesis and characterization of pH-responsive and folated nanoparticles based on self-assembled brush-like PLGA/PEG/AEMA copolymer with targeted cancer therapy properties: a comprehensive kinetic study. European journal of medicinal chemistry. 2012;50:416-27.

115. Heidari Majd M, Asgari D, Barar J, Valizadeh H, Kafil V, Abadpour A, et al. Tamoxifen loaded folic acid armed PEGylated magnetic nanoparticles for targeted imaging and therapy of cancer. Colloids and Surfaces B: Biointerfaces. 2013;106:117-25.

116. Song H, Su C, Cui W, Zhu B, Liu L, Chen Z, et al. Folic acid-chitosan conjugated nanoparticles for improving tumor-targeted drug delivery. BioMed research international. 2013;2013.

117. Hejazi R, Amiji M. Chitosan-based gastrointestinal delivery systems. Journal of Controlled Release. 2003;89(2):151-65.

118. TIAN XX, GROVES MJ. Formulation and biological activity of antineoplastic proteoglycans derived from Mycobacterium vaccae in chitosan nanoparticles. Journal of pharmacy and pharmacology. 1999;51(2):151-7.

119. Janes KA, Fresneau MP, Marazuela A, Fabra A, Alonso MaJ. Chitosan nanoparticles as delivery systems for doxorubicin. Journal of Controlled Release. 2001;73(2):255-67.

120. Katas H, Alpar HO. Development and characterisation of chitosan nanoparticles for siRNA delivery. Journal of controlled release. 2006;115(2):216-25.

121. Qi L, Xu Z, Jiang X, Hu C, Zou X. Preparation and antibacterial activity of chitosan nanoparticles. Carbohydrate Research. 2004;339(16):2693-700.

122. Luo Y, Zhang B, Cheng W-H, Wang Q. Preparation, characterization and evaluation of selenite-loaded chitosan/TPP nanoparticles with or without zein coating. Carbohydrate Polymers. 2010;82(3):942-51.

123. Dung TH, Lee S-R, Han S-D, Kim S-J, Ju Y-M, Kim M-S, et al. Chitosan-TPP nanoparticle as a release system of antisense oligonucleotide in the oral environment. Journal of nanoscience and nanotechnology. 2007;7(11):3695-9.

124. Gan Q, Wang T. Chitosan nanoparticle as protein delivery carrier—systematic examination of fabrication conditions for efficient loading and release. Colloids and Surfaces B: Biointerfaces. 2007;59(1):24-34.

125. Wang S-L, Yao H-H, Guo L-L, Dong L, Li S-G, Gu Y-P, et al. Selection of optimal sites for< i> TGFB1</i> gene silencing by chitosan–TPP nanoparticle-mediated delivery of shRNA. Cancer genetics and cytogenetics. 2009;190(1):8-14.

126. López-León T, Carvalho E, Seijo B, Ortega-Vinuesa J, Bastos-González D. Physicochemical characterization of chitosan nanoparticles: electrokinetic and

stability behavior. Journal of Colloid and Interface Science. 2005;283(2):344-51.

127. Nasti A, Zaki NM, de Leonardis P, Ungphaiboon S, Sansongsak P, Rimoli MG, et al. Chitosan/TPP and chitosan/TPP-hyaluronic acid nanoparticles: systematic optimisation of the preparative process and preliminary biological evaluation. Pharmaceutical research. 2009;26(8):1918-30.

128. Wu Y, Yang W, Wang C, Hu J, Fu S. Chitosan nanoparticles as a novel delivery system for ammonium glycyrrhizinate. International journal of pharmaceutics. 2005;295(1):235-45.

129. Berthold A, Cremer K, Kreuter J. Preparation and characterization of chitosan microspheres as drug carrier for prednisolone sodium phosphate as model for anti-inflammatory drugs. Journal of Controlled Release. 1996;39(1):17-25.

130. Di Costanzo F, Sdrobolini A, Gasperoni S. Capecitabine, a new oral fluoropyrimidine for the treatment of colorectal cancer. Critical reviews in oncology/hematology. 2000;35(2):101-8.

131. Venturini M. Rational development of capecitabine. European Journal of Cancer. 2002;38:3-9.

132. Pentheroudakis G, Twelves C. The rational development of capecitabine from the laboratory to the clinic. Anticancer research. 2001;22(6B):3589-96.

133. Camidge R, Reigner B, Cassidy J, Grange S, Abt M, Weidekamm E, et al. Significant effect of capecitabine on the pharmacokinetics and pharmacodynamics of warfarin in patients with cancer. Journal of clinical oncology. 2005;23(21):4719-25.

134. Frickhofen N, Beck F-J, Jung B, Fuhr H-G, Andrasch H, Sigmund M. Capecitabine can induce acute coronary syndrome similar to 5-fluorouracil. Annals of oncology. 2002;13(5):797-801.

135. Mercier C, Ciccolini J. Severe or lethal toxicities upon capecitabine intake: is DPYD genetic polymorphism the ideal culprit? Trends in pharmacological sciences. 2007;28(12):597-8.

136. Blesch KS, Gieschke R, Tsukamoto Y, Reigner BG, Burger HU, Steimer J-L. Clinical pharmacokinetic/pharmacodynamic and physiologically based

pharmacokinetic modeling in new drug development: the capecitabine experience. Investigational new drugs. 2003;21(2):195-223.

137. Ravi Kumar MN. A review of chitin and chitosan applications. Reactive and functional polymers. 2000;46(1):1-27.

138. Rowe RC, Sheskey PJ, Owen SC, Association AP. Handbook of pharmaceutical excipients: Pharmaceutical press London; 2006.

139. Wade A, Weller PJ. Handbook of pharmaceutical excipients: Pharmaceutical Press; 1994.

140. Butterworth C, Tamura T. Folic acid safety and toxicity: a brief review. The American journal of clinical nutrition. 1989;50(2):353-8.

141. Yang S, Tsai K, Peng C, Lin F, Shieh M. A Novel Detection of Early Colorectal Cancer by Chitosan Nanoparticles Conjugated with Folic Acid Annals of oncology. 2005;15(4):745-71.

Annexure I

LIST OF PUBLICATION

1. Javia AR, Seth AK. Development and optimization of Capecitabine Loaded Chitosan Nanoparticles for Colon Cancer Therapy. American Journal of PharmTech Research 2015;5(4):709-23.

AMERICAN JOURNAL OF PHARMTECH RESEARCH
Journal home page: http://www.ajptr.com/

Development and Optimization of Capecitabine Loaded Chitosan Nanoparticles for Colon Cancer Therapy

Ankur R. Javia*[1], A.K.Seth[1]
1. Department of Pharmacy, Sumandeep Vidyapeeth University, Piparia, Vadodara, Gujarat.

ABSTRACT

The goal of this study was to develop and optimize the Capecitabine loaded chitosan nanoparticles (CS-NPs)for improved colon cancer therapy, by enhancedsurface area, sustained drug release, reduced dose and hence, most importantly, reduced toxicity. Capecitabine loaded Chitosan nanoparticles were prepared by 3^2 full factorial designs, using ionotropic gelation method by cross-linking of chitosan (CS) with sodium tripolyphosphate (TPP). CS-NPs were prepared by dissolving chitosan in 1% (w/v) acetic acid solution under magnetic stirring at room temperature. The CS solution was diluted with deionized water to produce different concentration. The capecitabine was dissolved in CS solution using sonication and aqueous TPP solution was added drop wise using syringe to the mixture with moderate stirring for 30 min. The prepared nanoparticles were characterized by FT-IR spectroscopy and DSC to confirm the cross linking reaction between CS and cross-linking agent. From the % entrapment of capecitabine, nanoparticles were optimized using regression analysis, contour plots and check point analysis.Particle size of the optimized batch (CS-NPs-8) was found to be 87 nm. The Polydispersity index of the nanoparticles was found to be 0.113. The nanoparticles formed were spherical in shape with high zeta potentials, -35mV. *In vitro* release studies in phosphate buffer saline (pH 7.4) showed an initial burst effect and followed by a slow drug release. The drug release followed first order kinetics and was found to be diffusion controlled. Optimized formulation was also showing more % inhibition than drug alone in *In-vitro* anticancer study. From the accelerated study of optimized batch, it was found to be stable.

Keywords: Capecitabine, Colon cancer, Chitosan-TPP nanoparticles, HT-29.

*Corresponding Author Email: ankur_javia@yahoo.in
Received 27July 2014, Accepted13 August2014

Please cite this article as: Javia A *et al.*, Development and Optimization of Capecitabine Loaded Chitosan Nanoparticles for Colon Cancer Therapy. American Journal of PharmTech Research 2015.

INTRODUCTION

Nanotechnology is the designing of practical frameworks at molecular or nano scale[1]. Particles are considered as nanoparticleswhen one dimension is 100 nanometers or less in size[2]. The properties of numerous common materials change when framed from nanoparticles. This is commonly in light of the fact that nanoparticles have a more prominent surface area per weight than bigger particles; this makes them be more receptive to certain molecules. It is conceivable that medications as nanoparticles may give better solubility, prompting better absorption[3]. Additionally, medications may be contained inside of a molecular transporter, either to shield them from stomach acids or to control the drug release to a particular focused area, diminishing the probability of side effects. Nanoparticular drug delivery systems are submicron-sized particles (3-200 nm), devices, or systems that can be made, utilizing an assortment of materials including polymers (polymeric nanoparticles, micelles, or dendrimers), lipids (liposomes), virus (viral nanoparticles), and even organometallic compound (nanotubes). Capecitabine (Figure 1) is an pro-drug that is changed over to fluorouracil in the body tissues taking after the oral route. It is broadly utilized as a part of the treatment of metastatic colorectal growth and breast malignancy, since it is promptly ingested from the gastrointestinal tract. The prescribed every day dosage is huge, i.e., 1500 mg/m^2 and it has a short disposal half-life of 0.5–1h[4]. The unwanted impacts with capecitabine incorporate bone-marrow dipression, cardiotoxicity, looseness of the bowels, sickness and retching, stomatitis, dermatitis, and so on. Subsequently, preparing capecitabine as a controlled release (CR) medication would give more noteworthy or more *in vitro* and *in vivo* antitumor movement, in this way decreasing its harmful effects. Specifically, particular favorable circumstances of multi-particulate formulation, for example, microspheres, beads, and so forth., over other routinedosage form like tablets and capsules have been talked about before[5]. Nevertheless, the principle target of any CR dosage form is to get formulation that would permit the drg to stay in therapeutic window as far as possible. The improvement of such pharmaceutical structures can be accomplished by utilizing particular biocompatible polymers. Among numerous such polymers, hydrogels have been broadly utilized for creating CR devices. Subsequently, it would be of enthusiasm to pick such polymers that have suitable chemical composition, physicochemical nature, biodegradability, chemical stability, mechanical properties, drug release qualities, coveted pharmaceutical dosage form and route of administration[6]. Chitosan [poly (β-(1 → 4)-2-amino-2-deoxy-D-glucose)] is a deacetylated derivative of chitin, which is a naturally occurring polysaccharide, found abundantly in marine crustaceans, insects and fungi[7]. Chitosan is a

cationic, biocompatible and biodegradable polymer having many biomedical applications. Chitosan has many advantages, particularly in developing micro/nanoparticles. These include, its ability to control the release of active agents, it avoids the use of hazardous organic solvents while fabricating particles formulating dosage form, it is soluble in aqueous acidic solution, it is a linear polyamine containing number of free amine groups that are readily available for crosslinking, its cationic nature allows for ionic crosslinking with multivalent anions, it has muco-adhesive character, which increases the residual time at the site of absorption and so on. Chitosan has been extensively studied as a carrier for many drugs[8], proteins and gels for the entrapment of cells or antigens[9] in pharmaceutical industries.

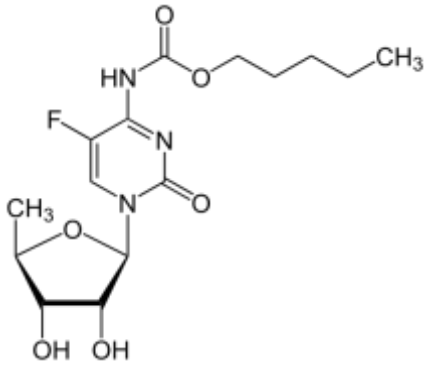

Figure 1: Chemical structure of Capecitabine

MATERIAL AND METHODS

Chitosan (CS, Deacetylation degree of 95% and molecular weight of 80 kDa), Tripolyphosphate (TPP) waspurchased from Balaji drugs (Surat). Capecitabine was obtained as a gift sample from Sun Pharma Research and Analysis Center (Vadodara). All other materials and reagents used in the study were analytical grade.

Preparation of Capecitabine Nanoparticles

Chitosan nanoparticles were prepared, by 3^2 factorial design, by ionic cross linking of chitosan solution with TPP anions. Chitosan was dissolved in 50ml aqueous solution of acetic acid (1% v/v) to prepare various concentrations (0.5mg/ml, 1mg/ml, 1.5mg/ml). Under magnetic stirring at room temperature, 0.5 mg/ml, 0.75 mg/ml, and 1.0 mg/ml concentration of 20 ml TPP aqueous solution was added drop wise using syringe needle into chitosan solution containing 25 mg of capecitabine. pH was adjusted to 6.0 by adding 0.1 N NaOH. The stirring was continued for about 30 minutes. The resultant nanoparticles suspensions were centrifuged at 12000 rpm for 30 minutes. Particles were settled down and separated from clear supernatant. The Particles obtained after centrifugation were finally freeze dried and stored in air tight close container. The formation of the nanoparticles

was because of the interaction be-tween the negative groups of the TPP and the positively charged amino groups of chitosan (ionic gelation) [10, 11] (Table 1).

Table 1: 3^2 Factorial Design of Chitosan Nanoparticles

Batch	Capecitabine (mg)	Chitosan in 1% v/v acetic acid (mg/50ml)	TPP in water (mg/20ml)
CS-NPs -1	25	25	10
CS-NPs -2	25	25	15
CS-NPs -3	25	25	20
CS-NPs -4	25	50	10
CS-NPs -5	25	50	15
CS-NPs -6	25	50	20
CS-NPs -7	25	75	10
CS-NPs -8	25	75	15
CS-NPs -9	25	75	20

Solubility Studies

Solubility of the drug was determined by saturation equilibrium method. Excess quantity of capecitabine was added in to the 10ml volumetric flask and then volume was made up to 10ml mark with water, and then mixture was place in incubator shaker overnight, to get saturated solution of drug. Next day, undissolved drug was separated from the solution by filtering the mixture from whatman filter paper. Supernatant was diluted appropriately with water and the absorbance was determined using UV-visible spectrophotometer. Concentration of the drug was calculated from the standard calibration curve of drug taken in water at 240 nm.

Characterization

Capecitabinecontent

Estimation of drug content was done as per the method reported earlier[12]. Nanoparticles of known weights were soaked in 50ml of water for 30 mints and sonicated using a probe sonicator for 15 mints to break the nanoparticles and facilitate extraction of the drug. The whole solution was centrifuged using a centrifuge to remove the polymeric debris and polymeric debris was washed twice with fresh solvent (water) to extract any adhered drug. The clear supernatant solution was analyzed for capecitabine content by UV spectrophotometer (Shimadzu 1800) at λmax value of 240 nm. The complete extraction of drug was confirmed by repeating the extraction process on the already extractedpolymeric debris.

Entrapment efficiency

At the end of the formation of nanoparticles, it was separatedfrom medium by centrifugation at 12000 RPM for 30 minutes. Then, the nanoparticles pellets and supernatant was separated. Then after, supernatant was appropriately diluted in water and absorbance was taken against water as a

reference on UV-Visible Spectrophotometer at 240nm. Percentage entrapment was calculatedusing following formula.

$$\%\ \text{DrugEntrapment} = \frac{\text{TotalDrugtaken} - \text{druginsupernatant}}{\text{Totaldrugtaken}} \times 100$$

***In-vitro* drug release**

In vitro release study of capecitabine from nanoparticles was carried out in PBS medium, according to a reported procedure[12]. A 4-5 cm long portion of the dialysis bag was made into a dialysis sac by folding and tying up one end of the bag with thread. It was then filled up with phosphate-buffer pH 7.4 and examined for the leaks. The sac was then emptied and NPs dispersion (equivalent to 10 mg drug) was accurately transferred into sac which served as the donor compartments. The sac was once again examined for leak and then suspended in the glass beakers containing 50 ml phosphate-buffer pH 7.4, which become the receptor compartment. Aliquots were taken at 1,2,3,4,5,6,7,8 12, 24, 48 and 72 hours and analyzed spectrophotometrically at 240 nm. Fresh buffer was used to replenish the receptor compartment at each time to maintain sink condition.

Particle size

The average particle size of nanoparticles was measured using a Malvern particle size analyser[8].

Zeta potential

Particle charge is a stability determining parameter in aqueous nanoparticles it is measured by electrophoresis and expressed as electrophoretic mobility (or) converted to the zeta potential (mV). Zeta potential was measured with a combination of laser Doppler velocimetry and phase analysis light scattering (Malvern instruments UK). A Smoluchowsky constant F (Ka) of 1.5 was used to calculate zeta potential values from the electrophoretic mobility[9].

Polydispersity index

The polydispersity index was determined using non-invasive back scatter technology which allows samples measurement in the range of 0.6 nm - 6 µm, freshly prepared capecitabine nanoparticles (800 µl) was placed in a folded capillary cell without dilution. The measurement was carried out using 4MW He-Ne laser as light source at a fixed angle of 173^{o}C the parameters were used for the experiments like medium temperature 25^{o}C.

Fourier transformer infrared spectroscopy

FT-IR spectra was taken to identify changes in chemical structure of the capecitabine nanoparticle. The samples were first lyophilized in freeze drier, and then grounded into homogeneous powders.

The spectra were acquired at 400–4000cm^{-1} wave numbers with a 4cm−1 resolution utilizing a Shimadzu FT-IR spectrophotometer.

Differential scanning calorimetry

Differential scanning calorimetry (Shimadzu DSC-60) analysis was performed using an automatic thermal analyzer. Aluminum pans were employed in the experiments for all samples and an empty pan, prepared in the same manner, was used as a reference. Samples of 3 mg were weighted directly into the aluminum pan which was firmly crimped around the lid to provide an adequate seal. The thermal analyses were conducted from ambient temperature to 300^{o}C at a pre-programmed heating rate of 10^{o}C per min.

Scanning electron microscopy

The morphology of optimizedCS-NPs-8 nanoparticles was examined by scanning electron microscopy (SEM) operated at an acceleration voltage of 10 kV. The samples were attached to aluminum stubs with double side adhesive carbon tape then gold coated and examined using a scanning electron microscope (Leo 1430 VPGermany).

MTT assay

Capecitabine, blank CS-NPs and capecitabine loaded CS-NPs was evaluated for its anti-colon cancer activity by using three different cell lines; HT-29, MCF-7 and Vero.Cells were preincubated at a concentration of 1×106 cells/ml in culture medium, taken in T flask, for 3 h at 37°C and 6.5% CO2. Then after cells were seeded at a concentration of 5×104 cells/well in 100µl culture medium and various amounts of compound (final concentration e.g. 100µM - 0.005µM) were added into microplates (tissue culture grade, 96 wells, flat bottom). Then cell cultures were incubated for 24 h at 37°C and 6.5% CO2 after which 10 µl MTT labeling mixture was added and incubatefurther for 4 h at 37°C and 6.5% CO2. Then in the last the formazan crystals that formed were solubilized by adding 150 µl solubilization solution (isopropanol containing 0.01N HCl)in each well and incubated for overnight and number of viable cells in each well was determined from the absorbance at 570 nm in a plate reader.

Statistical analysis

Data were expressed as means of three separateexperiments, and were compared by analysis of variance(ANOVA). A p-value <0.05 was considered statisticallysignificant in all cases.

Stability study

The stability study was carried out for Capecitabine loaded CS NPs and FA conjugated CS NPs as per ICH guidelines. Nanoparticles of the optimized formulation were placed in screw capped glass container and stored at various ICH storage condition which are 250 C ± 20C (60%± 5%RH) and

400 C ± 20C (75%± 5%RH) for a period of 90 days. The samples were analyzed for physical appearance and for the entrapement efficiency at regular interval of 15 days. Drug release was performed after 90 days.

RESULTS AND DISCUSSIONS

CS (Chitosan) nanoparticles can easily be prepared upon the incorporation of TPP solution to the CS solution under magnetic stirring, since the creation of nanoparticles depends mainly on the evolved ionic interaction of CS with TPP that eventually leads to the reduction of aqueous solubility of CS. The ratio between CS and TPP is critical and controls the size and the size distribution of the nanoparticles. The size characteristics have been found to affect the biological performance of CS nanoparticles. For this reason before the drug encapsulation into CS nanoparticles, the effect of CS/TPP ratio on the size characteristics of the nanoparticles was studied in order to find the optimum ratio that result to nanoparticles of low size and narrow size distribution.

Solubility

The solubility of capecitabine in water was found to be 25.32±0.12mg/ml which is very nearer to reported solubility of capecitabine. The standard calibration curve of the capecitabine was obtained by plotting the concentration from 5, 10, 20, 30 and 40µg/ml against its respective absorbance at 240nm (Figure 2).

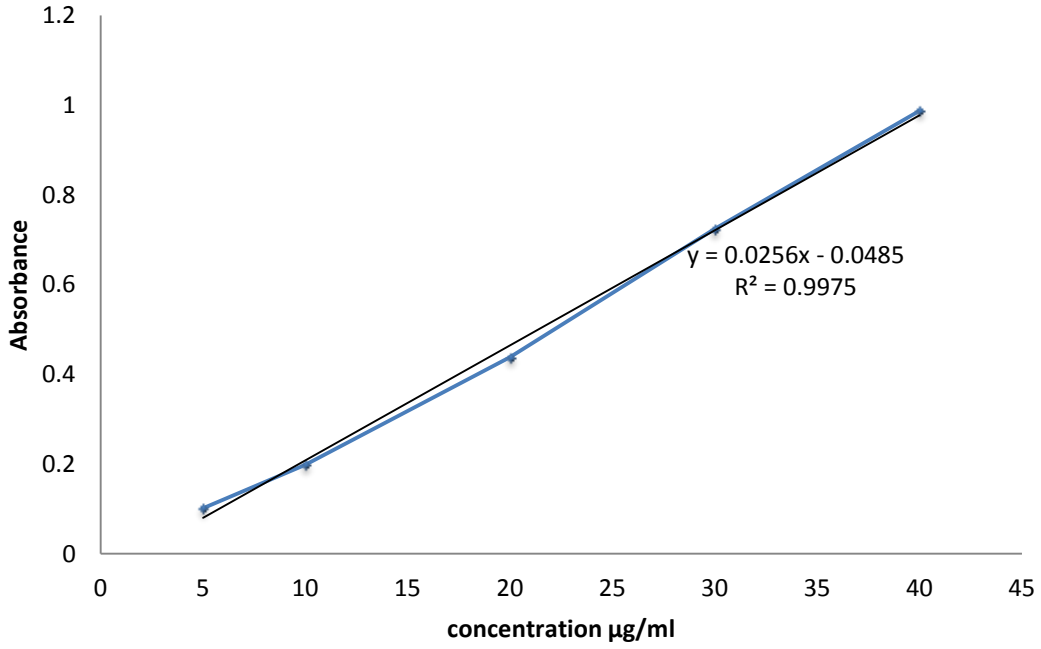

Figure 2: Calibration Curve of Capecitabine in Phosphate Buffer Solution pH 7.4

Table 2: Calibration Curve of Capecitabine in PBS pH 7.4 at λmax 240 nm

Sr. No.	Conc. (µg/ml)	Absorbance			Mean ± SD
		I	II	III	
1	5	0.105	0.099	0.101	0.101±0.003
2	10	0.199	0.201	0.196	0.198±0.002
3	20	0.438	0.441	0.435	0.438±0.003
4	30	0.724	0.72	0.728	0.724±0.004
5	40	0.987	0.99	0.985	0.987±0.002

n=3

Encapsulation efficiency and drug loading

The encapsulation efficiency and drug loading of capecitabine nanoparticles was measured using U.V spectroscopy. Entrapment efficiency was determined for all 09 batches and it was obtained in the range of 45 to 85%. The maximum entrapmentwas in batch CS-NPs-8, 85.74±2.36.This may be because of optimum concentration of chitosan as well as of TPP. Initially as concentration of TPP increases, the entrapment was also found to be increasing up to certain limit,but as concentration further increases, the entrapment was decreasing. This suggest that at lower level TPP is not sufficient enough to crosslink all chitosan used, and at higher concentration TPP might be causing the over cross linking which is reducing the entrapment. For chitosan, higher level was observed to cause maximum entrapment, which suggests that the 1:3 capecitabine chitosan ratio is optimum(Table 3 and figure 3).

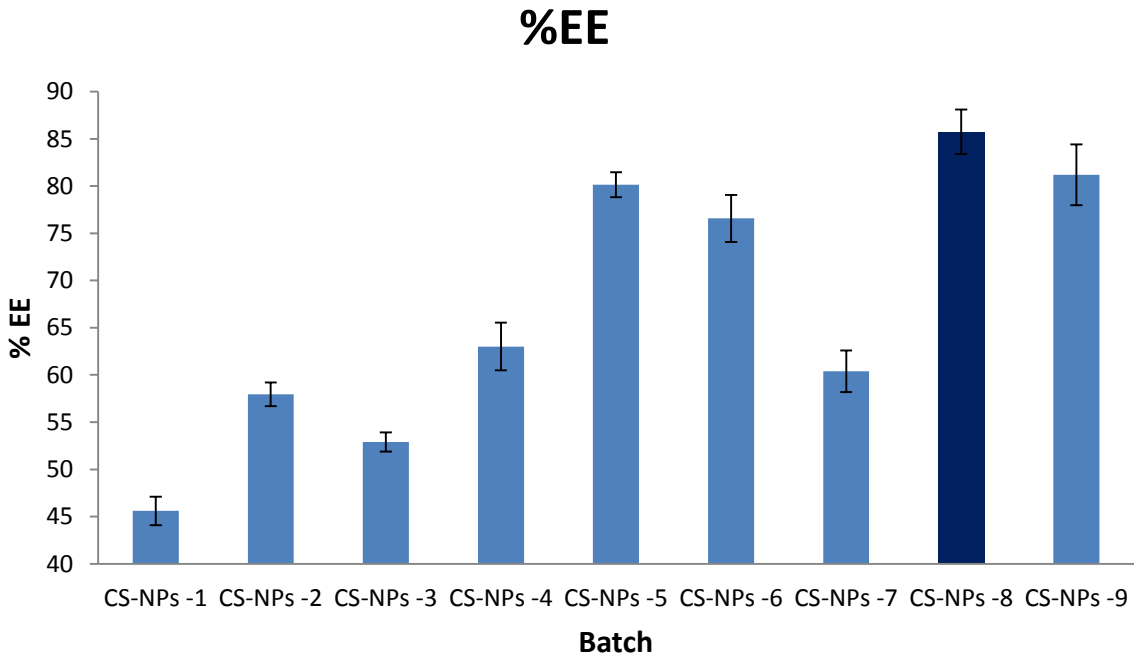

Figure 3: % Entrapment efficiency of capecitabine CS-NPs

Table 3. Data of % yield, % entrapment efficiency (EE) and % drug loading of capecitabine CS-NPs

Batch No.	%Yield	%EE	%Drug Loading
CS-NPs -1	69.6±1.4	45.6±1.5	25.18±0.62
CS-NPs -2	66.38±1.21	57.94±1.25	27.2±0.76
CS-NPs -3	62.07±0.95	52.9±1.023	24.85±.54
CS-NPs -4	65.2±2.06	63.01±2.53	27.56±0.91
CS-NPs -5	70.1±1.3	80.15±1.32	28.67±1.04
CS-NPs -6	73.9±0.96	76.57±2.5	25.87±0.82
CS-NPs -7	54.17±2.5	60.39±2.21	24.66±0.85
CS-NPs -8	69.64±1.11	85.74±2.36	29.9±0.91
CS-NPs -9	70.06±0.93	81.19±3.21	23.03±0.43

n=3

Optimization of formulation

Prepared chitosan nanoparticles were optimized by plotting the contour plots by considering the %EE as a response. Contour plot was drawn by Sigmaplot version 11.0. From the plot it was observed that the maximum entrapment ~85% was attributed to the +1 level of chitosan and 0 level of TPP variables, which represents the batch CS-NPs-8 (Figure 4).

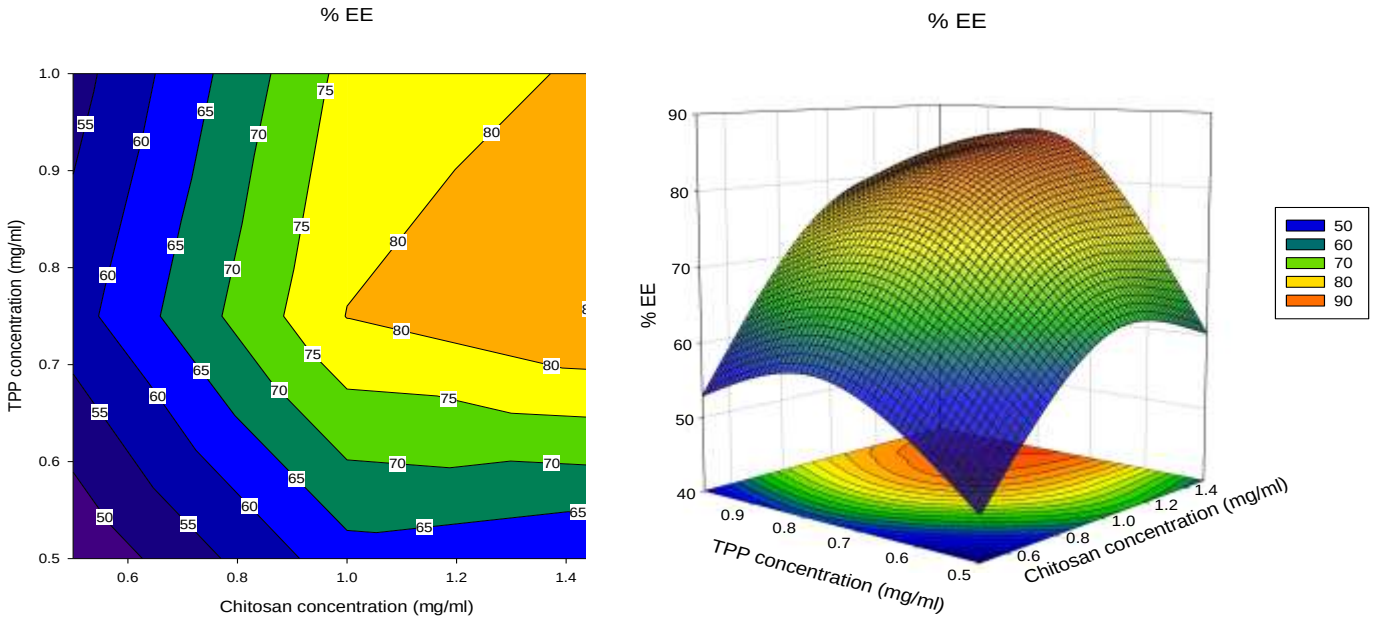

Figure 4: 2D and 3D Contour plots of variables on %EE

Particle size and PDI

Particle size is one of the most important parameters determining biocompatibilities and bioactivities of nanoparticles. Small nanoparticles have a higher intracellular uptake than large ones[14]. Reported that the gastrointestinal uptake of particles of 100nm was 15–250 folds greater than larger size microparticles. Since particle size plays a vital role in mucosal and epithelial tissue

uptake and intracellular trafficking of nanoparticles[13], it is possible to enhance the mucoadhesive properties of CS nanoparticles by decreasing its particle size, and thus to improve mucosal uptake of capecitabine-loaded nanoparticles. Average particle size distribution of CS-NPs-8 was found to be 87.23nm which quite good as per the nano perspective of the formulation and PDI was found to be 0.113 which shows that the optimized nanoparticles were exhibiting narrow size distribution which drastically reduce the possibility of the aggregation of the nanoparticles (Figure 5).

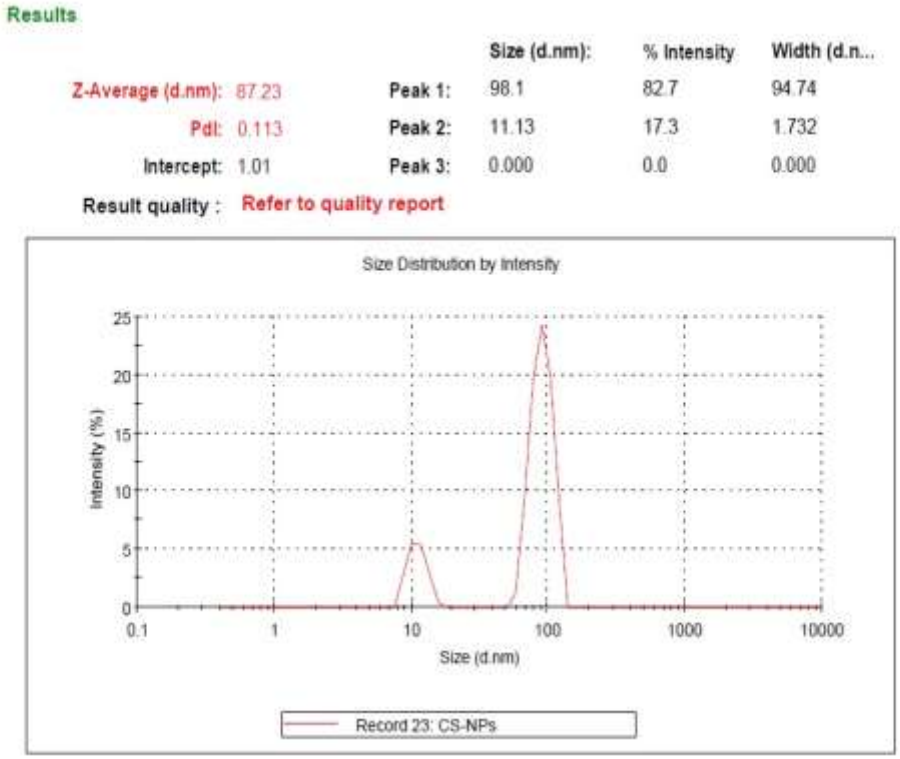

Figure 5: Particle size distribution of optimized formulation CS-NPs-8

Zeta potential

Sufficient zeta potential must exist at the surface of the nanoparticles in order to prevent the aggregation during the storage period. Zeta potential of the optimized bath CS-NPs-8 was analysed and was found to be -35.9mV which is sufficient enough to work as repulsion force between particles so that the stability of the nanoparticles will not be affected and particles will not undergoe the aggregation (Figure 6). Zeta potential is another key parameters contributing to various nutritional properties of CS nanoparticles. It has been well documented that CS possesses mucoadhesive properties, due to molecular attractive forces formed by an electrostatic interaction between positively charged CS and negatively charged mucosal surfaces. Since most tumor cell membranes are negatively charged, CS nanoparticles have recently been studied to develop tumor-specific delivery of anticancer drugs.

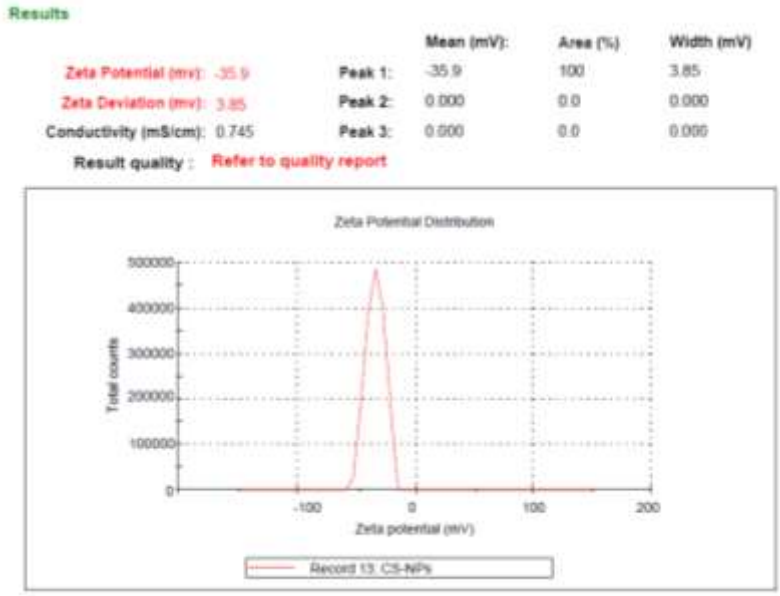

Figure 6: Zeta potential distribution of optimized formulation CS-NPs-8

Fourier transformer infrared spectroscopy

The intermolecular interaction between drug and excipients in nanoparticles was characterized by FT-IR.. first the FT-IR spectra of the capecitabine alone was taken and then the FT-IR spectra of the optimized formulation was taken and then both spectra was compared for the presence of the all the characteristic peaks of the capecitabine. From the comparison it was revealed that the capecitabine is not interacting with the chitosan or TPP as all the characteristic peaks of the drug was preserved in the formulation CS-NPs-8 (Figure 7).

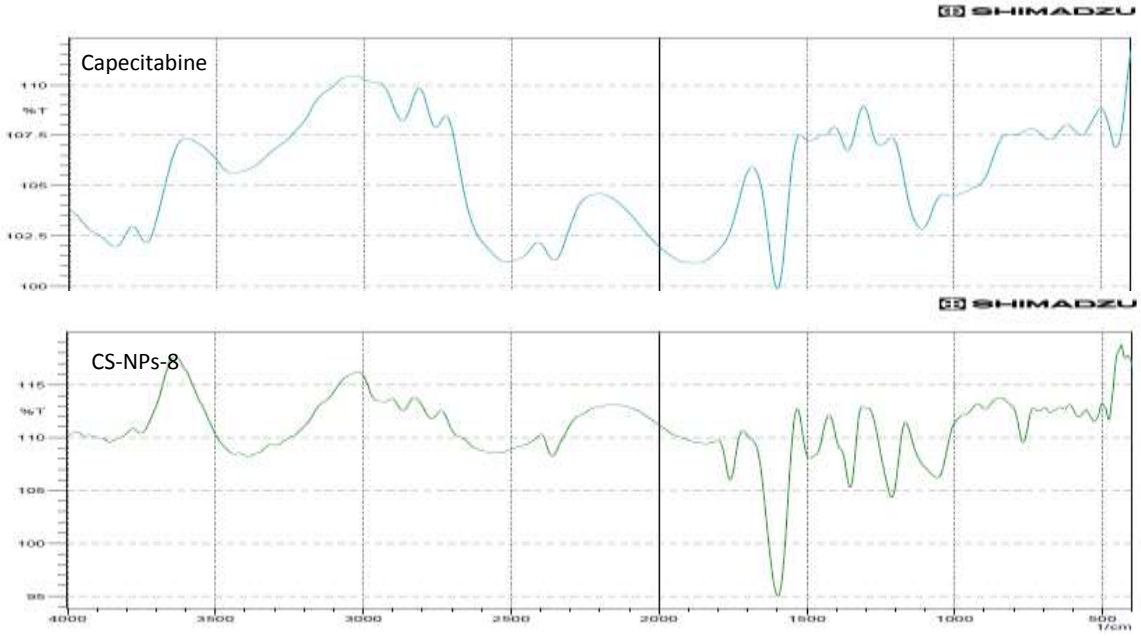

Figure 7: FTIR spectra of Capecitabine and CS-NPs-8

Differential scanning calorimetry

DSC thermogram of capecitabine exhibited a single endothermic peak at 123^{o}C, which corresponded to its intrinsic melting points. similarly, melting peak of capecitabine was identified in the DSC curves obtained from CS-NPs-8. The presence of phase transitions owing to capecitabine in the DSC analysis is evidence that capecitabine is physically compatible within the nanoparticles and exhibited thecrystalline state(Figure 8).

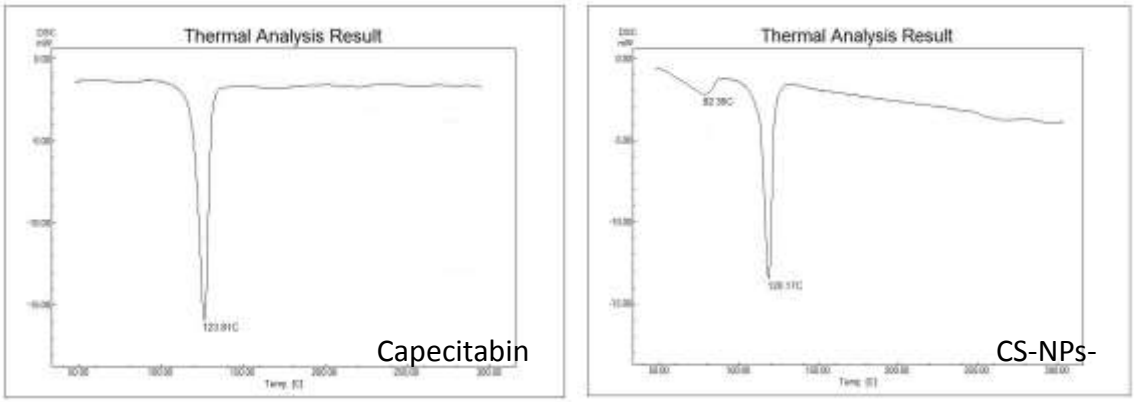

Figure 8: DSC thermogram of Capecitabine and CS-NPs-8

Scanning electron microscopy

Figure 9 represents the morphologies of the nanoparticles observed on SEM. It could be seen that all nanoparticles were regular spheres with smooth surface (diameters <100 nm).

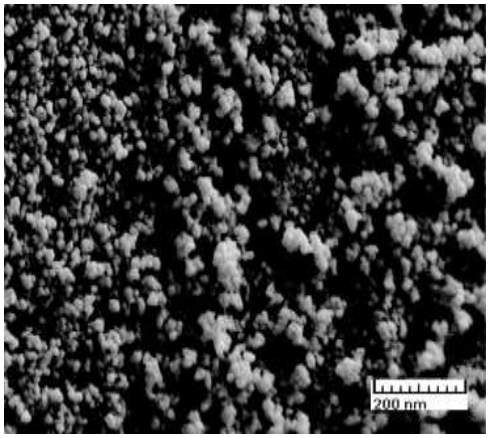

Figure 9: SEM of CS-NPs-8

***In-vitro* drug release of Capecitabine chitosan coated nanoparticles**

The cumulative percentage release of capecitabine from the prepared nanoparticles was obtained from 73.5±2.15 to 94.4±2.15 up to the 48 hours of duration.Highest drug release found in CS-NPs-8 might be because of the better through entrapment of the drug in chitosan network within nanoparticle. From the result of the drug release kinetic model drug release was found to be following first order and diffusion controlled. Initially the burst release was observed up to the

period of 8h and then after slow and gradual release was observed and after 48h the release was observed becoming linear(Figure 10).

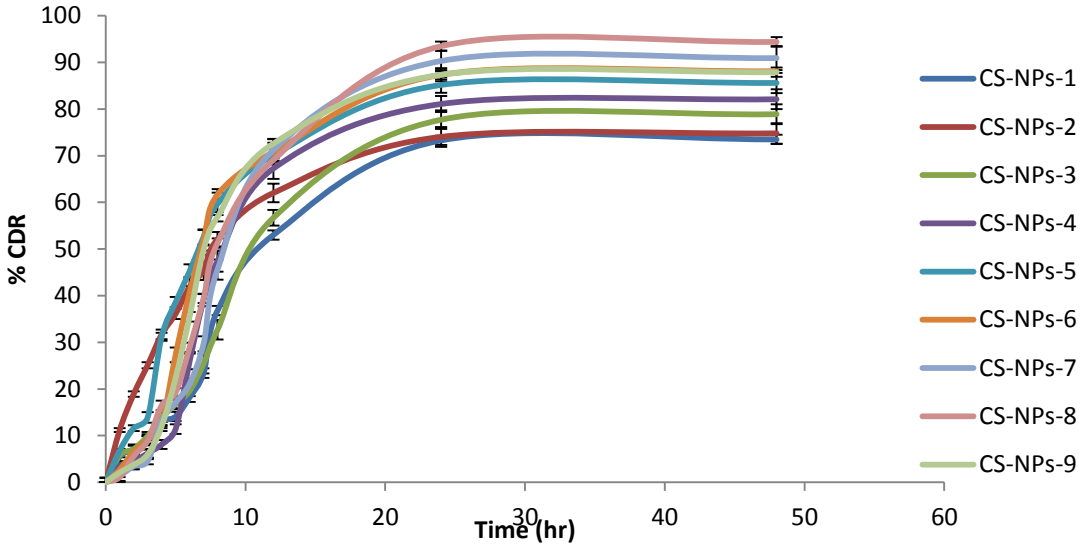

Figure 10: % cumulative drug release of CS-NPs

MTT assay

From the result of the MTT assay it was observed that the capecitabine loaded CS-NPs-8 was showing almost 50% more inhibition than the capecitabine alone in both the cancer cell line HT-29 and MCF-7, which is because of the nano size of the particles enabling the more ingestion the drug within the cells. However, growth inhibition was less in MCF-7 as compared to the HT-29 cell line which shows the better effect of drug in colon cancer than breast cancer. None of the samples have shown any cytotoxicity to the normal cell line Vero. This outcome suggest that the chitosan nanoparticles can be an important way to potentiate the anticancer effect in colon cancer (Figure 11).

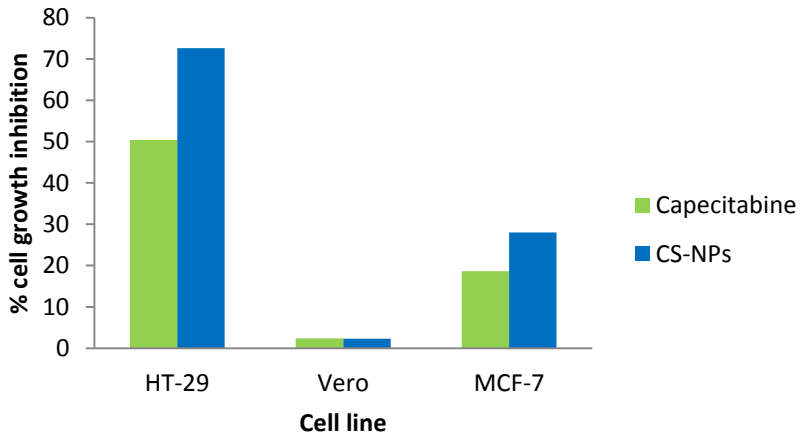

Figure 11: % inhibition of the cell growth by capecitabine and CS-NPs

CONCLUSION

Capecitabine loaded CS nanoparticles were successfully prepared under mild conditions by cross-linked with tripolyphosphate (TPP). The nanoparticles formulation of capecitabine was successfully optimized based on entrapment efficiency(85%) and sustain drug release up to 48h (92%), and optimized batch CS-NPs-8 was found to be having 87nm particle size, minimum Polydispersity (0.113), sufficient zeta potential (-35.9mV), spherical shape, and smooth surface and physical compatibility of drug in nanoparticles. Results from the stability studies at 25°C/60 ± 5% RH and 40°C/70 ± 5% RH indicated good stability of the optimized formulation as there was no significant change in the physical appearance, drug content and drug release. MTT assay shows the 50% rise in the anticancer activity of capecitabine as in chitosan nanoparticle form. So it can be concluded that the chitosan nanoparticles can be effectively used to drastically increase the anti cancer potency of the capecitabine in colon cancer in order to reduce its dose and hence its side effects.

REFERENCES

1. Cristina Buzea, Ivan Pacheco, and Kevin Robbie. Nanomaterials and Nanoparticles Sources and Toxicity. Biointerphases. 2007; 3(2): 217.
2. Eric Drexler K. Nano systems, Molecular Machinery, Manufacturing, and Computation. MIT PhD thesis: 1991.
3. Taniguchi N. on the Basic Concept of 'Nanotechnology. 1974; 2: 175-185.
4. Judson IR, Beale PJ, Trigo JM, Aherne W, Crompton T, Jones D, Bush E, and Reigner BA. human capecitabine excretion balance and pharmacokinetic study after administration of a single oral dose of 14C-labelled drug. Invest. New Drugs. 1999; 17: 49-56.
5. Agnihotri SA, Mallikarjuna NN, Aminabhavi TM. Recent advances on chitosan-based micro and nanoparticles in drug delivery. J. Control. Release. 2004; 100: 5-28.
6. Doelker E. Water-swollen cellulose derivatives in pharmacy. Peppas NA (Ed.), Hydrogels in Medicine II, CRC Press, Boca Raton, FL. 1987; 115.
7. Agnihotri SA, Aminabhavi TM. Formulation and evaluation of novel tableted chitosan microparticles for the controlled release of clozapine. J. Microencapsul. 2004; 21: 709-718.
8. Agnihotri SA, Aminabhavi TM. Controlled release of clozapine through chitosan microparticles prepared by a novel method. J. Control. Release. 2004; 96: 245-259.

9. Mi FL, Shyu SS, Chen CT, and Schoung JY. Porous chitosan microspheres for controlling the antigen release of Newcastle disease vaccine: preparation of antigen-adsorbed microsphere and in vitro release. Biomaterials. 1999; 20: 1603-1612.
10. Calvo P, Remunan Lopez C, Vila Jato JL and Alonso MJ. J Appl.Polym. Sci. 1997; 63: 125-132.
11. Shah S, Pal A, Kaushik V K, and Devi S. Preparation and characterization of venlaxine hydrochloride-loaded chitosan nanoparticles and in vitro release of drug. J. Appl. Polym. Sci. 2009; 112: 2876-2887.
12. Muller RH and Facobs C. Buparvasome muchoadhesive nanosuspension preparation optimization and long-term stability. Int. J. Pharm. 2002; 137: 151-161.
13. Wu Y, Yang WL, Wang CC, Hu JH and Fu SK. Chitosan nanoparticles as a novel delivery system for ammoniu glycyrrhizinate. Int. J. Pharm. 2005; 295: 235-245
14. Desai MP, Labhasetwar V, Amidon GL and Levy RJ. Gastrointestinal uptake of biodegradable microparticles: Effect of particle size. Pharm. Res. 1996; 13(12): 1838-1845.
15. Kahn and Jennifer. Nanotechnology. National Geographic. 2006; 4: 98-119.
16. Rodgers P. Nanoelectronics- Single file. Nature Nanotechnology, 2006; 1: 1-5.